THE UNIVERSITY OF QUEENSLAND

AUSTRALIA

Ecohydrology in space and time:

functioning and changes in the streamflow generation of catchments

Ralph Trancoso

Bachelor Forest Engineering

Masters Tropical Forests Sciences

Masters Applied Geosciences

A thesis submitted for the degree of Doctor of Philosophy at

The University of Queensland in 2016

School of Earth and Environmental Sciences

Abstract

Surface freshwater yield is a service provided by catchments, which cycle water intake by partitioning precipitation into evapotranspiration and streamflow. Streamflow generation is experiencing changes globally due to climate- and human-induced changes currently taking place in catchments. However, the direct attribution of streamflow changes to specific catchment modification processes is challenging because catchment functioning results from multiple interactions among distinct drivers (i.e., climate, soils, topography and vegetation). These drivers have coevolved until ecohydrological equilibrium is achieved between the water and energy fluxes. Therefore, the coevolution of catchment drivers and their spatial heterogeneity makes their functioning and response to changes unique and poses a challenge to expanding our ecohydrological knowledge. Addressing these problems is crucial to enabling sustainable water resource management and water supply for society and ecosystems.

This thesis explores an extensive dataset of catchments situated along a climatic gradient in eastern Australia to understand the spatial and temporal variation in their ecohydrological functioning and to potentially identify responses to climate- and human-induced changes. To address this aim, the thesis has four major objectives:

1) to investigate how streamflow similarity varies according to the annual water and energy balances and to determine to what degree biophysical drivers of runoff explain the observed spatial streamflow variability;
2) to determine the changes in the drivers of key streamflow characteristics across different regions and scales;
3) to examine long-term ecohydrological changes in the water and energy balances of catchments and separate out the climate- and human-induced components; and
4) to investigate trends in baseflow and separate the contribution of precipitation, potential evapotranspiration and elevated atmospheric CO_2 feedbacks with vegetation.

Three hundred and fifty five catchments were analysed spanning a tropical to Mediterranean climatic gradient in the Australian east coast over multiple periods of time. An extensive dataset was compiled and analysed, composed of: daily streamflow and precipitation time series, monthly satellite-based time-series of vegetation, model-based soil moisture and temperature, and spatial data of land-cover, topography, soil properties, physiography, bioregions and human population density. To address the first objective, catchments were classified using streamflow signatures and modelling was used to relate the spectrum of water and energy balances (Budyko framework) to the

drivers of runoff generation (Dunne diagram). To address the second objective a robust statistical modelling framework was applied to understand changes in streamflow drivers with regions and scales. In the third objective, the temporal displacement into the Budyko framework and its decomposition into climate and human-induced changes were examined. In the fourth objective, non-linear regressions and trend statistics were used to detect the influence of CO_2-vegetation feedbacks in baseflow. In addressing the four objectives, the following contribution to the ecohydrological knowledge has been made:

1) The catchments were classified into five hydrological regimes, which vary along the spectrum of water and energy balances (Budyko framework). The drivers of runoff generation (from the Dunne diagram) explained 77% of the streamflow similarity. The findings highlighted a formal mechanistic link between the Budyko Framework and the Dunne diagram.
2) Specific biophysical drivers govern the spatial variability of streamflow characteristics and therefore cannot be generalized across different regions. However, important drivers associated to climate and vegetation are consistent at both regional and continental scale but with differing importance. Catchment soil properties have a significant effect on streamflow characteristics, especially at regional scales.
3) Both climate- and land cover-induced changes are altering the water and energy balances of catchments towards a streamflow reduction. The land cover-induced contribution to changes in streamflow is greater in water-limited catchments while energy-limited and equitant catchments experienced more climate-induced changes. Catchments are consistently moving towards a drier equilibrium regardless their aridity and streamflow regimes.
4) A consistent spatio-temporal decline is observed in baseflow. Although the observed trends are mostly explained by climate forcings, residual baseflow trends attributed to other factors are best explained by increasing photosynthetic activity. The elevated atmospheric CO_2 and its associated vegetation feedbacks are reducing baseflow with more acute impacts in water-limited regions.

The thesis findings provide new insights into the ecohydrological functioning and changes in freshwater availability currently taking place in eastern Australia with potentially profound implications for sustainable water resource management in other water-limited regions. The understanding of ecohydrological feedbacks over a range of regimes and their sensitivity to climate-induced changes and human-induced landscape modifications is pivotal to ensure freshwater supply for societal and environmental needs in water scarce environments.

Declaration by author

This thesis is composed of my original work, and contains no material previously published or written by another person except where due reference has been made in the text. I have clearly stated the contribution by others to jointly-authored works that I have included in my thesis.

I have clearly stated the contribution of others to my thesis as a whole, including statistical assistance, survey design, data analysis, significant technical procedures, professional editorial advice, and any other original research work used or reported in my thesis. The content of my thesis is the result of work I have carried out since the commencement of my research higher degree candidature and does not include a substantial part of work that has been submitted to qualify for the award of any other degree or diploma in any university or other tertiary institution. I have clearly stated which parts of my thesis, if any, have been submitted to qualify for another award.

I acknowledge that an electronic copy of my thesis must be lodged with the University Library and, subject to the policy and procedures of The University of Queensland, the thesis be made available for research and study in accordance with the Copyright Act 1968 unless a period of embargo has been approved by the Dean of the Graduate School.

I acknowledge that copyright of all material contained in my thesis resides with the copyright holder(s) of that material. Where appropriate I have obtained copyright permission from the copyright holder to reproduce material in this thesis.

Publications during candidature

Peer-reviewed papers

Trancoso R., Larsen J.R., McVicar T.R., Phinn S., McAlpine C. (2017). CO_2 – Vegetation feedbacks and other climate changes implicated in reducing baseflow. *Geophysical Research Letters*, 44(5): 2310-2318, doi:10.1002/2017GL072759. (Incorporated as Chapter 5)

Trancoso R., Phinn S., McVicar T.R., Larsen J.R., McAlpine C.A., (2017). Regional variation in streamflow drivers across a continental climatic gradient. *Ecohydrology* e1816. DOI:10.1002/eco.1816 (Incorporated as Chapter 3)

Trancoso R., Larsen J.R., McAlpine C., McVicar T.R., Phinn S. (2016). Linking the Budyko framework and the Dunne diagram. *Journal of Hydrology* 535: 581-597. doi:10.1016/j.jhydrol.2016.02.017 (Incorporated as Chapter 2)

Trancoso R., Sano E.E., Meneses P, R. (2014). The spectral changes of deforestation in the Brazilian tropical savanna. Environmental Monitoring and Assessment 187(1): 1-15. DOI:10.1007/s10661-014-4145-3

Conference abstracts

Berghuijs, W., Woods, R.A., Aalbers, E., Trancoso R., Larsen, J. (2016). Recent changes in extreme floods across multiple continents. 2016 AGU Fall Meeting.

Trancoso R. (2015). Catchment biophysical drivers of streamflow characteristics. 2015 AGU Fall Meeting.

Trancoso R., McAlpine C., Phinn S., Larsen J.R., McVicar T.R. (2014). Hydrological similarity and controls of streamflow behaviour in eastern Australian catchments. 2014 AGU Fall Meeting.

Book chapters

Larsen, J., Leon, J., McGrath, C., Trancoso, R. (2013) Review of the catchment processes relevant to the Great Barrier Reef region. Australian Government. Great Marine Park Authority. e-book, 48p.

Publications included in this thesis

Trancoso R., Larsen J.R., McAlpine C., McVicar T.R., Phinn S. (2016). Linking the Budyko framework and the Dunne diagram. *Journal of Hydrology* 535: 581-597. doi:10.1016/j.jhydrol.2016.02.017 (Incorporated as Chapter 2)

Contributor	Statement of contribution
R. Trancoso (Candidate)	Research design/conceptualisation (90%) Data analysis/interpretation (100%) Write/edit paper (80%)
J. R. Larsen	Research design/conceptualisation (4%) Write/edit paper (6%)
C. McAlpine	Research design/conceptualisation (4%) Write/edit paper (6%)
T. R. McVicar	Research design/conceptualisation (1%) Write/edit paper (6%)
S. Phinn	Research design/conceptualisation (1%) Write/edit paper (2%)

Trancoso R., Phinn S., McVicar T.R., Larsen J.R., McAlpine C.A., (2017). Regional variation in streamflow drivers across a continental climatic gradient. *Ecohydrology* e1816. doi:10.1002/eco.1816 (Incorporated as Chapter 3)

Contributor	Statement of contribution
R. Trancoso (Candidate)	Research design/conceptualisation (80%) Data analysis/interpretation (100%) Write/edit paper (80%)
S. Phinn	Research design/conceptualisation (1%) Write/edit paper (4%)
T. R. McVicar	Research design/conceptualisation (1%) Write/edit paper (2%)
J. R. Larsen	Research design/conceptualisation (1%) Write/edit paper (2%)
C. McAlpine	Research design/conceptualisation (17%) Write/edit paper (12%)

Trancoso R., Larsen J.R., McVicar T.R., Phinn S., McAlpine C. (2017). CO_2 – vegetation feedbacks and other climate changes implicated in reducing baseflow. *Geophysical Research Letters*, 44(5): 2310-2318, doi:10.1002/2017GL072759. (Incorporated as Chapter 5)

Contributor	Statement of contribution
R. Trancoso (Candidate)	Research design/conceptualisation (76%) Data analysis/interpretation (100%) Write/edit paper (75%)
J. R. Larsen	Research design/conceptualisation (10%) Write/edit paper (10%)
T. R. McVicar	Research design/conceptualisation (10%) Write/edit paper (7%)
S. Phinn	Research design/conceptualisation (2%) Write/edit paper (3%)
C. McAlpine	Research design/conceptualisation (2%) Write/edit paper (5%)

Contributions by others to the thesis

Chapter 1 – This chapter was solely written by the candidate with editorial assistance from Clive McAlpine, Stuart Phinn, Joshua Larsen and Tim McVicar.

Chapter 2 – This chapter is a replication of the paper: *Linking the Budyko framework and the Dunne diagram.* The candidate conceived the idea for the chapter, conducted all analysis, interpreted results and wrote the first draft. Jeff Hanson, Peter Scarth and Ross Darnell gave useful assistance on data processing (acknowledged in the paper). Further writing improvements were made with editorial assistance of Clive McAlpine, Stuart Phinn, Joshua Larsen and Tim McVicar.

Chapter 3 – This chapter is a replication of the paper: *Regional variation in streamflow drivers across a continental climatic gradient.* The candidate conceived the idea for the chapter, conducted all analysis, interpreted results and wrote the first draft. Further writing improvements were made with editorial assistance of Clive McAlpine, Stuart Phinn, Joshua Larsen and Tim McVicar.

Chapter 4 – This chapter is a replication of the paper: *Disentangling vegetation gain and climate contributions to long-term streamflow changes.* The candidate conceived the idea for the chapter, conducted all analysis, interpreted results and wrote the first draft. Further writing improvements were made with editorial assistance of Clive McAlpine, Stuart Phinn, Joshua Larsen and Tim McVicar.

Chapter 5 – This chapter is a replication of the paper: *CO_2 – vegetation feedbacks and other climate changes implicated in reducing baseflow*. The candidate conceived the idea for the chapter, conducted all analysis, interpreted results and wrote the first draft. Further writing improvements were made with editorial assistance of Clive McAlpine, Stuart Phinn, Joshua Larsen and Tim McVicar.

Chapter 6 – This chapter was solely written by the candidate with editorial assistance from Clive McAlpine, Stuart Phinn, Joshua Larsen and Tim McVicar.

Statement of parts of the thesis submitted to qualify for the award of another degree

None

Acknowledgements

Back to 1999, when I had my first contact with science at undergraduate level and decided I would become a scientist undertaking my PhD overseas, I had no idea about the challenge I was posing to myself neither the long-term planning it would require. Eighteen years later I am now starting writing the acknowledgments of my PhD thesis reflecting about the massive intellectual, physical and emotional journey I have gone through. Reaching this point and having one of my career goals coming through is a pleasant sensation – good stuff!

I am thankful to my four supervisors who are all outstanding scientists from the different branches of science I have interest: landscape ecology, remote sensing, ecohydrology and catchment hydrology. I was fortunate enough to have received guidance along this 3.5 years journey - that helped me to become a much better scientist. Whilst challenging to manage distinct inputs and scientific styles, I learned different things from their expertise and constructed my own way of thinking and scientific style.

My principal advisor, Prof Dr Clive McAlpine, encouraged me to come to Australia when I first got in touch with him in 2012 and since then has always been enthusiastic about my ideas and provided me guidance, encouragement and support throughout the long and windy PhD road. My associated supervisor, Prof Dr Stuart Phinn, has always been available to hear and make his considerations touching the heart of the matter. These are two truly great men. They gave me liberty to conduct my research and made me feel like they believed in my capacity. That provided me confidence and motivation to keep moving forward no matter how big the challenge was. I truly admire them professionally, the way they approach research, and their respect for the individualities and wishes of their PhD students.

My other two associated supervisors, Dr Josh Larsen and Dr Tim McVicar joined the supervision team a bit further to strength the hydrological component of my research and they really did it. Josh has always been enthusiastic about my findings and helped me to improve my writing skills. I am also grateful to Josh for the opportunity to be involved as a tutor in the course Climatology and Hydrology (GEOS2101) for three years. Tim was the last to join the supervision team, yet I have learned a lot from him. He is a great scientist, and has an unbelievable capacity to pay attention to details. He greatly improved my research and I am lucky to have had the opportunity to work with him.

This research would have been impossible without the availability of: (i) streamflow time-series by the State governments of Queensland, New South Wales, Victoria and Tasmania; (ii) gridded

precipitation time-series by the Bureau of Meteorology; (iii) hydroclimatological and (iv) vegetation time series by CSIRO Land and Water; (v) Digital Elevation Model and (vi) national dynamic land cover by Geoscience Australia; (vii) soil spatial datasets by CSIRO Land and Water; and (viii) atmospheric CO_2 concentration time series by CSIRO.

I am also grateful to the University of Queensland and the Australian Government, which provided the funding for my PhD scholarship, tuition fees and conference travel.

The discussions with several colleagues in the Remote Sensing Research Centre, Landscape Ecology and Conservation Group and in other groups within the former School of Geography, Planning and Environmental Management - GPEM (now, School of Earth and Environmental Sciences - SEES) have indirectly contributed to make my own way. Particularly, Matt Watts, Jeff Hanson and Dr Peter Scarth assisted me with data processing in the early stages. Dr Ross Darnel kindly shared his expertise helping me to debug my R scripts a couple of times.

I was lucky enough to have met Nivea Siqueira when I first arrived at GPEM. Since then, she has been like a close aunt for my family and myself throughout our ups and downs here in Australia. Was great to meet "my big mate" Matt Rice at GPEM as well, he is such a great friend who has always been available to catch up and hear me. I am deeply thankful to both of you.

Still in Brazil, Dr Robert Miller and Dr Edson Sano encouraged me to come here when I was in doubt and their experience and wise words helped me to make the right decision.

I am also grateful to my family ("*The Trancosos*" – Adelaide, Elizabeth, Indra Raquel and Ingrid) as well as my family-in-law ("*The Sardinhas*" – Aureiza, Ijanil, Aline and Lorena). They helped me with their love and support. Special thanks to Aureiza, who came here three times, and has always been close, no matter how far a half planet is.

Last but foremost, I am deeply thankful to my wife Ingrid Sardinha Trancoso, who supported me wholeheartedly over the last eight years of my life and turned my career dream into our family goal. She encouraged me to come to Australia more than anyone, temporally stopped her promising career as a doctor, and quitted her jobs in Brazil to embrace the challenging adventure of a student lifestyle beside me overseas. In the meantime, during the last stages of my PhD, she made me father giving birth to our adorable little girl Evelyn, who flooded our lives with love and happiness. Evelyn, you are still young to understand it now, but if you read this in future, know that you made me a better man and that helped my PhD as well. Ingrid and Evelyn you are wonderful. I am truly lucky to have you both with me and proud to call you my family – this is my best achievement, all my love to you.

Keywords

Ecohydrology, catchment classification, Budyko framework, Dunne diagram, streamflow drivers, streamflow changes, baseflow trends, climate change, land cover change, CO_2 fertilization effect

Australian and New Zealand Standard Research Classifications (ANZSRC)

ANZSRC code: 040608, Surface Water Hydrology, 60%
ANZSRC code: 040607, Surface Processes, 20%
ANZSRC code: 040104, Climate Change Processes, 20%

Fields of Research (FoR) Classification

FoR code: 0406, Physical Geography and Environmental Geoscience, 70%
FoR code: 0502, Environmental Science and Management, 30%

Table of Contents

List of Figures

List of Tables

List of Abbreviations used in the thesis

ΔQ – Change in Q

ΔQ [%] – Change in Q relative to initial Q

ΔQ^c – Climate-induced change in Q

ΔQ^c [%] – Climate-induced change in Q relative to initial Q

ΔQ^h – Anthropogenic landscape-induced change in Q

ΔQ^h [%] – Anthropogenic landscape-induced change in Q relative to initial Q

AET – Actual evapotranspiration

AIC – Akaike Information Criterion

BFI – Baseflow Index

BIC – Bayesian Information Criterion

CO_2 – Carbon dioxide concentration in the atmosphere

cs – Cubic splines

DEM – Digital elevation Model

EC – East Coast

eCO_2 – Elevated Carbon dioxide concentration in the atmosphere

eCO_2–Veg – Feedbacks between vegetation and elevated carbon dioxide concentration

EM – Expectation Maximization

EQP – Streamflow elasticity

FDC – Flow Duration Curve

FNF – Frequency of no flow

fPAR – Fraction of Photosynthetic Active Radiation

fPARr – Fraction of Photosynthetic Active Radiation detrended from P and PET

GAMLSS – Generalized Additive Model for Location, Scale and Shape

GBR – Great Barrier Reef

GDR – Great Dividing Range

Ksat – Saturated Hydraulic Conductivity

LOESS – Locally Weighted Scatterplot Smoothing

MAD – Mean Absolute Deviation

MHC – Model based Hierarchical Clustering

n – Free parameter for partitioning of P into Q and AET in the Budyko framework

N – Sample size

NSW – New South Wales

P – Precipitation

P max – Maxima monthly P

PC1 – First Principal Components

PC2 – Second Principal Components

PCA – Principal Components Analysis

PET – Potential evapotranspiration

PET max – Maxima monthly PET

ps – Penalized splines

Q – Streamflow

Q10N – Normalized 10^{th} percentile streamflow

Q90N – Normalized 90^{th} percentile streamflow

Qb – Baseflow

Qbr – Baseflow detrended from P and PET

QLD – Queensland

R1 – Region one, tropical catchments (Cape York Peninsula, Wet Tropics and Einasleigh Uplands)

R2 – Region two, sub-tropical catchments (South East Queensland)

R^2 – Coefficient of determination

R3 – Region three, temperate catchments (South Eastern Highlands)

RLD – Rising Limb Density

RQP – Long-term runoff ratio

Rzero – Zero flow ratio

SFDC – Slope of the Flow Duration Curve

SM – Monthly Averaged Soil Moisture

SRTM – Shuttle Radar Topographic Mission

SSE – Sum Squared Error

TAS – Tasmania

VIC – Victoria

CHAPTER 1

INTRODUCTION

Most of the Australian freshwater supply relies on the east coast catchments. Currumbin Creek at Springbrook National Park, Queensland. Photo by Ralph Trancoso.

1.1 Background to the problem

Streamflow and catchments are two core subjects approached by this thesis. The overarching knowledge pursued is the understanding of catchment-scale ecohydrological mechanisms driving the natural variability and changes in the long-term annual streamflow. As a background to the research problems and objectives addressed by this thesis, this section will introduce why streamflow is important, how it is generated and how changes to the climate and landscape taking place within catchments are affecting streamflow processes.

1.1.1 Importance of catchments for streamflow generation

Streamflow plays a critical role in the water cycle and terrestrial ecosystems. Globally, the streamflow is the main source by which water returns to the oceans, while the evaporation from the oceans is the primary source by which water returns to the atmosphere, and the precipitation over the land is the primary source of streamflow generation (Oki, 2006).

Streamflow is generated by catchments, which are landscape units naturally delimited by topographic features that partition precipitation into evapotranspiration, percolation and streamflow according to their biophysical characteristics. Catchments use gravity to drain water downhill to an outflow point, often the ocean (Berry et al., 2006). Therefore, catchments are continuously cycling the water intake from the headwaters to the lower plains, generating streamflow and providing one of the most important ecosystem services – the freshwater yield (Poff et al., 1997).

Streamflow is the main source of freshwater for urban populations, agriculture and riverine ecosystems (Johnson et al., 2001). The quantity and quality of streamflow generation is largely influenced by the catchment characteristics as well as the climate-induced changes and human landscape modifications impacting the upstream catchment. Hence, the freshwater yield by catchments is given by the summation of these processes that are changing in space and time (Wagener et al., 2006). Likewise, streamflow is highly variable both within and among catchments in space and time. Climate- and human-induced changes in streamflow impact communities and economies through floods and droughts, which impact freshwater availability, economic activities and water-dependent ecosystems (Sterling et al., 2013; van Dijk et al., 2013).

1.1.2 Drivers of streamflow generation and change

The hydrological behaviour of catchments reflects the co-evolution of climate, soils, topography and vegetation (Dunne, 1983; Winter, 2001; Woods, 2003; Berry et al., 2006; Sivapalan, 2006). The

spatial and temporal heterogeneity of these biophysical characteristics makes the hydrological processes of each catchment unique (McDonnell et al., 2007). This uniqueness challenges the development of hypotheses that can adequately test the overall functioning of hydrological systems (Beven, 2000).

Understanding the factors driving streamflow behaviour has been the focus of scientists and water decision-makers worldwide (Postel and Richter, 2012). Changes in rainfall regimes associated with climate variability and change and anthropogenic landscape modifications are often identified as the main drives of streamflow changes (Sterling et al., 2013; Delworth and Zeng, 2014; Karoly, 2014; Zhou et al., 2015; Sarojini et al., 2016). While few studies have attempted to separate the effects of climate and landscape changes and rising levels of atmospheric CO_2 on streamflow using global models (Gedney et al., 2006; Piao et al., 2007), separating these individual effects remains challenging for observational studies (Wang et al., 2013). Understanding the relative influence of the drivers of change in freshwater availability is particularly important on water-limited regions that are more sensitive to changes because this resource is already scarce (Barnett et al., 2008; Seddon et al., 2016) and are inhabited by more than one third of world's population (Gilbert, 2011). These drivers of change are quite significant in Australia where its landscapes have been dramatically modified over the last 200 years (Walker et al., 1993; Butzer and Helgren, 2005) with forest clearing for cropping and grazing. However, in the last few decades an increase in biomass in woodland and forest ecosystems has been reported as a result of regrowth and CO_2 fertilization (Fensholt et al., 2012; Donohue et al., 2013; Liu et al., 2015; Evans, 2016).

Australia also is experiencing climate change as evidenced by a reduction in annual rainfall, most pronounced over eastern and south-west regions since 1950 (Delworth and Zeng, 2014; Karoly, 2014) and increasing temperature (Alexander and Arblaster, 2009). Increase in atmospheric demand and transpiration have also been reported (Zhang et al., 2016b), although the global dimming and stilling (Roderick and Farquhar, 2002; McVicar et al., 2012a) are offsetting that. Along the eastern seaboard, where most of the human population is concentrated, both climate-induced changes and human-induced landscape modifications may alter the hydrological cycle impacting catchment outflows. However, the detection of these hydrological changes, and particularly their attribution to drivers, is challenging due to the large variability of catchments (Beven et al., 1988) and their responses according to their specific physiographical characteristics (Sivapalan, 2006).

1.1.3 Climate change and variability impacts on streamflow

Globally, climate change and variability affect terrestrial ecosystems (Seddon et al., 2016) and freshwater availability with consequences for human health, economic activity, ecosystem function and geophysical processes (Milly et al., 2005; Collins et al., 2013). There is increasing evidence that the observed changes in hydroclimatological variables (Alkama et al., 2011; McVicar et al., 2012a; Ukkola and Prentice, 2013; Greve et al., 2014; Zhang et al., 2016b) are resulting in an overall increase in water fluxes, with an ongoing claim that any stationarity in water cycle has already been modified by anthropogenic climate change (Milly et al., 2008). Despite past controversies (Ohmura and Wild, 2002; Labat et al., 2004; Labat et al., 2005; Legates et al., 2005), there is an emerging consensus that global warming is intensifying the global water cycle (Huntington, 2006; Syed et al., 2010; Wu et al., 2010; Eicker et al., 2016).

Being the driest inhabited continent, Australian freshwater availability is quite sensitive to changes in climate forcings compared to other continents (Wu et al., 2010; Eicker et al., 2016; Seddon et al., 2016). This, however, was experienced by the first European settlers who faced cool and wet weather during 1788-1790 (La Niña) followed by hot weather and droughts from 1791 to 1793 (El Niño), limiting initiatives to establish European agricultural in the colony (Gergis et al., 2010). These five initial years were a good proxy to comprehend the natural variability of climate in Australia. The water scarcity and associated constraints to living in the driest populated continent, which also has the lowest proportion of rainfall converted to runoff (Finlayson and McMahon, 1988; McMahon et al., 2007), has shaped the Australian economy and society over the past 228 years. As a result, most human settlements were established in the wetter coastal regions with the majority of population now inhabiting Australia's east coast (ABS, 2014).

Australia's climate is highly variable, with a strongly seasonal, inter-annual and even inter-decadal variations. This diversity is driven by different climatic teleconnections occurring in the Pacific, Indian and Southern Oceans. These connections can be represented by four factors: El Niño or Southern Oscillation (ENSO), Inter-decadal Pacific Oscillation (IPO), Indian Ocean Dipole (IOD) and Southern Annular Mode (SAM) (Verdon-Kidd and Kiem, 2009). Fu et al. (2010) showed that the highest intense rainfall events occur over east coast for the period 1910-2006. In addition, they found strong relationships between the occurrence of extreme rainfall events and the Southern Oscillation Index (SOI) and the IPO especially during La Niña years. Increasing trends in the number of rain days were observed over southern and northern parts of the east coast between 1910 and 1998 at a rate of 6.4 - 9.2 days 100 years^{-1} (Haylock and Nicholls, 2000), while upward trends

for wet extremes were also detected over the continent between 1910 and 2005 at a rate of 1-2% decade-1 (Gallant and Karoly, 2010). The declines in Southern Australia occurred mainly between March and August which is closely related to the trend in SAM (Nicholls, 2010).

Considering the factors simultaneously controlling rainfall in Australia, this high seasonal, inter-annual and inter-decadal variation is expected. Such natural variability impacts water availability, especially for agriculture and urban areas. Potter and Zhang (2009) showed a streamflow decrease of 44% in Murray-Darling Basin between 1997 and 2006 due to an observed 13% reduction in rainfall. Australia's east coast has also become drier in recent decades, with a negative trend up to -5 mm/years from 1950 to 2009. These changes in rainfall patterns were partially explained by exceptionally wet years during the early 1950s and, in part, attributed to human-induced climate change (Cai and van Rensch, 2012). The natural variability of rainfall impacts Australian society through extreme events, such as these recent floods and droughts. The negative rainfall anomaly recorded between 1998 and 2008, which was popularly called as "Big Dry" or "Millennium Drought" was the worst drought since the arrival of European settlers (Gergis et al., 2012; van Dijk et al., 2013). However, the ongoing rainfall decline in south-eastern Australia appears worse than previous droughts (Timbal and Fawcett, 2012). Conversely, after this dry decade extreme consecutive rainfall events have occurred in Queensland, begetting severe floods that impacted population in different ways (van den Honert and McAneney, 2011). These events were later explained in light to an association of a negative Pacific Decadal Oscillation (PDO) and Interdecadal Pacific Oscillation (IPO) during La Niña years (Cai and van Rensch, 2012).

Evidence has shown that Australia is already experiencing climate change impacts, despite the difficulties of separating its effect from natural variability (Nicholls and Collins, 2006; Murphy and Timbal, 2008; Collins et al., 2013). Particularly with regard to Australian runoff, most studies have used output scenarios from global climate models (GCMs) as inputs into hydrological models to forecast potential changes on streamflow (Chiew and McMahon, 2002; Chiew et al., 2009b; Zhang and Chiew, 2009; Vaze et al., 2010). Model results often indicate that runoff tends to decrease more markedly than precipitation due the convergence of precipitation reduction and potential evapotranspiration increase (Chiew et al., 2009a; Vaze et al., 2011; Silberstein et al., 2012). The calibration period also has an important role in the predictability of rainfall-runoff models. Models can generally predict climate change impacts, since the future mean annual rainfall is not more than 15% higher or 20% wetter in relation to the model calibration period (Vaze et al., 2010). Model outcomes are also sensitive to climate change scenarios. In a comparison of climate change projections, derived from 23 GCMs for 210 catchments across southeast Australia, annual rainfall

changes ranged from -10% to 3% change per degree global warming, with the corresponding streamflow changes ranging between -23% to +4% (Chiew et al., 2009a). In addition, projections for 106 catchments in south-western Australia from 15 GCMs showed a median annual rainfall decline of 8%, which results in a median decline of 25% in runoff (Silberstein et al., 2012). This magnitude of runoff decline may significantly reduce water yields and freshwater availability for urban water supplies and agriculture, and threaten water-dependent ecosystems (Barron et al., 2012; McFarlane et al., 2012).

1.1.4 Landscape transformation and impacts on streamflow

With over seven Billion people inhabiting the world's catchments, human-induced landscape modifications can have a significant impact on catchment streamflow and freshwater availability (Sterling et al., 2013). Studies have been addressing the global impact of human activities such as forest clearing, regulation and irrigation for energy and food production on freshwater availability (Destouni et al., 2013; Sterling et al., 2013; Jaramillo and Destouni, 2014; Jaramillo and Destouni, 2015).

A large global network of experimental catchments has been implemented since the beginning of the last century with the aim of addressing the impacts of landscape changes on streamflow (Bosch and Hewlett, 1982; Andréassian, 2004; Brown et al., 2005). The results from experimental catchment studies are extensive, and comprehensive reviews have been developed about the theme. Bosch and Hewlett (1982) published a well-known review, grouping results of 94 experiments about hydrological impacts of deforestation. More recently, Andréassian (2004) expanded this review to include 137 catchments. The overall trend revealed by these experiments shows that deforestation leads to an increase in streamflow, whereas reforestation tends to reduce water yield. The changes in water yield however, are proportional to annual rainfall and proportion of the watershed affected. Other reviews concluded that streamflow impacts of reductions of forest cover by less than 20% of the catchment area could not be statistically detected (Sahin and Hall, 1996; Stednick, 1996). Paired catchment studies have shown that catchment flow impacts are more pronounced immediately following deforestation, and are attenuated in subsequent years. This hydrological behaviour occurs especially when deforested areas are abandoned, which is becoming a common practice worldwide. Giambelluca (2002) showed that whilst albedo from secondary forests reduces radiation efficiency, saturated hydraulic conductivity and the evaporative fraction increase gradually for up to around 30 years since abandonment of the deforested area. Brown et al. (2005) performed another comprehensive review that added 72 paired catchments in relation to

those from Bosch and Hewlett (1982), focusing on a total of 166 paired catchments. They showed that changes in water yield are proportional to biomass, vegetation types and percentage of catchment treated. It is important to note that most catchments from experimental studies are smaller than 2 km^2, mainly for the application of treatment (deforestation or reforestation) and control of natural variability of biophysical properties. However, the convenience in terms of experimentation conditions in many cases does not represent the real-world complexity of larger catchments.

Australian landscapes have been extensively transformed since the establishment of the first European settlements (Walker et al., 1993; Butzer and Helgren, 2005). Numerous studies have shown that these recent land cover changes (LCC) are also affecting the climate and water cycle in Australia (Gordon et al., 2003) and globally (Gordon et al., 2005; Scanlon et al., 2006; Scanlon et al., 2007). Comparisons between pre-European and modern land cover highlight that historical LCC has been contributing to observed regional climate changes by warming surface temperatures and decreasing rainfall (Timbal and Arblaster, 2006; McAlpine et al., 2007) where up to 50% of these changes can be explained by LCC (Pitman et al., 2004). Convective storms are also sensitive to LCC, with travel velocity and intensity increasing over agricultural and dense urban surfaces respectively (Gero et al., 2006). The replacement of woody vegetation by croplands and grasslands has caused significative changes in evapotranspiration during the past 200 years, decreasing by 10% water vapour flows at continental scale (Gordon et al., 2003). These shifts in water and energy fluxes attributed to LCC can also impact plant physiology and ecohydrological processes of catchments (McVicar et al., 2010).

Long-term experimental catchments studies have shown significant changes in the water and biogeochemical cycles after converting native vegetation to grain cropping and livestock pastures (Cowie et al., 2007; Radford et al., 2007; Thornton et al., 2007). A large deforested catchment in Queensland also increased streamflow by 78% (Siriwardena et al., 2006), whilst smaller increases were observed in other large Queensland catchments in the first years of clearing (Peña-Arancibia et al., 2012). However, further analysis showed an increase in peak flow and reduced low flows, also suggesting changes to catchment streamflow dynamics.

Recent study showed that in the last two decades, the forest cover in the Australian east coast has been increasing rather than decreasing (Liu et al., 2015) as a result of both regrowth and elevated CO_2-vegetation feedbacks (Ukkola et al., 2016). This is in the context of acceleration in native vegetation clearing in Queensland and New South Wales due to wind-back of vegetation management legislation (Evans, 2016). There is also evidence of increasing trends in actual

evapotranspiration for the same period (Zhang et al., 2016b), which can potentially lead to streamflow reductions (Sahin and Hall, 1996; Bruijnzeel, 2004; Brown et al., 2005; Farley et al., 2005; van Dijk and Keenan, 2007).

1.2 Problem statement

The relationship between landscape biophysical properties at the catchment scale (1-1000s km^2) and hydrological processes has been targeted by water related scientists. It is well-recognised that spatial and temporal heterogeneity of climate, soils, topography and vegetation control the water and energy balances differ among catchments with important consequences for runoff generation mechanisms. Two underlying hydrological theories regarding the coevolution of catchment properties and the hydrological behaviour are the Budyko framework (Budyko, 1974) and the Dunne diagram (Dunne, 1983). The Budyko framework describes the catchment long-term water and energy balances through a curvilinear relationship between Evaporative Index (Actual evapotranspiration (AET) / Precipitation (P)) and the Dryness Index (Potential evapotranspiration (PET) / P). The Dunne diagram describes how the runoff generation mechanisms – Horton overland flow, subsurface stormflow and return flow – change with biophysical variables and catchment properties. Despite the popularity of these well-established theories, the convergence between them is not well understood. This is important for Australian systems because developing this understanding will allow us to classify catchments with similar streamflow regimes and enhance the management of water resources.

Studies have investigated the relationship between catchment properties and streamflow characteristics at different scales (from local to global) and regions (all over the world) (Lacey and Grayson, 1998; Mwakalila et al., 2002; Beck et al., 2013a; Zhang et al., 2014; Beck et al., 2015). While there is a certain convergence about the main drivers, a substantial variability with regard to the dominance and contribution of drivers has been reported. Currently, we do not know if the contribution of drivers determining streamflow characteristics varies across different regions and spatial scales.

Previous evidence suggests that Australia is currently experiencing increased climate variability, land cover changes and climate change simultaneously (McAlpine et al., 2009). These processes are collectively driving changes in the ecohydrological feedbacks of catchments, altering their streamflow generation process in sometimes opposing directions (Tomer and Schilling, 2009; Wang and Hejazi, 2011; Jaramillo and Destouni, 2014). Climate change, variability and land use (i.e. deforestation, afforestation and natural regrowth) potentially affect catchment water and energy

balances differently. Understanding how these distinct drivers of change are currently impacting catchment streamflow is crucial to water resource knowledge and management.

The slow contribution component of streamflow (baseflow) ensures stability and persistence of water availability during the dry season (Smakhtin, 2001). However, it is sensitive to reductions in precipitation and increases in evapotranspiration currently occurring as a result of climate change and variability. In addition, recent studies have been reporting an increased photosynthetic activity as a response to changes in atmospheric CO_2 concentration (Ukkola et al., 2016). These changes in vegetation function are potentially impacting baseflow. However, there is little empirical analysis of the relative contribution of these documented changes in baseflow.

1.3 Thesis Aims and Objectives

The overall aim of this thesis is to understand the characteristics and controls of streamflow generation and to investigate how historical climate variability and landscape change influence the streamflow response along a sub-continental gradient of multiple catchments characteristics in eastern Australia. This major aim is partitioned in the following specific objectives.

Objective 1: Investigate how streamflow similarity varies according to the annual water and energy balances and determine to what degree the biophysical drivers of runoff generation explain the observed flow variability among catchments.

Rationale:
The spatial and temporal heterogeneity of climate, soils, topography and vegetation control the water and energy balances among catchments. Two well-known hydrological theories underpinning these processes are the Budyko framework of water and energy balances and the Dunne diagram of runoff generation mechanisms. This study investigates the process overlaps between these approaches and offer insights into the mechanics of catchment co-evolution.

Objective 2: Model streamflow characteristics with catchment biophysical factors across distinct regions and scales and determine changes in importance and contribution of drivers.

Rationale:
Streamflow characteristics are driven by specific flow-generation mechanisms, which are determined by the biophysical properties of catchments. They provide important environmental services for society, regulating water supply and quality, flood mitigation, and the biological diversity of aquatic and riverine ecosystems. This study investigates how the drivers of spatial variability of streamflow characteristics vary at the level of bioregional management (regional ($10^4 km^2$) and sub-continental scales ($10^7 km^2$)) in Australia.

Objective 3: Assess ecohydrologic shifts in the long-term water and energy balances of catchments and separate out the climate- and land cover-induced changes components.

Rationale:
Changing climate and landscape modifications impact the catchment water balance in different ways. While climate change impacts precipitation and potential evapotranspiration, landscape modifications impact actual evapotranspiration. The resultant ecohydrologic shift can therefore be separated according to the observed change trajectory each catchment has experienced. This study builds upon this concept to determine the dominant changing trajectory catchments experienced in the last four decades and its relationship with vegetation gain.

Objective 4: Investigate trends in baseflow and separate the contribution of precipitation, potential evapotranspiration and feedbacks between vegetation and elevated atmospheric CO_2.

Rationale:
Numerous studies indicate that precipitation, temperature and winds have been changing in the last decades in different regions around the world. In Australia, these changes are particularly acute and catchment streamflow has also been experiencing resulting changes. The increasing atmospheric CO_2 concentration raises photosynthesis activity and water consumption ultimately impacting catchment streamflow as well. The slow contribution component of streamflow (baseflow) is sensitive to such changes, but their impacts are yet poorly understood. This study quantifies the relative contribution of precipitation, potential evapotranspiration and atmospheric CO_2 in baseflow trends.

1.4 Thesis approach

This PhD applies an interdisciplinary framework to infer the catchment feedbacks with vegetation and climate and their relationship with landscape properties to generate streamflow. The catchments are the landscape units seen through the lens of hydrology, remote sensing and ecosystem sciences. The thesis integrates these three branches of science to address the aforementioned problems with an ecohydrological perspective (Figure 1.1). This holistic view, which integrates different branches of environmental sciences, is required to understand the relationships between hydrological processes and catchment properties and to distinguish the impacts of drivers of changes taking place in catchment streamflow.

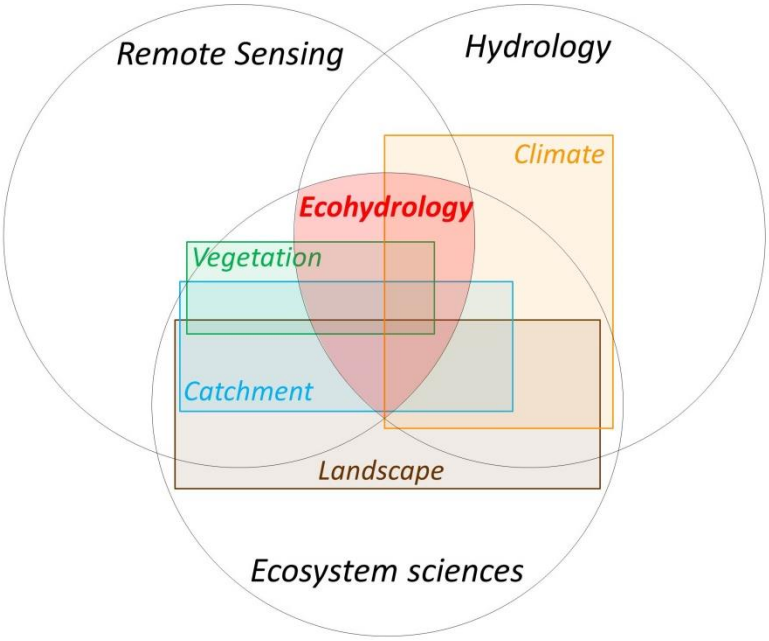

Figure 1.1 Interdisciplinary framework applied to infer the catchment ecohydrological feedbacks among vegetation, climate, landscape properties and ultimately the effect on streamflow generation. The circles represent the branches of science whereas colour rectangles represent the Earth's biophysical compartments. The main niche of knowledge my PhD addresses (i.e. Ecohydrology) is given by the intersection of science areas and biophysical compartments.

The thesis builds upon the spatio-temporal variability of catchment characteristics and hydrological, climatic and vegetation time-series to enhance the ecohydrological knowledge of Australian catchments. Firstly, it explores the spatial variability of a multiple gradient of biophysical characteristics (Figure 1.2) along 355 catchments in the Australian east coast (Table A1.1 in Appendix 1) to infer the dominant ecohydrological feedbacks of catchment functioning. Secondly, the thesis analyses the temporal changes in hydrological, climatic and vegetation time-series to assess the changes in the streamflow generation and determine the causal drivers.

A combination of approaches is applied, spanning areas such catchment hydrology, remote sensing and spatial analysis, and integrating them with modern data analysis techniques. The four objectives differ in terms of studied catchments, period and length of time-series, target hydrological metrics, hydroclimatic and landscape data and approaches used. Table 1.1 presents a comparative methodological overview of the four analytical chapters.

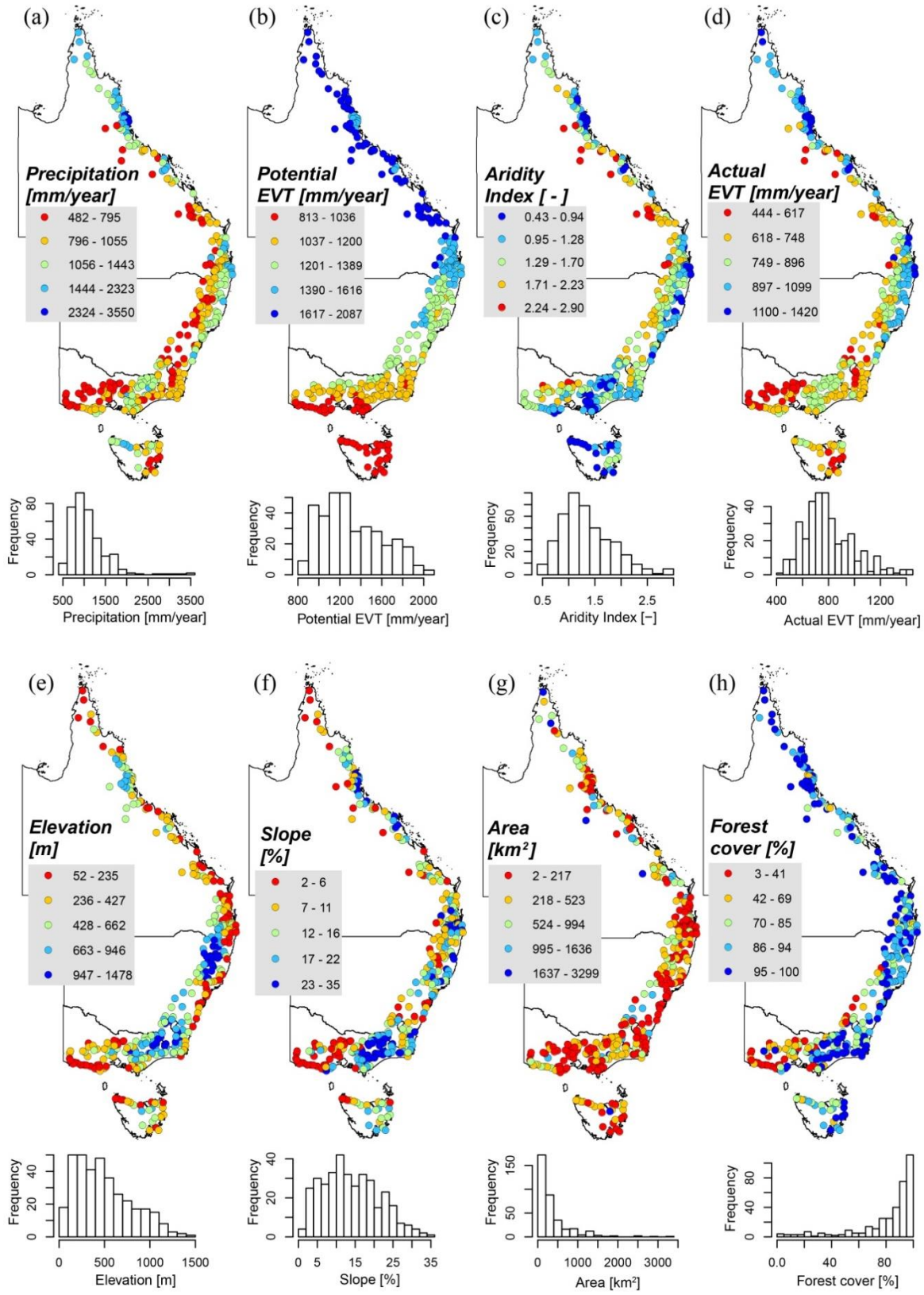

Figure 1.2 Multiple gradients of catchment biophysical characteristics along 355 catchments situated in the Australian east coast explored in this PhD thesis: (a) long-term annual precipitation; (b) long-term annual potential evapotranspiration; (c) long-term Aridity Index; (d) long-term annual actual evapotranspiration; (e) mean elevation; (f) mean slope; (g) catchment area; and (h) forest cover.

Table 1.1 Comparative methodological aspects of this PhD thesis per research objective.

ASPECTS	OBJECTIVE 1	OBJECTIVE 2	OBJECTIVE 3	OBJECTIVE 4
Climate domains	Tropical, Sub-tropical, Temperate and Mediterranean			
Number of catchments	355 unregulated catchments	354 / 40 / 51 / 69 unregulated catchments	193 / 47 unregulated catchments	315 / 44 unregulated catchments
Catchment area range (total area)	0.6 – 3,299.3 km^2 (126,328.7 km^2)	2.4 – 3,299.3 km^2 (126,328.1 km^2) / 16.1 – 2914.5 km^2 (22,880.3 km^2) / 7.1 – 1401.0 km^2 (13,474.2 km^2) / 4.5 – 1635.7 km^2 (19,867.3 km^2)	13.1 – 3,299.3 km^2 (86,480.7 km^2) /	6.8 – 3,299.3 km^2 (119,060 km^2) / 16.1 – 1,557.4 km^2 (18,826.4 km^2)
Period (time series length)	1980 – 2013 (33 years)	1980 – 2013 (33 years)	1971 – 2010 (40 years)	1981 – 2013 (32 years) / 1950 – 2013 (63 years)
Latitude range	-43.08 – -11.36	-43.08 – -11.36 / -20.39 – -11.36 / -29.38 – -24.42 / -38.70 – -33.20	-41.64 – -16.73	-43.08 – -11.36 / -41.46 – -17.34
Aridity range	0.43 – 2.90	0.43 – 2.90 / 0.43 – 2.88 / 0.77 – 2.13 / 0.54 – 2.10	0.48 – 2.86	0.43 – 2.90 / 0.48 – 2.10
Hydroclimatic data [(a)]	*Q, P, PET, AET*	*Q, P, PET, AET, T*	*Q, P, PET, AET*	*Q, P, PET*
Target hydrological metrics [(b)]	*RQP, EQP, BFI, RLD, SFDC, Q10N, Q90N, Rzero, PET/P* and *AET/P*	*RQP, BFI* and *Rzero*	Δ *PET/P,* Δ *AET/P, %*ΔQ, *%*ΔQ^c and *%*ΔQ^h	trends in *Qb* and *Qbr*,
Landscape and anthropogenic data [(c)]	Slope, soil depth, soil saturated hydraulic conductivity, fPAR and woody vegetation cover	Elevation, fPAR, woody vegetation cover, soil moisture, soil depth, saturated hydraulic conductivity, clay content, soil pH, soil plant available water capacity, soil bulk density	Land use, fPAR and biomass	fPAR, atmospheric CO_2 concentrations
Main approaches	Bayesian hierarchical clustering, Principal Components Analysis, Budyko framework and Generalized additive Model for Location, Scale and Shape	Random forests and Generalized additive Model for Location, Scale and Shape	Movement in Budyko space and decomposition of climate- and human-induced changes in Q	Mann-Kendall test, Sen-slope estimator and LOESS regressions

(a) Where: *Q* = streamflow; *P* = precipitation; *PET* = Potential evapotranspiration; *AET* = Actual evapotranspiration; and *T* = temperature.

(b) Where: *RQP* = runoff ratio; *EQP* = *Q* elasticity to *P*; *BFI* = baseflow index; *RLD* = rising limb density; *SFDC* = slope of the flow duration curve; *Q10N* = normalized 10th percentile of *Q*; *Q90N* = normalized 90th percentile of *Q*; *Rzero* = Zero flow ratio; *PET/P* = aridity index; *AET/P* = evaporative index; Δ*PET/P* = change in aridity index; Δ*PET/P* = change in evaporative index; *%*ΔQ = relative change in *Q; %*ΔQ^c = relative climate-induced change in *Q*; *%*ΔQ^h = relative human-induced change in *Q*; *Qb* = baseflow and *Qbr* = baseflow detrended from *P* and *PET*.

(c) Where: fPAR = fraction of photosynthetically active radiation.

1.5 Thesis outline

This PhD thesis covers contemporary themes in ecohydrology knowledge such as: (i) functioning; (ii) drivers; and (iii) changes. It is constructed using the "by publication" approach, where the analytical chapters are developed according to the scientific journal style they aim to be submitted. The Thesis is structured in six chapters. The first and last ones aim to introduce the research problems (Chapter 1) and summarize the overall contribution of knowledge (Chapter 6), while the four intermediate chapters (i.e. the analytical chapters) are prepared as research articles (Chapters 2 to 5). Figure 1.3 summarizes the structure of this PhD thesis in terms of chapter organization and linkages.

The first chapter (this chapter) provides background to the research problem and introduces the research questions and objectives in regard to the relevant gaps in knowledge. The second chapter addresses objective one, which assesses the hydrological similarity and classify streamflow regimes in light of the spectrum of water and energy balances and the drivers of streamflow generation. The third chapter addresses objective two, which analyses the regional variability of drivers of key hydrological characteristics. The fourth and fifth chapters address objectives three and four, analysing the shifts in water and energy balances of catchments induced by climate and landscape changes and trends in baseflow induced by climate and feedbacks between elevated CO_2 concentrations and vegetation functioning. The final chapter integrates the four studies together in terms of their main findings, contribution to scientific knowledge, and recommendations.

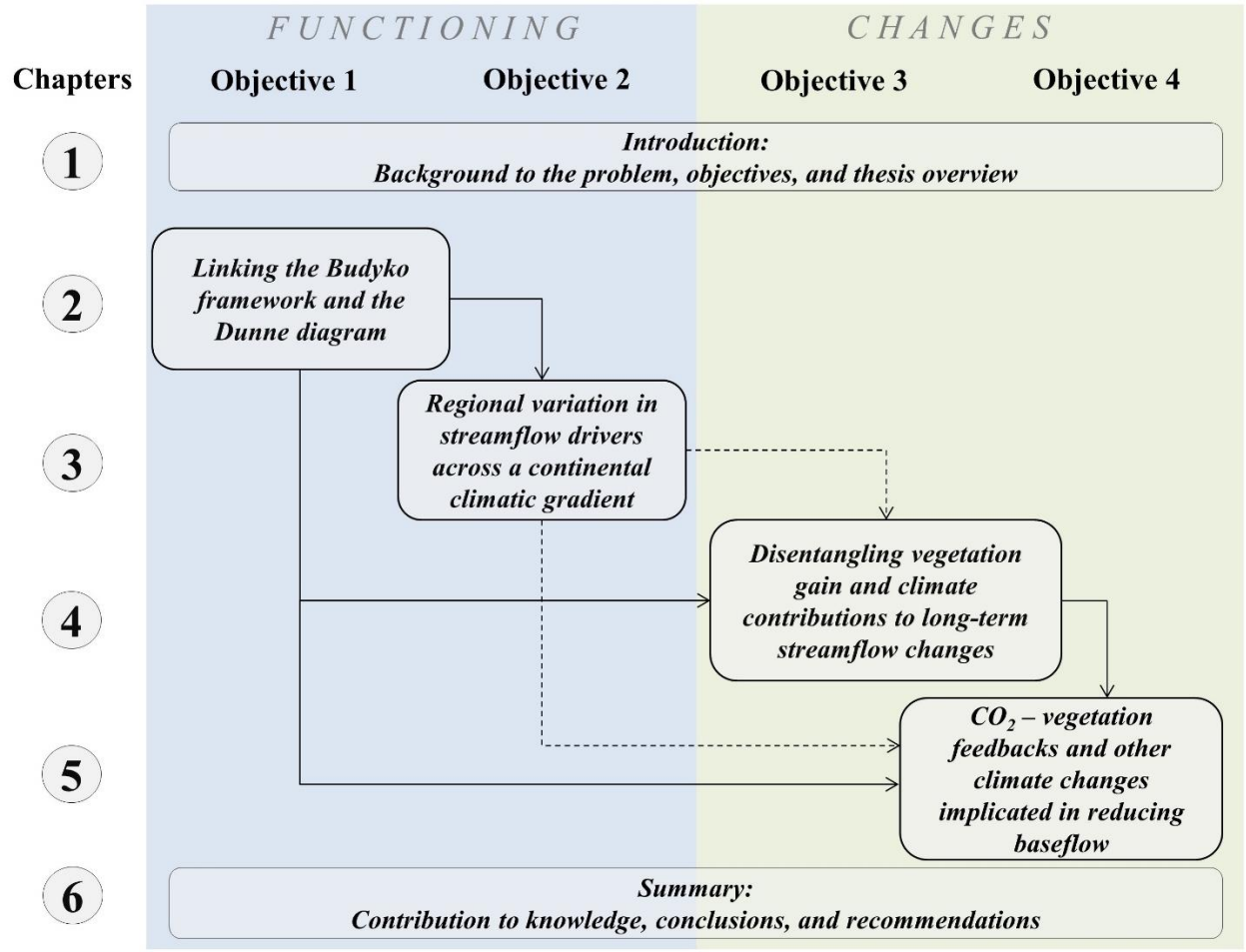

Figure 1.3. Diagram of the thesis structure highlighting the relationship among the four papers and the thesis chapters. Solid arrows denote the linkage is made by dataset and processes interpretation while dashed arrows mean that studies are linked by processes interpretation.

With regards to publications of the chapters / papers, the first paper (chapter 2) entitled "*Linking the Budyko framework and the Dunne diagram"* has been published in Journal of Hydrology.

The second paper (chapter 3) entitled *"Regional variation in streamflow drivers across a continental climatic gradient"* has been published in Ecohydrology.

The third paper (chapter 4) is entitled "*Disentangling vegetation gain and climate contributions to long-term streamflow changes".* The chapter is in the final stages of preparation to be submitted to Environmental Research Letters.

The fourth paper (chapter 5) entitled *"CO_2 – vegetation feedbacks and other climate changes implicated in reducing baseflow"* has been published in Geophysical Research Letters.

CHAPTER 2

LINKING THE BUDYKO FRAMEWORK AND THE DUNNE DIAGRAM

Quality freshwater yield is an ecosystem service provided by pristine catchments. Aire River, Beech Forest, Victoria. Photo by Paul Ryjkoff (source: flickr.com).

This chapter is based on the following manuscript:

Trancoso R., Larsen J.R., McAlpine C., McVicar T.R., Phinn S. (2016). Linking the Budyko framework and the Dunne diagram. *Journal of Hydrology* 535: 581-597.

2.1 Abstract

The spatial and temporal heterogeneity of climate, soils, topography and vegetation control the water and energy balances among catchments. Two well-known hydrological theories underpinning these processes are the Budyko framework and the Dunne diagram. Relating the scaling of water-energy balances (Budyko) and runoff generation mechanisms (Dunne) raises some important catchment comparison questions, namely: (i) how do streamflow characteristics vary according to the annual water and energy balances?; (ii) to what extent do biophysical drivers of runoff explain the observed streamflow variability?; and (iii) are there quantifiable process overlaps between these two approaches, and can they offer insights into the mechanics of catchment co-evolution? This study addresses these questions by analysing daily streamflow and precipitation time series data to quantify hydrological similarity across 355 catchments located along a tropical-temperate climatic gradient in eastern Australia. We used eight hydrological metrics to describe the hydrological response over a 33-year period (1980 to 2013). Hierarchical cluster, ordination analysis, the Budyko framework, and generalised additive models were used to evaluate hydrological similarity, extract the dominant response, and examine how the landscape and climatic characteristics of catchments influence the dominant streamflow response. The catchments were classified into five clusters based on the analysis of their hydrological characteristics and similarity, which vary along the annual water and energy balance gradient in the Budyko framework. Furthermore, we show that the streamflow similarity is explained by six catchment-specific biophysical factors that overlap with those described by the Dunne diagram for runoff generation, which in this case have the following order of relative importance: (i) Dryness Index; (ii) Fraction of Photosynthetically Active Radiation; (iii) Saturated Hydraulic Conductivity; (iv) Soil Depth; (v) Maximum Slope and (vi) Fraction of Woody Vegetation Cover. The research makes an important contribution to understanding of the role of biophysical controls on hydrologic similarity and formal process links between the Budyko Framework and Dunne diagram of runoff mechanisms.

Keywords: Streamflow regime; Catchment classification; Budyko framework; Dunne diagram; Hydrological similarity; Biophysical properties

2.2 Introduction

The hydrological behaviour of catchments reflects the coevolution of climate, soils, topography and vegetation (Dunne, 1983; Winter, 2001; Berry et al., 2006; Sivapalan, 2006; Pelletier et al., 2013). The interplay between these biophysical factors and climate forcings drives the variation in hydrological behaviour that emerges when comparing catchments (Troch et al., 2015). The spatial and temporal heterogeneity of these biophysical factors, and their interactions, make the hydrological processes of each catchment unique (McDonnell et al., 2007), challenging the development of new theories on the overall functioning of hydrological systems (Beven, 2000). Two established approaches in hydrology, (i) the convergence in long-term water and energy balances according to climatic factors - the Budyko framework - and (ii) the runoff generation mechanisms according to catchment properties - the Dunne diagram (Dunne 1983) - together encompass the key drivers of catchment co-evolution. The Budyko framework describes the catchment long-term water and energy balances through a curvilinear relationship between Evaporative Index [Actual evapotranspiration (AET) / Precipitation (P)] and the Dryness Index [Potential evapotranspiration (PET) / P] (Budyko, 1974). The Dunne diagram describes how the runoff generation mechanisms – Horton overland flow, subsurface stormflow and return flow – change with biophysical variables and catchment properties (Dunne, 1983). Figure 2.1 displays these well-known approaches that were developed for distinct insights, despite being both primarily driven by the atmospheric evaporative demand (x-axes in both schemes): being the Dryness Index in the Budyko framework and “Climate” in the Dunne diagram. This is, therefore, the logical starting point to examine the linkages between them. Linking these approaches can provide important mechanistic insights on what controls the similarity, or dissimilarity, in observed hydrological behaviour between catchments, as well as a more powerful conceptual tool to predict hydrological behaviour.

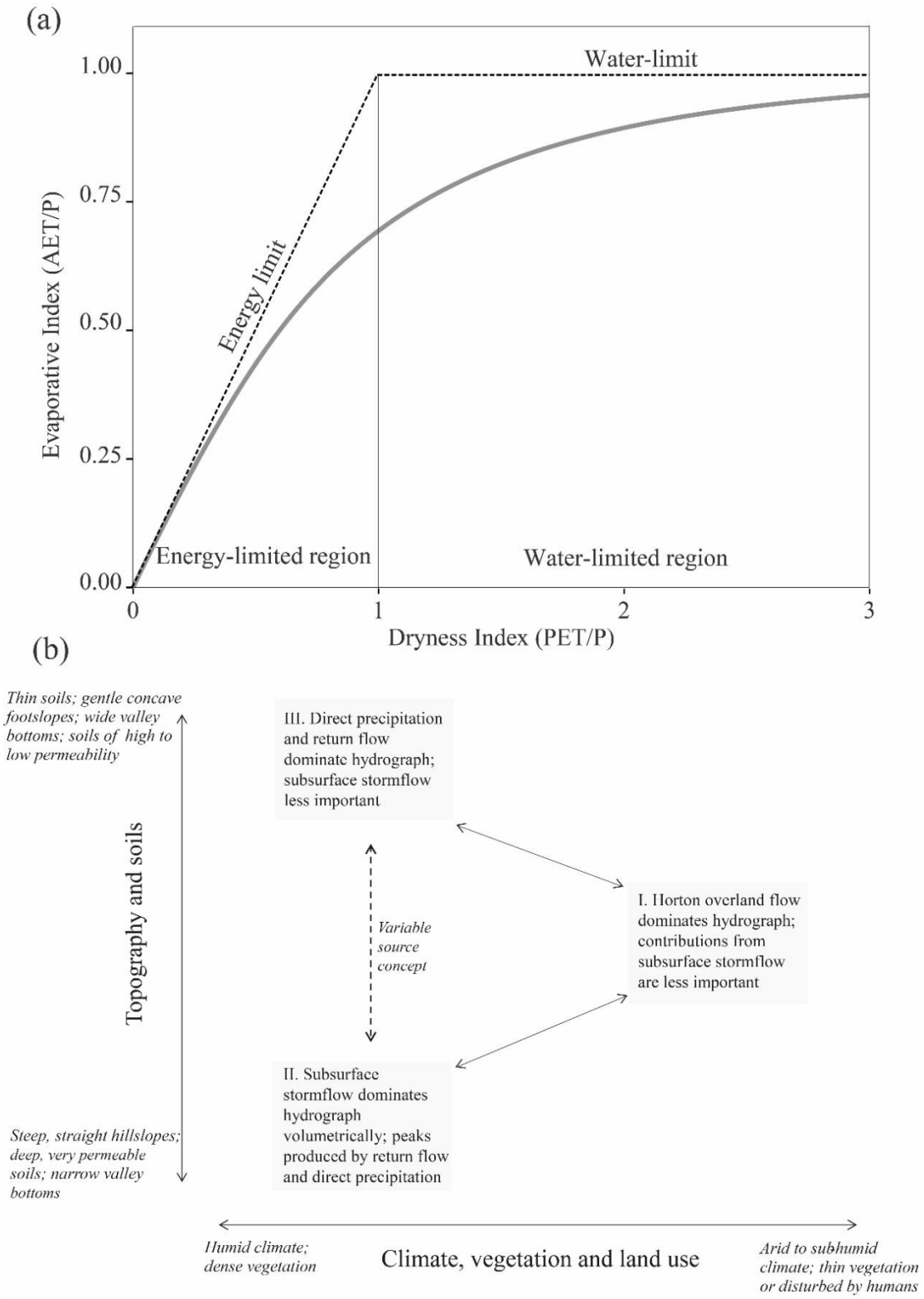

Figure 2.1 Schematic diagrams for each framework. (a) Budyko framework for annual water and energy balances. Catchments in the water-limited region have potential evapotranspiration greater the precipitation (i.e., PET > P), whereas those located in the energy-limited region have the water supply (assumed to be solely precipitation) greater than the evaporative demand (i.e., P > PET). The horizontal dashed line is the water-limit, where 100% of P becomes AET and the diagonal dashed line is the energy-limit, where 100% of PET is converted to AET; and (b) Qualitative diagram for the drivers of runoff mechanisms (adapted from Dunne, 1983) showing that the contribution of the three mechanisms of runoff generation changes according to biophysical controls.

In the absence of a formal theoretical connection between the Budyko framework and the Dunne diagram, it is necessary to explore observed streamflow behaviour from a sufficiently wide variety of catchment settings and ask whether the data supports such links emerging. In this case, a classification scheme is necessary to objectively organize and synthesize large observational datasets according to their biophysical traits and streamflow characteristics (McDonnell and Woods, 2004; Wagener et al., 2007; Sivakumar et al., 2014).

Previous studies have used a variety of classification approaches according to streamflow regimes (Botter et al., 2013), hydro-climatology (Berghuijs et al., 2014a; Carmona et al., 2014), catchment morphology (Beven et al., 1988), hydrological signatures (Sawicz et al., 2011), similarity indexes (Ali et al., 2012), landscape structure and land use (Wardrop et al., 2005) and water resource use and impact (Dynesius and Nilsson, 1994; Destouni et al., 2013; Jaramillo and Destouni, 2014). Olden et al. (2012) separated catchment classification approaches into those based on deductive or inductive reasoning. Deductive approaches are based on environmental datasets describing climate, topography, soils, geology, vegetation and land use to define spatial similarities and differences. Inductive approaches rely on gauged streamflow data using a combination of attributes to characterize streamflow regimes. The main advantage of the inductive approaches is that they are based on real hydrological measurements rather than surrogates. Table 2.1 presents a summary of relevant literature on catchment similarity studies, and specifically those based on flow signatures (inductive approaches) organising catchments according to their hydrological response to boundary conditions across a range of climatic and biophysical gradients. While classification approaches have so far provided promising results, it is widely agreed that a classification framework which coherently organizes catchments according to their structure and function is still required to optimally integrate the inductive and deductive classification strategies (McDonnell and Woods, 2004; Wagener et al., 2007; Sivakumar et al., 2014).

This chapter has three main aims: (a) to investigate how streamflow similarity and characteristics vary according to the annual water and energy balances using the Budyko framework; (b) to determine to what degree biophysical drivers of runoff (Dunne diagram) explain the observed flow variability among catchments; and (c) to evaluate whether links between these two approaches (Budyko framework and Dunne diagram) offer insights into the mechanics of catchment co-evolution. We do this by: (i) using long-term (1980-2013) streamflow and rainfall data for 355 catchments widely distributed over the climatic and topographic gradients of eastern continental margin of Australia to derive eight streamflow signatures, (ii) statistically classifying catchments with regard to their similarities in streamflow behaviour based on these signatures, (iii) evaluating

the consistency of the classification framework along the spectrum of water and energy balances, (iv) extracting the dominant streamflow spectrum from a multi-dimensional ordination space of streamflow signatures, and (v) modelling the extracted dominant streamflow spectrum with biophysical drivers of runoff. Following these steps, the paper approach is designed to test whether the drivers of runoff mechanisms explain the streamflow spectrum captured by the catchment classification, and hence reveal any links between the Budyko framework and the Dunne diagram.

Table 2.1 Summary of relevant literature on catchment similarity studies based on flow signatures in relation to the aims of this study, which are: (a) to investigate how streamflow similarity and characteristics vary according to the annual water and energy balances using the Budyko framework; (b) to determine to what degree biophysical drivers of runoff (Dunne diagram) can explain the observed flow variability within catchments; and (c) to evaluate whether links between the Budyko framework and the Dunne diagram offer insights into the mechanics of catchment co-evolution. We added the current study for completeness. Studies are ordered chronologically then alphabetically. The symbol 'n.r.' means 'not reported'.

Study	Approach to assess catchment similarity	Location/climate/ number of catchments/ size range of catchment/length of time series	Main output with regard to streamflow similarity / (relation with the three component aims of this study)
1. Mosley (1981)	Discriminant and cluster analysis by sum of square of distances	New Zealand/Temperate to polar/174/n.r./n.r.	Four groups of catchments with similar hydrologic regime / (a)
2. Ogunkoya (1988)	Cluster analysis by Euclidian distances	South-western Nigeria/Tropical/15/2-18.8 km^2/ < 1 year	Five regions hydrologically homogeneous / (a)
3. Pegg and Pierce (2002)	Discriminant and cluster analysis by Euclidian distances	Northern United States/ Cold/15/64,070-1,353,000 km^2/30 years	Six hydrologically distinct units exhibiting similar flow characteristics / (a)
4. Snelder et al. (2005)	Ordination and Euclidian distances	New Zealand/Temperate to polar/335/n.r./5-21 years	River Environment Classification (REC) groups catchments in 14 similar regions more consistent than other schemes / (a, b)
5. Leigh and Sheldon (2008)	Cluster analysis by Euclidian distances	Gulf of Carpentaria, Australia/Tropical/15/1077-17,382 km^2/20 years	Two groups related to flow magnitude and stability and three groups related to seasonality / (a)
6. Moliere et al. (2009)	Hierarchical agglomerative cluster analysis by Euclidian distances	Northern Australia/ Dry and tropical/28/318-107,150 km^2 /20 years	Catchments divided in four groups: Perennial; Seasonal; Dry seasonal and Seasonal-intermittent / (a, b)
7. Kennard et al. (2010)	Bayesian mixture modelling	Australian continent/ Dry, tropical, and temperate/830/6-222,674 km^2 /15-35 years	12 classes of flow regimes differing in seasonality, flow permanence, magnitude and frequency / (a, b)
8. Ley et al. (2011)	Cluster analysis by Self-Organizing Maps	Germany/Temperate, cold/53/9-1469 km^2/25 years	Five clusters of similarly behaving catchments with 67% of correspondence with clusters of physical characteristics / (a)
9. Patil and Stieglitz (2011)	Variability of flow duration curves	Northeast United States/Temperate/25/65-4163 km^2/19 years	Spatial variability in streamflow is determined by the high evaporative demand during the warm period / (a, b)
10. Sawicz et al. (2011)	Bayesian clustering scheme	Eastern half of United States/ Temperate and cold /280/67-10,096 km^2/10 years	Catchments separated into 9 homogeneous classes interpreted in light of climatic and landscape attributes / (a, b)
11. Ali et al. (2012)	Affinity propagation for clustering	Scotland/Temperate/36/0.44-1712.1 km^2/n.r.	Distinct combination of catchment properties are used to form five to nine groups with low agreement between outcomes / (a)

12. Coopersmith et al. (2012)	Decision trees with Iterative Dichotomiser 3 algorithm	Continental United States/Dry, temperate, and cold /428/ 500–10,000 km^2/53 years	Catchments are grouped in five regime behaviours primarily controlled by climate seasonality / (a, b)
13. Toth (2013)	Self-Organizing Maps by neural network	North-central Italy/Temperate/44/18-1303 km^2/ 3.5-10 years	Groups of three and six catchments are distinguished with an overall consistency with location, altitude and precipitation / (a, b)
14. Berghuijs et al. (2014a)	Manual grouping by trial and error based on visual observation	Continental United States/Dry, temperate, and cold /321/67-10,329 km^2/10 years	10 clusters with similar seasonal water balance behaviour consistent with flow signatures and Budyko framework / (a)
15. Sawicz et al. (2014)	Bayesian mixture-clustering algorithm and decision tree	Continental United States/Dry, temperate, and cold /314/67-10,096 km^2/38-40 years	12 clusters of catchments are formed for a baseline scenario and the clusters composition change on further decades / (a)
16. This study	Model-based hierarchical clustering	East coast of Australia/Tropical to temperate/355/0.6-3,299 km^2/23-33 years	Five clusters of similar hydrological behaviour consistent with the water and energy balance spectrum and explained by drivers of runoff mechanisms / (a, b, c)

2.3 Study Area and Materials

2.3.1 Study catchments

The study area covers the entire eastern margin of the Australian continent, covering an area > 10^6 km^2 that extends 4,000 km north-south and up to 200 km inland. We selected 355 catchments ranging in size from 0.6 to 3,299 km^2, with 79% being smaller than 500 km^2 (Figure 2.2a and 2.2b). All catchments were unregulated. To avoid nested catchments, we chose the most upstream gauging station per stream. The total surface area covered by all catchments was 126,398 km^2. For the 355 catchments, the 1980-2013 catchment-average annual average precipitation (P) ranged from less than 500 mm/year to more than 3,500 mm/year, with 88% within the 500-1,500 mm/year range (Figure 2.2c). The 1980-2013 Priestley-Taylor potential evapotranspiration (PET) ranges from 836 to 2,183 mm/year, with an average of 1,316 mm/year (Figure 2.2d). The major physiographic feature in mainland eastern Australia is the Great Dividing Range (GDR) with strong elevation gradients and rugged terrains (Figure 2.2e). Twenty-three per cent of the catchments drain west (to the interior of the continent, with a long flow path to the ocean, if at all) and 77% drain east, usually as smaller coastal systems with far shorter flow paths to the ocean. More than 70% of the 355 catchments have at least 80% of their surface covered by woody vegetation (Figure 2.2f), thus minimising the impact of land-use change on streamflow.

The north-south hydro-climatological gradients are driven by distinct climate regimes (equatorial, tropical, sub-tropical and temperate) which have a strong influence on the precipitation delivery and ultimately streamflow (Risbey et al., 2009). A strong orographic effect generally causes lower precipitation west of the GDR, as well as minor snow packs in the Alpine regions (Reinfelds et al., 2014). Seasonality (i.e., in-phase and out-of-phase local maxima of P and PET) is also a strong feature along the climatic gradient affecting the water and energy balances (Potter et al., 2005; Jothityangkoon and Sivapalan, 2009; Potter and Zhang, 2009).

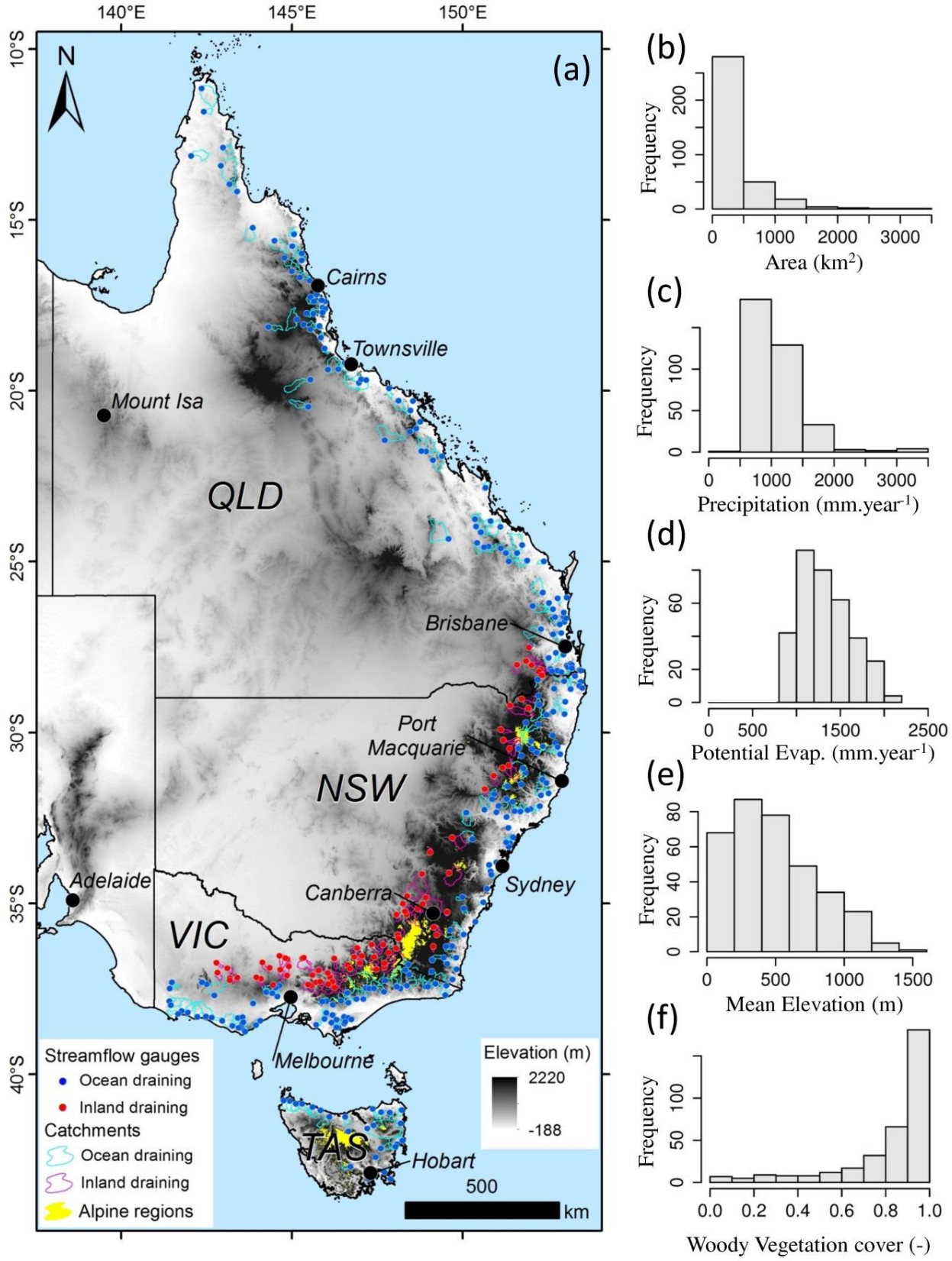

Figure 2.2 Distribution and characteristics of the study catchments. Part (a) shows the location of the 355 catchments in eastern Australia extending over four States: Queensland – QLD, New South Wales – NSW, Victoria – VIC and Tasmania – TAS. Frequency distributions of: (b) drainage area, (c) annual precipitation, (d) annual potential evapotranspiration, (e) mean elevation, and (f) woody vegetation cover are also provided.

2.3.2 Hydrological data

We used daily streamflow (Q) time series data from 1980 to 2013 (12,045 days over these 33 years) measured in m^3/s. The data were obtained from the water monitoring agencies of each State. We only used gauges with at least 70% valid Q data within these 33 years. We used gridded daily precipitation time series (~ 5 km pixel-size) developed by Jones et al. (2009) for the same period where Q data was available.

2.3.3 Ancillary data

A hydrologically-conditioned and drainage-enforced DEM with a 1 arc-second (~ 30 m) pixel-size derived from SRTM data produced by Geoscience Australia was used to map catchment boundaries (Wilson et al., 2011). The geographic coordinates of the streamflow stations were used as the catchment outlets.

In order to allocate catchments in the context of the Budyko framework and to model the controls of the long-term dominant streamflow behaviour we used monthly gridded dataset of Priestley-Taylor potential evapotranspiration with ~ 5 km pixel size (Donohue et al., 2010a), the fraction of photosynthetically active radiation absorbed by vegetation (fPAR) with spatial resolution of 1 km (Donohue et al., 2008) , digital maps of saturated hydraulic conductivity and soil depth (McKenzie et al., 2000) and vegetation classification with 250 m pixel-size (Lymburner et al., 2011). Catchment boundaries were used to extract the average daily precipitation time-series as well as the aforementioned ancillary data.

2.4 Methods

2.4.1 Flow signatures

Metrics which characterise long-term behaviour serve as flow signatures that integrate the influence of all the streamflow drivers (Shamir et al., 2005). While no single descriptor is able to capture the overall complexity of the hydrological behaviour of a catchment, the analysis of a set of complementary streamflow signatures provides insights into the overall catchment hydrological behaviour (Olden and Poff, 2003; Sanborn and Bledsoe, 2006; Kennard et al., 2010; Sawicz et al., 2011). This signature approach has been widely used to evaluate, compare and model the hydrological behaviour of catchments worldwide (Casper et al., 2012; Sawicz et al., 2014; Zhang et al., 2014). As a result, hundreds of hydrological signatures are currently available to characterize streamflow regimes (Yadav et al., 2007). However, signature metrics are often highly correlated

and therefore the choice of which signature to use risks introducing redundancy to the analysis, thereby potentially leading to data to be overfit (Olden and Poff, 2003).

The streamflow characteristics we considered pivotal to describe the hydrological response to boundary conditions of Australian catchments are partitioning of water release, baseflow contribution, flow sensitivity to rainfall, flow variability, degree of intermittency, and intensity of low and high flows. We selected eight streamflow signatures to characterize the catchment streamflow behaviour (Table 2.2). Six signatures were derived from Q records alone while the remaining two require P data in their calculation. The first four signatures were calculated using separate expressions, while the last four were based on the analysis of the Flow Duration Curve (FDC). Although the FDC-based streamflow signatures are long-term averages, they also reflect the seasonal variability along the climatic gradient.

Table 2.2 Summary of flow signatures used to represent the dominant streamflow characteristics and hydrological response of the 355 catchments (see Supplementary Information for detailed descriptions).

Flow signature	Acronym	Description	Temporal scale
Long-term runoff ratio	RQP	Cumulative faction of P released by Q.	33 years
Streamflow elasticity	EQP	Percentage of change in Q expected for a 1% change in P.	Annual
Rising Limb Density	RLD	Denotes the shape and smoothness of a hydrograph.	Daily
Baseflow Index	BFI	Fraction of Q resulting from slower water release components	Daily
Slope of the Flow Duration Curve	SFDC	Measure of flow variability based on the shape of the flow duration curve.	Daily
Normalized 10^{th} percentile streamflow	Q10N	Measure of the intensity and variability of high flows.	Daily
Normalized 90^{th} percentile streamflow	Q90N	Measure intensity and variability of low flows.	Daily
Frequency of no flow	FNF	Determines the fraction of time a stream is ephemeral	Daily

2.4.2 Data analysis

Grouping catchments with similar hydrological behaviour

Cluster analysis is the automated identification of groups with similar observations that are significantly different from other likewise similar groups (Fraley and Raftery, 2002). We used Model-based Hierarchical Clustering (MHC) with an Expectation-Maximization (EM) algorithm to divide catchments into clusters with similar hydrological behaviour based on the eight streamflow signatures. Behavioural hydrological similarity can be derived from signatures of catchments functional response and serve as the basis for model parameter transferability (Oudin et al., 2010). The main advantage of this approach, compared to the distance-based agglomerative clustering approach, is that MHC algorithm automatically infers the number of clusters and uses a Bayesian approach to model selection (Heller and Ghahramani, 2005). Following Burnham and Anderson (2002), we assessed the performance of 10 models with up to 20 clusters using the Bayesian Information Criterion (BIC) as implemented by Fraley and Raftery (2002). We also modelled a classification tree based on the MHC results to determine thresholds of flow signatures on clusters and allow further inclusions of other catchments into the clusters with similar hydrological behaviour. Following Jaramillo and Destouni (2015) we used the Wilcoxon rank test to determine whether the catchment clusters are significantly different in terms of flow signatures, Dryness Index and Evaporative Index.

Catchments with distinct flow characteristics in the context of the Budyko framework

The Budyko framework partitions catchment P (assumed to be the sole source of water) into Q and AET. It relates the catchment water and energy balances through AET, PET and P derived from observational data (Budyko, 1974). It has been widely used to study the long-term catchment water balance and to estimate the Evaporative Index as a function of the Dryness Index (Arora, 2002; Donohue et al., 2007; Zhang et al., 2008a; Gentine et al., 2012; van der Velde et al., 2014). Several equations are used to capture this relationship (Fu, 1981; Zhang et al., 2001; Zhang et al., 2008a; Gerrits et al., 2009; Donohue et al., 2012). Here, we use the original Budyko (1974) formula:

$$1 - RQP = \sqrt{\frac{\overline{PET}}{\bar{P}} tanh\left(\frac{\bar{P}}{\overline{PET}}\right)\left(1 - exp\left(-\frac{\overline{PET}}{\bar{P}}\right)\right)}; \quad (1)$$

where $\bar{Q}$, $\bar{P}$ and $\overline{PET}$ are long-term catchment-mean values for streamflow, precipitation and potential evaporation, where the Evaporative Index term assumes $\bar{P} = \bar{Q} + \overline{AET}$ over the long-term and storage changes (*dS*) are negligible.

In order to assess the displacement of catchment clusters across the Budyko framework, we also used the Choudhury (1999) formulation which uses a free parameter '*n*' to better fit observed data within the generalized Budyko framework to different catchment characteristics. This is given as:

$$1 - RQP = \frac{\bar{P}\,\overline{PET}}{(\bar{P}^n + \overline{PET}^n)^{1/n}}; \quad (2)$$

where *n* is a dimensionless parameter that modifies the partitioning of $\bar{P}$ between $\overline{AET}$ and $\bar{Q}$, encoding all factors driving this partitioning under a steady-state climate assumed by using long-term averages (Roderick and Farquhar, 2011). The *n*-parameter was optimised within each catchment cluster by minimising the least squares differences between observed Q and Q predicted by Equation (2).

We used the Mean Absolute Deviation (MAD) of the catchment data from the actual evaporative index positioned along the Budyko (1974) and Choudhury (1999) curves to evaluate whether the data points fell predominantly above or below the curves. We also used the Sum Squared Error (SSE) of the actual evaporative index as an estimate of scatter about the curves. Finally, we quantified the fraction of catchments within a given cluster that were above or below *PET*/*P* = 1 (i.e., water- or energy-limited).

Maximum variability of flow signatures as a proxy of the dominant streamflow behavior

Principal Components Analysis (PCA) has been used to explore continuous patterns in hydrological variability among catchments (Poff et al., 2006). Ordination techniques such as PCA have been widely used to progress beyond the correlation among multiple hydrologic signatures (Olden and Poff, 2003; Snelder et al., 2005; Poff et al., 2006; Sanborn and Bledsoe, 2006; He et al., 2011; Olden et al., 2012). We used PCA to extract the maximum unidimensional variance within a multi-dimensional space of eight correlated flow signatures. This allows the identification of patterns in the data based on their similarities and differences. We evaluated whether the first principal component (PC1) scores sufficiently capture the variance extracted from the eight streamflow signatures and can therefore be used as a proxy of the dominant streamflow behaviour.

Modelling flow variability with the drivers of runoff mechanism from Dunne's diagram

We used Generalized Additive Models for Location, Scale and Shape (GAMLSS) (Stasinopoulos and Rigby, 2007) to test whether the maximum variance among the eight flow signatures (PC1) is controlled by the drivers of flow characteristics as described in the Dunne diagram of runoff mechanisms (Dunne, 1983). We selected six variables to quantitatively represent the variables

described in the Dunne diagram (see Figure 2.1) and test whether this conceptual model explains the observed variability of flow signatures among catchments. The x-axis of the Dunne diagram is represented by a gradient of aridity, vegetation structure and land use. We use the Dryness index, fPAR and the catchment fraction of woody vegetation cover, respectively, to account for each of them. The y-axis of Dunne diagram is represented by a gradient of soil thickness, slope characteristics and soil permeability. Therefore, we used soil depth, maximum catchment slope and saturated hydraulic conductivity as proxies for Dunne's y-axis. We split the dataset, using random sampling with 90% for training and 10% for validation. We evaluated several possible models resultant from the interactions of the six explanatory variables to select the one with smallest Akaike Information Criterion (AIC) (Akaike, 1974) and then assess its fit using Nagelkerke R-squared (Nagelkerke, 1991). We used random forests with 5000 trees in order to assess the importance of each predictor on the response variable (Breiman, 2001). The importance is given by the relative increment on mean square error when the predictor is removed.

2.5 Results

2.5.1 Correlation, spatial distribution and variability of streamflow signatures

Catchments exhibited a spatial patterning in the similarities and differences both within and among the eight streamflow signatures. There was a general congruency in the spatial distribution of the signatures, suggesting it is useful to pursue comparative hydrology based on their classification. Flow signatures were chosen to represent different hydrological characteristics of flow response, but are often dependent on the same dominant hydrological processes. For example, higher groundwater and/or snowmelt availability leads to an increase in the baseflow contribution (BFI), which stabilises the flow response and converge high and low flows (Q10N and Q90N) toward the mean flow ensuring the perennial condition (FNF). In this sense, this dominant hydrological mechanism can control four flow signatures: BFI, Q10N, Q90N, and FNF. These signatures have correlation coefficient values (both Spearman's Rho and Pearson's) higher than 0.7 (Table 2.3), although they represent distinct characteristics of flow response. RQP and EQP are also highly negatively correlated because they are both rainfall dependent and RQP is a term in the equation for EQP. Both their correlation coefficients values were higher than 0.6, mainly because drier catchments with low RQP values are often more sensitive to rainfall changes, which lead to a higher EQP.

Table 2.3 Pairwise correlation of the flow signatures used in this study. Values above the framed and bold cells are Spearman's Rho rank non-parametric correlation coefficients, while values below the framed cells are linear Pearson's correlation coefficients.

		Spearman's Rho correlation coefficients							
		RQP	EQP	RLD	BFI	SFDC	Q10N	Q90N	FNF
Pearson cor. coefficients	RQP	**1**	-0.70	0.23	0.39	-0.01	-0.35	0.48	-0.50
	EQP	-0.61	**1**	-0.32	-0.45	0.19	0.44	-0.49	0.46
	RLD	0.20	-0.19	**1**	0.12	-0.30	0.18	0.05	-0.06
	BFI	0.36	-0.46	0.06	**1**	-0.15	-0.84	0.77	-0.78
	SFDC	-0.01	0.08	-0.23	-0.09	**1**	-0.19	-0.09	0.12
	Q10N	-0.33	0.44	-0.10	-0.84	0.12	**1**	-0.79	0.74
	Q90N	0.40	-0.47	0.20	0.79	0.27	-0.73	**1**	-0.91
	FNF	-0.34	0.37	0.19	-0.59	-0.22	0.54	-0.43	**1**

The driest catchments with RQP < 0.15 were generally those draining to the west of the GDR and south-western VIC. Most catchments with RQP values > 0.45 were located in northern QLD with a smaller number in the central and north coast of NSW and south-east QLD (Figure 2.3a). In general, higher EQP values (> 3.5) were observed in the drier regions (PET/P > 2) whereas catchments with lower EQP values (< 1.5) were concentrated in the wetter regions (PET/P < 1) and/or those receiving snowfall in the Alpine regions (Figure 2.3b). These findings are in accordance with Arora (2002). Catchments with the highest streamflow vulnerability to long-term changes in precipitation are located in the inland draining catchments and southwest VIC. The change in streamflow was at least 4.5 times greater than the observed change in precipitation for catchments located in the drier environments. Catchments with lower sensitivity to precipitation variability were located in northern QLD, the Victorian Alps and the north coast of Tasmania (TAS) (Figure 2.3b).

Catchments with higher RLD values (> 0.55) have a more rapid response to precipitation events, and were mostly located in the mountainous regions of the Australian Alps and in the central coast of NSW. Lower RLD values (< 0.4) occurred mostly within the western draining catchments of the GDR, and in shorter flow path coastal catchments with uniform precipitation supply in western Victoria and northern TAS (Figure 2.3c). Higher BFI values (> 0.6) occurred in catchments located in the wetter regions of north QLD, the Victorian Alps, and the north coast of TAS (Figure 2.3d). It is important to highlight that despite the similarity in BFI values, the flow paths (overland-flow, return-flow and subsurface-flow) incorporated into this slow flow component are likely to vary markedly among catchments. For example, it is likely that for far north QLD catchments have groundwater inputs dominating their BFI, while snowmelt will make a major contribution to BFI

for a small number of catchments that develop a seasonal snowpack in Australia's alpine areas (Figure 2). In contrast, the lowest BFI values (> 0.15) generally coincide with ephemeral catchments.

Ephemeral streams for at least one-third of the year (SFDC = 0) are mostly concentrated in western draining catchments of the GDR in QLD and in western VIC where the catchments drain into the Murray-Darling Basin. Catchments with a low to intermediate SFDC values (< 6.0) were distributed across the lowland east coast catchments (Figure 2.3e). In contrast, the 135 catchments with steeper flow duration curves (> 6.0) were mostly associated with lower annual precipitation (P = 885±259 mm/year) and higher elevations (E = 395±263 m). This notation used henceforward denotes the mean ± one standard deviation, comprising the 66% central of the referred data distribution.

Higher Q10N values (> 20) were found mainly in catchments from south-east TAS, western VIC and those draining west (inland) of the GDR. A noticeable cluster of catchments with a more equal distribution of high streamflow magnitudes (i.e., Q10N values < 10.0) occurred in the Victorian Alps catchments receiving snowfall and in the north coast of TAS. Another smaller group emerged in the wetter (PET/P < 1.2) coastal regions of QLD and NSW (Figure 3f). A major cluster with catchments ephemeral for at least 10% of the year (Q90N = 0) occurred in the west of VIC, whereas small clusters were scattered along eastern Australian coast. Catchments with less variability in magnitude of low flows, with at least 15% of low flows greater than the average flows (Q90N > 0.15), were concentrated in northern TAS, eastern and the west coast of VIC and far north QLD (Figure 2.3g).

The perennial catchments (FNF < 0.05) comprised 60.2% of the total number of catchments, with the remainder being ephemeral (FNF > 0.05). The truly perennial catchments, with water flowing permanently comprised only 27.9% of the total number of catchments. Perennial catchments were predominantly located in the wetter regions (PET/P < 1.2), while catchments which were ephemeral for > 33% of the time occurred almost exclusively within arid environments (PET/P > 2) (Figure 2.3h).

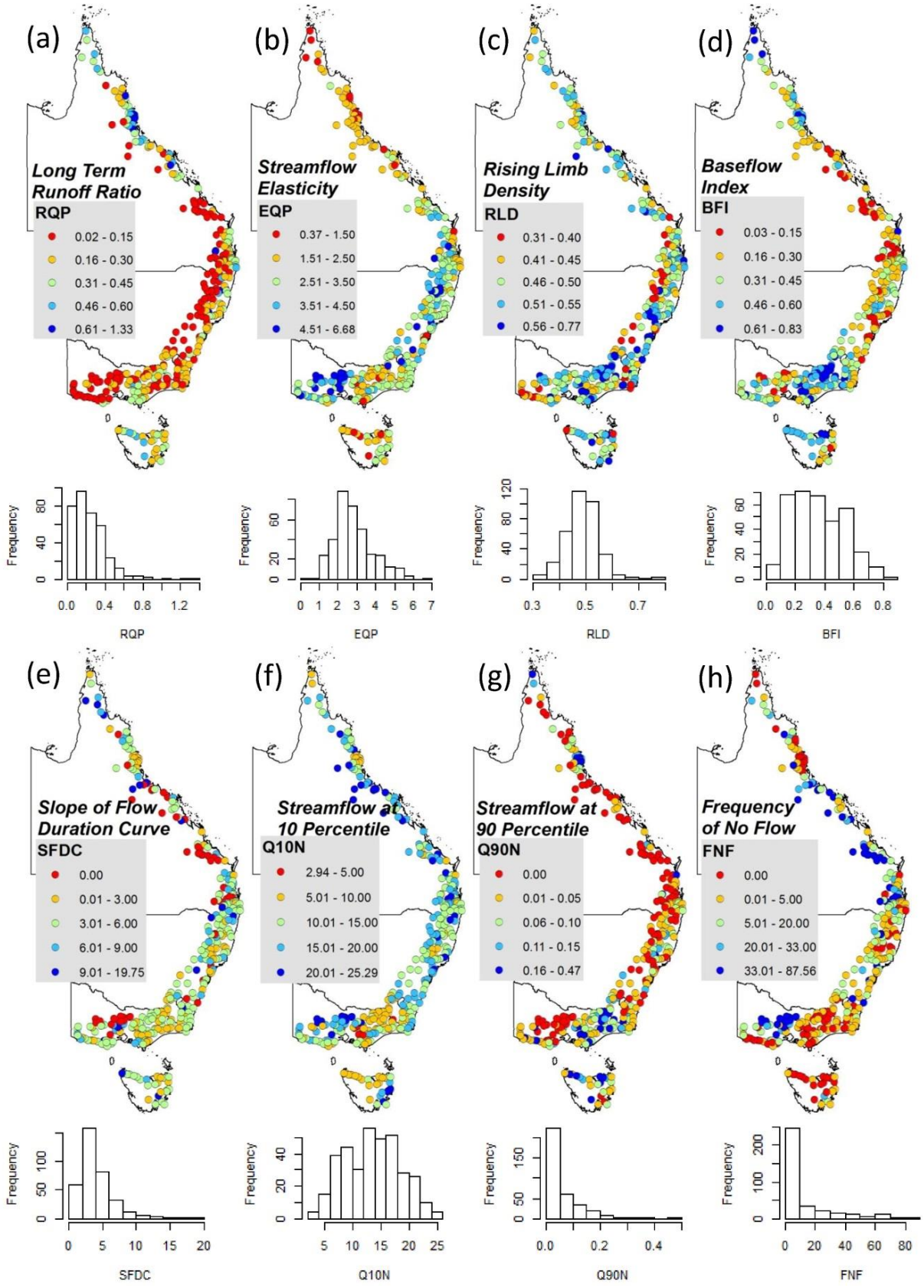

Figure 2.3 Spatial distribution and frequency of the eight flow signatures including: (a) Long-term runoff ratio (RQP), (b) Streamflow elasticity (EQP), (c) Rising limb density (RLB), (d) Baseflow index (BFI), (e) Slope of the flow duration curve (FDC), (f) Streamflow at 10 percentile (Q10N), (g) Streamflow at 90 percentile (Q90N), and (h) Frequency of no flow days (FNF).

2.5.2 Hydrological similarity of catchments

Using the EM algorithm, we assessed 10 statistical models with up to 20 components (or clusters). The five component ellipsoidal Gaussian finite mixture model with equal shape had maximum BIC (5752.7) and was selected as the optimal model for the hierarchical clustering of catchments based on the streamflow signatures. Figure A2.1 (Appendix 2) displays the variation in BIC across the different models and different number of components.

The five catchments clusters display distinct hydrological patterns according to the eight flow signatures (Figure 2.4). Some signatures such as RQP, BFI, SFDC, and Q10N showed consistent trends among clusters and were influential in separating and aggregating catchments. Other signatures, such as EQP, RLD, Q90N, and FNF, only showed major differences between several clusters. For instance, EQP and Q90N distinguished clusters D and E, RLD separated clusters A and E, and FNF was the primary flow signature separating clusters A and B.

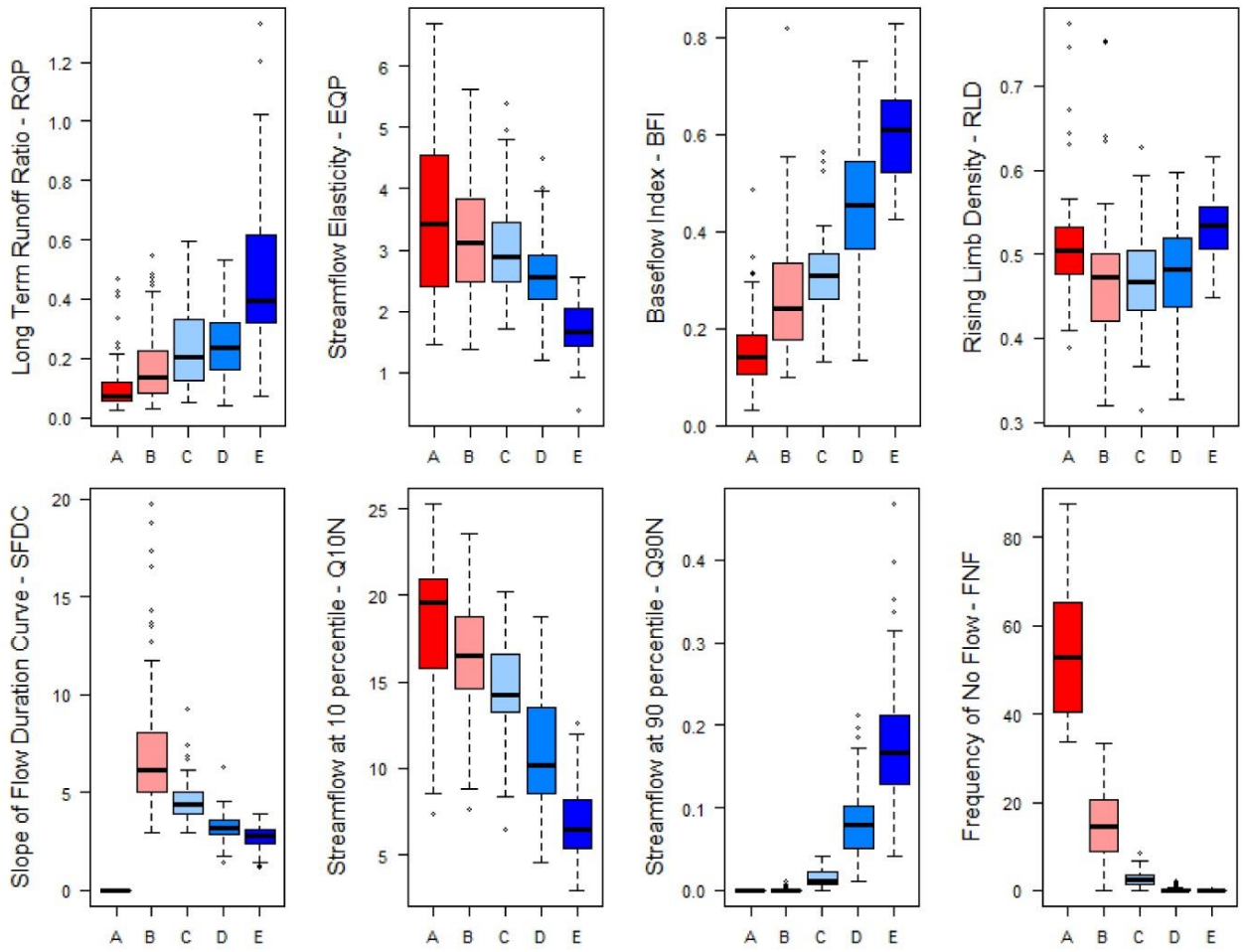

Figure 2.4 Box-Whisker plots of flow signatures by catchment clusters derived from the ellipsoidal Gaussian finite mixture model. The boxes are bound by the 25th and 75th percentiles of the datasets, while the heavy mid-line displays the median value. The upper and lower 'whiskers' represented by the dashed lines are the upper quartile plus 1.5 times the interquartile distance (IQD) and the lower quartile minus 1.5 times the IQD, where IQD refers to the inter-quartile distance. Dots are data points out of this range. See Table 2 for a brief definition of flow signatures and Supplementary Information for detailed description. Table A4.1 shows the statistical significance of an unpaired Wilcoxon rank sum test on the differences between the distributions of flow signatures by catchment clusters.

2.5.3 Cluster shifts according to long-term water and energy balances in the Budyko framework

The Budyko framework was used to verify shifts in the long-term water and energy balances that may exist among the catchment clusters. We find a clear gradation from clusters A to E ranging from catchments with highly seasonally variable and ephemeral flows, erratic low and high flows. There was a high sensitivity to precipitation changes (cluster A) in water-limited environments, to catchments with highly stable and perennial flows, low variability in both low and high flows, and low sensitivity to changes in precipitation (cluster E) in environments that become energy-limited (Figure 2.5).

Interestingly, there is no obvious regional dominance in the distribution of clusters along the eastern margin of Australia, although some broader spatial patterns exist. These distinctions include catchments within clusters A and B, which occur predominantly in the drier regions (PET/P > 2) draining to the west of the GDR (including inland-flowing streams of western VIC), and southern TAS. Cluster C occurs predominantly along transitional zones between dry and wet environments (PET/P = 1.34 ± 0.37). Clusters D and E are mostly located in the areas with higher annual precipitation that are also more evenly distributed throughout the year (which tend to be east draining coastal catchments), and in catchments that receive snowmelt in the Australian Alps.

With respect to the distribution of clusters around the Budyko curve (Figure 5 II), they are clearly moving along a gradient from strongly water-limited (PET/P = 2.03 ± 0.51) (cluster A) to mostly energy-limited catchments (PET/P = 0.82 ± 0.23) (cluster E) (Figure 2.5). It is interesting that this gradient holds despite the large spatial range of each cluster, suggesting the large seasonal differences in the distribution of P and PET do not necessarily lead to unique streamflow behaviours. Rather, the annual values of P, PET and AET can adequately capture the main drivers of the water and energy balances.

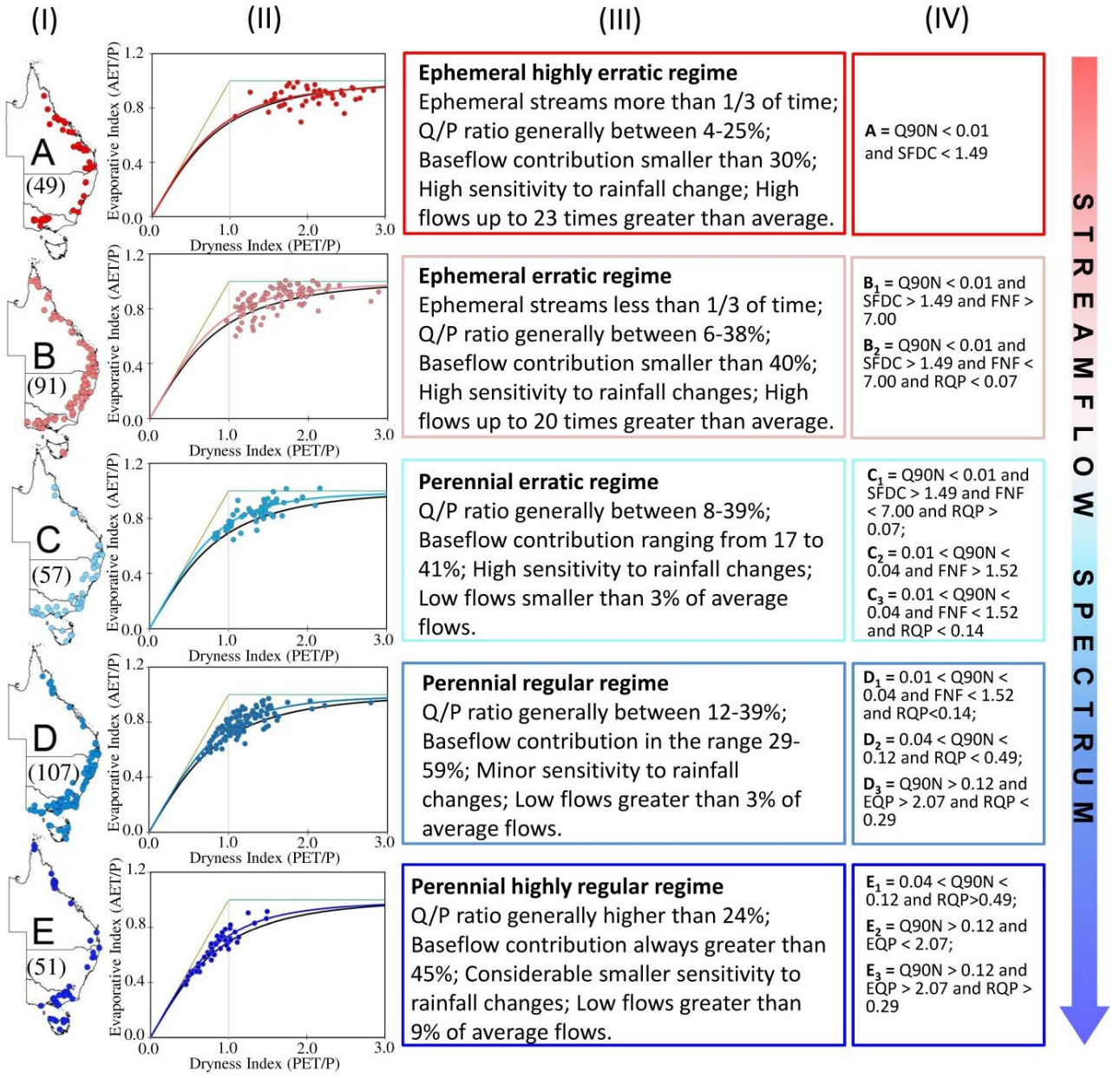

Figure 2.5 Spatial distribution, long-term annual water and energy balances and flow characteristics of catchment clusters. Column (I) shows the spatial distribution of catchments by cluster. The numbers in parenthesis under each of the cluster letters are the number of catchments in this cluster. Column (II) show the original Budyko (1974) curve (black) and Choudhury (1999) parametrised curves (coloured). See Table 2.2 for details regarding curves. Brown, green and grey lines, respectively, represent energy-limit, water-limit and the threshold between water- and energy-limited environments. Column (III) documents the main hydrological characteristics of the catchment clusters along the streamflow spectrum. Thresholds were determined using 10th and 90th percentiles of flow signatures by catchment cluster. Column (IV) reports the flow signatures threshold for allocating catchments to clusters with similar streamflow behaviour. Values are determined using a classification tree where the subgroups are distinct tree branches (see Figure A2.2 in Appendix 2 for details). Table A2.1 (Appendix 2) shows the statistical significance of an unpaired Wilcoxon rank sum test on the differences between the distributions of flow signatures by catchment clusters.

In cluster A catchments (N = 49) the Budyko curve is slightly overestimating AET losses from these catchments, and a greater partitioning of P to Q is required from this equation as streamflow intermittency and PET/P both increase. This is also reflected in the value of *n*, which is the lowest of all the clusters, meaning that as a fraction of P, more Q is generated relative to AET compared to catchments in other clusters. The prolonged ephemeral conditions characteristic of this cluster precludes their occurrence in temperate TAS. Catchments from cluster B (N = 91) are also almost entirely (except for one) water-limited. The increase in streamflow intermittency with increasing PET/P is a consistent pattern, highlighting the rapid depletion of catchment storage as atmospheric demand (PET) increases.

Although the catchments comprising clusters A and B are almost entirely water-limited, an interesting transition occurs from high to lower streamflow intermittency which is manifested within the Budyko framework as a shift from a slight over-prediction to slight under-prediction of AET. This suggests there are thresholds in the partitioning of P into Q and AET in response to subtle changes in the water and energy balances, which is also supported by the higher *n* values fitted for cluster B. In cluster C catchments (N = 57) a transition to energy-limited environments is observed with 12.28% of the catchments. This cluster also has the highest fitted *n* values, suggesting these catchments are partitioning more P into AET over Q than all others along the eastern Australian margin.

Considering the distance from the water- to energy-limit threshold (PET/P = 1), it is likely that many catchments from cluster D (N = 107) might be "equitant". Catchments considered "equitant" are those switching between energy- and water-limited on a seasonal basis (if intra-annual time steps are adopted) and/or between wetter versus drier years (McVicar et al., 2012b). The streams with more stable and perennial flows are represented by cluster E (N=51), with 78.43% of these catchments occurring within the energy-limited region of the Budyko curve. The remaining catchments occurring in the water-limited region had BFI values > 50% (BFI = 0.56 ± 0.17), indicating higher catchment storages can be maintained with increasing PET. The slower flow components in these catchments may be the result of distinct factors (e.g., strong anti-phase seasonality between P and PET in the tropics, snowmelt in alpine regions and water retention in upland swamps). The *n* value fitted to this cluster is also low, consistent with the progression to energy-limited environments being linked to a greater partitioning of P into Q rather than AET. The optimised Choudhury (1999) curves fitted best to all catchment cluster datasets with smaller SSE and MAD when compared to the original Budyko curve. The range in the *n*-parameter from 2.05 (cluster A) to 2.55 (cluster C) suggests that the clusters are formed by catchments with different

characteristics with distinct mechanisms determining the partitioning of P between AET and Q (Table 2.4).

Table 2.4 Statistical descriptors of catchment clusters distribution on the Budyko (1974) and the Choudhury (1999) curves. MAD and SSE of the actual evaporative index measure the dispersion (direction and spreading of clusters); whereas the proportion of catchments within the water-limited environments describes the primary limit of actual evaporation that the clusters are predominantly enclosed. The *n*-parameter was optimised by catchment cluster.

Cluster	Number of catchments	% water-limited catchments	Budyko (1974)		Choudhury (1999)		
			MAD	SSE	*n*	MAD	SSE
A	49	100.00%	-0.006	0.218	2.05	0.004	0.209
B	91	98.90%	0.035	0.576	2.37	0.005	0.445
C	57	87.72%	0.054	0.330	2.55	0.003	0.188
D	107	71.96%	0.052	0.629	2.48	0.004	0.385
E	51	21.57%	0.028	0.134	2.28	0.002	0.120

2.5.4 Extracting the long-term dominant streamflow behaviour

We used the maximum unidimensional variance from PCA analysis to extract the broader patterns in streamflow behaviour from the eight flow signatures and represent the dominant streamflow behaviour along the climatic and topographic gradients (Figure 2.6). The first two principal components (PC1 and PC2) explained 63.7% of the total variability within the eight flow signatures. PC1 explained 45.7% of total variance, and had a stronger correlation with the main flow signatures (RQP, BFI, Q90N, EQP, Q10N, and FNF). PC2 explained 18.0% of the variance and was correlated with SFDC, RLD and FNF. The superimposition of the previous cluster analysis with the space comprised by PC1 and PC2 denotes that the extracted variance within the eight flow signatures is consistent with the catchment separation from our classification outcome (Figure 2.6a). Importantly, the clusters from the previous analyses are best separated by the PC1. Because PC1 is strongly correlated with six out of eight flow signatures and explains almost half of the total variance, we consider it a reliable proxy of the dominant streamflow behaviour. PC1 is proportionally related to BFI, RQP, and Q90N and inversely related to EQP, Q10N, and FNF (Figure 6b).

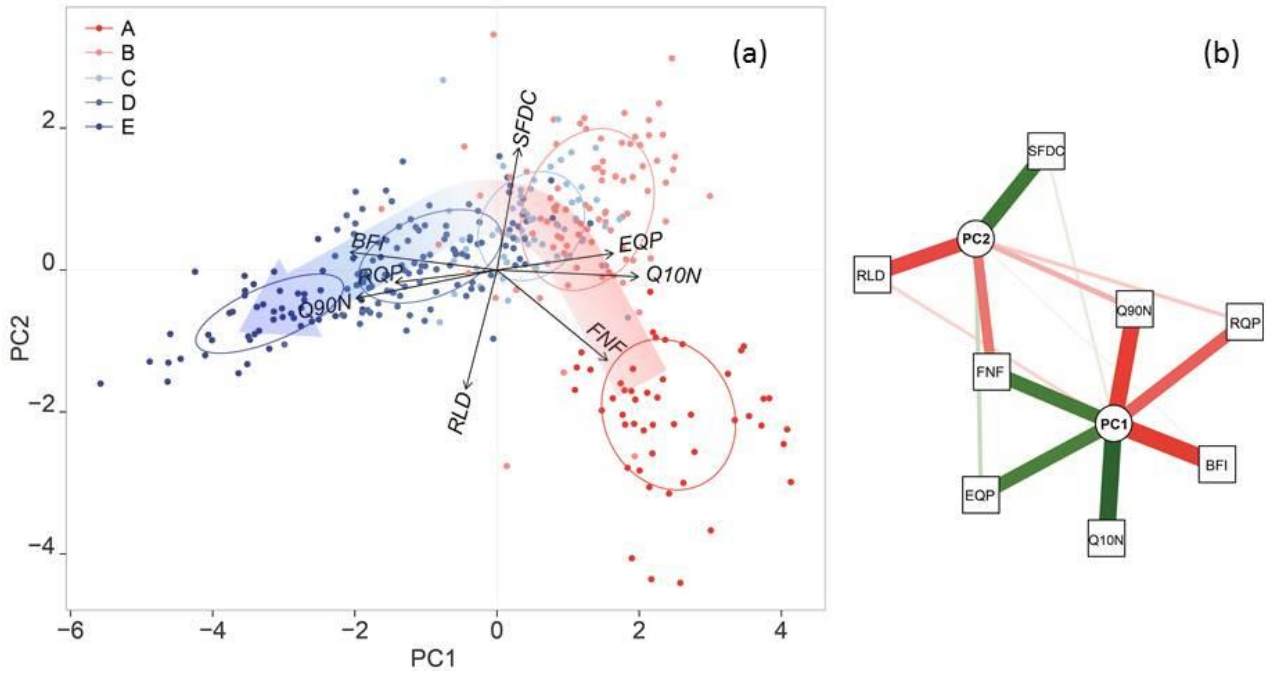

Figure 2.6 Principal Components Analysis (PCA) for the eight streamflow signatures. (a) Biplot of PCA, where the dots are catchments coloured according to the clustering analysis, the small arrows are flow signatures, and the confidence ellipsoids show the 50% central of each catchment cluster. The coloured curved arrow shows the direction of the streamflow spectrum referred in Figure 4, which is inversely proportional to PC1. (b) Loadings from the two first principal components of the eight flow signatures are shown with Green lines being positively correlated and Red lines negatively correlated. Thicker and darker lines are more correlated. The acronyms refer to the flow signatures (see Table 2.1 for details).

2.5.5 Does the Dunne diagram explain the dominant streamflow behaviour?

Having extracted the dominant streamflow response from the eight flow signatures using PCA, we next test whether, and to what extent, the drivers of flow characteristics in the Dunne diagram explain this behaviour. The statistical family distribution that best fitted the response variable was the skew normal type 2.The fitted non-linear model (AIC=1066.7) used six biophysical explanatory variables to explain 77.0% of the variance observed in the dominant streamflow response (PC1). The six predictors used to represent the Dunne diagram and explain the dominant streamflow behaviour of the catchments as described by PC1 were: (i) Dryness Index; (ii) average Fraction of Photosynthetically Active Radiation (fPAR); (iii) fraction of wood vegetation cover; and (iv) maximum slope; (v) average soil depth from A and B horizons; and (vi) saturated hydraulic conductivity (K_{sat}) within the A horizon (Table 2.5). These variables had an acceptable level of collinearity ($r < 0.5$). The validated global deviance was 112.16 with mean prediction error of 3.20. More details regarding the implementation and validation of the statistical modelling are provided in Figure A2.2 (Appendix 2).

Table 2.5 Parameter coefficients of the non-linear model fitted to explain the dominant streamflow behaviour. Predictors were rescaled to have mean zero and variance one. PC1 was used as response variable whereas the drivers of the runoff mechanisms pointed by the Dunne diagram are the explanatory variables.

Link to conceptual model	Model predictors	Coefficients parameters Estimate	Std. Error	t value	P
	Intercept	0.49	0.05	9.00	< 0.001
Dunne diagram x-axis	*cs* (Dryness index)	0.35	0.11	3.20	< 0.001
	ps (fPAR)	0.18	0.10	1.84	< 0.001
	ps (Fraction of wood veg.)	1.13	0.06	18.58	< 0.001
Dunne diagram y-axis	*cs* (Maximum slope)	-0.27	0.05	-5.36	< 0.001
	ps (Soil depth)	-0.70	0.07	-10.34	< 0.001
	ps ($\log(K_{sat})$)	0.79	0.08	10.04	< 0.001

* where *cs* refers to the cubic spline and *ps* to the penalised B-spline smothers.

The random Forest analysis revealed the predictors to be in the following relative order of importance: (i) Dryness Index; (ii) fPAR; (iii) K_{sat}; (iv) soil depth; (v) slope and (vi) fraction of woody vegetation cover. Biophysical variables representative of the x-axis on the Dunne diagram explained 62.9% of the variability whereas the remaining 37.1% of the variability was explained by variables representative of the y-axis. Figure 2.7 displays the partial effects of the predictors on the dominant streamflow behaviour (PC1). In the upper plots representing x-axis of the Dune diagram, the effect is closer to linear with some inflections, especially for the Dryness Index. Interestingly, this inflection is very close to 1, the threshold between water- and energy-limited regions in the Budyko framework. As expected, the vegetation variables are inversely proportional to PC1 with generally less vegetation cover in catchments from clusters A and B. The fPAR steadily increases up to 0.45 followed by a linear decay while the fraction of woody vegetation cover follows a linear downward trend with minor oscillations. With regard to the variables representative of the y-axis on the Dunne diagram, the effect is more non-linear and the benefit of smoother additive terms is clearly exhibited especially for the soil depth and K_{sat}. These controls are mostly influencing PC1 values in the negative range, comprising catchments from clusters D and E. The soil depth, an important catchment storage component, peaks around 0.8 m and gradually decreases showing clearly the development of deeper soils in wetter catchments. The contribution of K_{sat} to PC1 follows a similar trend observed in the soil depth with increasing K_{sat} (in log space) from clusters C to E, however with greater variability at higher values.

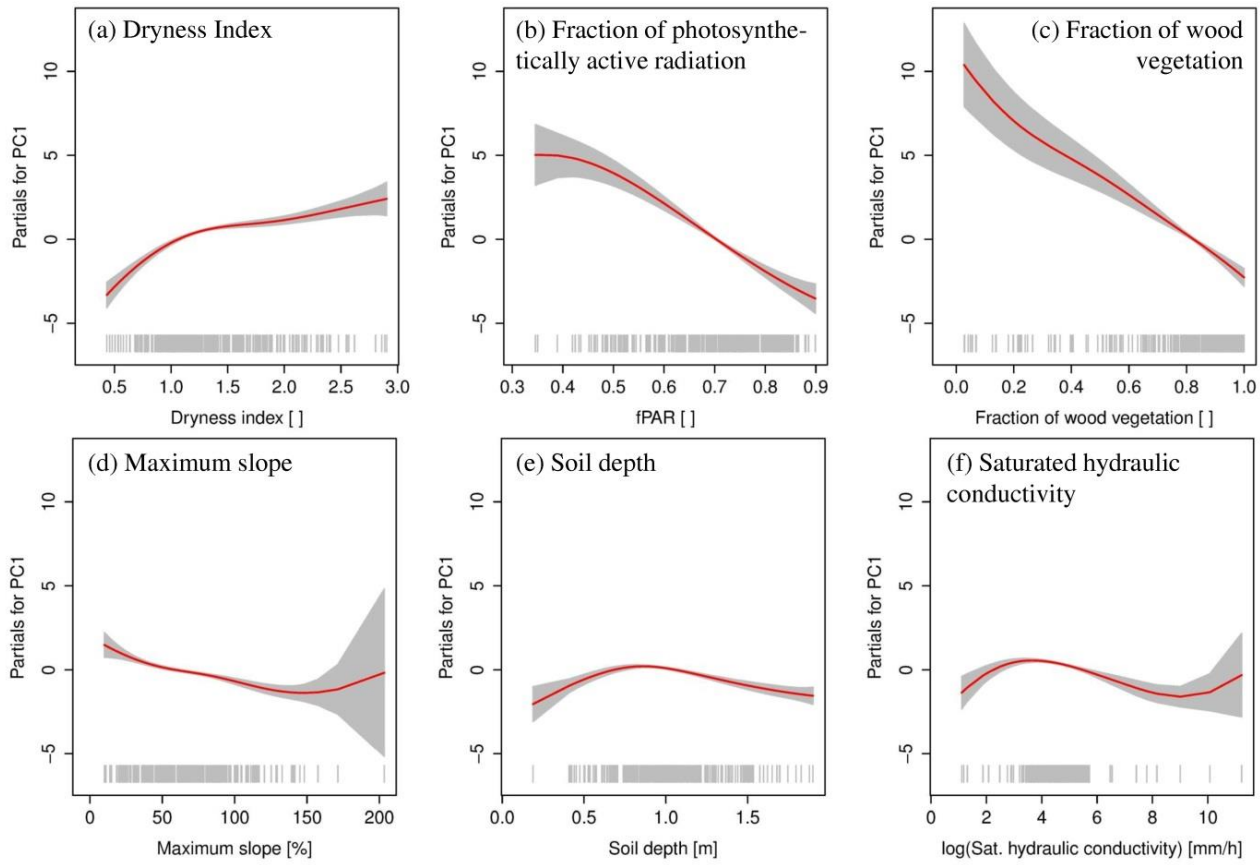

Figure 2.7 Partial effects for each explanatory variable from the Dunne diagram for the drivers of runoff mechanisms on the dominant streamflow behaviour (PC1). The upper three sub-plots (i.e., (a) to (c)) represent x-axis and the bottom three sub-plots (i.e., (d) to (f)) the y-axis of the Dunne diagram. Red lines are the smoothed partial effects, grey shades around them show the standard errors (± 1 SE) and the grey rug ticks show the distributions of the explanatory variables.

2.6 Discussion

2.6.1 Characteristics and drivers of streamflow behaviour along a large climatic gradient

We aimed to test for conceptual links between the Budyko framework and Dunne diagram using classification techniques of streamflow behaviour. In doing so, we were able to better characterise how streamflow behaviour changes over a large climatic (latitudinal) and topographic (elevation) gradients along the entire eastern continental margin of Australia. We found that the: (i) Dryness Index; (ii) fPAR; (iii) K_{sat} from A horizon; (iv) average soil depth from A and B horizons; (v) maximum slope; and (vi) fraction of woody vegetation cover explain 77% of the maximum variability observed in the dominant streamflow behaviour. These controls are consistent with previous studies which have used a variety of empirical approaches to test the importance of these six catchment-attributes (Snelder et al., 2005; Poff et al., 2006; McVicar et al., 2007; Kennard et al., 2010), and can be considered the key biophysical drivers of streamflow behaviour. Table 2.1 shows

that our research has distinct novel aspects compared to earlier studies that primarily focus on classifying streamflow similarity. The framework we present links the conceptual understanding of the quantitative approach to long-term water and energy balances (i.e., Budyko framework) and how catchment biophysical properties drive runoff processes (i.e., Dunne diagram).

The links between the variability in streamflow characteristics and drivers based on our analysis are summarised in Figure 2.8. Both the variability in catchment streamflow characteristics and the key biophysical drivers of streamflow follow clear transitions from water- to energy-limited environments. This is important for comparative hydrology (Woods, 2003; Wagener et al., 2007), demonstrating that judiciously selected streamflow signatures can be combined through a classification approach and linked to catchment biophysical drivers (i.e., climate, vegetation, soils and topography).

The main controlling factors of streamflow behaviour are commonly reported as some combination of climate, topography, soils, and vegetation / land cover (Dunne, 1983; Sefton and Howarth, 1998; Woods, 2003; Yadav et al., 2007; Li et al., 2014). Therefore, there is also some degree of feedback between the biophysical controls empirically quantified here and it is likely that the importance of a certain predictor in explaining the streamflow behaviour is partially dependent on the other drivers. As examples fPAR (a proxy of moisture depletion) is dependent on the Dryness Index (moisture availability) while soil depth and hydraulic conductivity are the result of the co-evolution between climate vegetation and topography (Dryness Index, fPAR, woody vegetation cover and slope). Over the long-term, these soil physical properties have been primarily developed in response to the moisture availability dictated by the catchment water and energy balances (Berry et al., 2006; Yetemen et al., 2015).

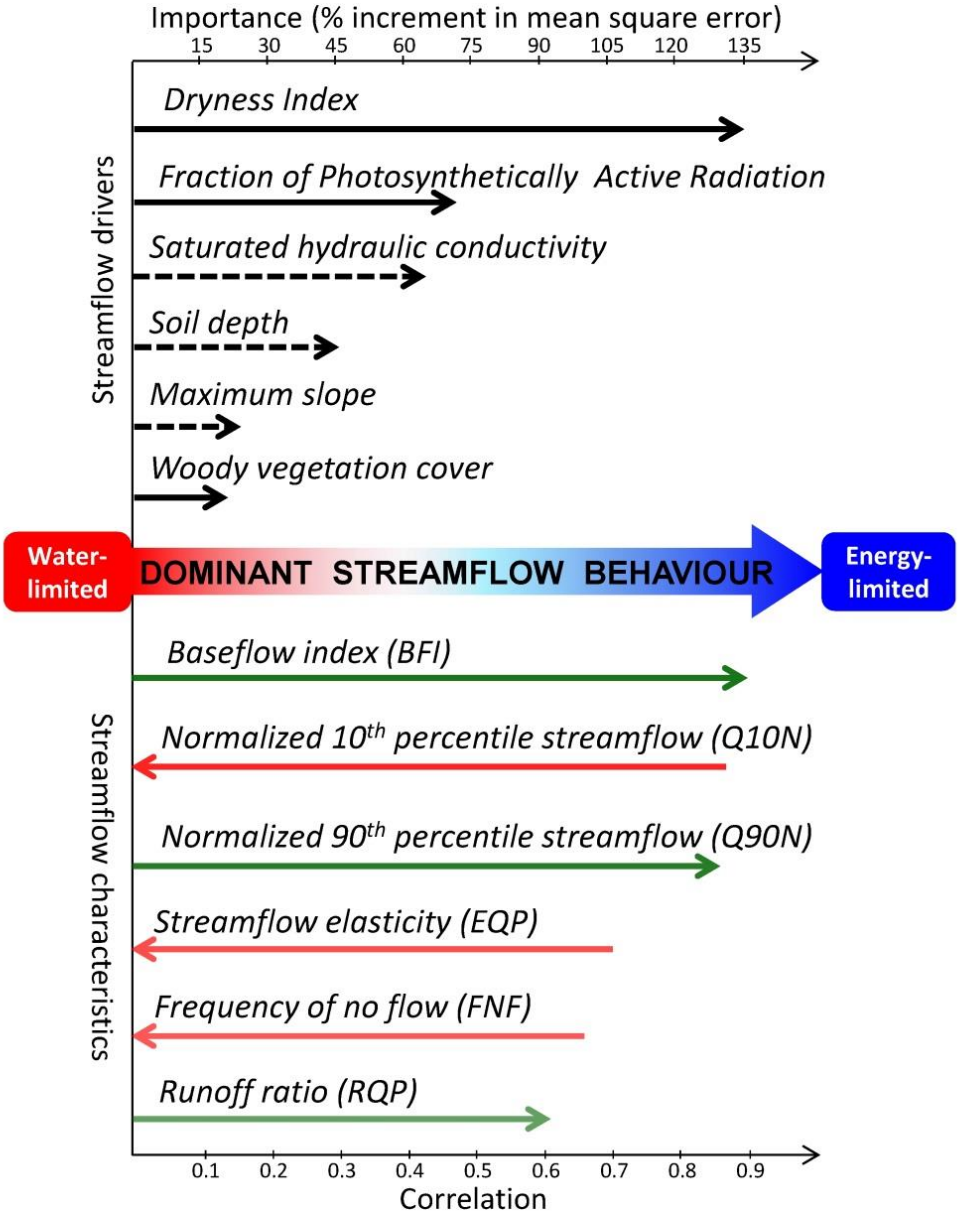

Figure 2.8 Conceptual framework for drivers and characteristics of the dominant streamflow spectrum. The thicker coloured arrow represents the spectrum of dominant streamflow behaviour varying from water-limited to energy-limited catchments along the Australian east coast (1980-2013). The main characteristics of flow regime are displayed below the streamflow spectrum, whereas the flow regime drivers appear above. Longer arrows have higher correlation (flow regime characteristics) and importance (flow regime drivers), with green indicating positive correlation and red negative correlation. Flow drivers with normal arrows represent the x-axis in the Dunne diagram whilst dashed arrows represent the y-axis. The importance criterion accounts for the average relative increment in MSE when the variable is removed from the models. Only six of the possible eight signatures are shown here due to their higher correlation with PC1 (see Figure 2.6b for details).

2.6.2 Links between the Budyko framework and the Dunne diagram

The clusters of hydrological similarity resulted from the classification of catchments according to flow signatures are consistent with the water and energy balances within the Budyko framework (Figure 2.9a). The key biophysical drivers within the Dunne diagram relate to both the dominant streamflow behaviour and the clusters of hydrological similarity that emerge from our classification approach. The Dunne diagram divides the biophysical drivers into the appropriate axes representing climate and vegetation (x-axis) and topography and soils (y-axis). The six biophysical controls, highlighted in a qualitative sense on the two axes of the Dunne diagram, explained most of the variability observed in PC1 (Figure 2.9b). The approximate positioning of the dominant streamflow behaviour within the Dunne diagram was determined by the relative ability of each axis to explain the variability in the first principal component (PC1) when plotted orthogonal (i.e., 90-degrees) to each other. As the x-axis explained 62.9% of the variability within PC1 the arrow angle from the dominant streamflow behaviour (PC1) was placed closer to this axis (33.3 degrees). If this method was applied to another case study with a greater degree of topographic regional dominance, rather than climatic dominance (as experienced here), we expect an angle greater than 45 degrees. After placing the maximum streamflow variability (PC1) in accordance with the dominant axes on the Dunne diagram, the main streamflow signatures driving this variance within PCI also appear consistent with the biophysical controls. Specifically, BFI, RQP and Q90N all increase right to left with increasingly humid climates and vegetation density, and Q10N, EQP, FNF increase left to right with increasingly arid to sub-humid climates and less vegetation cover (increasing Dryness Index). SFDC and RLD are also consistent with the biophysical controls of the Dunne diagram y-axis, increasing and decreasing, respectively, with increasing slope, soil depth and saturated hydraulic conductivity (see Figure 2.6 for details). These relations between flow signatures and catchment properties have been previously highlighted for BFI (Lacey and Grayson, 1998; Schneider et al., 2007; Beck et al., 2013b), RQP and FNF (Zhang et al., 2014), 10^{th} and 90^{th} percentiles streamflow (Ssegane et al., 2012) and FDC (Castellarin et al., 2004; Castellarin et al., 2007; Cheng et al., 2012).

The three runoff generation mechanisms considered in the Dunne diagram (i.e., Horton overland flow, subsurface stormflow and return flow) are also consistent with the clusters of hydrological similarity as well as the biophysical controls. It is expected that water-limited ephemeral catchments with highly erratic flow regimes (cluster A) have Horton overland flow dominating their hydrographs, which is also reinforced by the higher values of FNF, Q10N and EQP for these catchments. Conversely, catchments from cluster E, which are mostly energy-limited with perennial

and highly regular flow regimes, tend to have their hydrographs dominated by subsurface stormflow (higher BFI values) with peaks influenced by direct precipitation (denoted by greater RQP) and return flow indicated by lower soil depth and saturated hydraulic conductivity. Topographic and soil variations may be important drivers distinguishing flow regimes in catchments from clusters A to B in water-limited regions and E to D in energy-limited regions. As a result, steeper catchments have increasing values of SFDC, with direct precipitation and return flow dominance in their hydrographs also because nothing stays for long in storage. It is worth noting that catchments from intermediate clusters may have a fractional combination of the three runoff mechanisms driving their hydrographs, whereas clusters A and E are likely to have more dominant contributions from those highlighted mechanisms.

Our catchment classification approach divided the catchments along the eastern margin of Australia into five groups based on similar hydrological functioning. It is of course reasonable to expect that the number of clusters may change according to the study region, choice of flow metrics, the range of climate and flow conditions included, and the classification approach (Wagener et al., 2006; Kennard et al., 2010; Sawicz et al., 2011; Berghuijs et al., 2014a). However, if conducted in a similar way, the output of these comparative techniques should still yield maximum streamflow variance within the three runoff generation categories proposed by Dunne. This convergence between the aridity gradient and runoff generation mechanisms also means that the classification framework partitions the water and energy balances in a manner consistent with the Budyko framework (Budyko, 1974) and provides a robust link with the catchment biophysical characteristics. We therefore argue that an output from a catchment classification scheme based on representative flow signatures should be related to the long-term water and energy balances and be explained to some extent by the catchment co-evolution factors contained within the Dunne diagram regardless of the dataset characteristics such as region and number of catchments. It is therefore reasonable to expect that the relative importance of the axes on the Dunne diagram, as well as the contribution of the individual variables within them, will shift according to the regional dominance of the drivers of runoff mechanisms.

Simple runoff models have been used to partially quantify the Dunne diagram based on the partitioning between infiltration and saturation excess overland flow (Larsen et al., 1994), and to evaluate the relationship between the Budyko framework and the Dunne diagram (Li et al., 2014). Our results further demonstrate that the controls proposed by Dunne also emerge within large, long-term Q observational datasets summarised using a classification approach. Our findings relate streamflow characteristics (inductive classification approach to biophysical drivers) and the water

and energy balances (deductive classification) using observational data, developing a way to link the Budyko framework with the biophysical controls and runoff characteristics within the Dunne diagram. Conceptually, this link should have its basis in the co-evolution of catchment streamflow behaviour with biophysical drivers (Figure 9b) as catchments shift along the Budyko curve from water- to energy-limited regions (shown with the clusters identified in this study in Figure 2.9a).

In the context of the catchment co-evolution factors within the Dunne diagram, the dominant streamflow behaviour (PC1) is dependent on both axes (climate and vegetation on the x-axis, and topography and soil properties on the y-axis). Within the Budyko framework, the dominant streamflow behaviour (PC1) is an outcome of the atmospheric water supply and atmospheric evaporative demand. Likewise, the dominant streamflow behaviour (PC1) relates to both the biophysical factors driving flow characteristics on the Dunne diagram and the Dryness Index on the Budyko framework, revealing an important linkage between these two well-known schemes (Figure 2.9).

Whilst there has been progress using modelling and analytical approaches to link annual water and energy balances (e.g., Budyko framework) with biophysical streamflow controls (e.g., Dunne diagram) (Li et al., 2014), the co-evolution feedbacks that develop within and among catchments mean that separating cause and effect is difficult in lumped or distributed physical models. Several studies have implicitly, or explicitly, tested some of the specific controls provided by the Dunne diagram within the Budyko framework, such as the role of soil water storage capacity (Milly, 1994; Gentine et al., 2012), topography (Nippgen et al., 2011), soil permeability (Yokoo et al., 2008), vegetation (Donohue et al., 2012), soil moisture (Yin et al., 2014), and elevation (Berghuijs et al., 2014b; Reinfelds et al., 2014). An alternative approach, which we have pursued here, is to ask "what information can long-term streamflow data reveal about the variation and similarity in streamflow behaviour and to what extent are these characteristics explained by biophysical controls?" If large datasets are used, then a classification approach is needed to constrain the large heterogeneity in streamflow characteristics. Our findings using such a dataset highlight important overlaps and consistencies between the two schemes that can inform future work which seeks to develop formal theoretical links.

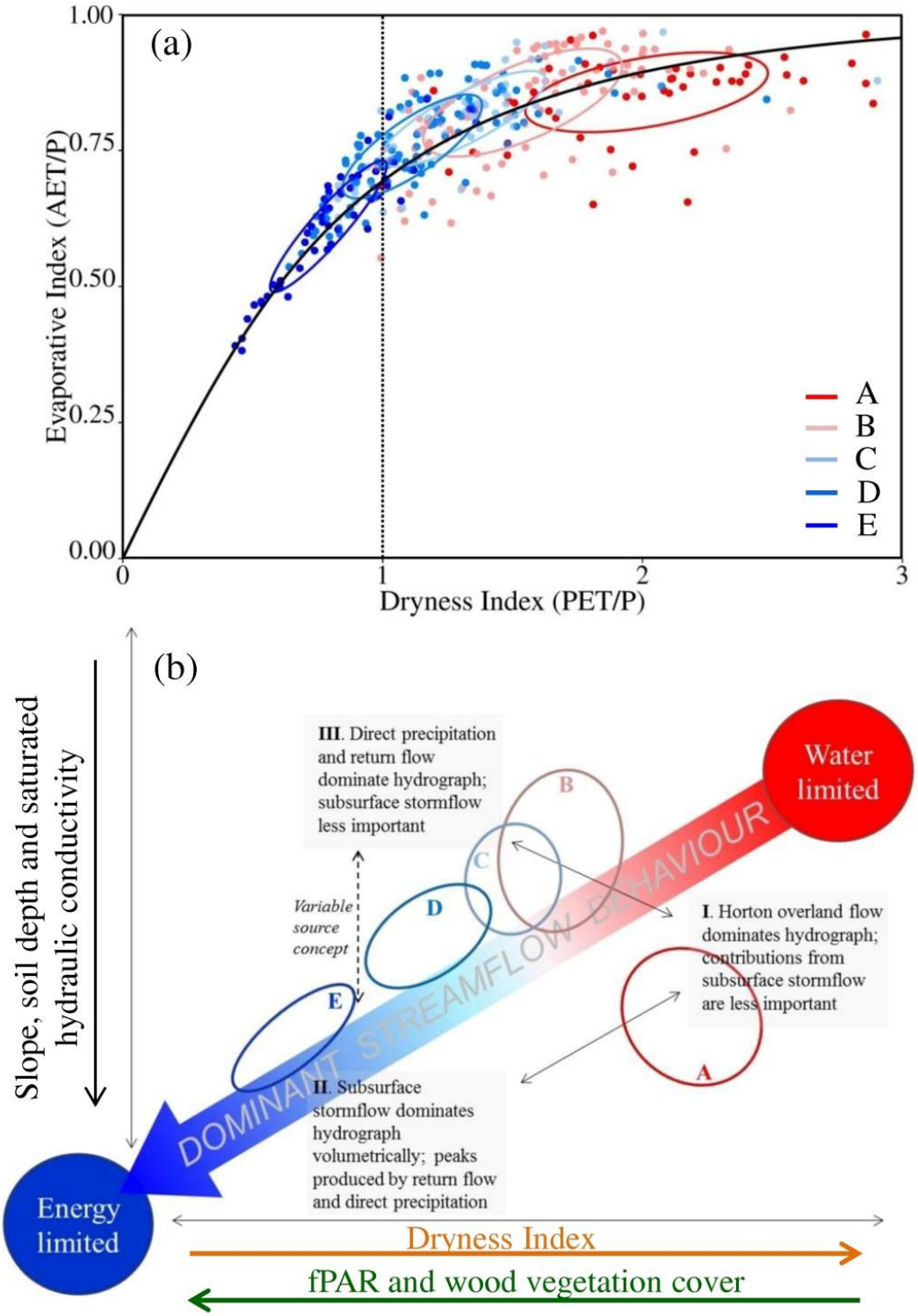

Figure 2.9. Graphic representation of the catchment classification results and the linkage between the Budyko framework and the Dunne diagram. (a) Catchment clusters plotted on Budyko framework with data ellipses based on the 66% probability range (average ± 1 standard deviation). Catchment clusters from A to E present a gradient of streamflow characteristics (see Figure 4 for details).(b) Dominant streamflow response spectrum and catchment clusters in the context of Dunne's diagram that relates the distinct runoff processes to their major controls (adapted from *Dunne*, 1983). The Dryness Index is increasing to the right (i.e. PET > P, as shown by the arrowhead) and fPAR and woody vegetation are increasing to the left (as shown the arrowhead).

2.7 Conclusion

We mapped the distribution of eight long-term (1980-2013) flow signatures to provide insights into the hydrological functioning of 355 catchments along topographic and climatic continental gradients in eastern Australia. The catchment classification of eight key hydrological signatures identified five clusters with distinct hydrological functioning along the streamflow spectrum. Within each cluster similar hydrological behaviour existed despite the large climatic and topographic gradients. The dominant streamflow behaviour is consistent with the catchment clusters and integrates an important fraction of the variability within the flow signatures. The classification output organised catchments along a spectrum of hydrological characteristics, which is consistent with the distribution of catchments along the hydro-climatic regions on Budyko framework. The drivers of the long-term dominant streamflow behaviour are consistent with the Dunne diagram of runoff mechanisms with the following catchment attributes provided in decreasing relative order of importance, being: (i) Dryness Index; (ii) Fraction of Photosynthetically Active Radiation; (iii) Saturated Hydraulic Conductivity; (iv) Soil Depth; (v) Maximum Slope; and (vi) Fraction of Woody Vegetation Cover.

The study represents a substantial methodological advance in the use of a sequence of well-established data analysis techniques to classify catchments based on their hydrological functioning. The catchment clusters follow a consistent pattern along the hydro- climatic gradients and are driven by the biophysical drivers of runoff mechanisms (Dunne diagram). This represents a novel approach based on streamflow characteristics (inductive classification) that independently organises catchments along the spectrum of water and energy balances and is statistically controlled by the catchment co-evolution factors normally used to organize catchments by deductive classification. Our findings suggest a more definitive convergence along the water and energy balance spectrum with the biophysical drivers and streamflow characteristics, providing new insights into how a catchment classification scheme links two well established theories in hydrology: the Budyko framework and the Dunne diagram.

CHAPTER 3

REGIONAL VARIATION IN STREAMFLOW DRIVERS ACROSS A CONTINENTAL CLIMATIC GRADIENT

The Great Divinding Range defines catchment boundaries across the Australian east coast. Mount Edwards, Queensland. Photo by Glen Ross (source: flickr.com).

This chapter is based on the following manuscript:

Trancoso R., Phinn S., McVicar T.R., Larsen J.R., McAlpine C. (2016). Regional variation in streamflow drivers across a continental climatic gradient. *Ecohydrology*.

3.1 Abstract

Streamflow characteristics are driven by specific flow-generation mechanisms, which are in turn determined by the biophysical properties of catchments. They provide important environmental services for society and ecosystems, regulating water supply and quality, flood mitigation, and the biological diversity of aquatic ecosystems. This study investigates how the drivers of streamflow characteristics vary at the level of regional management (regional (10^4 km^2) and continental scales (10^7 km^2)) in eastern Australia. Three hydrological signatures were used to represent streamflow characteristics: runoff coefficient, baseflow index and zero flow ratio. Long-term streamflow data and 24 spatially distributed biophysical properties from 354 catchments in eastern Australia were analysed with random forest and generalised additive beta regression models to determine the dominant drivers of streamflow characteristics. We found that the main drivers of streamflow characteristics cannot be generalized from region to region and that specific biophysical variables govern their spatial variability. However, some important drivers such as the Dryness Index and the fraction of photosynthetically active radiation from vegetation explain the variability of streamflow characteristics at both regional and continental scales with differing importance. Our findings also suggest that soil properties have a significant effect on streamflow characteristics at regional scales. However, the relative importance of these soil properties varies among regions depending on the streamflow characteristics. This paper demonstrates that: the drivers of streamflow characteristics are scale- and region-dependent; and biogeographically different regions have specific mechanisms governing streamflow. It opens an avenue to better connect the management perspectives of ecology and hydrology.

Keywords: Streamflow characteristics; Streamflow signatures; Catchment properties, Mixed-effect models; Beta regressions; Climate effect; Vegetation effect.

3.2 Introduction

Drivers of streamflow characteristics are investigated at different spatial extents, including local (10^2 km^2; e.g., Soulsby et al. (2010)), regional (10^4 km^2; e.g., Zhang et al. (2014)) and global (Beck et al., 2015). While global studies have revealed that the Dryness Index, precipitation seasonality and topographic slope are the dominant catchment properties influencing streamflow characteristics (Beck et al., 2013b; Beck et al., 2015), finer spatial scale studies suggest that their relative importance shows greater regional variability (Lacey and Grayson, 1998; Mwakalila et al., 2002; Zhang et al., 2014). Therefore, studies within a region of relatively uniform climatic and biophysical characteristics are often not able to reliably explain ecohydrological processes and inform catchment management decisions in other regions. This problem of cross-regional variability of catchment biophysical properties and their influence on streamflow characteristics, which is at the heart of streamflow regionalisation, is not yet well understood. Therefore, important questions such as: (i) "how does the relative influence of the dominant drivers of streamflow characteristics vary at continental scales and across biogeographically-contrasting regions?"; and (ii) "to what degree can studies in one region be used to inform decisions in other regions?" are yet to be fully answered. In addition, there is a need to understand process-based knowledge of streamflow variation at the regional scales adopted by management and policy frameworks common in biodiversity conservation (Mac Nally et al., 2002) and ecological assessments (Klein et al., 2009). The increased availability of spatial data that are important biophysical drivers (e.g., climate, topography, soil and vegetation) of streamflow within catchments encourages their use in making progress towards answering these important questions. Here, we examine variation in these metrics at the biogeographic regional level to determine the ecohydrological characteristics influencing streamflow, as this is the typical management scale used in biodiversity / ecology, policy and management.

Streamflow characteristics are determined by the hydrological processes within the catchment, which in turn, are driven by the inter-relation and co-evolution of catchment biophysical properties (Berry et al., 2006). Subsequently, different combinations of catchment properties leads to divergent partitioning of water and energy balances and flow paths between catchments that ultimately determine streamflow characteristics.These differences have been the focus of hydrological and ecological research for the last five decades. While hydrologists are usually interested in the magnitude, frequency, duration, timing and rate of change of streamflow (Sopper and Lull, 1965), ecologists typically seek insight into the ecological process and biological patterns within riverine and aquatic ecosystems (Minshall and Winger, 1968). This difference in objectives results in

ecological management priorities at spatial resolutions and scales usually not considered in hydrological studies, but can nonetheless have important regional hydrological implications. This paper therefore seeks to examine the processes that can explain streamflow variability at the regional scales of biodiversity management, and whether this provides a meaningful avenue for linking biodiversity and water resource management.

A common way to summarize key streamflow characteristics of catchments is through the use of 'streamflow signatures' (Sawicz et al., 2011; Trancoso et al., 2016) as thy provide a glimpse into the holistic functioning of the catchment and the relationship between landscape structure and catchment responses (Wagener et al., 2007). The main streamflow signatures of interest are typically: (i) flow variability (i.e. slope of the flow duration curves - Coopersmith et al., 2012); (ii) slow flow components (i.e. baseflow index - Beck et al., 2013b); (iii) recession rates (van Dijk, 2010); (iv) runoff ratio (i.e. fraction of precipitation converted to runoff - Zhang et al., 2014); (v) magnitude of low and high flows (i.e. 10th and 90th streamflow percentiles - Ssegane et al., 2012); (vi) magnitude of extreme events (i.e. minimum and maximum streamflow - Villarini and Smith, 2010) and; (vii) the degree of flow intermittency (Moliere et al., 2009).

The long-term spatial variability of streamflow characteristics is primarily determined by spatial variations in the key drivers, especially precipitation and actual evapotranspiration (and their characteristics), which are then further modified by catchment biophysical properties such as vegetation, topography, soil and physiography (Dunne, 1983; Winter, 2001; Wolock et al., 2004; Berry et al., 2006). However, we do not know how these drivers combine to determine variations in streamflow characteristics at different regions and spatial scales - e.g., regional (10^4 km^2) and sub-continental (10^7 km^2). Likewise, the reason for adjacent streams with similar biophysical properties having different streamflow characteristics is often difficult to determine (Costigan et al., 2015). Conversely, biogeographically different regions may have similar streamflow characteristics resulting from distinct processes whereby catchments have coevolved (Trancoso et al., 2016).

When these processes are investigated at larger spatial extents (i.e., intra-continental and global scales), the regionally-specific factors governing streamflow characteristics are often overlooked. This paper explores the differences in hydrological processes between sub-continental (10^7 km^2) and regional (10^4 km^2) scales using a widely-distributed catchment database, and among three biogeographic regions, all with differences in climate, terrain, soils and vegetation. The aims of this research are threefold:

(i) to determine the changes in the relationships between streamflow characteristics and catchment properties along regional and sub-continental scales and across biogeographically-contrasting regions;

(ii) to examine how dynamic catchment biophysical properties (i.e., vegetation and climate) affect key hydrological characteristics within and between regions; and

(iii) to infer the processes governing streamflow variation at larger biogeographic regional scales in order to better inform how biodiversity management scales can link with water resource management.

We address these aims using statistical modelling of a long-term ecohydrological dataset for 354 catchments in eastern Australia by testing the importance and weight of 24 explanatory variables to explain three of the most informative streamflow characteristics across the East Coast and three biogeographically-contrasting regions that define current biodiversity management boundaries. We also apply a novel modelling approach using a Generalized Additive Model for Location Scale and Shape (GAMLSS) with beta distribution for the response variable (fully described in the Methods) to account for the spatial variability of streamflow characteristics. This paper is structured in seven sections. Section 3.3 presents the conceptual model used, section 3.4 describes the study area and data, section 3.5 describes the methods, section 3.6 presents our findings and addresses the three objectives, section 3.7 discusses the findings in light of the relevant literature and section 3.8 summarises the conclusion of our study.

3.3. Conceptual Model

The conceptual basis of this research builds on the catchment co-evolution concept, whereby the development of spatial patterns in landscape features and the hydrological response of catchments are closely connected (Troch et al., 2013; Troch et al., 2015). We, therefore consider five primary hydrological drivers that may have coevolved over time to control the streamflow characteristics at the catchment scale: climate, vegetation, soils, topography and physiography (Figure 3.1). It is widely accepted that climate is the foremost control governing the supply of moisture and energy (i.e., precipitation and potential evapotranspiration), which in turn help determine the weathering processes largely underpinning the coevolution of the other drives. The interaction between climate and vegetation regulates actual evapotranspiration, whilst the landscape features determine the way that the non-evaporated water (i.e., precipitation - actual evapotranspiration) is transported within the catchment (i.e., by different flow paths such as overland flow, infiltration and soil or

groundwater storage supply) that ultimately define the streamflow characteristics (Dunne, 1983; Winter, 2001; Wolock et al., 2004; Berry et al., 2006).

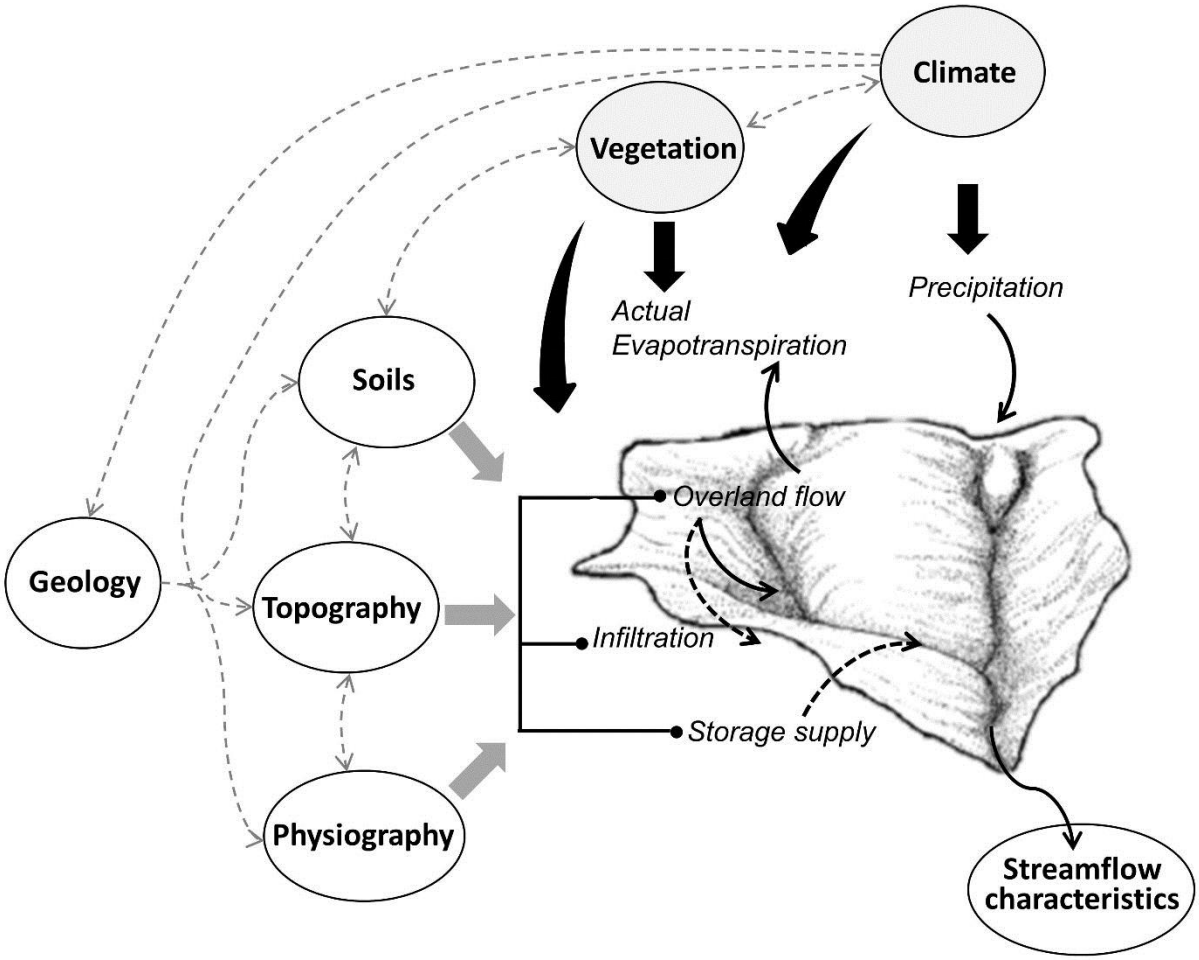

Figure 3.1. Conceptual model of the biophysical properties of catchments and how they influence flow paths and streamflow characteristics. Climate and vegetation, represented with shaded ellipses and black arrows, are dynamic properties sensitive to landscape and climate change, whereas the non-shaded ellipses are largely static at anthropogenic timescales. Grey dashed lines represent interactions between biophysical properties.

3.4 Study Site and Data

3.4.1 Study regions

The study area encompasses the whole eastern seaboard of Australia (including Tasmania) referred to here as the continental scale. It covers approximately 1,000,000 km^2, extending 200 km inland and ~3,600 km north-south. This area varies in climatic and biophysical properties including the amount and seasonality of precipitation, potential evapotranspiration, topography, vegetation, soils and physiography. We used 354 unregulated, non-nested catchments of which the majority (77%) drained east towards the coast and the remainder drained inland. Three widely-distributed and

biogeographically-contrasting regions (Thackway and Cresswell, 1995) were selected to test for regional variation in the patterns of influence of the dominant drivers on streamflow characteristics (Figure 3.2). These regions followed the bioregions from the Interim Biogeographic Regionalisation for Australia (IBRA7), which are classified according to climate, topography, soil and vegetation types (IBRA, 2013). Region 1, extending ~1,150 km north-south and 400 km east-west, encompasses three adjacent tropical IBRA bioregions (Cape York Peninsula, Wet Tropics and Einasleigh Uplands) and includes 40 catchments (Table 3.1). Region 2 extends ~700 km north-south and 160 km east-west, represents subtropical catchments from South East Queensland containing 51 catchments. Region 3, extends ~680 km north-south and 530 km east-west, and comprises 69 catchments from the South Eastern Highlands with a temperate climate and mountainous terrain. A summary of physiographic and hydroclimatic catchment characterisation for the entire dataset and the three regions is provided in Table 3.1.

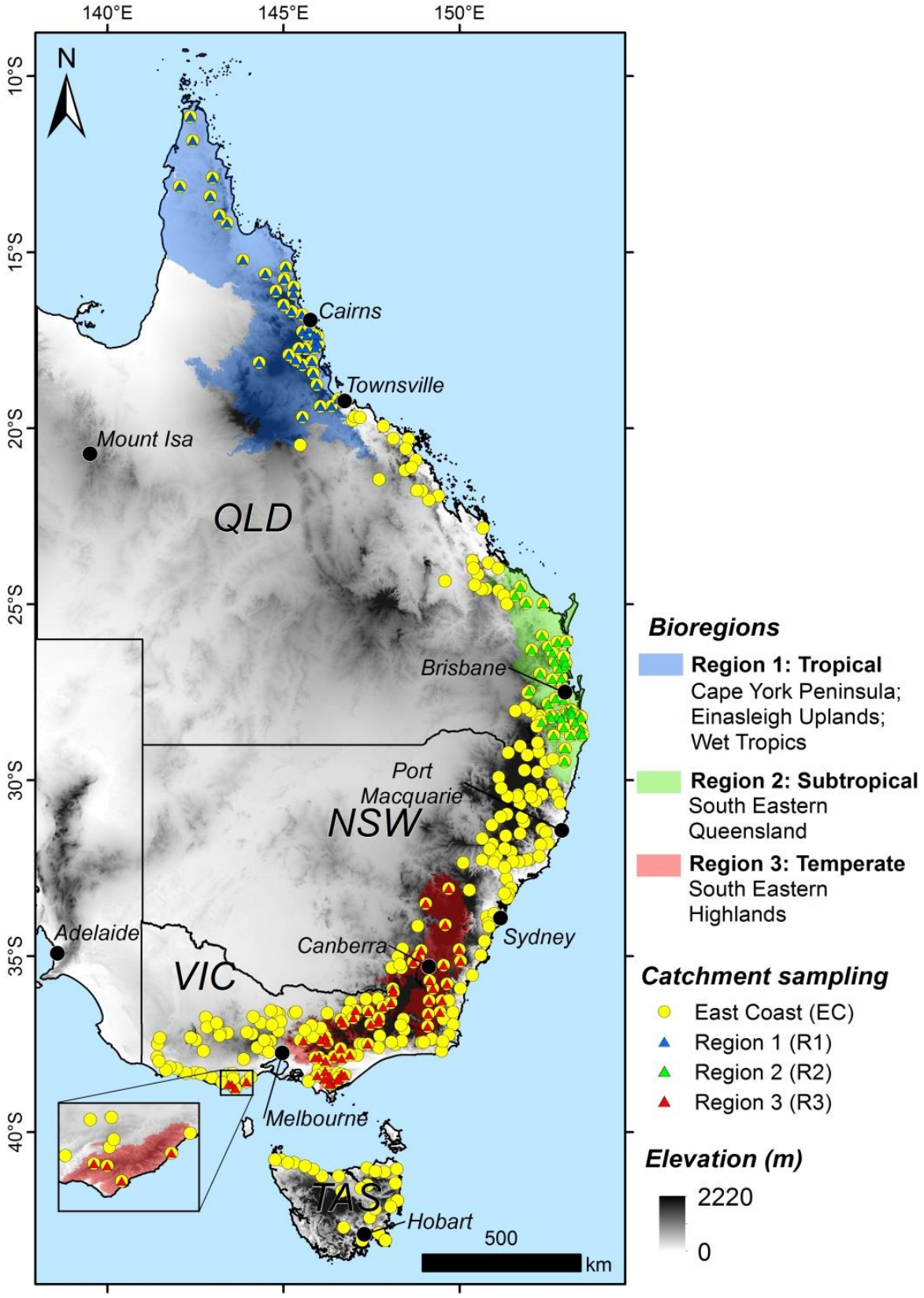

Figure 3.2 Study area with multi-scale sampling design encompassing 354 catchments along the east seaboard and the three distinct regions. QLD, NSW, VIC and TAS are abbreviations for Queensland, New South Wales, Victoria and Tasmania respectively. The inset in the bottom left shows an isolated sub-section of Region 3.

Table 3.1 Summary physiographic and hydroclimatic catchment characteristics for the full dataset and separately for the three regions. The statistics are: number of catchments, average ± standard deviation of area, elevation, and for the 1980- 2013 annual average precipitation (*P*), streamflow (*Q*), actual evapotranspiration (*AET*) and the seasonal variability in the supply of water and energy given by the difference between the month of maximum precipitation (*Pmax*) and month of maximum potential evapotranspiration (*PETmax*). *AET* was obtained as the difference between *P* and *Q*.

Region	Number of catchments	Average ± Standard Deviation					
		Area (km^2)	Elevation (m)	P (mm/year)	Q (mm/year)	AET (mm/year)	Pmax-PETmax (months)
East Coast	354	361 ± 429	491 ± 306	930 ± 272	203 ± 298	727 ± 150	2.83 ± 1.47
Region 1	40	572 ± 656	451 ± 218	1672 ± 744	625 ± 567	1047 ± 238	3.59 ± 1.52
Region 2	51	264 ± 341	301 ± 195	1189 ± 342	233 ± 269	956 ± 143	2.25 ± 1.68
Region 3	69	288 ± 320	666 ± 250	1031 ± 246	284 ± 191	747 ± 79	2.96± 1.04

3.4.2 Data

We used daily streamflow (*Q*) data from 1980 to 2013 across the 354 catchments to compute long-term streamflow characteristics (Trancoso et al., 2016). All selected gauges have at least 70% of *Q* data for these 33 years (12,045 days). We only used years with a complete record. Catchment boundaries were defined using a hydrologically-conditioned and drainage-enforced DEM with a 30 m pixel size (Wilson et al., 2011). We mapped the upstream area of each streamflow gauge using their geographic coordinates. The catchment boundaries were used to calculate catchment averaged daily precipitation from a gridded precipitation time series with ~ 5 km pixel-size (Jones et al., 2009) and for the other explanatory data used to predict streamflow characteristics. We used the climate, topography, vegetation, soils, and physiography of the catchments (Table 3.2). Because precipitation is one of the input variables to calculate runoff coefficients, we did not include it as an explanatory variable in our models to account for the effect of the other catchment biophysical properties.

Table 3.2 Listing of the 24 explanatory variables assessed to model streamflow characteristics with sources and description. Metrics with empty brackets are non-dimensional.

Explanatory variables (Units)	Source	Description
Climatic		
1. Dryness index ( )	Budyko (1974)	Determines the balance between atmospheric supply and demand of moisture by the ratio of long-term Potential Evapotranspiration and Precipitation extracted from gridded time-series (~5km pixel size)
2. Monthly maximum air temperature (° C)	Jones et al. (2009)	Long-term average maximum monthly air temperature (determined as item 1).
3. Monthly minimum air temperature (° C)	Jones et al. (2009)	Long-term average minimum monthly air temperature (determined as item 1).
4. Seasonality index ( )	Feng et al. (2013)	Measures the magnitude and concentration of the rainy season by combining the extent of precipitation concentration in the wet season with the mean annual precipitation normalized by the maximum mean annual precipitation (determined as item 1).
5. Annual average precipitation (mm)	Jones et al. (2009)	Long-term mean annual precipitation (determined as item 1).
Topography		
6. Fraction of erosional landscapes ( )	Gallant and Dowling (2003)	Fraction of non-deposition catchment surface based on an index that determines the flatness in valleys (Multi-resolution valley-bottom flatness) determined using DEM with 30 m pixel-size.
7. Average slope (%)	Wilson et al. (2011)	Average inclination of the catchment surface in per cent determined using DEM with 30 m pixel-size.
8. Maximum slope (%)	Wilson et al. (2011)	Maximum Inclination of the catchment surface in per cent determined using DEM with 30 m pixel-size.
Vegetation		
9. Monthly average fPAR ( )	Donohue et al. (2008)	Long-term monthly average of the fraction of Photosynthetically Active Radiation (fPAR) absorbed by vegetation estimated by AVHRR and MODIS imagery with 1 km of spatial resolution
10. Annual range of fPAR ( )	Donohue et al. (2008)	Long-term average of the fPAR annual range estimated by AVHRR and MODIS imagery with 1 km of spatial resolution
11. Fraction of woody vegetation cover ( )	Lymburner et al. (2011)	Determined by grouping the natural arboreal vegetation of MODIS imagery classification with 250 m pixel-size
12. Annual average of actual evapotranspiration (mm)	Raupach et al. (2012)	Long-term total annual evaporation and transpiration by soil and vegetation (determined as item 1).

Soils		
13. Monthly average of soil moisture ( )	Raupach et al. (2012)	Long-term monthly average relative soil moisture from upper layer (determined as item 1).
14. Average soil depth ($AB_{horizon}$) (m)	McKenzie et al. (2000)	Determines the volume of water for storage capacity and for vegetation use (determined using digital maps).
15. Saturated Hydraulic Conductivity (mm/h)	McKenzie et al. (2000)	Indicates the vertical drainage capacity of a soil as well as the likelihood of surface runoff and erosion (determined as above).
16. Average clay content (%)	ASRIS (2015)	The argillic component (< 2 um mass fraction of the < 2 mm) of soil texture is determined using the pipette method and affects most chemical and physical properties and indicates some processes of soil formation (extracted from gridded data with ~ 270 m pixel size).
17. Average pH ( )	ASRIS (2015)	Indicates the degree of weathering and controls nutrient availability and many chemical reactions (determined as item 16).
18. Average plant available water capacity (mm)	ASRIS (2015)	Primary control on biological productivity and soil hydrology (determined as item 16).
19. Average bulk density in top 30 cm (g/cm^3)	ASRIS (2015)	Density of the whole soil (including coarse fragments) in mass per unit volume by a method equivalent to the core method Depends on the composition and degree of compaction, and relates with suitability for root growth and permeability (determined as item 16).
Physiography		
20. Area (km^2)	Schumm (1956)	Drainage area upstream the station from which the surface runoff in derived (determined with catchment boundaries mapped using DEM with 30 m pixel-size).
21. Perimeter (km)	Schumm (1956)	The length of the ridge line along the topographic divide that delineates the catchment area (determined as item 20).
22. Circularity Ratio( )	Miller (1953)	It indicates how circular a catchment shape is and is determined by the catchment area divided by the area of a circle whose perimeter is equal to the length of the ridge line of the catchment (determined as item 20).
23. Shape factor( )	Snyder (1938)	Describes the general runoff concentration behaviour of the catchment. It is determined considering the distance between the catchment outlet (here the location of streamflow station) and the catchment centroid and the longest dimension of the catchment (determined as item 20).
24. Compactness coefficient ( )	Bendjoudi and Hubert (2002)	It indicates how elongated a catchment shape is and is calculated by the ratio of the perimeter of the catchment to the perimeter of the circle whose area is equal to the catchment area (determined as item 20).

3.5 Methods

We used three streamflow signatures to represent streamflow characteristics (see details in section 3.5.1). We considered over 70 possible explanatory biophysical variables in our initial exploratory analysis and eliminated the highly correlated ($r > 0.7$) variables and those with low predictability (i.e., low Akaike Information Criterion (AIC) and the R-squared (R^2)) for the sake of parsimony. We then assessed the importance of the 24 selected as potential explanatory variables with random forests (see details in section 3.5.2) for the entire East Coast catchment and the three regions. GAMLSS with beta distribution models were fitted to the calibration data and validated against the independent data (see details in section 3.5.3). This approach allowed us to determine the performance, weights and the partial effect of the explanatory variables across the regions (Figure 3.3).

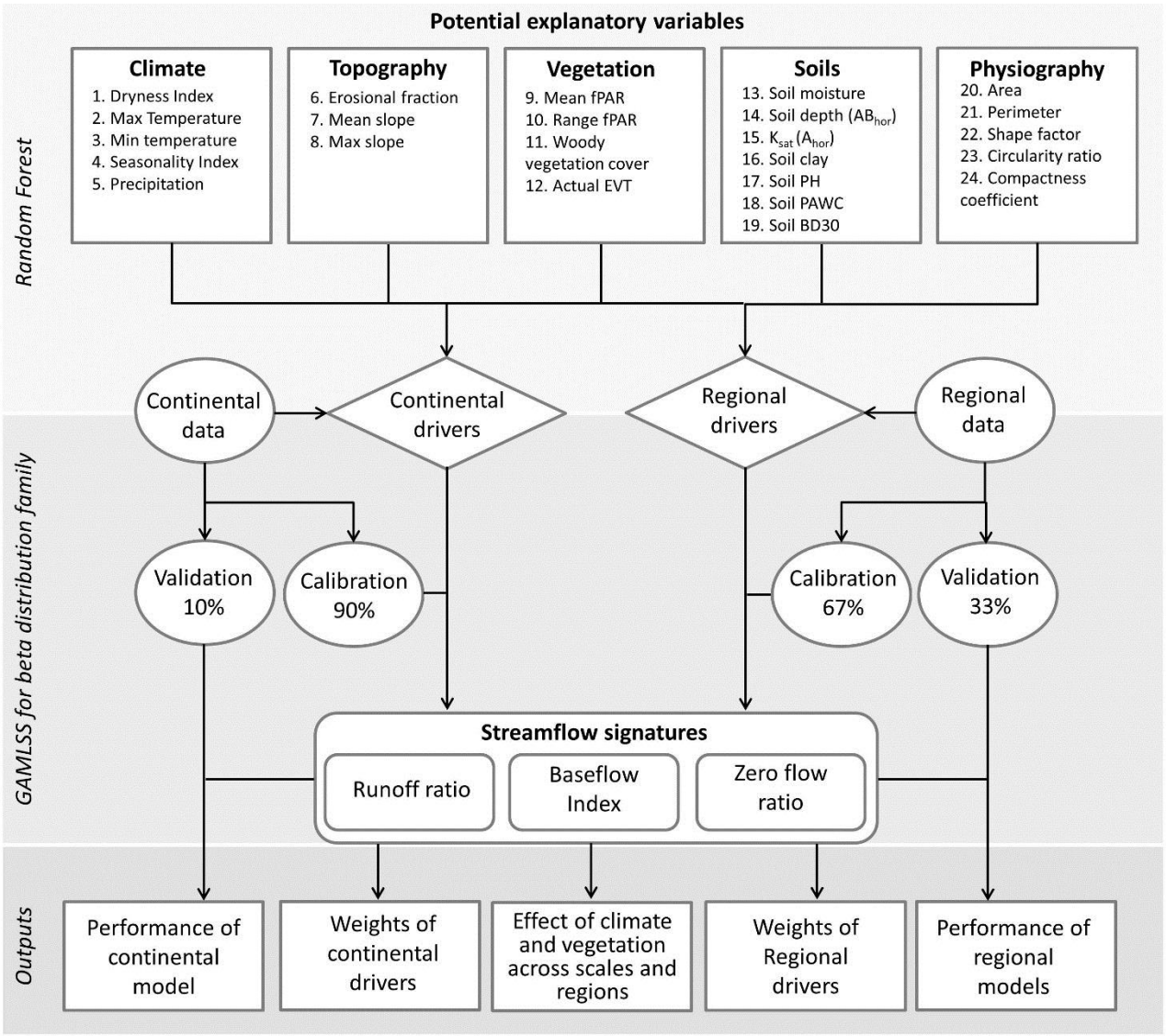

Figure 3.3 Flowchart of the modelling framework.

3.5.1 Streamflow characteristics

Streamflow characteristics are commonly represented by flow signatures as proportions, for example runoff ratio, slope of the flow duration curve and baseflow index. These types of proportional streamflow signatures are bounded by zero and one. The metrics explored here are: (i) runoff ratio – the amount of runoff relative to the amount of precipitation received; (ii) zero flow ratio – represents intermittency and is defined as the proportion of time that water is not flowing; and (iii) baseflow index – defined as the proportion of the 'slow' component contribution to the streamflow (Table 3.3). Here we adopt the widely accepted baseflow definition as the portion of flow that comes from groundwater storage and other delayed sources – i.e., wetlands, lakes, snow and ice melting and channel bank storage (Hall, 1968; Smakhtin, 2001; Beck et al., 2013b). While numerous techniques are available to separate baseflow from streamflow, we used the Lyne and Hollick (1979) algorithm as its performance has been widely reviewed within Australian environments (Nathan and McMahon, 1990; Lacey and Grayson, 1998; Ladson et al., 2013; Li et al., 2013). Whilst there are many additional streamflow signatures to choose from, for the sake of parsimony in our analysis we focus on these three as they provide different perspectives on the governing hydrological processes and their variability between regions. These characteristics are also extremely relevant for both ecology and water resource management (Poff et al., 1997; Bunn and Arthington, 2002).

Table 3.3 Summary of streamflow characteristics and signatures.

Streamflow characteristic	Signature [acronym]	Source	Equation
Partition of Precipitation (P) into Streamflow (Q)	Long-term runoff coefficient [R_{QP}]	Milly (1994)	$R_{QP} = \frac{\sum_{i=1}^{n} Q}{\sum_{i=1}^{n} P}$ (1)
Fraction of slow component contribution into Q	Baseflow Index [BFI]	Lyne and Hollick (1979)	$BFI = \sum_{i=1}^{n} \frac{Q_b(i)}{Q(i)}$ (2)
Degree of intermittency	Zero flow ratio [R_{zero}]	Zhang et al. (2014)	$R_{zero} = \frac{N_{NF}}{N_S}$ (3)

(1) where Q and P are the long-term cumulative streamflow and precipitation;
(2) where Q_b and Q are the baseflow contribution over streamflow in a long-term basis;
(3) where N_{NF} is the number of zero flow days, and N_S is the total number of days within the streamflow time series.

Following Jaramillo and Destouni (2015) we used the Wilcoxon rank test to determine whether the three regions were significantly different in terms of these streamflow characteristics. The significance of the test results was also assessed using the Bonferroni correction (i.e., p-value $\leq$ 0.0125).

3.5.2 Assessing the importance of explanatory variables

We used random forests models in order to assess the importance of each explanatory variable on the response variable (Breiman, 2001). Random forests are a combination of classification trees that randomly select a set of possible explanatory variables without overfit. They are used for both predictions and to assess variable importance. The importance was computed by permutation, where the difference between prediction errors (mean square error - MSE) before and after the permutation of variables was averaged and normalized by the standard deviation. This procedure considered 3,000 trees. The importance is therefore given by the relative increment of MSE when the variable is removed. For the sake of model parsimony we only included the drivers which incremented the MSE by at least 5% when removed from the models and correlation coefficients lower than 0.6.

3.5.3 Statistical modelling of streamflow characteristics

We used Generalized Additive Models for Location, Scale and Shape (GAMLSS) (Stasinopoulos and Rigby, 2007) to model streamflow signatures with catchment biophysical properties as explanatory variables. GAMLSS are semi-parametric, as they use parametric distributions for the response variable and non-parametric smoothing functions for the explanatory variables. The beta distribution is appropriate for modelling rates and proportions (Ferrari and Cribari-Neto, 2004). GAMLSS is able to account for streamflow signatures scaled between zero and one by mixing continuous and discrete distributions when the response variable contains either of these cases (Ospina and Ferrari, 2010; Ospina and Ferrari, 2012).

Because our response variables are bounded between zero and one, we used beta (for R_{QP} and *BFI*) and zero-inflated beta (for R_{zero}) distributions to implement the non-linear beta regressions. The penalised B-splines (Eilers and Marx, 1996) non-linear smoothing function were used as additive terms. The degree of smoothing is selected automatically using penalized maximum likelihood in the gamlss package in R (Stasinopoulos and Rigby, 2007). To estimate the accuracy of the predictions of flow signatures, we randomly split the dataset using 90% for calibration and 10% for validation for the whole East Coast and 67% for calibration and 33% for validation in each of the three regions (Figure 3.3). We used a bootstrapping approach with 2,000 samples and assessed the model performance with the AIC and R^2.

We applied spline correlograms to examine spatial autocorrelation on streamflow characteristics and model residuals and test how the covariance of data pairs evolves as a function of distance. This is a nonparametric procedure to estimate spatial dependence as a continuous function of distance (BjØrnstad and Falck, 2001). The bootstrap algorithm with 1,000 resamples was used to estimate a confidence envelope around the covariance function.

3.6 Results

3.6.1 Streamflow characteristics across scales and regions

The streamflow signatures showed high variability throughout the East Coast and the three regions of eastern Australia (Figure 3.4). The regions with contrasting biophysical properties represent catchments with distinct streamflow characteristics. The Wilcoxon rank sum test showed each region to be statistically different in terms of the distribution of at least one of the assessed streamflow signatures. The test compared the frequency distribution of streamflow characteristics of the four regions (i.e., including the entire East Coast as a region in this analysis) and identified two distinct distributions for R_{QP}, and three for both *BFI* and R_{zero}, see Figure 4 parts (a), (b) and (c), respectively.

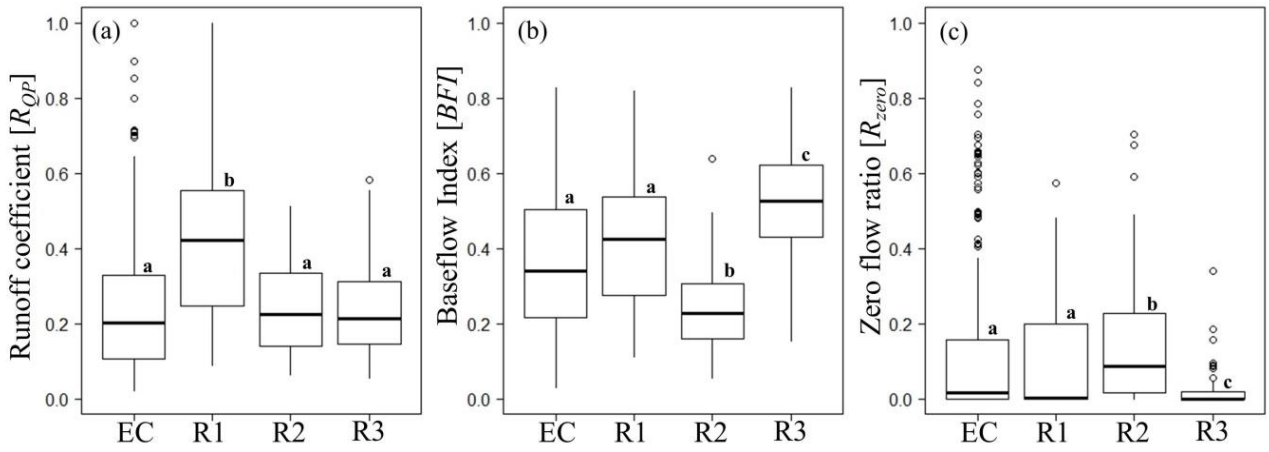

Figure 3.4 Box-Whisker plots of streamflow characteristics across the East Coast and the three biogeographical regions in eastern Australia: (a) Runoff coefficient, (b) Baseflow index, and (c) Zero flow ratio. The boxes are bound by the 25th and 75th percentiles of the datasets, while the heavy mid-line displays the median value. The upper and lower 'whiskers' represented by the vertical lines are the upper quartile plus 1.5 times the interquartile distance (IQD) and the lower quartile minus 1.5 times the IQD, where IQD refers to the inter-quartile distance. Dots are data points out of this range. Letters above the boxes denote whether the distributions of streamflow characteristics are significantly different among regions. Different letters indicate statistically different distributions (p-value < 0.0125 with Bonferroni correction) according to the Wilcoxon rank sum test.

There was no significant spatial structure in each of the streamflow characteristics, indicating the assumption of spatial independence of streamflow characteristics within and among the regions is justified (Figure A3.1 in Appendix 3).

3.6.2 Model performance of streamflow characteristics

The GAMLSS with beta distribution function showed a good overall performance in predicting streamflow indices using 24 catchment biophysical properties as explanatory variables (Table 3.4). The generally low standard deviations highlight the stability of the model fit regardless of catchment allocation for calibration or validation. The model fit was generally poorer at the sub-continental scale when compared to the three regions. Tests for goodness of fit of all selected models for the three streamflow characteristics returned *p*-values ≤ 0.05, thereby indicating good model fit. Similarly, residuals of the best models using the spline correlograms showed no significant spatial structure and therefore the assumption of spatial independence of the residuals was valid (Figure A3.2 in Appendix 3).

Table 3.4 Model parameter performance summary statistics using cross-validation with 2,000 bootstrap samples of three streamflow signatures across the whole East Coast (EC) and separately for each bioregion. R1 = Tropical catchments, R2 = Subtropical catchments and R3 = Temperate catchments. AIC is the Akaike Information Criterion and R^2 is the R-square value. Statistics are show for the mean ± standard deviation.

Streamflow signature	Region	Mean ± Standard deviation	
		AIC	R^2
Runoff Coefficient [R_{QP}]	EC	-617.9 ± 29.9	0.73 ± 0.02
	R1	-37.4 ± 11.8	0.92 ± 0.03
	R2	-107.6 ± 16.3	0.91 ± 0.03
	R3	-118.8 ± 10.8	0.89 ± 0.03
Baseflow Index [BFI]	EC	-578.2 ± 10.4	0.72 ± 0.04
	R1	-62.7 ± 21.6	0.88 ± 0.05
	R2	-80.9 ± 16.4	0.86 ± 0.03
	R3	-92.0 ± 8.6	0.85 ± 0.02
Zero Flow Ratio [R_{zero}]	EC	-382.2 ± 18.1	0.62 ± 0.03
	R1	-28.8 ± 26.8	0.88 ± 0.03
	R2	-64.8 ± 11.4	0.84 ± 0.05
	R3	-60.2 ± 14.1	0.69 ± 0.05

3.6.3 Drivers of streamflow characteristics

Dominant biophysical drivers

Figure 3.5 summarizes the modelling results and provides insights into biophysical controls of streamflow characteristics within the regions and for all East Coast catchments. Overall, the main

drivers governing the variability of streamflow characteristics are: (i) Dryness Index (relative importance greater than 5% in 100% of the 12 models); (ii) soil moisture (relative importance greater than 5% in 91.7% of models; and (iii) mean fPAR (relative importance greater than 5% in 83.3% of models). These explanatory variables represent the influence of climate, soils (hydro-pedological function), and vegetation respectively. Topography and physiography showed importance greater than 10% on streamflow characteristics only at regional scales for *BFI* and R_{zero}, which indicates that at the sub-continental scale *Q* generation variability was not primarily controlled by these explanatory variables. The Dryness Index and soil moisture appeared to exert a similar level of control over streamflow characteristics across all regions and at different spatial scales (Figure 3.5).

Runoff coefficient

An important mechanistic insight that emerges for R_{QP} is the strong negative relationship with Dryness Index and positive relationship with soil moisture (Figure 3.5), showing that the partitioning of *P* into *Q* is primarily determined by moisture availability (which in turn is related to the Dryness Index) across all regions. The inverse effects of the Dryness Index and the Seasonality Index also highlights that the partition of P into *Q* is controlled by the balance between the long-term atmospheric evaporative demand and intra-annual *P* variation. For instance, while the Dryness Index had a high weight in Region 1 which receives higher average annual precipitation, the Seasonality Index had a stronger weight in Region 3 that presents more mountainous catchments and a more seasonal climate. Another important variation was the different effects of soil variables across the regions. While the soil variables do not have a strong effect on R_{QP} variability at the continent scale, they do have a stronger effect and higher importance regionally. For example, in Region 1 the lower total soil depths and hydraulic conductivity in combination with high precipitation tended to increase R_{QP} values (Figure 3.5) probably by promoting runoff via infiltration excess overland flow. This effect, however, varies according to the subsurface lithology as denoted by the positive weight of soil pH (acidic soils tend to have lower R_{QP}). Conversely, for mountainous catchments in Region 3, R_{QP} values increase with increasing soil depth as most of the streamflow water relies on hillslope hydrological process with major streamflow contributions from sub-surface storages.

Baseflow index

With regard to *BFI*, the Dryness Index, mean fPAR and mean soil moisture were the most consistent controls with mostly positive and higher effects across the East Coast and the three separate regions (Figure 3.5). However, while soil moisture increases with *BFI* for all regions,

Region 1 presented an inversely proportional behaviour between *BFI* and seasonality and fPAR. This suggests that in tropical regions, both increasingly out of phase delivery of precipitation and increasingly photosynthetically active vegetation tends to diminish baseflow. A possible explanation is that the higher precipitation in tropical regions may be generating more overland flow, which tends to reduce the slow component contribution to the streamflow. Region 1 was also influenced by topography, with positive and negative effects for erosional fraction and slope respectively, indicating that steeper catchments in the tropics may have higher quick flow contributions probably due to the association with orographic *P*-generation effects and increasing overland flow. Soil characteristics have also shown relevance controlling *BFI* at continental and regional scales (Figure 3.5). Yet, the relevant soil characteristic controlling *BFI* varied across the different regions. Higher soil depth and conductivity tended to increase *BFI* for all eastern seaboard catchments, whereas clay content increased *BFI* in steeper catchments from Region 3. Furthermore, catchments from Regions 1 and 2 show a negative effect of hydraulic conductivity and bulk density on *BFI* respectively, highlighting that soil water may not be an important storage in Region 2 and preferential flow possibly dominates connectivity in Region 1. Interestingly, the minimum temperature had a high importance in the east coast region because it is a consistent proxy to summarise the variability of the large climatic gradient across the region and hence explain the *BFI*. Conversely, when the individual regions are considered separately the temperature variability is more homogeneous. Thus, others specific drivers better explained the *BFI* variability (i.e., *AET* in R1 and Mean Slope in R2). In Region 3, where catchments from both humid and dry tropics are encompassed, the temperature variability remains a good predictor of the *BFI*.

Zero flow ratio

The most consistent controls for streamflow intermittency across the different regions were Dryness Index and precipitation with positive and negative effect in R_{zero} respectively (Figure 3.5). However, in Region 1 soil moisture and depth were also important drivers controlling the negative effect in R_{zero}. This highlights that the intermittency of this array of tropical catchments is strongly determined by the subsurface storage characteristics. Precipitation does not appear to have an impact on R_{zero} in Region 1, probably because it is more sensitive to the storage capacity due to the highly seasonal precipitation regime here, but in other regions they are more sensitive to *P* than storage capacity. Catchment area also had a negative influence on R_{zero} in Region 1, which means that smaller catchments tend to be more intermittent within tropical regions. At the continental scale the minimum annual temperature and mean fPAR had a positive relationship with R_{zero}. This shows that the higher intermittency occurred in colder catchments with higher photosynthesis activity. At

the regional scale, the controls of intermittency are highly dependent on soil characteristics. For example, the intermittency of tropical catchments (R1) is strongly dependent on the available depth for moisture storage, while subtropical catchments (R2) are less influenced by soil depth. Wet season intensity is probably less, meaning the storage capacity may not always be reached, whereas in the tropics the storage capacity may be a much more limiting factor given the amount of rain available in the wet season. Similarly, temperate catchments (R3) tend to be more intermittent in soils with reduced saturated hydraulic conductivity with lower clay content.

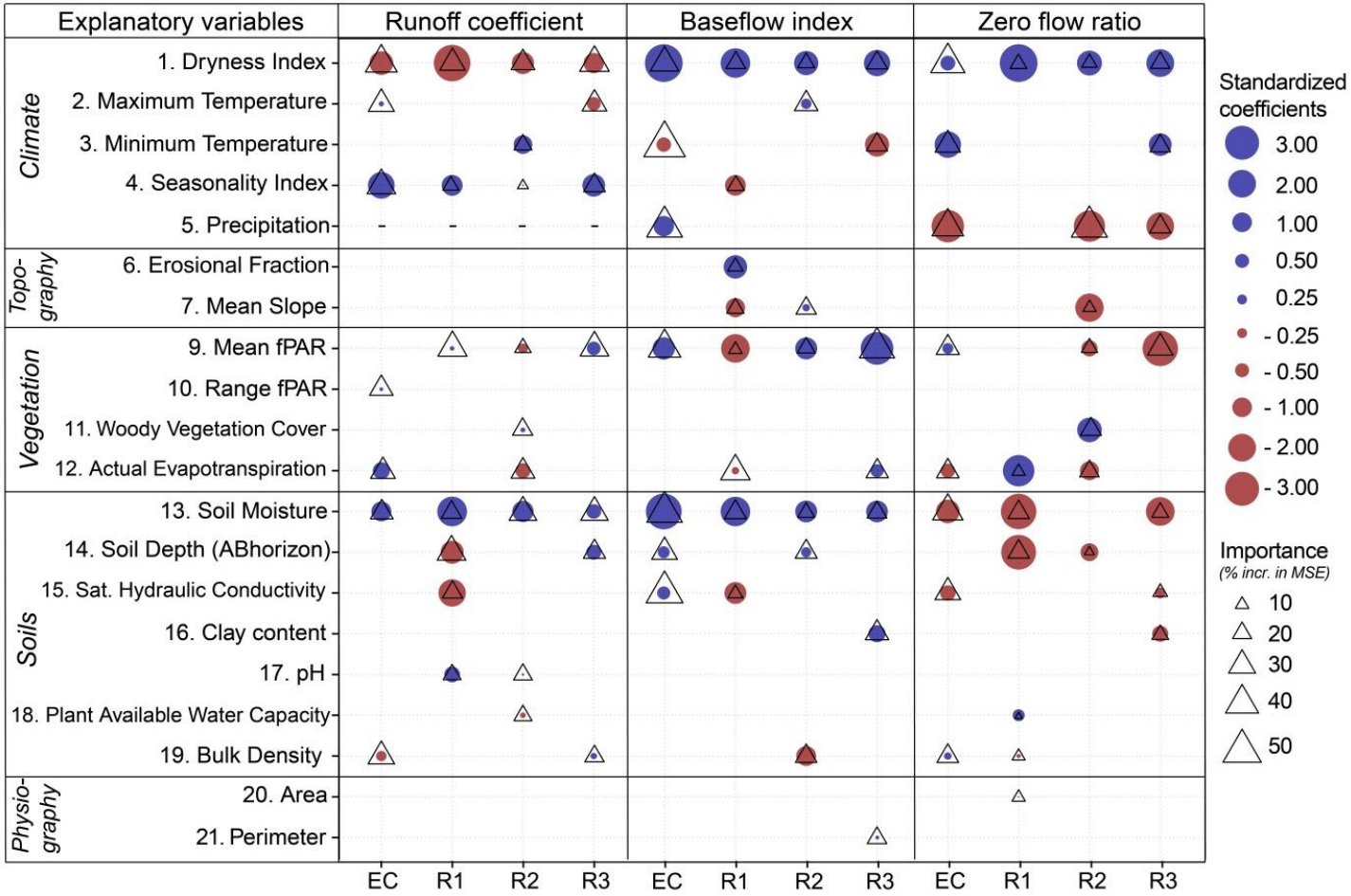

Figure 3.5 Standardized coefficients and importance of explanatory variables included in the subcontinent- and regional-level models. Explanatory variables were rescaled to have mean = 0 and variance = 1. Red and blue circles indicate negative and positive effects on flow signatures, respectively. Circle size indicates the magnitude of effects. Triangle size indicates the relative increment in the mean square error when the variable is excluded from the model. EC comprises catchments all over the East Coast; R1 is Region 1 comprised of tropical catchments; R2 is Region 2 including sub-tropical catchments from South East Queensland; and R3 is Region 3 with catchments from South Eastern Highlands; see Figure 2 for locations and Table 1 for basic physiographic and hydroclimatic catchment characteristics. Small dashes in runoff coefficient models indicate precipitation was not considered as it is in the response variable. Empty cells and explanatory variables not shown (i.e., #8, #22, #23 and #24) had importance lower than 5%.

3.6.4 Variability in climate and vegetation effects on streamflow characteristics

Figure 3.6 shows the degree to which the variability in streamflow characteristics are captured by the biophysical properties used in our models. It suggests that distinct regions have regionally-specific mechanisms driving the streamflow regime and the effects of climate and vegetation on streamflow appear highly variable. Some regions have the same response observed at continental scales (e.g., Dryness Index effect in R_{QP}, fPAR effect on *BFI* for East Coast and Region 2, and fPAR effect on R_{zero} for Regions 1 and 3), and on the other hand relationships between explanatory and response variables may differ when comparing between biogeographic regions (e.g., Dryness Index effect on R_{QP} for Regions 2 and 3 and fPAR effect on *BFI* for Regions 2 and 3). This highlight that these dynamic catchment biophysical properties may affect hydrological characteristics in different manners when experiencing shifts.

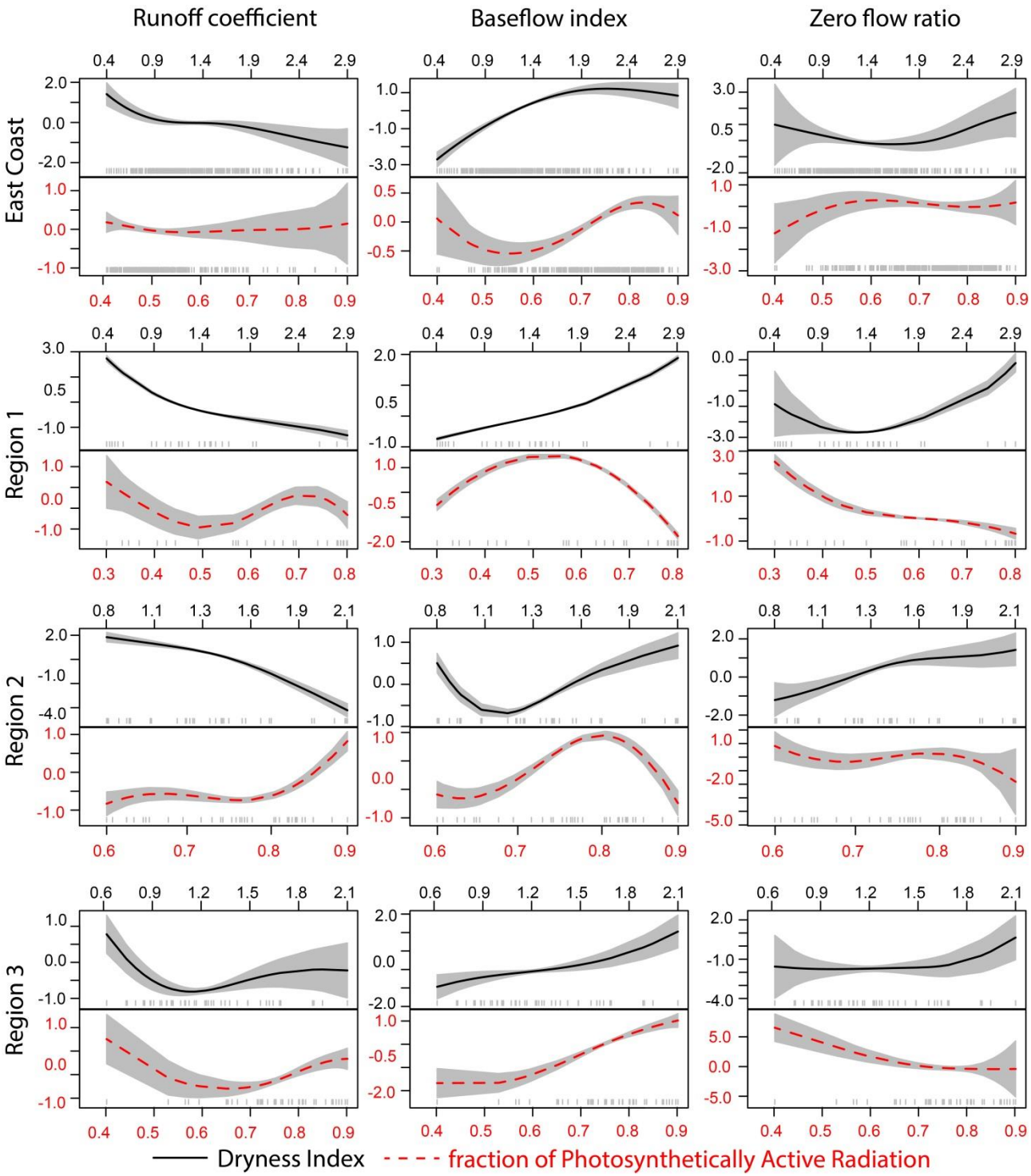

Figure 3.6 Partial effect (shown on the Y-axis) of climate (Dryness Index) and vegetation (fraction of Photosynthetically Active Radiation - fPAR) on streamflow characteristics by region. Filled and dashed lines are the B-spline smoothed partial effects of climate and vegetation respectively, grey shades around them show the standard errors (± 1 SE) and the small grey bars (aka 'rug ticks') on the bottom of each plot illustrate where the catchment-averages are located for the Dryness Index (upper pane of each sub-plot and upper X-axis labels) and fraction of Photosynthetically Active Radiation (bottom pane of each sub-plot and lower X-axis labels).

3.7 Discussion

3.7.1 Cross-regional similarities and differences

The drivers of long-term annual runoff coefficients are to the first order generally considered highly dependent on precipitation and potential evapotranspiration (or Dryness Index), with soil moisture and seasonality also playing an important role (Wolock and McCabe, 1999). Regional-scale studies have also reported permeability and geology as important controls of runoff coefficients (Ogunkoya et al., 1984; Norbiato et al., 2009). Our results are consistent with these drivers as saturated hydraulic conductivity and soil bulk density are associated with permeability and pH is, among other factors, a product of parent material weathering. Numerous studies have demonstrated the effect of land cover on runoff coefficients (Sriwongsitanon and Taesombat, 2011; Wang et al., 2012; Zhang et al., 2014). Our findings are consistent with this, yet vegetation variables were not the primary drivers of runoff (Donohue et al., 2010b). Rather, Dryness Index and soil moisture were more important to explain R_{QP} variability. This agrees with the findings by Hümann et al. (2011) that have previously highlighted the crucial effect of soil properties for runoff generation in German mountain ranges. In this study, specific soil properties emerged as important explanatory variables in regional models, with a stronger effect and importance at the regional-scale compared to the continent-scale (Figure 3.5). The regional soil properties controlling streamflow characteristics are generally consistent with relevant hydrological processes driving the streamflow regimes, such as soil depth and greater storage in tropical catchments and clay content and lower water residence time in temperate mountainous catchments.

In a global-scale study, the most important factors driving *BFI* were mean annual potential evaporation, mean snow water equivalent depth, and abundance of surface water bodies (Beck et al., 2013b). For global tropical catchments, mean annual precipitation and dryness index explained the major variability of baseflow recession rates (Peña-Arancibia et al., 2010). Our modelling results for *BFI* for the entire East Coast catchments are consistent with these global drivers and with the drivers reported by van Dijk (2010), who studied catchments from the same region. However soil characteristics (soil moisture, depth and saturated hydraulic conductivity) were also important in this study (Figure 3.5). Previous studies with *BFI* are consistent with our findings of the importance of substrate and soil characteristics for *BFI*. For instance, Schneider et al. (2007) highlight the importance of soils and the dominant paths of water movement to explain *BFI* variability across European catchments whilst Ahiablame et al. (2013) suggested that hydrological properties of soils may govern *BFI* variability at the regional scale in the USA. Likewise, van Dijk (2010) pointed out that the explanation of *BFI* can be improved if the relevant substrate properties

are also considered. This highlights the importance of soils in mediating slow flow component of streamflow through factors influencing both storage and transport, and that regional variability in the influence of soil properties are likely a trade-off between these factors.

At regional scales, previous work has found a mixture of controlling variables on streamflow characteristics. A regional study in south-eastern Australia found geology and ecological vegetation classes were the most important factors determining baseflow (Lacey and Grayson, 1998). Similarly, baseflow recession rates have been related to drainage density, geologic index, and ruggedness number in a regional scale study in the US (Brandes et al., 2005) while Bloomfield et al. (2009) reported lithology and aquifer structure as the most important controls on *BFI* in UK. Conversely, lithology was not reported as important for catchment streamflow in Zimbabwe (Mazvimavi et al., 2005). In Mediterranean catchments, a regional-scale modelling study showed that the changes soil and aquifer permeability with changing geology was the main driver of baseflow variability (Longobardi and Villani, 2008). For catchments within semi-arid Tanzania, the drivers of *BFI* were identified as climate and geology (Mwakalila et al., 2002). These findings combined show that geology related variables consistently emerges as a driver for *BFI* regionally, but not as often at continental scales. Our results are in accordance with this, although we only used surrogates for geology (i.e., topography, soils and physiography variables). For instance, soil moisture and clay content were identified as the main soil drivers of *BFI* in temperate regions (Region 3) whereas topographic controls (erosional fraction and slope) were more relevant in tropical and subtropical regions (Regions 1 and 2). Nevertheless, these drivers were not important at the scale of the entire East Coast. Vegetation (fPAR and actual evapotranspiration) were also important in explaining *BFI* variability in all regions. Similar insights have been made with regard to the forest growth stage and *BFI* (Lacey and Grayson, 1998) and soil moisture reduction has also been related to woody vegetation (Traff et al., 2015).

Intermittent streams have received little attention compared to perennial streams despite the fact that their cumulative discharge can contribute to more than half of the length and 30% of discharge of the global river network (Datry et al., 2014). While studies regarding controls on the degree of intermittency are not as common as for R_{QP} and *BFI*, the available literature suggests that intermittency should be associated with climate, geology, topography and land cover (Zhang et al., 2014; Costigan et al., 2016), yet the in-depth mechanisms interacting to control this intermittency in water-limited catchments remains poorly understood (Tooth, 2000). Our results build on these findings and provide additional evidence that specific soil properties may play a key role in explaining the variability in flow intermittency within regions. For instance, we show (Figure 3.5)

that soil moisture and depth were important to tropical and sub-tropical regions, while in temperate regions soil moisture, hydraulic conductivity and clay content were more important in explaining intermittency variability. In terms of processes interpretation, flow intermittency in tropical regions is most sensitive to soil storage parameters, since they generally receive a lot of water in the wet season. This means intermittency depends on this storage volume and its rate of release during the dry season. The other regions were more sensitive to precipitation and dryness index, since they are more limited by the amount of water available to be put into storage, rather than the amount of actual storage available.

To summarise, our findings sheds light on the variability of the dominant drivers of streamflow characteristics across regions and scales and provides meaningful insights into relevant hydrological processes and connections with landscape properties at distinct biogeographic regions.

3.7.2 Model generality

When models are generalized (calibrated in one region and used for predictions in other regions) and extrapolated (calibrated at regional scale and used for predictions at continent scale) the goodness of fit is substantially reduced (Figure 3.7). This shows that model generalizations and extrapolations can lead to inaccurate predictions and might be less useful at providing mechanistic insights into hydrological processes governing streamflow characteristics (Oudin et al., 2008). An explanation for the goodness of fit reduction lies in the disparity of catchment biophysical properties across the regions governing the flow paths and ultimately the streamflow characteristics within catchments. Despite the similarity in the statistical distributions of streamflow characteristics observed in some regions (e.g., East Coast, Region 2 and Region 3 for runoff coefficient), the drivers controlling the hydrological mechanisms are different, therefore making the model generality inaccurate. Previous studies highlighted the importance of regionalization of model parameters to make predictions in ungauged basins (Yadav et al., 2007; Zhang et al., 2008b) and recognized the ecological implications of regional differences (Hughes and James, 1989). Here we show that the calibration of regional models was strongly influenced by local characteristics of vegetation and soils and that specific coefficients assigned regionally cannot be transferred to other regions.

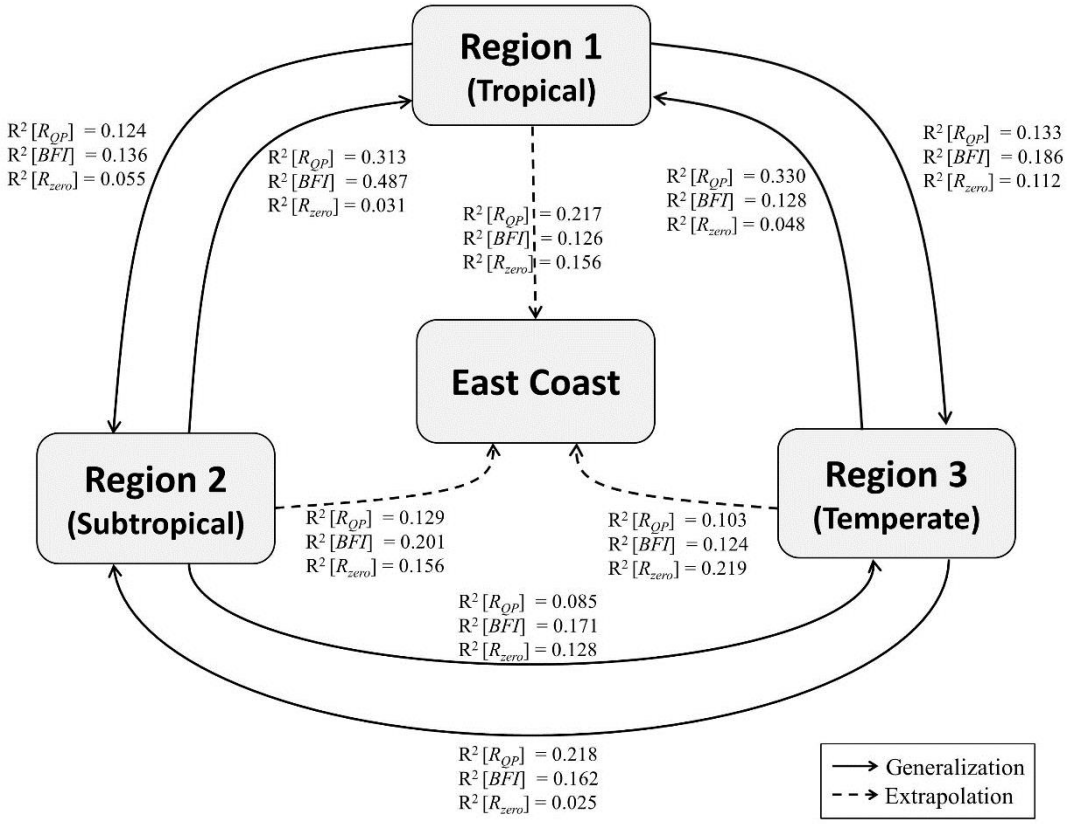

Figure 3.7. Goodness of fit (R^2) of the application of regional models to the other studied regions and extrapolation for the entire East Coast for R_{QP}, BFI and R_{zero}.

3.7.3 Implications for water resource management

This study investigated the regional variation in the dominant controls of three streamflow characteristics. The results are relevant to both human and natural systems. We pointed out the dominant catchment properties driving hydrological processes and ultimately streamflow characteristics that deliver relevant water-based ecosystem services to humans and the natural environment across distinct regions. The relevance to water resource management is that our findings highlighted the most important biophysical properties governing, noting that maintaining this functioning (to some degree) is a worthwhile management goal to avoid hydrological alterations (Mackay et al., 2014). Particularly in Region 1, where there is a concern regarding overland flow generation and transport of sediments to the Great Barrier Reef (Thorburn et al., 2013; Wilkinson et al., 2013) we show that catchments with lower Dryness Index, soil depth and hydraulic conductivity tend to produce more runoff and therefore could be prioritized for management strategies to reduce overland flow (Thorburn, 2013). Regions 2 and 3 include catchments playing important roles for urban water supply for cities like Brisbane (2.4 million people), Melbourne (5.2 million) and Canberra (0.4 million). We show that in subtropical catchments (R2) characteristics such as lower bulk density, higher soil depth and steeper relief are associated with higher baseflow contributions and lower flow intermittency. The same streamflow

characteristics in temperate catchments (R3) were explained by higher clay contents and lower minimum temperatures, which highlights that hydrological characteristics desired for the sake of water supply rely on specific catchment properties that vary between regions. From a management and policy perspective, catchments from different regions are expected to experience variable changes in streamflow characteristics as a result of climate change and vegetation modification. Also, given the successful extraction of unique factors governing key streamflow characteristics at these regions are already used for biodiversity conservation and ecology policies, this study shows that it is possible to co-opt water management at the same scale. Under the impacts of climate and land cover changes these regions are facing (McAlpine et al., 2009), these controls on streamflow may shift at decadal timescales at variable rates (Figure 6), which is critical to understand for future water management planning. In addition, our findings suggest that catchment management decisions based on assumptions made from generalizations or extrapolations from other regions may result in misleading guidelines and inappropriate management actions for the targeted catchment (Figure 3.7).

3.8 Conclusion

This study shows that several selected drivers, such as the dryness index and the fraction of photosynthetically active radiation from vegetation, explained the variability of flow characteristics at both regional and continental scales with distinct importance in the models. Soil properties had a significant effect on streamflow characteristics especially at regional scales. The importance and weights of these soil properties did vary across regions, and depended on the streamflow characteristics. The regional scale soil effects may contribute to the disparity between the importance of climate and vegetation effects that we have found across regions.

Our results showed that models used to estimate streamflow characteristics should not be generalised, as the explanatory variables and their importance changes from region to region and across scales. Hence, models calibrated in one region should not be used to inform decisions in other regions. Although useful to determine the primary controls in broader scales, studies undertaken at a continent scale may not be sensitive enough to capture regional controls and offer insights into regional-specific features driving variability of streamflow characteristics in biogeographically or hydrologically different regions.

The differences captured by our models across regions and scales provide useful insights for understanding the effects of catchment biophysical properties on specific streamflow characteristics. In general, climate, vegetation and soil moisture played key roles in explaining

streamflow characteristics in all regions, while soil properties helped to explain regional variability of streamflow regimes.

This study provides a methodological advance in using a combination of random forest and generalised additive models with beta distribution, for cross-regional and multi scale modelling in the field of ecohydrology. Our approach and its results have provided acceptable performances and cross-regional discrimination ability for determining the streamflow characteristics with catchment biophysical properties.

CHAPTER 4

DISENTANGLING VEGETATION GAIN AND CLIMATE CONTRIBUTIONS TO LONG-TERM STREAMFLOW CHANGES

Interactions between climate and land cover changes drive catchment streamflow. Agriculture at Barossa valley, South Australia. Photo by Steve Ryan (source: flickr.com).

This chapter is based on the following manuscript:

Trancoso R., Larsen J.R., McVicar T.R., Phinn S., McAlpine C. *Disentangling vegetation gain and climate contributions to long-term streamflow changes*. To be submitted to *Environmental Research Letters*.

4.1 Abstract

The water and energy balances of catchments are simultaneously affected by climate- induced change and land cover modification with significant implications for society and the environment. Disentangling these impacts is an important research priority to understanding current changes in streamflow and to inform water resource management. Here we explore the spatio-temporal dimension of water and energy balances of 193 catchments situated along a climatic gradient in eastern Australia by decomposing the climate- and land cover-induced changes in the long-term mean annual streamflow within the Budyko framework. We found that both climate-induced changes and land cover change are altering the water and energy balances of catchments in eastern Australia towards a streamflow reduction. We found a consistent displacement of catchments towards drier conditions. Although the observed streamflow reduction is driven by increasing aridity and evapotranspiration, the land cover-induced contribution was consistently higher in water-limited catchments while climatic-induced changes were higher in energy-limited catchments. We also found that the reduction in surface water is consistent with an increase in the photosynthetic activity of vegetation and a gain in biomass. Given the projected changes in future climate, the observed surface water reduction in eastern Australia may be more acute tan previously recognised, affecting societal water supply and environment, especially in regions already facing water scarcity.

Keywords: Streamflow changes; Climate change; Land cover changes, Budyko decomposition; Vegetation gain.

4.2 Introduction

Contemporary changes in climate and land surface conditions are impacting the hydrological cycle, and ultimately global water resources, via multiple pathways (Tomer and Schilling, 2009; Destouni et al., 2013; Wang et al., 2013; Jaramillo and Destouni, 2014; Tan and Gan, 2015). Disentangling the relative influence of how climate and anthropogenic land cover changes drive streamflow (Q) change is of critical importance for effective water resource adaptation and management. Climate changes impact Q largely through changes in precipitation (P), potential evapotranspiration (PET), and snowpack, while anthropogenic land cover change mainly impacts Q via changes in actual evapotranspiration (AET) rates (Tomer and Schilling, 2009).

While progress has been made in understanding climate change (Milly et al., 2005) and anthropogenic modification (Destouni et al., 2013; Sterling et al., 2013; Woodward et al., 2014) impacts on Q, much of the research focus has centred on anthropogenic modifications that decrease native vegetation cover (*e.g.*, clearing), causing a decrease in AET, and hence when experiencing steady-state conditions an increase in Q (Andréassian, 2004; Brown et al., 2005). Irrigation and flow regulation are also commonly reported anthropogenic drivers of Q reduction (Jaramillo and Destouni, 2015). However, there is also increasing evidence that many parts of the world are experiencing vegetation changes that can increase AET and decrease Q (Liu et al., 2015), such as native vegetation recovery following deforestation (*e.g.*, forest regrowth) (Beck et al., 2013a), reforestation (Feng et al., 2016) and CO_2 fertilization, particularly in water limited regions (Donohue et al., 2013; Ukkola et al., 2016; Trancoso et al., 2017a). Vegetation recovery following anthropogenic modification is likely to increase AET and decrease Q, however the scale of this potential impact across water and energy balance gradients is poorly known (Bruijnzeel, 2004; van Dijk and Keenan, 2007; Liang et al., 2015; Li et al., 2017). One possible reason is that many climate and land cover changes commonly occur simultaneously, and are difficult to disentangle at the catchment scale, especially at larger and heterogeneous catchments (Li et al., 2017; Zhang et al., 2017). Larger and heterogeneous catchments integrate multiple feedbacks happening simultaneously in a range of scales varying from leaves to landscapes, which are aggregated at catchment scale, compensating local effects (Wilk et al., 2001; Rodriguez et al., 2010).

The east coast of Australia is a good example of a heterogeneous region experiencing simultaneous land cover and climatic changes. In terms of land cover, extensive clearing of native vegetation began, and has been largely ongoing, since the arrival of European settlers in the late 1700s (Walker et al., 1993; Butzer and Helgren, 2005). However, from 1970 onwards, native vegetation policies have been changing and clearing fluctuated accordingly (Bradshaw, 2012; Evans, 2016). While

clearing continues in some areas (e.g. Brigallow Belt and Fitzroy Basin), many other regions have ceased clearing and logging native vegetation in the 1990s, which was then followed by an expansion of timber plantations or natural regeneration. This is important because the recovery of vegetation within previously cleared landscapes is likely contributing to documented increases in vegetation greenness (Fensholt et al., 2012) and biomass (Liu et al., 2015), in addition to CO_2 fertilisation effects (Donohue et al., 2013; Ukkola et al., 2016; Trancoso et al., 2017a). In terms of climate for the east coast of Australia, there is strong evidence for P declines (Delworth and Zeng, 2014) increased P variability (Goutam et al., 2017) and P extremes (Zhang et al., 2013; Bao et al., 2017), increases in PET and AET (Zhang et al., 2016b) and hence reduction in Q (Ukkola et al., 2016; Zhang et al., 2016a). However, despite these observed changes in land cover and climate, reliably quantifying their separate impacts on surface water resource availability remains a major research and management challenge.

In order to better understand these impacts, this study examines changes to the long-term water and energy balances of 193 catchments along a large aridity and streamflow regimes gradient on the east coast of Australia. Using the long-term displacement trajectory of catchments (Wang and Hejazi, 2011) along the Budyko curve (Budyko, 1974), which can simultaneously distinguish climate (P and PET) from land cover induced changes to AET and Q (Wang and Hejazi, 2011), our objectives are to:

(i) quantify the direction and magnitude of long-term shifts in the water and energy balances of catchments and how they scale across aridity and streamflow regimes gradients;
(ii) evaluate the relative impact of climate and land use changes on long-term water and energy balances; and
(iii) investigate whether these relative climate and land cover change impacts are linked to known land use patterns, as well as long-term changes in catchment photosynthetic activity and biomass.

The chapter is structured in four sections: section 4.2 introduces the problem and aims; section 4.3 describes the data and approach; section 4.4 presents the results and discussion and section 4.5 draws the conclusion. The approaches related to each of our three objectives are described, respectively, in three subheadings of section 4.3.3 and, likewise, the results and discussion for each objective are reported in sections 4.4.1, 4.4.2 and 4.4.3, respectively.

4.3 Material and methods

4.3.1 Study area and data

The study was conducted along a continental climatic gradient of 193 catchments in eastern Australia spanning Tropical, Sub-tropical, Temperate and Mediterranean climates. The catchments are a subset of those described in Trancoso et al. (2016), but with longer and more complete time series. We used daily Q time-series from 1971 to 2010 (40-years), aggregated to the annual scale. We only used catchments with at least 95% of valid daily Q in entire time-series, with any missing days were filled using linear interpolation. We mapped catchment boundaries using a hydrologically conditioned digital elevation model (Wilson et al., 2011) with a 30 m of spatial resolution. The catchment's drainage areas range from to 13.1 km^2 to 3299.3 km^2, with latitude varying from 16.73 S to 41.64 S and aridity index ranging from 0.48 to 2.86. We used daily gridded P (Jones et al., 2009) and monthly gridded Priestly-Taylor PET time-series (Raupach et al., 2012), then aggregated to the annual scale, with approximately 5 km of spatial resolution. The catchment boundaries were used to extract average daily values for each catchment. We used a 50 m land use map that combines catchment scale land use data (CLUM) from all Australian states with the date of mapping ranging from 1997 to 2012 derived from Landsat-like satellite data and field information (ABARES, 2014). We also used biomass maps with spatial resolution of 0.25º from 1993 and 2010 (Liu et al., 2015) and fraction of Photosynthetically Active radiation (fPAR) from 1990 and 2010 with ~ 1 km of spatial resolution (Donohue et al., 2008).

4.3.2 Approach

Assessing long-term shifts in the water and energy balances

Exploratory analysis of our dataset revealed that the average change point of all Q time-series is not significantly different (one sample t-test, $p < 0.001$) from 1990, the mid-point between 1971 and 2010. Utilising this, our analysis compares how the earlier 20-year period (1971 – 1990; denoted T1 herein) changed in relation to the later 20-year period (1991 – 2010; denoted T2 herein). We therefore, use the long-term annual average of T1 and T2. Over these long time scales, the variability in storage can be neglected and therefore the AET can be determined as the difference between P and Q.

To allocate catchments within the Budyko framework and to examine the displacement from period T1 to T2, we computed the dryness index (PET/P) and evaporative index (AET/P) for each period. In this approach, following Tomer and Schilling (2009), horizontal displacement indicates change in atmospheric demand, whereas vertical displacement reveals change in catchment water use. Per

Liang et al. (2015), we calculated the changes of direction (θ) and magnitude (β) from T1 to T2. These analyses are presented across the aridity and streamflow regimes. The three aridity regimes follow McVicar et al. (2012b): (i) water-limited (PET/P > 1.2); (ii) equitant (0.8 > PET/P < 1.2 or catchments that are water-limited and energy-limited for parts of the year); and (iii) energy-limited (PET/P < 0.8). The streamflow regimes follow Trancoso et al. (2016) classification of Australia's east coast catchments.

Evaluating climate vs anthropogenic impacts in Budyko space

Changes in the water and energy balances can be related using Choudhury (1999) formulation of the Budyko framework (see Figure A4.1 in Appendix 4), which tracks the ratio of mean annual AET to mean annual P (*i.e.*, Evaporative Index) with the ratio of PET to P (*i.e.*, Dryness Index) as a one parameter (*n* which is italic herein the distinguish it from the number of catchments represented by a non-italic lower case n herein) power-law function:

$$AET = \frac{P \times PET}{(P^n + PET^n)^{1/n}}, \quad (1)$$

Using this approach, catchments experiencing a changing climate will vary their water and energy balances by moving along the Budyko curve, while land cover modifications only impact the partitioning of P into Q and AET (the vertical axis). This follows the 'decomposition' method of Wang and Hejazi (2011). Since the land cover modifications only impact AET in the Budyko framework, this was isolated first as:

$$\Delta Q^L = P_2(AET_{2`}/P_2 - AET_2/P_2), \quad (2)$$

where ΔQ^L is the magnitude of the land cover-induced change on Q, $AET_{2`}$ is the actual evapotranspiration as predicted by the Budyko curve for T2 (using n values calibrated separately for each catchment), P_2 is the precipitation in T2, and AET_2 is the actual evapotranspiration in T2 obtained by the difference between P and Q. The climate-induced change on Q is then obtained as the difference:

$$\Delta Q^C = \Delta Q - \Delta Q^L, \quad (3)$$

where ΔQ^C is the magnitude of the climate-induced change on Q and ΔQ is the total change in streamflow between the two periods:

$$\Delta Q = Q_2 - Q_1, \quad (4)$$

where Q_1 and Q_2 are the long-term mean annual streamflow for the first and second time periods respectively.

Changes in water and energy balances of catchments with vegetation gain

To assess whether the observed hydrological changes relate to vegetation gain we calculated the increment in fPAR and biomass from 1990 (end of T1) to 2010 (end of T2) and select s subset of 47 catchments with Δ fPAR ≥ 0.1 and increasing biomass. We then used a land use map to determine the dominant land use categories of catchments. In addition, for each catchment, we have determined the change in calibrated *n* parameter across the two periods from Choudhury (1999) form of the Budyko framework (equation 1).

4.4 Results and discussion

4.4.1 Long-term shifts in the water and energy balances

We found strong evidence that changes in P, PET and AET across the last four decades have impacted the water and energy balances of eastern Australian catchments towards a drier surface and atmosphere. All aridity and streamflow regimes have increased PET and reduced P, hence aridity has increased from T1 to T2 (Table 4.1 and Figure 4.1a). This is consistent with observed declining trends in P associated with a complementary increasing trends of PET (Gordon et al., 2003; Timbal and Fawcett, 2012; Delworth and Zeng, 2014; Karoly, 2014; Traff et al., 2015; Sarojini et al., 2016). Most catchments also experienced an increase in AET, with the greatest increases occurring in energy-limited and equitant regions that have predominantly perennial streamflow regimes (Table 4.1 and Figure 4.1a).

Table 4.1. Human- and climate-induced long-term annual changes in aridity and hydrological regimes from period 1971-1990 to 1991-2010.

Regime classes	n [-]	ΔP [mm]	ΔPET [mm]	ΔAET [mm]	ΔQ [mm]	ΔQ^L [mm]	ΔQ^C [mm]
Aridity regime							
Water-limited	85	-66.3	29.3	-7.0	-59.3	-27.2	-32.1
Equitant	79	-110.5	31.2	33.5	-144.0	-63.9	-80.1
Energy-Limited	29	-133.9	25.9	35.6	-169.5	-57.1	-112.4
Hydrological regime							
Ephemeral highly erratic	14	-84.5	28.3	-41.1	-43.4	-15.4	-28.0
Ephemeral erratic	54	-78.9	30.0	1.2	-80.1	-37.2	-42.9
Perennial erratic	30	-102.5	29.2	35.3	-137.8	-75.0	-62.7
Perennial regular	64	-109.3	30.8	23.5	-132.7	-51.4	-81.3
Perennial highly regular	31	-87.7	27.2	33.2	-120.9	-39.4	-81.5
All catchments	193	-95.5	29.6	14.7	-110.2	-46.4	-63.8

The displacement tends to be smaller for lower aridity values because there is less of an option for the catchments to move into the energy-limited region, whereas as the aridity increases, so does the variability, and therefore the displacement becomes larger. While the displacements in the energy-limited and equitant regions tend to be dominated by changes in the evaporative index, in the water-limited-region, the increasing dryness index is clearly dominating. Interestingly, this in interpreted as wetter catchments are trending towards a drier land surface but a wetter atmosphere (less Q and more AET). On the other hand, drier catchments are trending towards drier surfaces and drier atmospheres (less Q and less AET). The consistent displacement towards higher atmospheric demands (*i.e.*, higher dryness index) is gradually moving catchments into the adjacent aridity regions; *i.e.*, catchments originally energy-limited are moving towards the equitant region, equitant catchments are moving towards the water-limited region and water-limited catchments are getting drier (Figure 4.1b). This provides important observational evidence clearly supporting non-stationarity in the long-term hydrological cycle (Milly et al., 2008), with important implications for future water resource availability if these trends persist. With regards to the displacement by streamflow regimes, all regimes are moving towards the upper right direction (*i.e.*, increasing both aridity and evaporative indices). However, there is also a clear gradation in the dominance of these components according to streamflow regime (*i.e.*, runoff generation processes). In the perennial regular regime catchments, the increase in evaporative index is dominant. In contrast, for the ephemeral erratic regime catchments, the increase in the aridity index dominates the displacement (Figure 4.1c).

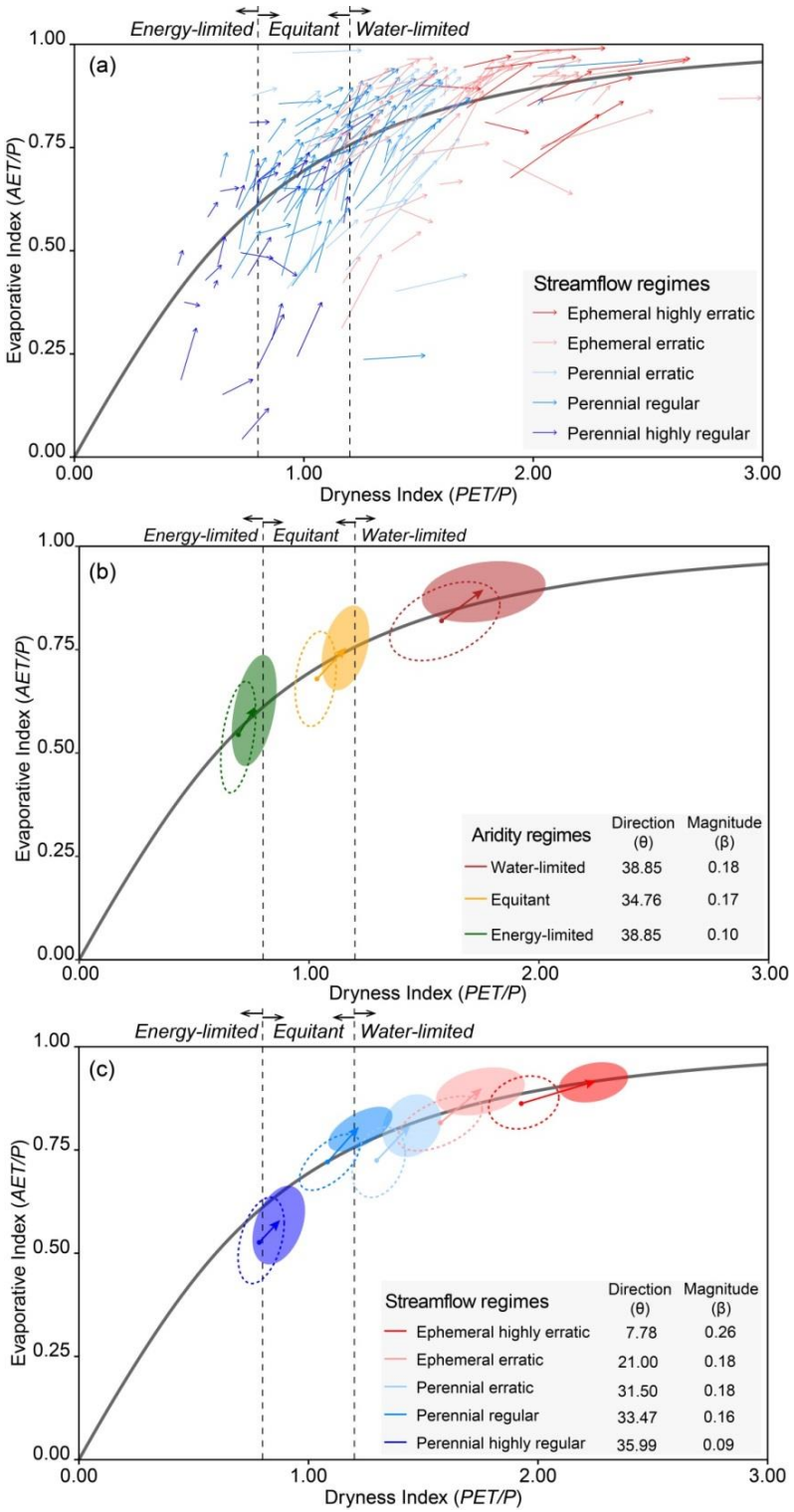

Figure 4.1 Displacement in the Budyko framework space from 1971-1990 compared to 1991-2010 across 193 catchments. (a) Arrows display the displacement of individual catchments from the pre-change (starting point) to post-change period (arrowhead). Colours refer to a spectrum of streamflow regimes. (b) Averaged displacement of the 30% central cluster of aridity regime: water-limited (PET/P ≥ 1.2), equitant (0.8 > PET/P < 1.2) and energy-limited (PET/P ≤ 0.8) catchments. (c) Averaged displacement of the 30% central cluster of streamflow regime. In (b) and (c) dashed ellipses represent the pre-change values while filled ellipses are the post-change values. Arrows denote the displacement of ellipses centroids. The legend shows the changes of direction (θ) and magnitude (β). The number of catchments in each strata used in (b) and (c) are reported in Table 4.1.

4.4.2 Separating climate and anthropogenic induced changes to water and energy balances across aridity and streamflow regimes

We found that 96% of the 193 catchments showed long-term annual average Q declines when comparing the 1971-1990 and 1991-2010 periods. The magnitude of change ranged from -545.6 mm to +106.9 mm, with a mean of -110.4 mm and a standard deviation of 106.6 (Figure 4.2a). Energy-limited and equitant catchments showed the greatest reduction in total Q compared to the water-limited catchments. Likewise, the greatest magnitude of decrease occurred in catchments with perennial Q. This is somewhat expected given these catchments originally had a greater annual Q to begin with (Figure 4.2a).Large variability was observed in the climate- and land cover-induced contributions to the magnitude of changes in total Q (Figure 4.2b). The energy-limited and equitant catchments with perennial regimes had major contributions in Q changes also because they have greater annual Q to begin with (Figure 4.2b). However, when these climate- and land cover induced changes are considered in relative terms, this reveals that water-limited and equitant catchments with ephemeral flow regimes are more sensitive (Figure 4.2c).

The greatest relative reductions in Q occurred mostly in the central and southern sections of the east coast catchments whereas tropical (Queensland) and temperate (Tasmanian) catchments experienced relatively minor Q reductions (Figure 4.3a). When looking at the dominance of climate- (50.3%) or land cover induced changes (49.7%) in Q, some interesting patterns emerge including: (i) Q changes in the Australian Alps are mostly dominated by climate modifications; (ii) Q changes in Tasmanian catchments were mostly attributed to land cover impacts; (iii) a major cluster of land cover induced changes emerged in the north coast of New South Wales; and (iv) a few smaller clusters of climate-induced dominated changes emerged along the Queensland coast. The observed climate-induced Q reductions in the Snowy Mountains (see Figure 4.3b) are consistent with the evidence for decreasing snow cover (Hennessy et al., 2008; Green and Pickering, 2009), and its expected impact on Q as a result of climate change (Berghuijs et al., 2014b; Reinfelds et al., 2014).

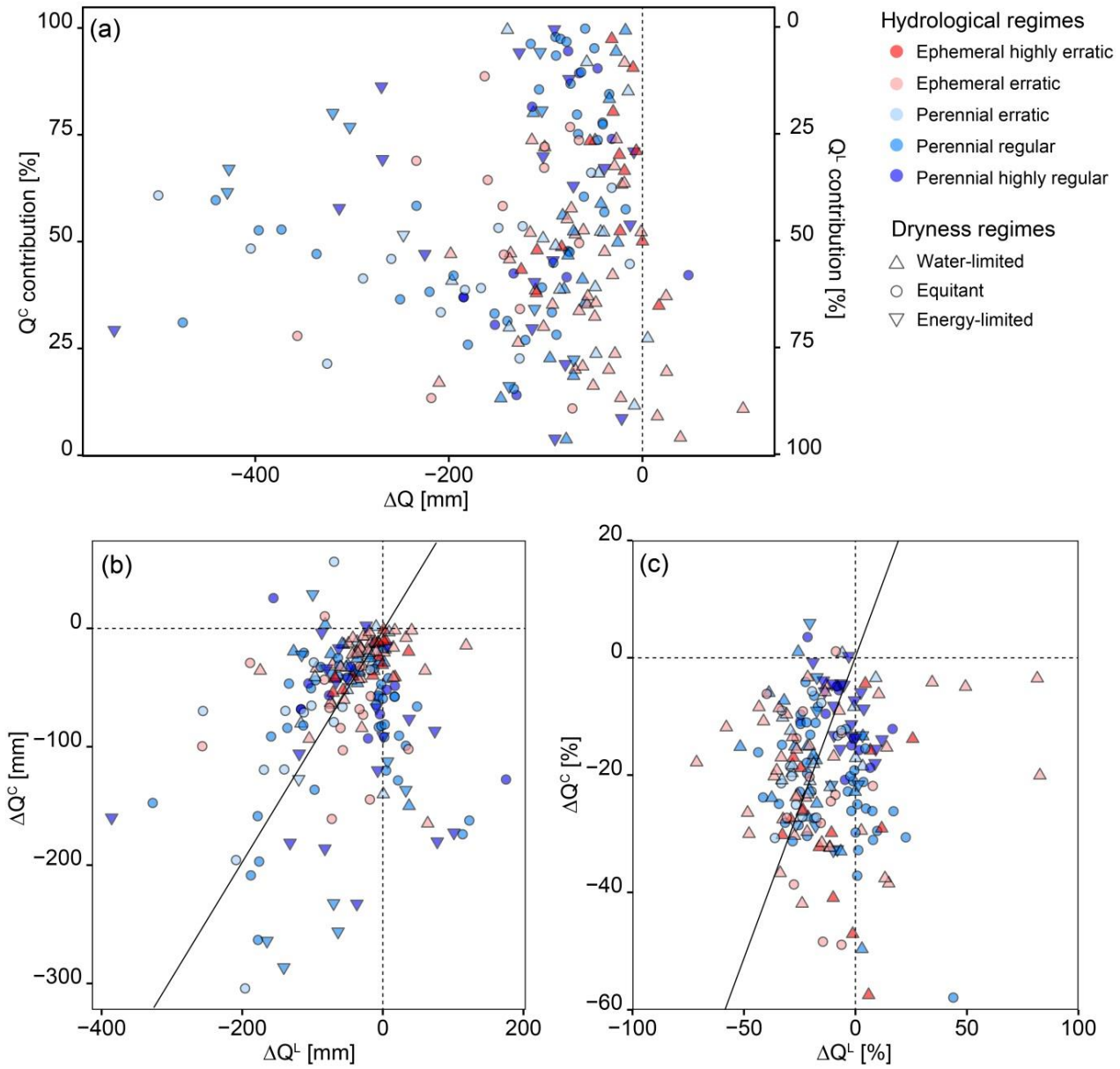

Figure 4.2 Climate- and direct land cover-induced changes in the streamflow of 193 catchments by dryness and streamflow regimes. (a) Magnitude of change in streamflow (ΔQ [mm]) in relation to prechange period and relative contribution of climate- (ΔQ^C [%]) and land cover-induced (ΔQ^L [%]) components. (b) Magnitude of climate- (ΔQ^C [mm]) and land cover-induced (ΔQ^L [mm]) components of streamflow change. (c) Relative change of climate- and land cover-induced components [%] in relation to the 1971-1990 period. Colours refer to the spectrum of streamflow regimes and symbols refer to the dryness regime.

The spatial distribution of climate- and land cover-induced relative changes in Q also provides relevant insights into the possible cause of Q declines (Figure 4.3c and 4.3d). Both climate- and land cover-induced change are simulataneously contributing to reductions in Q. The climatic contribution component is consistent with evidence for both decreasing P trends (Delworth and Zeng, 2014; Sarojini et al., 2016) and increasing AET trends (Zhang et al., 2016b).

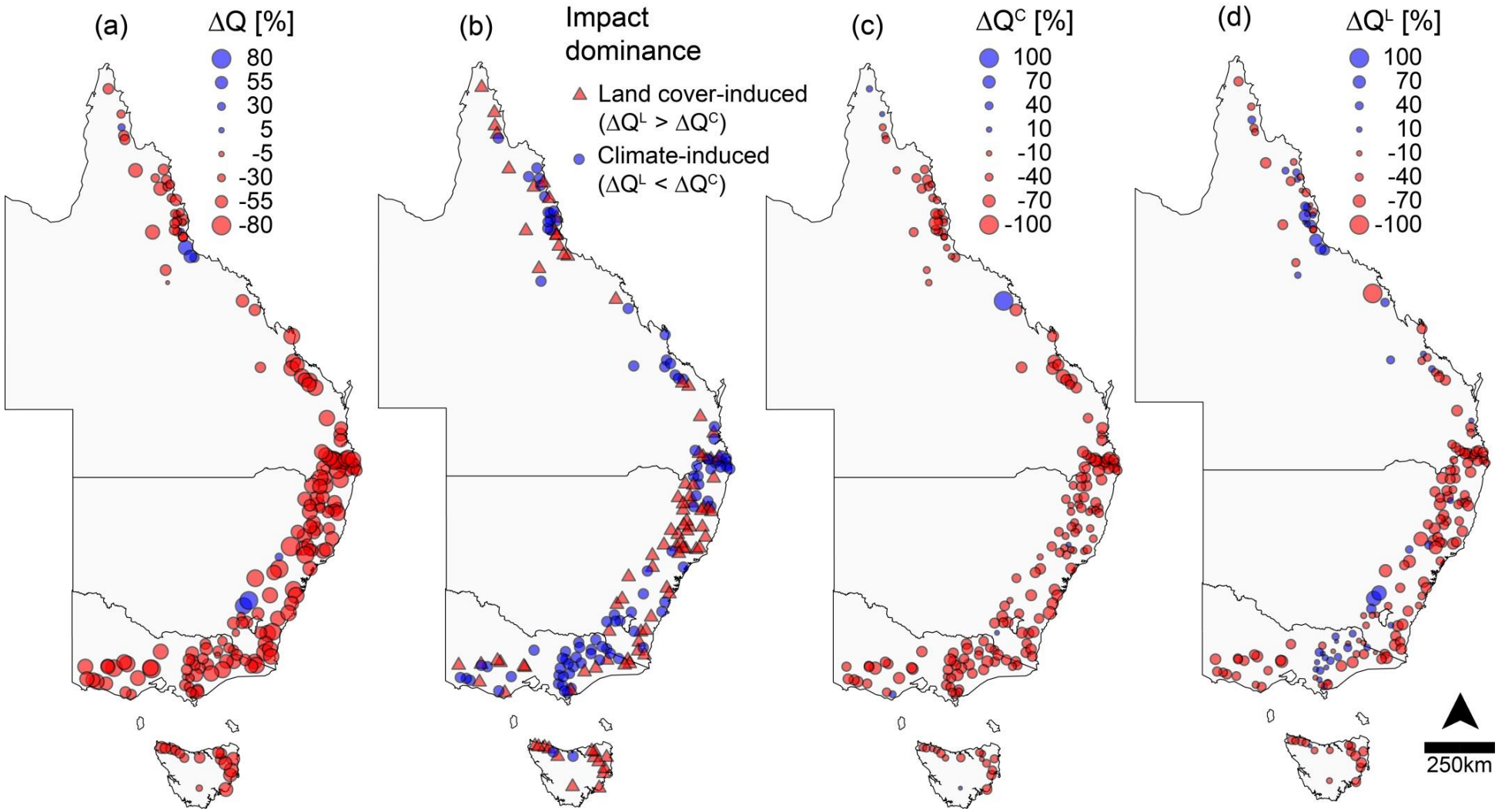

Figure 4.3 Spatial distribution of changes in the streamflow of 193 catchments: (a) change in 1991-2010 streamflow relative to the 1971-1990 pre-change period (ΔQ [%]); (b) dominance of either climatic- or land cover-induced impact; (c) climate-induced (ΔQ^C [%]) and (d) land cover-induced (ΔQ^L [%]) changes in streamflow relative to the 1971-1990 period.

Next, we examine the impact of climate- and land cover-induced Q changes relative to existing surface water resources and streamflow processes for the 193 catchments. We then group catchments according to aridity and streamflow regimes to assess the overall differences and sensitivity these regimes have regarding the relative role of climate and humans in Q changes. Figure 4.4a shows that water-limited catchments are most sensitive to both climate- and land cover-induced modifications, and that this sensitivity decreases for equitant and energy-limited regimes. While energy-limited catchments on average are dominated by climate-induced changes, equitant and water limited catchments are dominated by landscape-induced changes (Figure 4.4a). These results are supported by previous studies showing the influence of changing aridity and other factors such as land cover on the water and energy balances (Gudmundsson et al., 2016), where water-limited regions are more sensitive to all factors that influence Q (Ukkola et al., 2016). With regards to streamflow regimes, Figure 4.4b shows that the contributing pattern of climate- and land cover-induced modifications is not as clear. Yet, in ephemeral highly erratic regimes the climate-induced contribution was far greater than the land cover-induced contribution when compared to the other regimes. In ephemeral and perennial erratic regimes the land cover-induced contribution was slightly greater than the climate contribution. Perennial highly regular regimes had smaller contributions of both climate- and land cover-induced modifications compared to the other regimes, and these contributions are substantially increased in perennial regular regimes (Figure 4.4b). Considering the relationship between the water and energy balances and the streamflow generation processes (Trancoso et al., 2016), the climate and land cover-induced impacts on water and energy balances can implicate in changes in essential hydrological processes for society and environment (Bunn and Arthington, 2002; Lytle and Poff, 2004),

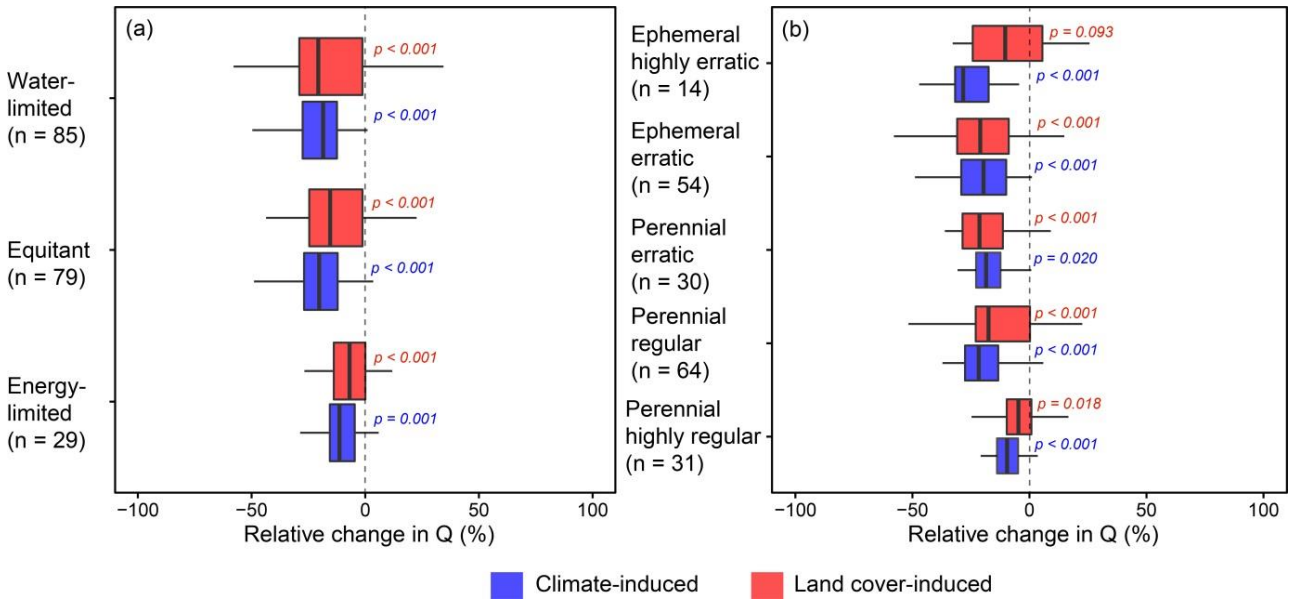

Figure 4.4 Relative climate- and land cover-induced contribution on streamflow changes in relation to pre-change period. Changes are compared among (a) water-limited (PET/P ≥ 1.2), equitant (0.8 > PET/P < 1.2) and energy-limited (PET/P ≤ 0.8) catchments and (b) among streamflow regimes (see Trancoso et al (2016) for a full description of streamflow regimes). Box plot statistics include the median (internal thick vertical line), interquartile range (IQR - denoted by the box), and horizontal lines (or whiskers) are calculated as $\pm 1.58 \times \mathrm{IQR}/\sqrt{n}$. The p-values beside the boxes refer to the probability that the mean impacts are not different from zero using a one sample t-test.

4.4.3 Changes in water and energy balances of catchments with vegetation gain

Next, we ask whether the observed reductions in Q are associated with vegetation gain. We then determine the changes in fPAR and biomass that took place from the end of T1 (1990) to the end of T2 (2010) and select 47 catchments with Δ fPAR ≥ 0.1 and increasing biomass and group them by dominant land use class (Table 4.2). We find that fPAR and biomass have increased in all land use categories from 1990 to 2010. These increases are consistent with observed changes in the Evaporative Index and in the *n* parameter from the Choudhury (1999) Budyko type model, that accounts for catchment properties and partition of P into Q and AET (Table 4.2). This is strong evidence that the increasing AET in catchments may relate to changes in vegetation functioning and water-use efficiency.

Table 4.2. Hydrological and vegetation changes for the catchments with Δ fPAR ≥ 0.1 and increasing biomass per dominant land use. Vegetation metrics represent change in the 2010 signal (end of T2) relative to the 1990 signal (end of T1), expressed as a percentage of the 1990 signal.

Dominant land use	n [-]	Δ fPAR [%]	Δ biomass [%]	Δ *n* [-]	Δ PET/P [%]	Δ AET/P [%]	Δ Q^L [%]	Δ Q^C [%]
Natural vegetation	23	22.39	7.29	0.34	17.39	19.71	-16.44	-25.19
Forestry	7	18.11	5.93	0.56	8.98	13.70	-17.60	-12.84
Grazing	10	19.86	16.81	0.38	11.57	17.29	-11.79	-19.22
Grazing and forestry	7	28.84	11.03	0.49	6.79	13.47	-16.87	-10.77
Total	47	22.18	9.74	0.38	13.19	16.92	-13.64	-19.94

Catchments dominated by grazing and forestry experienced major changes in fPAR, biomass and the *n* parameter (Table 4.2). Considering the 96 catchments with dominant land cover-induced impact (*i.e.*, the red triangles in Figure 4.3b), fPAR increased in 83.5% and biomass increased in 88.7% between the two periods. Interestingly, even catchments with large extents of native vegetation cover have experienced significant land cover-induced changes in Q, consistent with increases in the *n* parameter as well as in fPAR and biomass (Liu et al., 2016). The overall consistency between increasing fPAR, biomass gain, increasing AET and *n* parameter, and decreasing Q regardless the land use aligns with upward trends in vegetation greenness (Fensholt et al., 2012; Liu et al., 2015) that can be attributed to several potential factors: reforestation, natural regrowth (Arnold et al., 2012) and changes in vegetation feedbacks due to elevated atmospheric CO_2 (Donohue et al., 2013; Lu et al., 2016; Ukkola et al., 2016; Yang et al., 2016b). Despite the substantial impact of land cover-induced changes on Q, the climate-induced contribution was generally greater across all land use types.

The observed Q reductions due to land cover changes are also supported by an increase in fPAR and vegetation biomass across the majority of Australian east coast (Liu et al., 2015). Increasing biomass via either reforestation or natural regrowth is likely to lead to a reduction in Q (Andréassian, 2004; Bruijnzeel, 2004; Brown et al., 2005; van Dijk and Keenan, 2007; Liang et al., 2015). The major cluster of land cover-induced changes in the northern coast of New South Wales is consistent with the Australian hotspot of biomass gain, where an increment of up to 2 Mg C ha^{-1} $year^{-1}$ has been reported (Liu et al., 2015), thus linking increases in AET with vegetation regrowth following anthropogenic land cover changes.

Interestingly, the small number of catchments that had increased Q are located in the dry tropics or in the alpine region (Figure 4.3a). They also had the largest relative contribution of land cover driven impacts (Figure 4.2a and 4.3b). The observed increases in the dry tropics are within the Brigalow region (Evans, 2016), which experienced extensive clearing of open woodland / savannah

for agriculture and grazing during the 1980s (in the pre-change period). Such land-cover modifications increase cathment runoff (Cowie et al., 2007; Thornton et al., 2007; Peña-Arancibia et al., 2012). The incresing Q observed in the catchments adjacent to the Australian Capital Territory, for example, is consistent with a loss in biomass across this region between 1993 and 2012 (Liu et al., 2015). Likewise, southern catchments with increasing Q due to land cover changes (Figure 4.3d) also experienced a loss in vegetation biomass up to -2 Mg C ha^{-1} $year^{-1}$ (Liu et al., 2015). Increasing Q as a result of decreasing biomass and AET is a well-known catchment response consistent with field experiments worldwide (Brown et al., 2005; Andréassian et al., 2012). However, the climate component dominated their hydrological response (Figure 4.3b and 4.3c), resulting in an overall decline in Q.

Where deforestation is the major land cover change, AET is expected to increase. However, the hydrological impact of vegetation gain has received comparatively little attention (Andréassian, 2004; Li et al., 2017; Zhang et al., 2017). Exceptions apply in regions that experienced extensive reforestation (Xu et al., 2014; Liang et al., 2015; Feng et al., 2016; Ning et al., 2016). Although many regions globally have experienced considerable historical deforestation, a global reversal in forest loss has been reported (Liu et al., 2015) and many parts of the world, especially water-limited, are getting greener (Fensholt et al., 2012). This is consistent with a global increase in AET during the last three decades. Evidences have also pointed out that irrigation and streamflow regulation not only increased AET, but also reduced local runoff variability over the last century (Jaramillo and Destouni, 2015). Our results show that a recent increase in fPAR and biomass due to vegetation regrowth (Bruijnzeel, 2004; Beck et al., 2013a), reforestation (Xu et al., 2014) and CO_2 fertilization (Donohue et al., 2013; Ukkola et al., 2016; Trancoso et al., 2017a), in addition to climate changes, is a likely contributor to the overall increasing AET and decreasing Q along the east coast of Australia.

4.5 Conclusion

The research findings presented here show that over the last four decades, catchments situated along the Australian east coast experienced significant changes in streamflow as a result of both climate change and direct land cover-induced modifications. These changes altered the water and energy balances of catchments towards a drier condition (higher aridity) with higher AET and therefore less Q. This displacement within the Budyko framework space is consistent across all catchments regardless of the streamflow regimes, aridity regimes and land-use characteristics. We have also found that the reduction in Q seems to be associated with an increase in the photosynthetic activity of vegetation and a gain in biomass. Overall the contribution of climate and direct-human induced changes in Q changes was similar, despite the large spatial variability in the dominance of these drivers. However, water-limited catchments experienced slightly more direct land cover-induced changes than climatic changes on Q changes, whereas in equitant and energy-limited catchments the contribution of climate was slightly greater than land cover-induced changes. The consistent climatic shift towards a higher atmospheric demand (*i.e.,* higher aridity), catchments within energy-limited region are gradually moving to the equitant region, equitant catchments are moving to water-limited region and water-limited catchments are becoming drier. We also show that the land cover-induced reductions in Q are consistent with vegetation gain (*i.e.,* increasing photosynthesis activity and biomass). These observed changes suggest a reduction in surface water availability and have important implications for environmental and societal water supply needs.

.

CHAPTER 5

CO_2 – VEGETATION FEEDBACKS AND OTHER CLIMATE CHANGES IMPLICATED IN REDUCING BASEFLOW

Vegetation feedbacks with atmosphere determine the catchment freshwater budget. Mamu rainforest, Wooroonooran National Park, Queensland. Photo by Angus Mckenzie (source: flickr.com).

This chapter is based on the following manuscript:

Trancoso R., Larsen J.R., McVicar T.R., Phinn S., McAlpine C. (2017) CO_2 – vegetation feedbacks and other climate changes implicated in reducing baseflow. *Geophysical Research Letters*, 44(5): 2310-2318, doi:10.1002/2017GL072759.

5.1 Abstract

Changes in the hydrological cycle have a significant impact in water-limited environments. Globally, some of these regions are experiencing declining precipitation trends yet are simultaneously becoming greener, partly due to vegetation feedbacks associated with increasing atmospheric CO_2 concentrations. Reduced precipitation together with increasing rates of actual evapotranspiration diminishes streamflow, especially baseflow, a critical freshwater dry-season resource. Here we assess recent changes in baseflow in Australia from 1981-2013 and 1950-2013 and separate the contribution of precipitation, potential evapotranspiration and other factors on baseflow trends. Our findings reveal that these other factors influencing the baseflow trends are best explained by an increase in photosynthetic activity. These results provide the first robust observational evidence that increasing atmospheric CO_2, and its associated vegetation feedbacks are reducing baseflow in addition to other climatic impacts. These findings have broad implications for water resource management, especially in the world's water-limited regions.

Keywords: Elevated atmospheric CO_2; CO_2 fertilization; Baseflow; Vegetation feedbacks; Climate change; Trends.

5.2 Introduction

Human activity and climatic change are altering the terrestrial water cycle (Sterling et al., 2013). Shifts in precipitation (P) (Chou et al., 2013; Greve et al., 2014), atmospheric demand (potential evapotranspiration - PET) (McVicar et al., 2012a), evaporative fluxes from the land surface (actual evapotranspiration - AET) (Zhang et al., 2016b), and streamflow (Q) (Wang and Hejazi, 2011; Ukkola et al., 2016; Zhang et al., 2016a) have all been detected (Collins et al., 2013). However, attribution to anthropogenic causes (Sarojini et al., 2016) such as land-cover change (Sterling et al., 2013), increasing concentrations of greenhouse gases (Gedney et al., 2006; Delworth and Zeng, 2014) and other climate changes (Karoly, 2014) as opposed to long-term natural variability remains challenging. These impacts are especially acute within water-limited regions (PET > P), where recent global increases in vegetation greenness are attributed to 'fertilization' through elevated atmospheric CO_2 concentrations (eCO_2) (Donohue et al., 2013; Liu et al., 2015).

In water-limited regions, the implications of the vegetation feedbacks for the hydrological cycle are potentially profound, as the eCO_2-driven enhancement of catchment leaf area (Donohue et al., 2013) and rooting depth (Iversen, 2010; Bond and Midgley, 2012) potentially offsets the leaf-level reduction of water-use due to decreasing stomatal conductance (Bonan, 2008; Donohue et al., 2017). This potentially leads to increasing rates of AET (when water is available), which may in turn reduces streamflow (Ukkola et al., 2016), especially of the baseflow (Qb or 'slow-flow') component. Adding to these vegetation impacts on the hydrological cycle are concurrent changes to climate drivers (P and PET) that primarily govern the magnitude and direction of streamflow changes (Piao et al., 2007). How these changes operate in combination to impact streamflow is a critical issue to resolve given 35.5% of the world's population live in water-limited environments and rely on this scarce resource (Gilbert, 2011).

Here, we focus on disentangling climate forcing and eCO_2-driven vegetation feedback impacts on Qb, for two reasons: (i) streamflow is highly influenced by P variability, thus any impacts due to changes in vegetation functioning are best observed through the Qb lens as this component arguably exhibits greater sensitivity to catchment characteristics, such as vegetation cover, not hydroclimatic changes; and (ii) this is the portion of streamflow derived from groundwater storage and other delayed sources (Smakhtin, 2001) which temporally dominates streamflow generated by catchments. Thus Qb plays a pivotal role in the water supply to agriculture, urban areas and ecosystems, especially during periods of low or no P. Furthermore, there is currently a poor understanding of how shifts in Qb sources – e.g. groundwater and snow melt (Taylor et al., 2013;

Berghuijs et al., 2014b) and drivers – e.g. P, PET and eCO_2 (Piao et al., 2007) impact this critical resource.

To address this issue, we first separate Qb from total streamflow and assess trends in Qb, P, and PET from 1981-2013 in 315 catchments located across a large climatic gradient in eastern Australia. We next separate the relative contribution of climatic drivers (P and PET) from all other potential factors. We also used a subset of 44 catchments with longer time-series availability (1950-2013) to analyse the sensitivity of trend slopes of Qb, P and PET to the length of time-series and assess the robustness of the results with a shorter Qb time-series (see Materials and Methods).

5.3 Methods

5.3.1 Study area and data

The study focused on eastern Australia. We used two datasets of catchments according to the available length of streamflow (Q) time-series. The first dataset comprised 315 catchments with Q data from 1981 to 2013 (33 years) (56% are water-limited, i.e. $PET/P \geq 1.2$; 36% are equitant (McVicar et al., 2012b), i.e. $1.2 < PET/P > 0.8$; and 11% are energy-limited, i.e. $PET/P \leq 0.8$). The second dataset had a longer Q time-series (1950-2013; 64 years) containing fewer (44) catchments (50% water-limited; 39% equitant; and 11% energy-limited). All catchments are unregulated and not nested. They are a subset of the Trancoso et al. (2016) dataset used for catchment Q regime classification, and range from wet-dry tropical savanna woodland (far north Queensland) to cold-temperate rainforest (Tasmania). The catchments were primarily located in headwaters (mountainous forested areas) rather than lowland agricultural landscapes and had experienced little human-induced land-use change in the past 65 years. The 1981-2013 series catchment areas range from 6.8 to 3,299 km^2 (total area is 119,060 km^2), latitude 11.36 - 43.08^o S, and the dryness index (PET/P) ranges from 0.43 to 2.90. The 1950-2013 series catchment areas range from 16.1 to 1,557km^2 (total area is 18,826 km^2), latitude 16.73 - 41.64^o S, and the dryness index ranges from 0.48 to 2.10. These range of dryness index values encompass those where catchment rooting depth is maximum(Yang et al., 2016a) and so presents an opportunity where eCO_2-driven vegetation feedbacks, including increased rooting depths (Iversen, 2010; Bond and Midgley, 2012), influencing the Qb response are maximized.

We only used catchments with at least 95% valid daily Q in each time-series. Data were obtained from the Queensland, New South Wales, Victorian and Tasmanian state-government water monitoring agencies. We used daily gridded precipitation (Jones et al., 2009) and monthly Priestley-Taylor PET (Raupach et al., 2012) time-series with spatial resolution of ~5 km for the same period

of Q data availability. Time-series of monthly fraction of Photosynthetically Active Radiation (fPAR) (Donohue et al., 2008) from 1981 to 2013 with ~ 1 km of spatial resolution were also used. We used catchment boundaries to extract the average values of these gridded datasets per catchment or the catchment centroid to extract the gridded value when the catchment area was smaller than the grid-size. We also compared our results with 1981-2013 annual atmospheric CO_2 concentrations from Cape Grim Baseline Air Pollution Station (Tasmania).

5.3.2 Approach

We separated baseflow (Qb) from Q by applying the Lyne and Hollick (1979) algorithm to daily time-series. We then created annual time-series of Qb, P, PET and fPAR by summing the first three and averaging the last. Only years with complete records are used. Next, we used the Mann-Kendall test (Helsel and Hirsch, 2002; Hamed, 2008) to detect monotonic trends in Qb, P and PET. The magnitude of the trend was estimated using Kendall's Tau statistic (Sen, 1968; Helsel and Hirsch, 2002). Trends are quantified as mm/year/year (i.e. $mm.a^{-2}$). We used the second smaller dataset with longer Q (1950–2013) to assess the sensitivity of Qb, P and PET trend slope estimation to the time-series length, using roughly 5-year intervals.

To interpret the observed Qb trends we used : (i) the Budyko framework (Budyko, 1974); (ii) temporal phase offsets between the month of P maxima and month of PET maxima averaged per-catchment across the entire time-series (Donohue et al., 2010b); and (iii) streamflow regimes as developed by Trancoso et al. (2016). Next, we estimated the relative contributions of P, PET and the non-explained fraction (i.e. other factors) to Qb trends. We considered the sum of these contributions to be the total trend: $\mathrm{Qb(trend)} = \mathrm{Qb[P](trend)} + \mathrm{Qb[PET](trend)} + \mathrm{Other\ factors(trend)}$, with the other factors trend calculated as the residual.

Given that the relation between Qb and P and Qb and PET is often non-linear, local regressions (LOESS) were used to detrend Qb and remove the contribution of P and PET to the Qb time-series (Qbr). This was performed by sequentially taking the regression residuals, first between Qb and P, and then between Qb and PET, and finally multiplying the residuals by the long-term mean Qb. We then repeated the trend analysis on the Qbr time-series to determine: (i) to what extent climate factors (P and PET) contributed to the original Qb trends; and (ii) the relative contribution of the remaining trend (other factors) not explained by climate factors in the original Qb time-series.

To examine whether the other factors contributing to the trends in Qbr can be explained by vegetation feedbacks associated with increasing CO_2 concentrations, we first obtained time-series of vegetation greenness (fPAR) detrended for climatic (P and PET) effects (fPARr), using the same

approach described above for Qb. We then assessed whether the remaining Qbr trends were consistent with fPARr trends, and in addition, whether the remaining fPARr trends were consistent with trends in atmospheric CO_2 concentrations. We also used a one sample t-test to infer whether mean climate and the eCO_2-driven vegetation feedback impacts on Qb trends were significantly different from zero across the different aridity and streamflow regime categories (Trancoso et al., 2016).

5.4 Results and discussion

In terms of Qb, 75% of catchments are declining for 1981-2013, with the majority of these declines (78%) up to -1 $mm.a^{-2}$ (Figure 5.1a), yet only 56% of catchments experience decreasing P and of these 78% are decreasing by more than -1 $mm.a^{-2}$ (Figure 5.1b). PET trends are almost uniformly (96%) increasing, and with 88% of these catchments increasing by > 0.5 $mm.a^{-2}$ (Figure 5.1c). Similar results were found for 1950–2013 (Figure A5.1a-c in Appendix 5). While these trends are somewhat sensitive to the timescale over which they are determined and methods used to calculate the variables of interest, our sensitivity analysis suggests these trends are generally robust (Figures A5.2 and A5.3 in Appendix 5).

Interestingly, the magnitude of the Qb trend increases with decreasing aridity (PET/P), and experiences the greatest magnitude within equitant catchments (i.e., where conditions switch between being energy- and water-limited seasonally (McVicar et al., 2012b) or are exclusively energy-limited (Figure 5.1d). However, these larger magnitudes (i.e. > 5 $mm.a^{-2}$) are mostly increasing trends as opposed to the majority (75%) of declining trends and therefore are likely to be driven by distinct mechanisms given the large variability of streamflow drivers across the study area (Trancoso et al., 2017b).

It is also important to highlight that despite the largest absolute declines in Qb occurring in equitant and energy-limited environments (Figure 5.1d), the larger proportion of available Qb in these catchments results in a lower sensitivity to change in comparison to water-limited environments which have lower Qb at the beginning of the study period. The generation and contribution of Qb to long-term average streamflow is already known to relate well to aridity spatially (Trancoso et al., 2016), yet represents an important finding that the combined impact of changing drivers on Qb also follows this spectrum in water- and energy-availability over time (Figure 5.1e and Figure A5.4 in Appendix 5). We also found no relationship between the magnitude of the trends in Qb, P and PET with seasonality (month of P maximum – month of PET maximum) or streamflow regime (Figure A5.5 in Appendix 5).

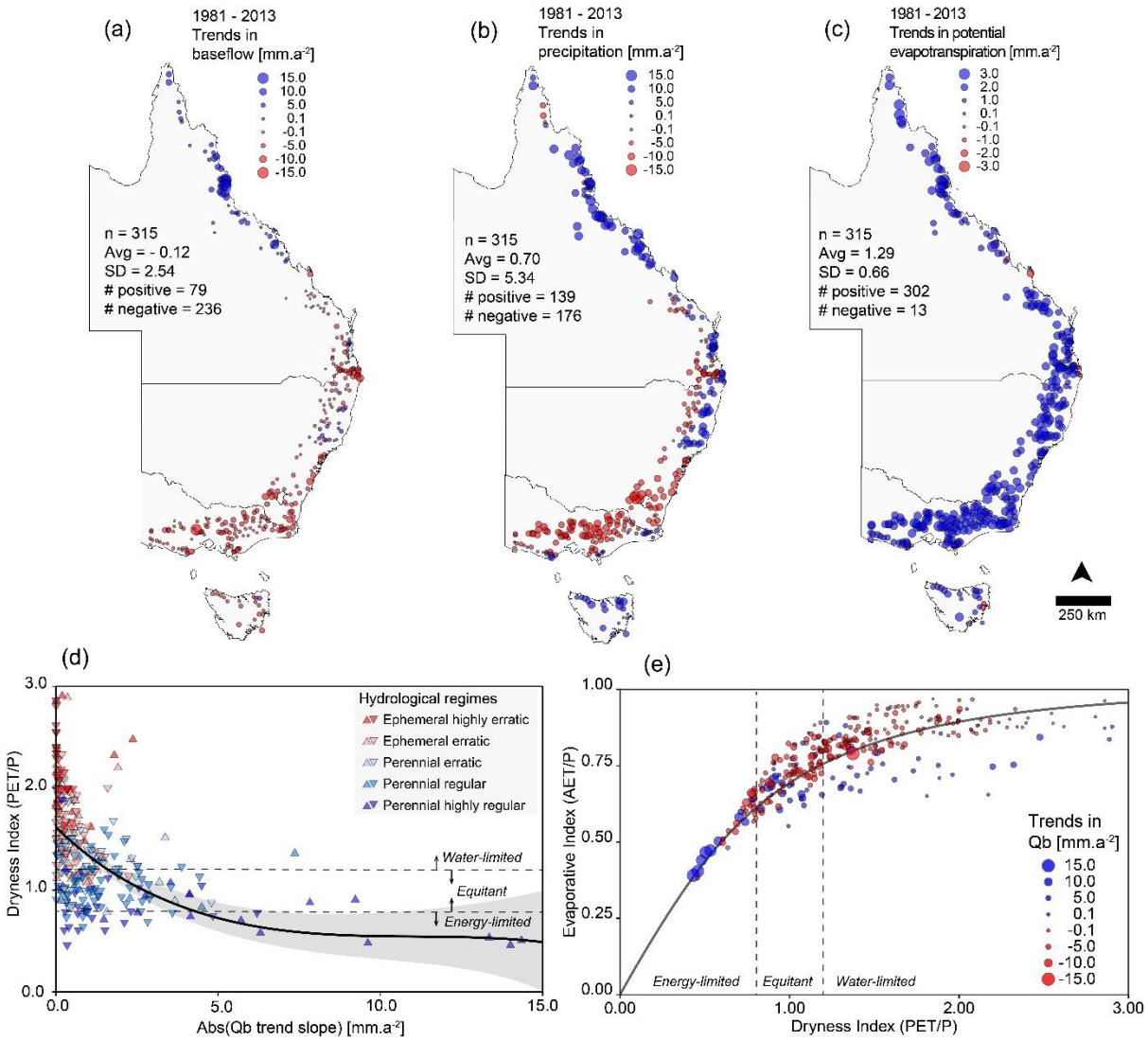

Figure 5.1 Trends in (a) baseflow (Qb), (b) precipitation (P) and (c) potential evapotranspiration (PET) for 1981–2013. (d) Relationship between absolute magnitude of Qb trends and the dryness index (PET/P) for 1981-2013 (n = 315 catchments). Upward triangles have increasing trends and downward triangles decreasing trends. Symbol colours refer to the hydrological regime derived from eight streamflow indices (Trancoso et al., 2016). The solid black line shows the average increase in Qb trends with decreasing dryness for all catchments and the grey shaded area is the 95% confidence interval. (e) 1981-2013 Qb trends in the context of the Budyko framework; solid grey line is the Budyko (1974) curve. Dashed lines in parts (d) and (e) define the water-limited, equitant and energy-limited regions.

Within the ternary space defined by the relative contributions of P, PET and other factors influencing the 1981-2013 Qb trends (Figure 5.2), the region with the highest density of catchments had 30-50% P and 20-40% PET contributions to observed changes in Qb. Importantly, this demonstrates that 25-40% of changing Qb must be explained by other factors, with 67% of catchments retaining a declining Qb trend after climatic effects are accounted for. The longer time-series (1950-2013) also supports these findings with 75% of catchments exhibiting declining Qb

trends with 10-25% of Qb changes attributed to other factors (Figure A5.6 in Appendix 5). These additional factors potentially include: (i) catchment storage changes; (ii) changes in seasonality of climate drivers; (iii) streamflow changes due to land-cover changes, and (iv) eCO_2-driven vegetation feedbacks (denoted eCO_2–Veg herein). Given the persistence of the long-term (64 years) declines in Qb (Figure A5.7a-b in Appendix 5), they are unlikely to be maintained exclusively by catchment storage changes, which generally balance or become very small over long time scales (Budyko, 1974). We did not find any relation between the Qb trend with climate effects removed and the seasonal offset in water- and energy-availability (Figure A5.8 in Appendix 5). Land-cover changes are also known to cause similar feedbacks (Sterling et al., 2013), however we used only headwater catchments with high native vegetation cover and little or no contemporary land-cover change (Trancoso et al., 2016). Thus, after discounting the first three other factors, we next examine whether the remaining Qbr trends (i.e., Qb trends after climate effects are removed) can be attributed to eCO_2–Veg.

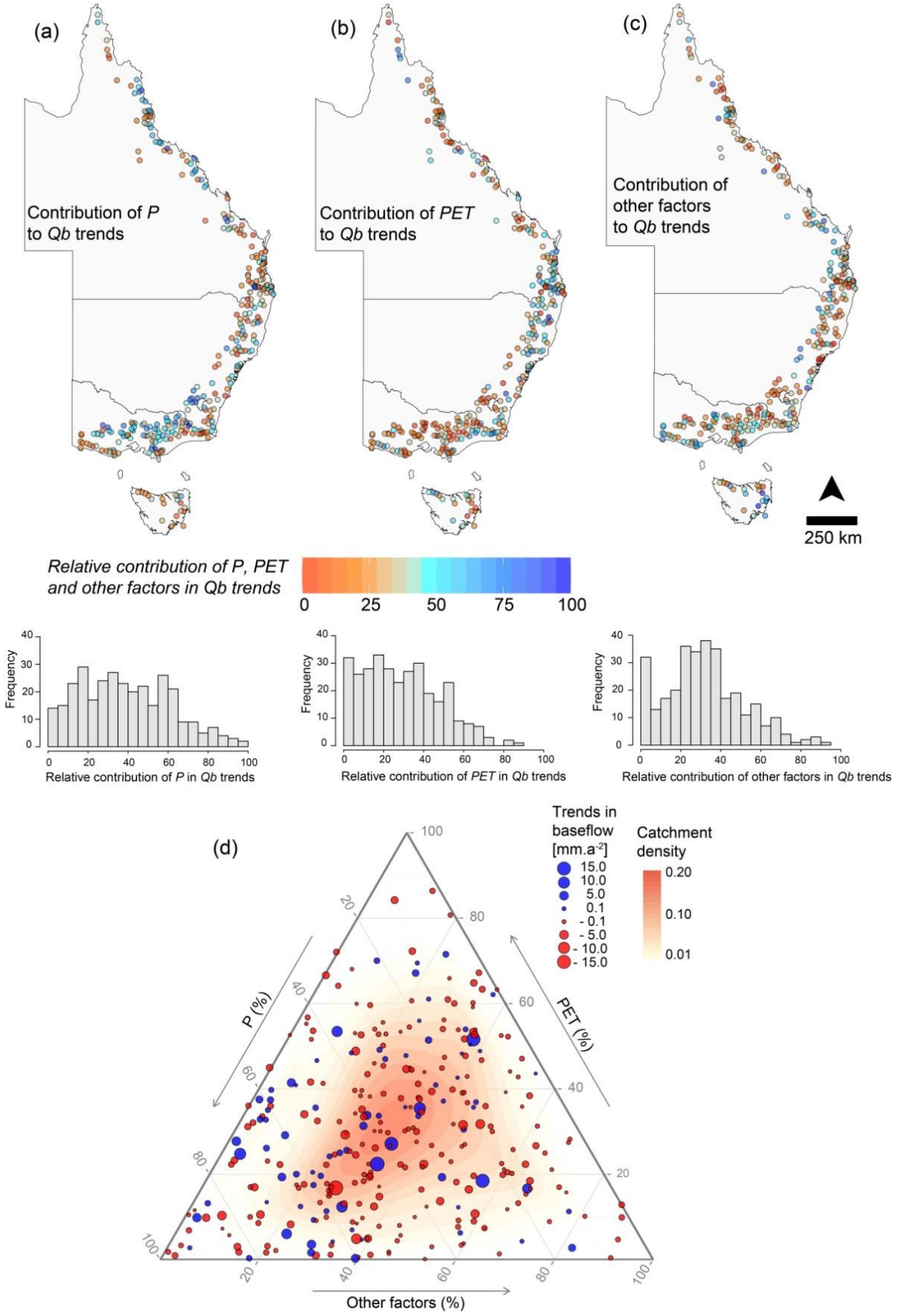

Figure 5.2 Spatial distribution of the relative contributions of (a) P, (b) PET and (c) other factors on Qb trends with histograms showing the relative distribution of each component for 1981-2013. (d)

Ternary diagram integrating the relative contributions of P, PET and other factors on Qb trends. Catchment density refers to the relative frequency of catchments within the ternary space.

To do this, we first assess 1981-2013 fPAR trends (Donohue et al., 2008), which reveals 91.1% of the 315 catchments exhibited an increasing fPAR trend. When climate effects on fPAR trends were removed (i.e. fPARr, Figure A5.9b in Appendix 5), 90.8% of the 315 catchments retained increasing fPARr trends. We propose this increase in fPARr is best explained by a continuously increasing atmospheric CO_2 concentration resulting in increased leaf-level water-use efficiency which invokes an increasing Leaf Area Index (LAI) that is most noticeable in water-limited and equitant environments (Donohue et al., 2013; Lu et al., 2016). Other limiting factors such as light and nutrients can be discounted as they are unlikely to maintain persistent trends, nor apply uniformly to almost all catchments. If eCO_2 is the main driver of fPARr trends (Lu et al., 2016) across almost all studied catchments, then this implies sub-annual AET rates have also increased (when water is available) through some combination of landscape-level photosynthetic enhancement (Donohue et al., 2013) and/or deeper roots at the plant level (Iversen, 2010; Bond and Midgley, 2012) changing the subsurface distribution of water in a catchment and hence the generation of Q. Both these processes seemingly offset the reduction in leaf-level stomatal conductance (Bonan, 2008; Donohue et al., 2017), ultimately contributing to Qb declining.

The extent of this eCO_2–Veg hydrological impact can be detected in 59.3% of the 315 catchments, as these experience declining Qbr trends while simultaneously displaying increasing fPARr trends (Figure A5.9 in Appendix 5). Focusing on the 210 catchments with declining Qbr trends and binning the relative contribution of the Qbr trends to the overall Qb trends into deciles, reveals a linear relationship with fPARr trends (Figure 5.3a), demonstrating that a robust mechanistic link exists between eCO_2–Veg feedbacks and declining Qbr. Although changes in both fPARr and Qbr are roughly balanced over the last 30 years (Figure 5.3b), during the last decade changes in fPARr appear to be consistently outpacing changes in Qbr. This raises the important question as to whether Qbr changes will also rise in response, or whether there is a limit to the influence of fPARr changes on Qbr under eCO_2. Nonetheless, the overall increase in fPARr across all catchments is consistent with the trend in atmospheric CO_2 concentrations observed at Cape Grim, Tasmania (Figure 5.3c and Figure A5.10 in Appendix 5), which is further observational evidence to support the attribution of increasing fPARr to eCO_2-Veg feedbacks.

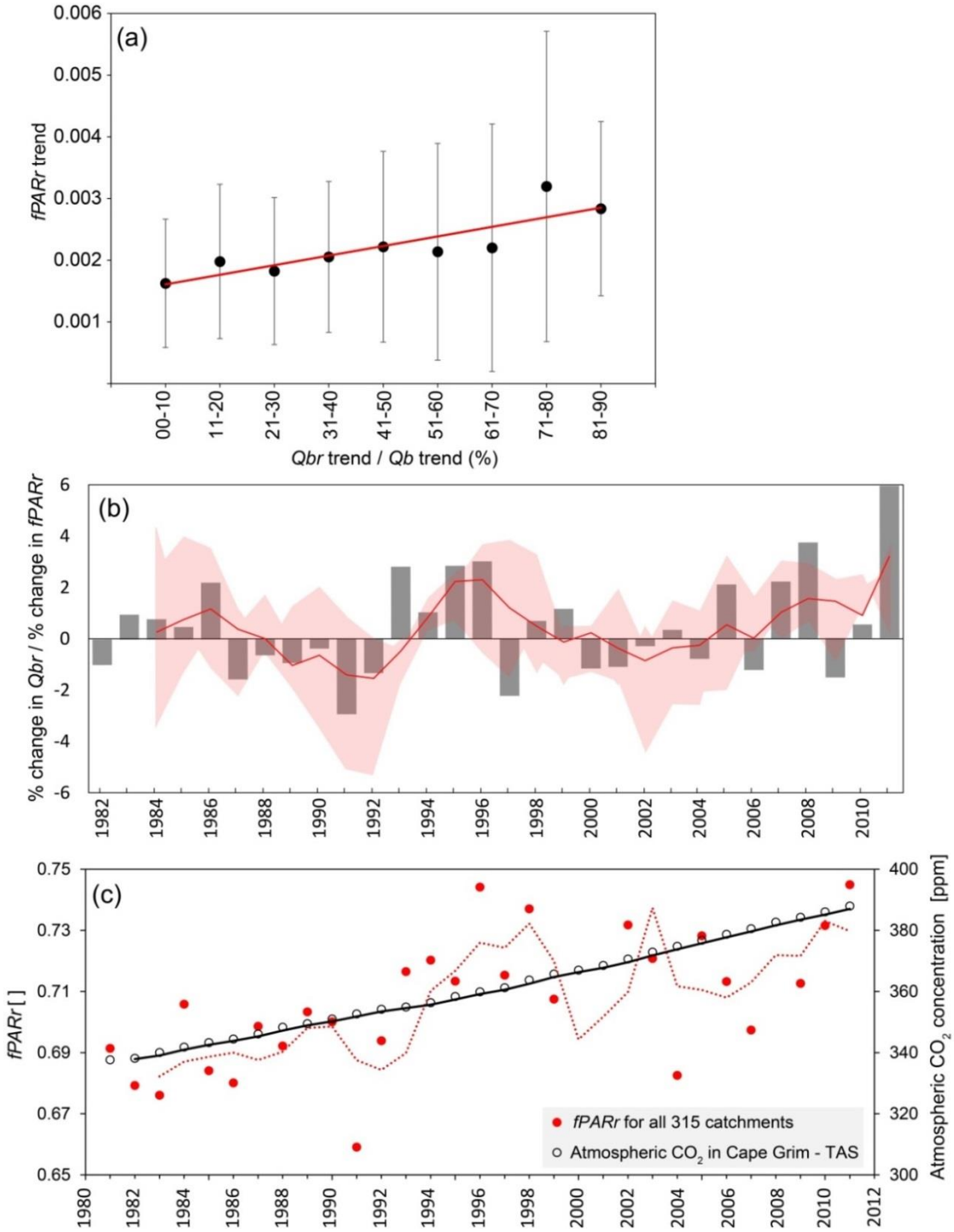

Figure 5.3 Impact of eCO_2–Veg on Qb. (a) Relationship between the Qbr trends relative to the total Qb trends and fPARr trends for the 210 catchments with declining Qbr. Means (black dots) and standard deviations (vertical bars) are shown for each group of binned catchments. The linear trend line ($y = 0.0002x + 0.0015$, $R^2 = 0.75$ and $p<0.001$) is shown in red. (b) Ratio of the annual relative change in Qbr to the annual relative change in fPARr averaged across all 315 catchments (grey bars). Red line is the 3-year moving averages for all 315 catchments and red shaded area is the envelope composed by the same analysis for the five hydrological regimes introduced in Figure 5.1d. (c) Annual time-series of fPARr averaged across all 315 catchments and Cape Grim atmospheric CO_2 concentrations. Red dotted line is the 3-year moving averages for fPARr, and the black line is the 2-year moving averages in atmospheric CO_2 concentrations (Spearman correlation coefficient (r_s) = 0.643; $p < 0.001$). See Figure A5.10 in Appendix 5 for the linear relationship between atmospheric CO_2 concentrations and fPAR across the aridity spectrum.

Having systematically accounted for all potential factors influencing Qb, we are confident the identified relationship between Qbr and fPARr is causal rather than only correlative. Next we evaluate the relative impacts of climate effects (P and PET) and eCO_2–Veg feedbacks separately on Qb. We use the 1981-2013 catchment average Qb as a benchmark to evaluate these impacts, and find firstly a clear association with aridity, namely minor impacts in energy-limited environments ($PET/P \leq 0.8$), increasing climatic impacts which reduce Qb in equitant environments ($1.2 < PET/P > 0.8$), and increasing climate effects and eCO_2–Veg feedbacks which combine to cause the largest Qb impact in water-limited environments ($PET/P \geq 1.2$) (Figure 5.4a). Secondly, these impacts can be separated by hydrological flow regime, which shows catchments with highly stable and perennial streamflow receive little or even slightly positive climate and eCO_2–Veg impacts that increase Qb (Figure 5.4b). Given these catchments are almost exclusively energy-limited, this positive feedback with eCO_2–Veg likely reflects the conditions under which increased leaf-level water use efficiency also increases Qb at the catchment scale. The 1950-2013 analysis supports these findings with an overall similar pattern, albeit with lower contributions and variability from both climate and eCO_2–-Veg (Figure A5.11 in Appendix 5). The remaining streamflow regimes increase in flow variability and transition from perennial to ephemeral conditions, and are almost exclusively declining in Qb due to the increasing impact of both climate and eCO_2–Veg feedbacks, with the greatest impact on relative Qb occurring within perennial but variable flow regimes.

Although climatic changes have the greatest impact on Qb, which is consistent with previous work by (Piao et al., 2007), this study reveals that eCO_2–Veg feedbacks also play a critical role as water limitation and baseflow variability increase. This corroborates previous findings that catchment evapotranspiration is increasing and depleting total streamflow, especially in sub-humid and semi-arid areas (Ukkola et al., 2016). However, our work also highlights that the combined impacts of climate change and eCO_2–Veg feedbacks on surface water resources may be better observed through baseflow, since no significant actual evapotranspiration impacts were found for arid (Ukkola et al., 2016) or tropical catchments (Yang et al., 2016b) using streamflow. It is also worth noting that very dry (i.e. arid) catchments are underrepresented in this, and most previous comparative studies, constraining our understanding of the hydrological response of these regions. We also have not directly accounted for potential feedbacks between eCO_2 and P and PET (Delworth and Zeng, 2014; Karoly, 2014; Roderick et al., 2015), and our use of a radiation-based method for PET (Priestley–Taylor) may not represent the entire atmospheric demand process (McVicar et al., 2012a). However, in the absence of reliable long-term wind data we are not able to use a more physically-based form of PET (McVicar et al., 2012a). In this context, we note that our increasing PET trends contrasts with declining pan evaporation trends (Roderick and Farquhar,

2002; McVicar et al., 2012a). Therefore, assuming complementarity, any overestimate in the contribution of PET to Qb trends would result in an underestimate of the eCO_2–Veg feedbacks considered here.

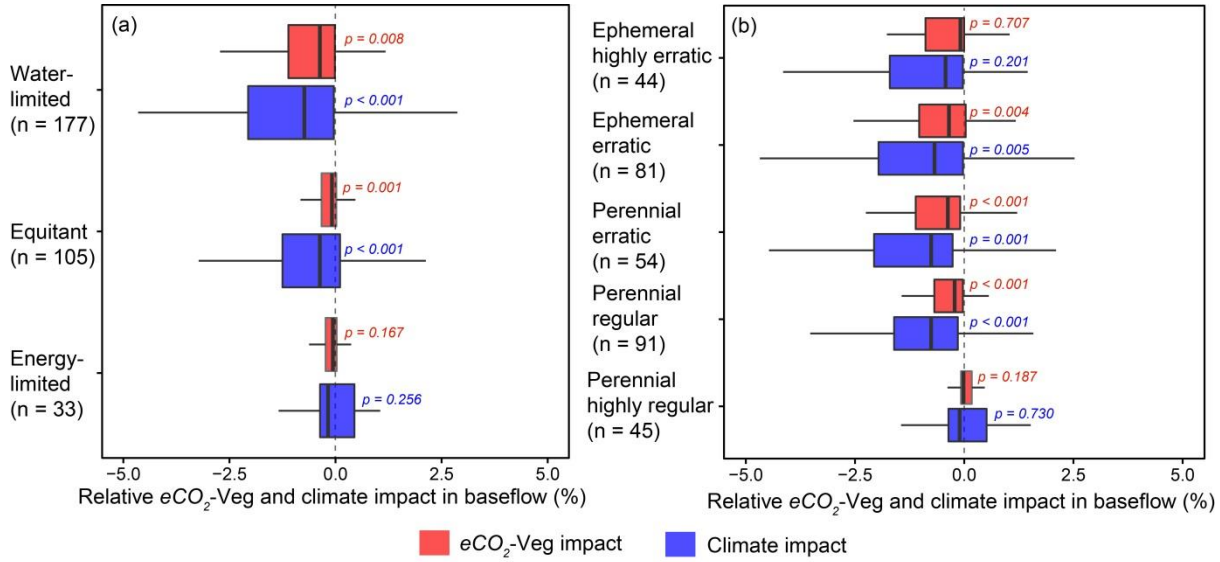

Figure 5.4 Impact of eCO_2–Veg feedbacks and climate (P + PET) on Qb trends relative to the long-term mean annual Qb. Impacts are compared across: (a) water-limited (PET/P ≥ 1.2), equitant (0.8 > PET/P < 1.2) and energy-limited (PET/P ≤ 0.8) catchments, and (b) the five hydrological flow regimes (Trancoso et al., 2016). Box plot statistics include the median (internal vertical line), interquartile range (IQR - denoted by the box), and horizontal lines (or whiskers) are calculated as $\pm 1.58 \times IQR\sqrt{n}$. The p-values beside the boxes refer to the probability that the mean impacts are not different from zero using a one sample t-test.

Current climate projections for eastern Australia suggest lower supply of P, higher PET demand, and therefore lower Qb (Collins et al., 2013). However, they do not account for eCO_2–Veg feedbacks that need to be acknowledged to ensure sustainable water resource management, especially during future droughts. This study used observational data of the hydrological cycle over ~30- and ~60-year periods to demonstrate that such climate impacts are indeed occurring. However, these impacts are also compounded by eCO_2–Veg feedbacks, and are highly differentiated according to water and energy availability (aridity) as well as streamflow generation processes. Using a data-driven approach applied over a broad climatic gradient, we provide direct evidence demonstrating how long-term eCO_2–Veg feedbacks impact Qb. This is important because such evidence is difficult to establish using climate projections coupled to land surface models that generally do not capture the ecohydrological feedbacks described here (Collins et al., 2013; Swann et al., 2016; Knauer et al., 2017). Results from such models typically yield additional soil or surface water through increased leaf-level water use efficiency, which recent modelling studies suggest could reduce drought severity (Swann et al., 2016) and increase runoff (Knauer et al., 2017), a

result generally not supported by our, and others (Ukkola et al., 2016; Yang et al., 2016b), observational evidence. Importantly, our findings also highlight the vulnerability of streamflow in water-limited environments to the combined influence of changing climate drivers and CO_2 fertilization of vegetation, and that these reductions of available water resources need to be considered more thoughtfully in water planning and allocation for both humans and ecosystems. This impact may also extend to the availability of other hydrologically linked water resources such as groundwater (Taylor et al., 2013), which can dominate the supply of Qb, with any reduction in recharge further compounding the uncertainty surrounding future water availability.

5.5 Conclusion

We separated the impact of changing climate forcings (precipitation and potential evapotranspiration) and CO_2-driven vegetation feedbacks on catchment baseflow – the portion of streamflow derived from groundwater storage and other delayed sources that plays a critical role in water supply to agriculture, urban areas and ecosystems. We show that the widespread reductions in baseflow not associated with climate forcings are best explained by increasing photosynthetic activity due to increased atmospheric CO_2, offsetting leaf-level increases in water use efficiency. This observational evidence emphasises the importance of considering the combined impacts of changing climate drivers and CO_2-driven vegetation feedbacks on water resources, especially in regions already experiencing water scarcity (i.e., water-limited) where the relative impacts are largest.

CHAPTER 6

SUMMARY AND CONCLUSION

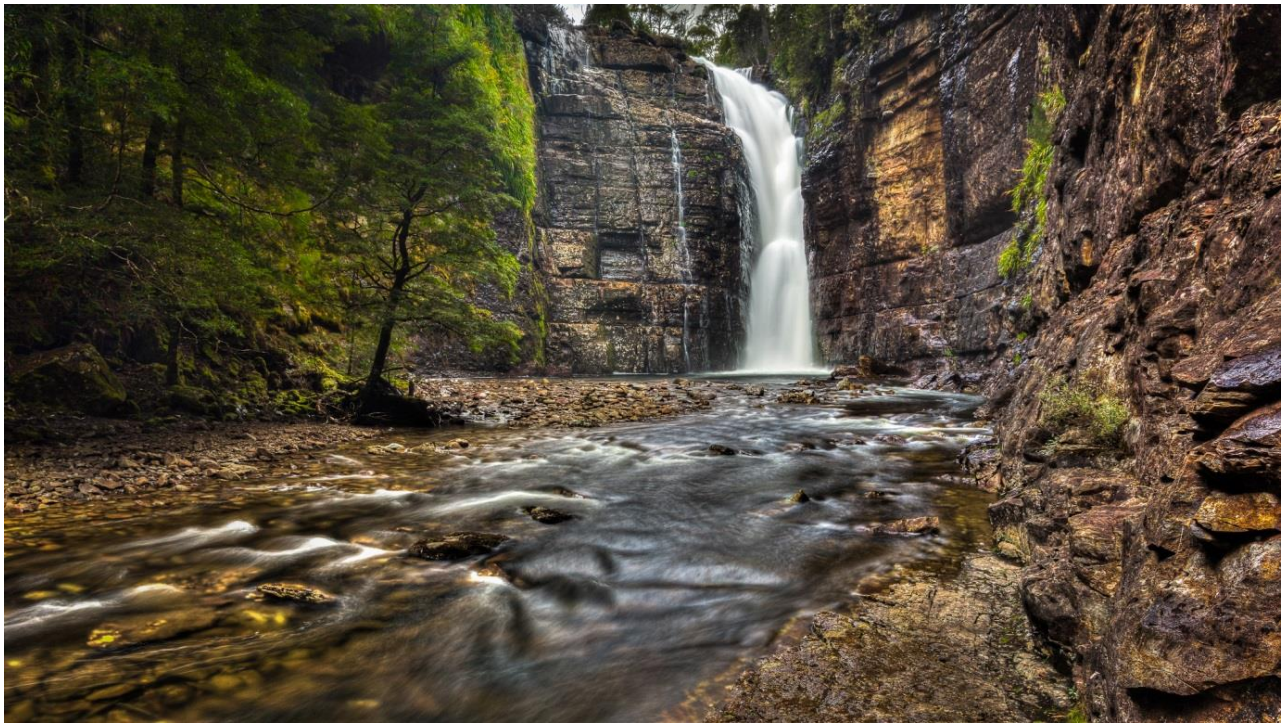

How do we maintain the essential ecohydrological processes to ensure freshwater yield in a changing world? Harnett Falls at Mersey River. Walls of Jerusalem National Park, Tasmania. Photo by Gavin Owen (source: flickr.com).

6.1 Overview

The primary aim of this chapter is to summarise the key research findings in relation to the broad objectives described in section 1.3 and the specific objectives described in the introduction of the analytical chapters (i.e. sections 2.2, 3.2, 4.2 and 5.1). The overall contribution of these findings is then discussed in light of improvements to the field of ecohydrology. Finally, I highlight the implications for water resource management and make recommendations for future research.

The overarching aim of this thesis was to understand the characteristics and controls of streamflow generation and to investigate how historical climate-induced changes and human-induced landscape transformations influenced the streamflow along a broad-scale gradient of catchment biophysical characteristics (see Figure 1.2). To achieve this, I explored the spatial and temporal variability of a dataset from 355 catchments along the Australian east coast. The data included streamflow and precipitation time series, satellite-based time-series of vegetation properties, model-based soil moisture and temperature surfaces, and a range of spatial data of land-cover, topography, soil properties, physiography, bioregions and human population density.

The research targeted two key problems in order to enhance ecohydrological knowledge: (i) the functioning of catchments influencing streamflow generation; and (ii) the changes in streamflow generation induced by climate and landscape modifications (see Figure 1.3). To address the first problem, I used long-term averages (33 years) of hydrological metrics (i.e. streamflow signatures) to represent catchment' streamflow "steady-state" and explored the spatial variability of hydrological behaviours to typify hydrological regimes (objective 1) and determine the dominant biophysical drivers of hydrological functioning (objective 2). To address the second problem, I used the temporal dimension to quantify changes in the streamflow, climate forcings and vegetation to then separate the climate-induced and human induced changes on streamflow (objective 3) as well the changes attributed to CO_2-vegetation feedbacks (objective 4).

6.1.1 Objective 1

The first objective, addressed in Chapter 2, investigated how streamflow similarity varies according to the annual water and energy balances and to determine to what degree biophysical drivers of runoff explain the observed spatial streamflow variability. This objective was decomposed into three aims: (a) to investigate how streamflow similarity and characteristics vary according to the annual water and energy balances using the Budyko framework; (b) to determine to what degree biophysical drivers of runoff (Dunne diagram) explain the observed flow variability among

catchments; and (c) to evaluate whether links between these two approaches (Budyko framework and Dunne diagram) offer insights into the mechanics of catchment co-evolution.

I firstly mapped the distribution of eight long-term (1980-2013) streamflow signatures to provide insights into the hydrological functioning of 355 catchments along the eastern Australia. I then classified the catchments into five streamflow regimes with distinct hydrological functioning. By using PCA, I extracted the maximum unidimensional variability of the eight streamflow signatures to represent the dominant streamflow behaviour, which is consistent with the streamflow regimes classified. The classification output also organised catchments along the spectrum of water and energy balances within the Budyko framework. The drivers of runoff mechanisms from the Dunne diagram explained 77% of the variability of the dominant streamflow behaviour with the following order of importance: (i) Dryness Index; (ii) Fraction of Photosynthetically Active Radiation; (iii) Saturated Hydraulic Conductivity; (iv) Soil Depth; (v) Maximum Slope; and (vi) Fraction of Woody Vegetation Cover.

This chapter represents a methodological advance in the use of a sequence of well-established data analysis techniques to classify catchments based on their hydrological functioning. The classified streamflow regimes follow a consistent pattern along the hydro- climatic gradients (Budyko framework) and are driven by the biophysical drivers of runoff mechanisms (Dunne diagram). It represents a novel approach based on streamflow characteristics (inductive classification) that independently organises catchments along the spectrum of water and energy balances and is statistically controlled by the catchment co-evolution factors normally used to organize catchments by deductive classification. Using a catchment classification scheme coupled with other data analysis techniques I showed the link between two well established theories in hydrology: the Budyko framework and the Dunne diagram.

6.1.2 Objective 2

The second objective (Chapter 3) aimed to identify the catchment-scale biophysical drivers of key streamflow characteristics across distinct regions and scales and determine changes in importance and contribution of drivers. The specific objectives were: (a) to determine the changes in the relationships between streamflow characteristics and catchment properties along regional and sub-continental scales and across biogeographically-contrasting regions; (b) to examine how dynamic catchment biophysical properties (i.e. vegetation and climate) affect key hydrological characteristics within and between regions; and (c) to infer the processes governing streamflow variation at larger biogeographic scales in order to better inform linkages between water resource management and biodiversity management.

The study explored 354 catchments in the whole east coast as well as three subsets within biogeographically contrasting regions. Three key long-term streamflow signatures were used to represent important hydrological characteristics - i.e. partitioning of P into Q; contribution of delayed sources to Q; and degree of intermittency. I determined the importance and weight of 24 potential biophysical drivers using random forest and Generalised Additive Model for Location Scale and Shape (GAMLSS).

The study identified the overall and regional drivers of streamflow characteristics. While the dryness index and the fraction of photosynthetically active radiation from vegetation explained the variability of streamflow characteristics at both regional and continental scales, soil properties had a significant effect especially at regional scales. Moreover, the importance and weights of these soil properties varied across regions, and depended on the streamflow characteristics.

I concluded that models used to estimate streamflow characteristics should not be generalised across regions and spatial scales, as the explanatory variables and their importance changes from region to region and across scales. Hence, models calibrated in one region should not be used to inform decisions in other regions. Despite the utility to determine the primary controls in broader scales, studies undertaken at a continent scale may not be sensitive enough to capture regional controls and offer insights into regional-specific scales. The study provided a methodological advance in using a combination of random forest and GAMLSS with beta distribution, for cross-regional and multi scale modelling in the field of ecohydrology.

6.1.3 Objective 3

The third objective (Chapter 4) aimed to assess ecohydrologic shifts on long-term water and energy balances of catchments and separate out the climate- and human-induced changes components. This overarching aim had three sub-objectives: (a) to quantify the direction and magnitude of long-term shifts in the water and energy balances of catchments and how they scale across aridity and streamflow regimes gradients; (b) to evaluate the relative impact of climate and land use changes on long-term water and energy balances; and (c) to examine whether these relative climate and land use change impacts are linked to known land use extents, as well as long term changes in catchment photosynthetic activity and biomass.

This study explored the changes in the water and energy balances of two long-term periods (20 years) of 193 catchments spanning the entire east coast. I used the displacement within the Budyko framework to display the changes in the water and energy balances and the decomposition approach proposed by Wang and Hejazi (2011) to separate the changes in Q induced by climate change and

variability and anthropogenic landscape modifications. I then assessed the change components in light of streamflow and aridity regimes and anthropogenic landscape categories.

The research findings showed that over the last four decades, catchments located along the entire east coast of Australia experienced changes in streamflow as a result of both climate and direct human-induced modifications. These changes altered the water and energy balances of catchments towards drier conditions with higher AET and therefore less Q. Overall, the contribution of climate and direct-human induced changes to changes in Q was similar, despite the large spatial variability in the dominance of these drivers. However, Q changes in water-limited catchments have been influenced slightly more by land cover-induced changes than climatic changes, whereas in equitant and energy-limited catchments the contribution of climate was slightly greater than human-induced changes. With the consistent climatic shift towards a higher atmospheric demand (i.e. higher aridity), catchments within energy-limited region are gradually moving to the equitant region, equitant catchments are moving to water-limited region and water-limited catchments are becoming drier. We also show that the land cover-induced reductions in Q are consistent with vegetation gain (i.e., increasing photosynthesis activity and biomass). These observed changes suggest a reduction in surface water availability and have important implications for environmental and societal water supply needs.

6.1.4 Objective 4

Finally, the fourth objective (Chapter 5) investigated trends in baseflow (Qb), climate forcings and vegetation and then separated the contribution of precipitation, potential evapotranspiration and feedbacks between vegetation and elevated atmospheric CO_2 on baseflow trends. To address this issue the specific objectives were: (a) to assess trends in baseflow, precipitation and potential evapotranspiration; (b) to separate out the relative contribution of precipitation, potential evapotranspiration and other factors influencing baseflow trends; (c) to evaluate residual trends (after Qb – P – PET is accounted for) in baseflow and relate it with the residual trends in vegetation greenness (fPAR trends with effect of precipitation and potential evapotranspiration removed).

The study explored trends in hydroclimatological and vegetation time-series in two multi-temporal datasets with 44 (1950-2013) and 315 (1981-2013) catchments in eastern Australia. Because Q is highly influenced by P variability, the study focused on Qb trends to distinguish long-term changes in vegetation functioning. I used trend statistics and LOESS regression to remove the effect of P and PET from Qb and fPAR time-series and then quantify the fraction of Qb trends explained by climate and eCO_2-vegetation feedbacks along the aridity and streamflow regimes.

The findings reveal that these other factors influencing the baseflow trends are best explained by an increase in photosynthetic activity. These results provide the first robust observational evidence that increasing atmospheric CO_2, and its associated vegetation feedbacks are reducing freshwater availability in eastern Australian catchments in addition to other climatic impacts. Using a data-driven approach applied over a broad climatic gradient, I provided evidence demonstrating how long-term Veg – eCO_2 feedbacks impact Qb. I also highlighted the vulnerability of streamflow in water-limited environments to the combined influence of changing climate drivers and CO_2 fertilisation of vegetation, and that these reductions of available water resources need to be considered more thoughtfully in water planning and allocation for both humans and ecosystems. This impact may also extend to the availability of other hydrologically linked water resources such as groundwater, which can dominate the supply of Qb, with any reduction in recharge further compounding the uncertainty surrounding future water availability.

6.2 Contributions to the field

This PhD research makes important theoretical and applied contributions to the fields of ecohydrology and catchment hydrology in advancing the understanding of the functioning and changes in the streamflow generation process. In particular, it contributes to understanding the ecohydrology and catchment hydrology of eastern Australian catchments and the impact of elevated CO_2 levels on the latter. Figure 6.1 presents a schematic overview of the key findings and main knowledge contributions of this thesis as well as how the four objectives link together to make a meaningful contribution to our understanding of the functioning and changes to the streamflow generation process.

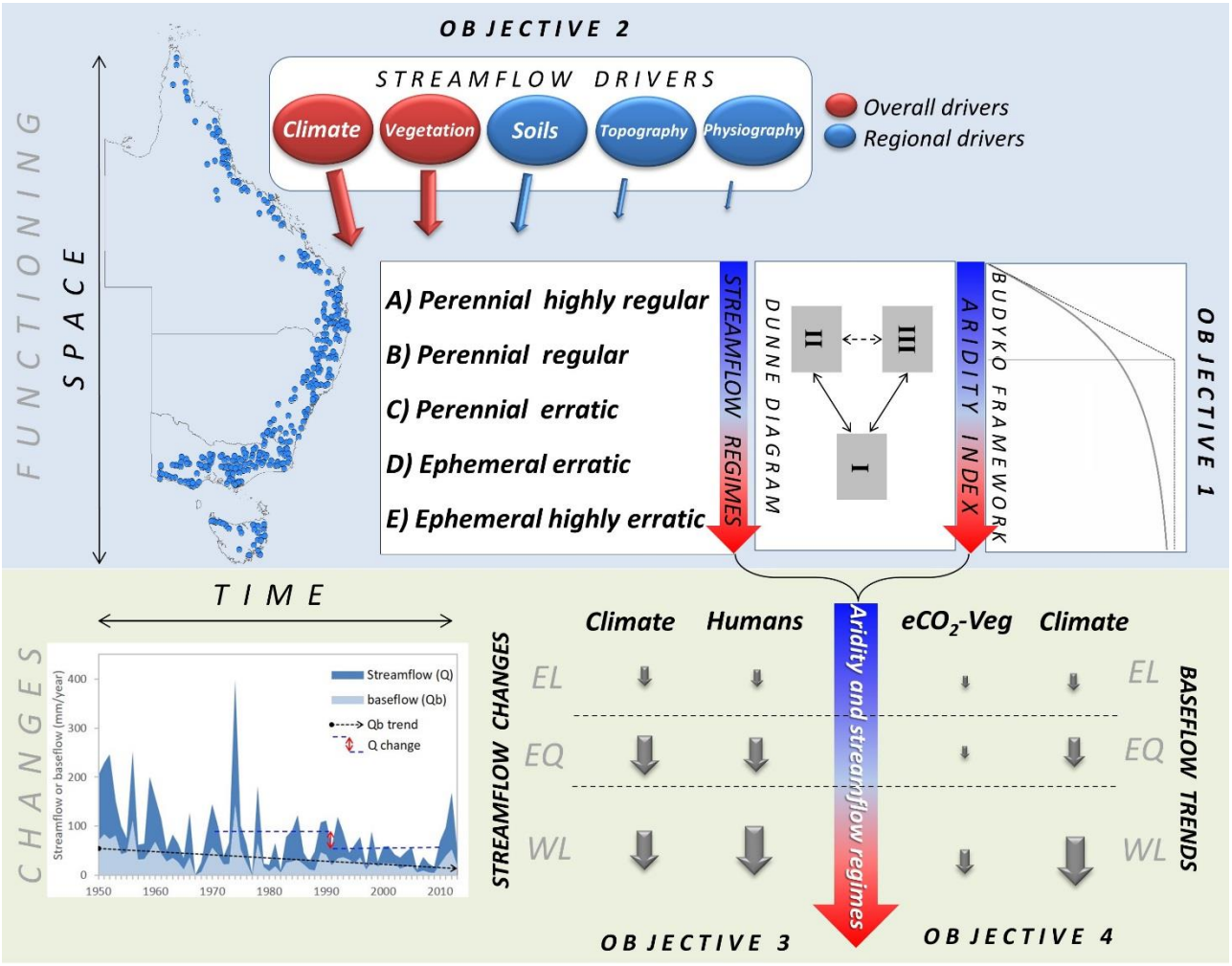

Figure 6.1 Summary of key findings and main contribution to the field of ecohydrology of this thesis concerning functioning and changes in streamflow generation. In the objective 1, the roman numerals in the Dunne diagram refer to the dominance in hydrograph of: (I) Horton overland flow; (II) subsurface stormflow; and (III) direct precipitation and return flow (see Figure 2.9 for details). The objective 2 illustrates the overall dominant drivers of streamflow and those more important at regional scale. Arrows sizes refer to the average weight of effect explaining streamflow characteristics (See figure 3.5 for details). In the objectives 3 and 4 the direction and size of the grey arrows illustrates the directions and magnitudes of change in streamflow and trends in baseflow. Arrows are scaled by the maximum effect per objective (see figures 4.4, A4.10 and 5.4 for details). EL, EQ and WL refer to the energy-limited, equitant, and water-limited aridity regimes respectively.

6.2.1 Functioning of streamflow generation processes

I firstly show that the catchment dataset spanning multiple gradients of biophysical characteristics follow a spectrum of streamflow characteristics, which can be divided into five categories of streamflow regimes. Furthermore, the streamflow spectrum scales well with aridity and is explained by the drivers of runoff mechanisms from the Dunne diagram. Hence, this work shows a convergence of two important underlying theories in hydrology linking the Budyko framework (Budyko, 1974) and the Dunne diagram (Dunne, 1983).

The study also represent a significant methodological advancement in the field of catchment classification as it shows that two different classification approaches (inductive and deductive) can be linked as long as the dominant streamflow spectrum is properly represented.

Interestingly, the regimes are not spatially aggregated, which means that despite the similarity in hydrological behaviour, the specific hydrological processes of catchments in eastern Australia are driven by distinct mechanisms. For instance, catchments with perennial highly stable streamflow regimes occur in both tropical and alpine climatic domains and are driven by both high annual precipitation and snowmelt. Likewise, in the opposite extremity of the streamflow spectrum, ephemeral catchments with highly erratic streamflow occur in dry tropical environments as well as in Mediterranean and sub-tropical coastal regions. This highlights that regional controls may play an influential role on the intermittency of streamflow.

This finding from Objective 1 guided the second objective of this thesis, where I showed that the controls of key hydrological characteristics vary across regions. Thus, biogeographically distinct regions, with a similar range in terms of specific hydrological characteristics have distinguishable biophysical drivers controlling the spatial variability of streamflow characteristics. This is an important contribution to the field given the ongoing focus on global studies (Beck et al., 2013b; Beck et al., 2015). I show that despite the valuable contribution brought by the understanding of dominant drivers of global variability, these studies are not sensitive enough to detect factors driving regional variability. Thus, they have more scientific than management value as they neglect regional processes and are unable to guide water resource management at the scale policies are implemented, decisions are made and freshwater is used. Hydrological processes and drivers change according to the scale at which they are assessed and global-scale generalizations should not inform decisions at local, regional and even continental scales.

The study also has distinct novel methodological aspects by applying a combination of modelling techniques (random forest and GAMLSS with beta distribution) to tackle ecohydrological problems.

6.2.1 Changes in streamflow generation processes

With regards to changes in streamflow, while significant progress has been made to distinguish climate-induced changes from landscape-induced modifications (Tomer and Schilling, 2009; Wang et al., 2013; Jaramillo and Destouni, 2014; Tan and Gan, 2015), there is little evidences from Australian catchments, where acute climatic changes and biomass increases (Liu et al., 2015) have been reported. I separate, for the first time, the large-scale reductions on streamflow due to changes in climate and vegetation regrowth. This phenomenon is consistent across the Australian east coast.

The approaches used in this work can also distinguish the fraction of change attributed to each one of these components and their dominance all over the coast. A novel aspect of this research is the sensitivity of streamflow to climate-induced changes and landscape-induced modifications across the aridity and streamflow regimes. I show that water-limited catchments have been more sensitive to landscape-induced modifications while climate-induced changes played a major role in the streamflow reduction of energy-limited catchments. Likewise, the streamflow regimes follow a similar pattern. I also highlight that aridity experienced remarkable changes over the last four decades and that all catchments have become drier because of climate-induced changes. This is a critical finding for the scientific branches of climate change and ecohydrology with important implications for societal and environmental health.

Another key finding of my research that adds to the current pool of knowledge is the hydrological impacts of the long-term eCO_2 feedbacks with vegetation. My analysis suggests that these feedbacks are reducing baseflow together with climatic forcings. This work, for the first time, separates the contribution of P, PET, and eCO_2-veg feedbacks to baseflow trends and reveals that the relative reductions on streamflow are more acute in water-limited catchments that are already facing water scarcity. These outcomes provide meaningful novel aspects to the science of CO_2 fertilization over water-limited areas and enhance our understanding about ecohydrological interactions among climate forcings, vegetation and delayed streamflow sources. The implications for freshwater supply are highly significant, as baseflow dominates the surface freshwater yield during both the dry season and drier years.

6.3 Implications for management

These research outcomes underscore important challenges regarding future water supply and management, with important implications for the environment and society. Given the observed streamflow reductions, what can we expect for the future of water supply along the Australian east coast? Are essential water dependent societal needs, such as food production and urban domestic use impacted and threatened? How can the advancements in scientific knowledge achieved by this research bridge management and influence policy making and stakeholders? This section briefly discusses the issues highlighted above.

Firstly, concerning climate forcings, reducing carbon dioxide emissions will help diminish the observed P reduction and PET increase (climate-induced change) as well as the eCO_2-vegetation feedbacks also identified as a driver of reduction in freshwater availability. While Australia already has a comprehensive guideline to target climate change mitigation established by the Climate Change Authority Act 2011, the findings of this research show that climate change already has an

acute detrimental impact on freshwater availability. This highlights that the current framework of activities may not be enough to ensure the freshwater supply for basic societal needs, especially considering the ongoing scenario of growing demand and reducing availability. Urban centres and agricultural regions may need to reconsider alternative sources previously considered unsuitable due to high cost. This also has important implications for urban populations with a potential rise in the prices of food, domestic water use and hence in the overall cost of living.

Secondly, the increasing human consumption pressure on water resources may also reduce environmental flows (Poff et al., 1997; Naiman et al., 2008; Kennard et al., 2010), posing a risk to the downstream riverine environments dependent on the same sources over extracted by humans. Alternative sources currently not explored for societal needs and serving to wildlife conservation may also be threatened by growing human demand and reduced availability.

Thirdly, the new insights into streamflow regimes and drivers of streamflow characteristics can potentially assist decision-makers regarding the suitability of catchments for freshwater supply, both at present and in the future. In addition, the regional drivers of streamflow characteristics can help bridging water resource management and biodiversity conservation at bioregion scales. Integrated catchment management programs should be encouraged to conserve essential catchment biophysical drivers to achieve specific management goals such as reduction of overland flow and sediment load in reef catchments and maximization of recharge and release in urban and agricultural supply catchments.

Finally, taking into account the streamflow reductions in regions already facing water scarcity, the dominant biophysical drivers of key streamflow characteristics may be of assistance in the identification of ungauged catchments with desirable characteristics for expansion of supply sources network (e.g. higher baseflow, lower intermittency and higher runoff ratio).

6.4 Approach and limitations

Ecohydrology in an emerging inter-disciplinary field of knowledge that has made major advances in the last decades. Some aspects inherent to these advancements are the range of publicly available catchment datasets, the emerging data processing techniques and the advancement of computer performance. My background in environmental and spatial sciences, remote sensing and hydrology helped me to identify this unique opportunity to undertake world-class research and make a solid contribution to the field of ecohydrology in my PhD. One of the greatest gains I developed was the ability to handle and analyse large datasets. This allowed me to compile and integrate data from different sources and to automate modern data analysis techniques to reveal the subtle patterns of

this thesis. It is worth noting that the current availability of free datasets, diffusion of scripting knowledge and advancement of computers supports the new generation of scientists and their ability to solve complex inter-disciplinary problems. That would not have been possible ten years ago.

It is important to mention the limitations with regard to the datasets and approach used in this thesis. Firstly, this thesis addresses only the annual time scale (i.e., long-term mean, change in the steady-state and trends), which means that there are a range of other temporal scales that would certainly also provide additional mechanistic insights if they were assessed (e.g. seasonality). The gridded precipitation data does not have the same quality across the study region, as it is strongly dependent on the gauge density. This means that some catchments may have errors in P estimates. However, as most of the analyses were performed with long-term averages at the annual scale, these errors tend to be minimised. The most critical catchments are likely to be the mountainous ones that receive regular orographic rainfall as well as those with low gauge density in the surrounding area. The streamflow data may also have problems in some catchments as the accuracy depends on the sampling effort to construct the rating curve – i.e. the proper representation of the natural water level and streamflow range of each river. Another constraint concerns the potential evapotranspiration data, as I use a radiation method (Priestley – Taylor) that may not adequately represent the atmospheric demand process. However, the absence of reliable long-term wind data precludes the use of a more physically-based form of PET. The soil data has limitations as well taking into account the limited number of field measurements and methods used extrapolate and generate the spatial datasets. Lastly, this study lacks a reliable source of atmospheric CO_2 concentrations and its spatial and temporal variability. However, this is a challenge faced for most researches, as these measurements are costly and the methods available to measure the past trends are limited and constrain the construction of spatially explicit time-series.

6.5 Future Research

The findings of this thesis offer a scope to develop future research.

First, it is important to test the catchment classification scheme developed here considering a large number of streamflow signatures exploring their complementarity and redundancy based on orthogonality for selection of metrics before the classification. This prior exploratory data analysis based on a large range of streamflow signatures would allow the classification of rivers with different streamflow characteristics and could potentially suit other regions worldwide or even global datasets with a broader streamflow regime spectrum. It is also important to test to what extent the relationship between the spectrum of water and energy balances (Budyko framework)

and drivers of runoff characteristics (Dunne diagram) holds with different or broader spectrum of streamflow regimes.

Second, there is a need to evaluate the importance of soil properties to explain the variability in streamflow characteristics at regional scales both in Australia and globally. Given the limitations of the Australian soil dataset (e.g. coarse resolution and low number of data points), it is recommended to repeat the analysis once improved soil data is available to better capture the soil effects already discussed. I would also recommend exploring smaller spatial extents, as the regional scales considered here are yet quite large. With this, new subtle patterns concerning the drivers of streamflow characteristics may emerge and hence enhancing the utility for water resource management and conservation of essential catchment ecohydrological processes for freshwater yield.

Thirdly, there are important questions concerning the patterns of streamflow change as well as the climate-induced and anthropogenic landscape-induced in development countries in South America and Africa. Understanding global drivers of changes using empirical evidence rather than modelling is also a promising outreach of this research. While the data availability may be a constraint for these directions for future research, there is certainly data availability for larger catchments, although the majority of them are regulated. I would also recommend examining streamflow changes over multiple periods as well as the trajectory that single catchments undertake within the Budyko framework in light of climate and landscape modifications. The pre-selection of catchments that experienced a range of landscape changes with long-term data availability (e.g. >80 years) to perform a more detailed temporal analysis (i.e. annual and/or decadal timescales) could potentially reveal new insights into the changes in the water and energy balances the specific landscape changes could lead to.

These recommendations for investigation expansion for other regions as well as to global scale also apply for assumptions regarding eCO_2-vegetation feedbacks and streamflow reductions in other water-limited regions worldwide. An important consideration for future studies is the inclusion of CO_2 time-series to relate with satellite-based vegetation data. The CO_2 time-series can be derived from flux-towers, remote sensing or both. This could provide a source of validation for the eCO_2-vegetation feedbacks addressed in the objective 4.

6.6 Conclusion

Catchment streamflow integrates the ecohydrological feedbacks of vegetation and atmosphere over a range of scales (i.e. at leaf, plant and landscape levels) and in space and time. This thesis makes an important contribution towards understanding streamflow generation functioning and the impacts of rapid changes in climate and landscapes currently taking place. This is particularly important for eastern Australia, as the study region includes over 80% of the Australian population and the freshwater supply for domestic use, food production, and ecosystem health strongly relies on the functioning and changes of streamflow generation addressed by this thesis. In a broader context, the findings of my PhD research advance the pool of knowledge regarding the underlying ecohydrological feedbacks generating streamflow in a range of climatic settings, especially in water-limited areas, where over one third of the global human population currently inhabit and struggle against water scarcity.

REFERENCES

ABARES, 2014. Catchment Scale Land Use of Australia - 2014. Bioregional Assessment Source Dataset.

ABS, 2014. Australian Population Grid, 2011 ABS, Canberra.

Ahiablame L, Chaubey I, Engel B, Cherkauer K, Merwade V, 2013. Estimation of annual baseflow at ungauged sites in Indiana USA. *Journal of Hydrology* **476**: 13-27. DOI:10.1016/j.jhydrol.2012.10.002

Akaike H, 1974. A new look at the statistical model identification. *Automatic Control, IEEE Transactions on* **19**(6): 716-723. DOI:10.1109/TAC.1974.1100705

Alexander LV, Arblaster JM, 2009. Assessing trends in observed and modelled climate extremes over Australia in relation to future projections. *International Journal of Climatology* **29**(3): 417-435. DOI:10.1002/joc.1730

Ali G, Tetzlaff D, Soulsby C, McDonnell JJ, Capell R, 2012. A comparison of similarity indices for catchment classification using a cross-regional dataset. *Advances in Water Resources* **40**(0): 11-22. DOI:doi:10.1016/j.advwatres.2012.01.008

Alkama R, Decharme B, Douville H, Ribes A, 2011. Trends in Global and Basin-Scale Runoff over the Late Twentieth Century: Methodological Issues and Sources of Uncertainty. *Journal of Climate* **24**(12): 3000-3014. DOI:doi:10.1175/2010JCLI3921.1

Andréassian V, 2004. Waters and forests: from historical controversy to scientific debate. *Journal of Hydrology* **291**(1): 1-27.

Andréassian V, Lerat J, Le Moine N, Perrin C, 2012. Neighbors: Nature's own hydrological models. *Journal of Hydrology* **414**: 49-58. DOI:doi:10.1016/j.jhydrol.2011.10.007

Arnold S, Thornton C, Baumgartl T, 2012. Ecohydrological feedback as a land restoration tool in the semi-arid Brigalow Belt, QLD, Australia. *Agriculture, Ecosystems & Environment* **163**(0): 61-71. DOI:10.1016/j.agee.2012.05.020

Arora VK, 2002. The use of the aridity index to assess climate change effect on annual runoff. *Journal of Hydrology* **265**(1–4): 164-177. DOI:doi:10.1016/S0022-1694(02)00101-4

ASRIS, 2015. Australian Soil Resource Information System.

Bao J, Sherwood SC, Alexander LV, Evans JP, 2017. Future increases in extreme precipitation exceed observed scaling rates. *Nature Clim. Change* **7**(2): 128-132. DOI:10.1038/nclimate3201

Barnett TP, Pierce DW, Hidalgo HG, Bonfils C, Santer BD, Das T, Bala G, Wood AW, Nozawa T, Mirin AA, Cayan DR, Dettinger MD, 2008. Human-Induced Changes in the Hydrology of the Western United States. *Science* **319**(5866): 1080-1083. DOI:10.1126/science.1152538

Barron O, Silberstein R, Ali R, Donohue RJ, McFarlane DJ, Davies P, Hodgson G, Smart N, Donn M, 2012. Climate change effects on water-dependent ecosystems in south-western Australia. *Journal of Hydrology* **434–435**(0): 95-109. DOI:10.1016/j.jhydrol.2012.02.028

Beck H, Bruijnzeel L, van Dijk A, McVicar T, Scatena F, Schellekens J, 2013a. The impact of forest regeneration on streamflow in 12 meso-scale humid tropical catchments. *Hydrology and Earth System Sciences Discussions* **10**: 3045-3102.

Beck HE, de Roo A, van Dijk AIJM, 2015. Global Maps of Streamflow Characteristics Based on Observations from Several Thousand Catchments. *Journal of Hydrometeorology* **16**(4): 1478-1501. DOI:10.1175/JHM-D-14-0155.1

Beck HE, van Dijk AIJM, Miralles DG, de Jeu RAM, Bruijnzeel LA, McVicar TR, Schellekens J, 2013b. Global patterns in base flow index and recession based on streamflow observations from 3394 catchments. *Water Resources Research* **49**(12): 7843-7863. DOI:10.1002/2013WR013918

Bendjoudi H, Hubert P, 2002. The Gravelius compactness coefficient: critical analysis of a shape index for drainage basins. *Hydrological Sciences Journal* **47**(6): 921-930. DOI:doi:10.1080/02626660209493000

Berghuijs WR, Sivapalan M, Woods RA, Savenije HHG, 2014a. Patterns of similarity of seasonal water balances: A window into streamflow variability over a range of time scales. *Water Resources Research* **50**(7): 5638-5661. DOI:doi:10.1002/2014WR015692

Berghuijs WR, Woods RA, Hrachowitz M, 2014b. A precipitation shift from snow towards rain leads to a decrease in streamflow. *Nature Climate Change* **4**(7): 583-586. DOI:10.1038/nclimate2246

Berry SL, Farquhar GD, Roderick ML, 2006. Co-Evolution of Climate, Soil and Vegetation, Encyclopedia of Hydrological Sciences. John Wiley & Sons, Ltd. DOI:doi:10.1002/0470848944.hsa011

Beven KJ, 2000. Uniqueness of place and process representations in hydrological modelling. *Hydrology and Earth System Sciences* **4**(2): 203-213. DOI:doi:10.5194/hess-4-203-2000

Beven KJ, Wood EF, Sivapalan M, 1988. On hydrological heterogeneity — Catchment morphology and catchment response. *Journal of Hydrology* **100**(1–3): 353-375. DOI:doi:10.1016/0022-1694(88)90192-8

BjØrnstad O, Falck W, 2001. Nonparametric spatial covariance functions: Estimation and testing. *Environmental and Ecological Statistics* **8**(1): 53-70. DOI:10.1023/A:1009601932481

Bloomfield JP, Allen DJ, Griffiths KJ, 2009. Examining geological controls on baseflow index (BFI) using regression analysis: An illustration from the Thames Basin, UK. *Journal of Hydrology* **373**(1–2): 164-176. DOI:10.1016/j.jhydrol.2009.04.025

Bonan GB, 2008. Forests and Climate Change: Forcings, Feedbacks, and the Climate Benefits of Forests. *Science* **320**(5882): 1444-1449. DOI:10.1126/science.1155121

Bond WJ, Midgley GF, 2012. Carbon dioxide and the uneasy interactions of trees and savannah grasses. *Philosophical Transactions of the Royal Society of London B: Biological Sciences* **367**(1588): 601-612. DOI:10.1098/rstb.2011.0182

Bosch JM, Hewlett J, 1982. A review of catchment experiments to determine the effect of vegetation changes on water yield and evapotranspiration. *Journal of hydrology* **55**(1): 3-23.

Botter G, Basso S, Rodriguez-Iturbe I, Rinaldo A, 2013. Resilience of river flow regimes. *Proceedings of the National Academy of Sciences* **110**(32): 12925-12930. DOI:10.1073/pnas.1311920110

Bradshaw CJA, 2012. Little left to lose: deforestation and forest degradation in Australia since European colonization. *Journal of Plant Ecology* **5**(1): 109-120. DOI:10.1093/jpe/rtr038

Brandes D, Hoffmann JG, Mangarillo JT, 2005. Base flow recession rates, low flows, and hydrologic features of small watersheds in pennsylvania, USA. *JAWRA Journal of the American Water Resources Association* **41**(5): 1177-1186. DOI:10.1111/j.1752-1688.2005.tb03792.x

Breiman L, 2001. Random Forests. *Machine Learning* **45**(1): 5-32. DOI:10.1023/A:1010933404324

Brown AE, Zhang L, McMahon TA, Western AW, Vertessy RA, 2005. A review of paired catchment studies for determining changes in water yield resulting from alterations in vegetation. *Journal of hydrology* **310**(1): 28-61.

Bruijnzeel LA, 2004. Hydrological functions of tropical forests: not seeing the soil for the trees? *Agriculture, Ecosystems & Environment* **104**(1): 185-228.

Budyko MI, 1974. Climate and life. International Geophysics Series, 18. Academic press New York, New York.

Bunn ES, Arthington HA, 2002. Basic Principles and Ecological Consequences of Altered Flow Regimes for Aquatic Biodiversity. *Environmental Management* **30**(4): 492-507. DOI:10.1007/s00267-002-2737-0

Burnham KP, Anderson DR, 2002. Model selection and multimodel inference: a practical information-theoretic approach. Springer Science & Business Media.

Butzer KW, Helgren DM, 2005. Livestock, Land Cover, and Environmental History: The Tablelands of New South Wales, Australia, 1820–1920. *Annals of the Association of American Geographers* **95**(1): 80-111. DOI:10.1111/j.1467-8306.2005.00451.x

Cai W, van Rensch P, 2012. The 2011 southeast Queensland extreme summer rainfall: A confirmation of a negative Pacific Decadal Oscillation phase? *Geophysical Research Letters* **39**(8): L08702. DOI:10.1029/2011GL050820

Carmona AM, Sivapalan M, Yaeger MA, Poveda G, 2014. Regional patterns of interannual variability of catchment water balances across the continental U.S.: A Budyko framework. *Water Resources Research* **50**(12): 9177-9193. DOI:doi:10.1002/2014WR016013

Casper MC, Grigoryan G, Gronz O, Gutjahr O, Heinemann G, Ley R, Rock A, 2012. Analysis of projected hydrological behavior of catchments based on signature indices. *Hydrology and Earth System Sciences* **16**(2): 409-421. DOI:10.5194/hess-16-409-2012

Castellarin A, Camorani G, Brath A, 2007. Predicting annual and long-term flow-duration curves in ungauged basins. *Advances in Water Resources* **30**(4): 937-953. DOI:DOI:doi.org/10.1016/j.advwatres.2006.08.006

Castellarin A, Galeati G, Brandimarte L, Montanari A, Brath A, 2004. Regional flow-duration curves: reliability for ungauged basins. *Advances in Water Resources* **27**(10): 953-965. DOI:DOI:doi.org/10.1016/j.advwatres.2004.08.005

Cheng L, Yaeger M, Viglione A, Coopersmith E, Ye S, Sivapalan M, 2012. Exploring the physical controls of regional patterns of flow duration curves – Part 1: Insights from statistical analyses. *Hydrol. Earth Syst. Sci.* **16**(11): 4435-4446. DOI:10.5194/hess-16-4435-2012

Chiew FHS, McMahon TA, 2002. Modelling the impacts of climate change on Australian streamflow. *Hydrological Processes* **16**(6): 1235-1245.

Chiew FHS, Teng J, Vaze J, Kirono DGC, 2009a. Influence of global climate model selection on runoff impact assessment. *Journal of Hydrology* **379**(1–2): 172-180. DOI:10.1016/j.jhydrol.2009.10.004

Chiew FHS, Teng J, Vaze J, Post DA, Perraud JM, Kirono DGC, Viney NR, 2009b. Estimating climate change impact on runoff across southeast Australia: Method, results, and implications of the modeling method. *Water Resources Research* **45**(10): W10414. DOI:10.1029/2008WR007338

Chou C, Chiang JCH, Lan C-W, Chung C-H, Liao Y-C, Lee C-J, 2013. Increase in the range between wet and dry season precipitation. *Nature Geoscience* **6**(4): 263-267. DOI:10.1038/ngeo1744

Choudhury B, 1999. Evaluation of an empirical equation for annual evaporation using field observations and results from a biophysical model. *Journal of Hydrology* **216**(1–2): 99-110. DOI:doi:10.1016/S0022-1694(98)00293-5

Collins M, Knutti R, Arblaster J, Dufresne J-L, Fichefet T, Friedlingstein P, Gao X, Gutowski W, Johns T, Krinner G, 2013. Long-term climate change: projections, commitments and irreversibility. In: Stocker, T.F. et al. (Eds.), Climate Change 2013: The Physical Science Basis. Contribution of Working Group I to the Fifth Assessment Report of the Intergovernmental Panel on Climate Change. Cambridge University Press, Cambridge, pp. 1029-1136. DOI:10.1017/CBO9781107415324.024

Coopersmith EJ, Yaeger MA, Ye S, Cheng L, Sivapalan M, 2012. Exploring the physical controls of regional patterns of flow duration curves - Part 3: A catchment classification system based on regime curve indicators. *Hydrology and Earth System Sciences* **16**(11): 4467-4482. DOI:doi:10.5194/hess-16-4467-2012

Costigan KH, Daniels MD, Dodds WK, 2015. Fundamental spatial and temporal disconnections in the hydrology of an intermittent prairie headwater network. *Journal of Hydrology* **522**: 305-316. DOI:10.1016/j.jhydrol.2014.12.031

Costigan KH, Jaeger KL, Goss CW, Fritz KM, Goebel PC, 2016. Understanding controls on flow permanence in intermittent rivers to aid ecological research: integrating meteorology, geology and land cover. *Ecohydrology*: n/a-n/a. DOI:10.1002/eco.1712

Cowie BA, Thornton CM, Radford BJ, 2007. The Brigalow Catchment Study: I*. Overview of a 40-year study of the effects of land clearing in the brigalow bioregion of Australia. *Soil Research* **45**(7): 479-495. DOI:10.1071/SR07063

Datry T, Larned ST, Tockner K, 2014. Intermittent Rivers: A Challenge for Freshwater Ecology. *BioScience*. DOI:10.1093/biosci/bit027

Delworth TL, Zeng F, 2014. Regional rainfall decline in Australia attributed to anthropogenic greenhouse gases and ozone levels. *Nature Geoscience* **7**(8): 583-587. DOI:10.1038/ngeo2201

Destouni G, Jaramillo F, Prieto C, 2013. Hydroclimatic shifts driven by human water use for food and energy production. *Nature Clim. Change* **3**(3): 213-217. DOI:DOI:doi.org/10.1038/nclimate1719

Donohue RJ, McVicar TR, Roderick ML, 2010a. Assessing the ability of potential evaporation formulations to capture the dynamics in evaporative demand within a changing climate. *Journal of Hydrology* **386**(1–4): 186-197. DOI:doi:10.1016/j.jhydrol.2010.03.020

Donohue RJ, Roderick M, McVicar T, 2010b. Can dynamic vegetation information improve the accuracy of Budyko's hydrological model? *Journal of Hydrology* **390**(1): 23-34.

Donohue RJ, Roderick ML, McVicar TR, 2007. On the importance of including vegetation dynamics in Budyko's hydrological model. *Hydrology and Earth System Sciences* **11**(2): 983-995. DOI:doi:10.5194/hess-11-983-2007

Donohue RJ, Roderick ML, McVicar TR, 2008. Deriving consistent long-term vegetation information from AVHRR reflectance data using a cover-triangle-based framework. *Remote Sensing of Environment* **112**(6): 2938-2949. DOI:doi:10.1016/j.rse.2008.02.008

Donohue RJ, Roderick ML, McVicar TR, 2012. Roots, storms and soil pores: Incorporating key ecohydrological processes into Budyko's hydrological model. *Journal of Hydrology* **436–437**(0): 35-50. DOI:doi:10.1016/j.jhydrol.2012.02.033

Donohue RJ, Roderick ML, McVicar TR, Farquhar GD, 2013. Impact of CO_2 fertilization on maximum foliage cover across the globe's warm, arid environments. *Geophysical Research Letters* **40**(12): 3031-3035. DOI:10.1002/grl.50563

Donohue RJ, Roderick ML, McVicar TR, Yang Y, 2017. A simple hypothesis of how leaf and canopy-level transpiration and assimilation respond to elevated CO_2 reveals distinct response patterns between disturbed and undisturbed vegetation. *Journal of Geophysical Research: Biogeosciences* **122**(1): 168-184. DOI:10.1002/2016JG003505

Dunne T, 1983. Relation of field studies and modeling in the prediction of storm runoff. *Journal of Hydrology* **65**(1–3): 25-48. DOI:doi:10.1016/0022-1694(83)90209-3

Dynesius M, Nilsson C, 1994. Fragmentation and Flow Regulation of River Systems in the Northern Third of the World. *Science* **266**(5186): 753-762. DOI:10.1126/science.266.5186.753

Eicker A, Forootan E, Springer A, Longuevergne L, Kusche J, 2016. Does GRACE see the terrestrial water cycle "intensifying"? *Journal of Geophysical Research: Atmospheres* **121**(2): 733-745. DOI:10.1002/2015JD023808

Eilers PHC, Marx BD, 1996. Flexible smoothing with B-splines and penalties. 89-121. DOI:10.1214/ss/1038425655

Evans MC, 2016. Deforestation in Australia: drivers, trends and policy responses. *Pacific Conservation Biology* **22**(2): 130-150. DOI:10.1071/PC15052

Farley KA, Jobbágy EG, Jackson RB, 2005. Effects of afforestation on water yield: a global synthesis with implications for policy. *Global Change Biology* **11**(10): 1565-1576. DOI:10.1111/j.1365-2486.2005.01011.x

Feng X, Fu B, Piao S, Wang S, Ciais P, Zeng Z, Lu Y, Zeng Y, Li Y, Jiang X, Wu B, 2016. Revegetation in China[rsquor]s Loess Plateau is approaching sustainable water resource limits. *Nature Clim. Change* **advance online publication**. DOI:10.1038/nclimate3092

Feng X, Porporato A, Rodriguez-Iturbe I, 2013. Changes in rainfall seasonality in the tropics. *Nature Climate Change* **3**(9): 811-815. DOI:doi:10.1038/nclimate1907

Fensholt R, Langanke T, Rasmussen K, Reenberg A, Prince SD, Tucker C, Scholes RJ, Le QB, Bondeau A, Eastman R, Epstein H, Gaughan AE, Hellden U, Mbow C, Olsson L, Paruelo J, Schweitzer C, Seaquist J, Wessels K, 2012. Greenness in semi-arid areas across the globe 1981–2007 — an Earth Observing Satellite based analysis of trends and drivers. *Remote Sensing of Environment* **121**: 144-158. DOI:10.1016/j.rse.2012.01.017

Ferrari S, Cribari-Neto F, 2004. Beta Regression for Modelling Rates and Proportions. *Journal of Applied Statistics* **31**(7): 799-815. DOI:10.1080/0266476042000214501

Finlayson B, McMahon T, 1988. Australia vs the world: a comparative analysis of streamflow characteristics. *Fluvial geomorphology of Australia*: 17-40.

Fraley C, Raftery AE, 2002. Model-Based Clustering, Discriminant Analysis, and Density Estimation. *Journal of the American Statistical Association* **97**(458): 611-631. DOI:doi:10.2307/3085676

Fu B, 1981. On the calculation of the evaporation from land surface. *Scientia Atmospherica Sinica* **5**(1): 23-31.

Fu G, Viney NR, Charles SP, Liu J, 2010. Long-Term Temporal Variation of Extreme Rainfall Events in Australia: 1910–2006. *Journal of Hydrometeorology* **11**(4): 950-965. DOI:10.1175/2010JHM1204.1

Gallant AJE, Karoly DJ, 2010. A Combined Climate Extremes Index for the Australian Region. *Journal of Climate* **23**(23): 6153-6165. DOI:10.1175/2010JCLI3791.1

Gallant JC, Dowling TI, 2003. A multiresolution index of valley bottom flatness for mapping depositional areas. *Water Resources Research* **39**(12): 1347. DOI:doi:10.1029/2002WR001426

Gedney N, Cox PM, Betts RA, Boucher O, Huntingford C, Stott PA, 2006. Detection of a direct carbon dioxide effect in continental river runoff records. *Nature* **439**(7078): 835-838. DOI:10.1038/nature04504

Gentine P, D'Odorico P, Lintner BR, Sivandran G, Salvucci G, 2012. Interdependence of climate, soil, and vegetation as constrained by the Budyko curve. *Geophysical Research Letters* **39**(19): L19404. DOI:doi:10.1029/2012GL053492

Gergis J, Gallant A, Braganza K, Karoly D, Allen K, Cullen L, D'Arrigo R, Goodwin I, Grierson P, McGregor S, 2012. On the long-term context of the 1997–2009 'Big Dry' in South-Eastern Australia: insights from a 206-year multi-proxy rainfall reconstruction. *Climatic Change* **111**(3-4): 923-944. DOI:10.1007/s10584-011-0263-x

Gergis J, Garden D, Fenby C, 2010. The Influence of Climate on the First European Settlement of Australia: A Comparison of Weather Journals, Documentary Data and Palaeoclimate Records, 1788–1793. *Environmental History* **15**(3): 485-507. DOI:10.1093/envhis/emq079

Gero AF, Pitman AJ, Narisma GT, Jacobson C, Pielke RA, 2006. The impact of land cover change on storms in the Sydney Basin, Australia. *Global and Planetary Change* **54**(1–2): 57-78. DOI:10.1016/j.gloplacha.2006.05.003

Gerrits AMJ, Savenije HHG, Veling EJM, Pfister L, 2009. Analytical derivation of the Budyko curve based on rainfall characteristics and a simple evaporation model. *Water Resources Research* **45**(4): W04403. DOI:doi:10.1029/2008WR007308

Giambelluca TW, 2002. Hydrology of altered tropical forest. *Hydrological Processes* **16**(8): 1665-1669. DOI:10.1002/hyp.5021

Gilbert N, 2011. Science enters desert debate. *Nature* **477**(7364): 262.

Gordon L, Dunlop M, Foran B, 2003. Land cover change and water vapour flows: learning from Australia. *Philosophical Transactions of the Royal Society of London. Series B: Biological Sciences* **358**(1440): 1973-1984.

Gordon L, Steffen W, Jönsson BF, Folke C, Falkenmark M, Johannessen Å, 2005. Human modification of global water vapor flows from the land surface. *Proceedings of the National Academy of Sciences of the United States of America* **102**(21): 7612-7617. DOI:10.1073/pnas.0500208102

Goutam K, Ashok M, Leung LR, 2017. Changes in temporal variability of precipitation over land due to anthropogenic forcings. *Environmental Research Letters* **12**(2): 024009.

Green K, Pickering CM, 2009. The Decline of Snowpatches in the Snowy Mountains of Australia: Importance of Climate Warming, Variable Snow, and Wind. *Arctic, Antarctic, and Alpine Research* **41**(2): 212-218. DOI:10.1657/1938-4246-41.2.212

Greve P, Orlowsky B, Mueller B, Sheffield J, Reichstein M, Seneviratne SI, 2014. Global assessment of trends in wetting and drying over land. *Nature Geoscience* **7**(10): 716-721. DOI:10.1038/ngeo2247

Gudmundsson L, Greve P, Seneviratne SI, 2016. The sensitivity of water availability to changes in the aridity index and other factors—A probabilistic analysis in the Budyko space. *Geophysical Research Letters*: n/a-n/a. DOI:10.1002/2016GL069763

Hall FR, 1968. Base-Flow Recessions—A Review. *Water Resources Research* **4**(5): 973-983. DOI:10.1029/WR004i005p00973

Hamed KH, 2008. Trend detection in hydrologic data: The Mann–Kendall trend test under the scaling hypothesis. *Journal of Hydrology* **349**(3–4): 350-363. DOI:10.1016/j.jhydrol.2007.11.009

Haylock M, Nicholls N, 2000. Trends in extreme rainfall indices for an updated high quality data set for Australia, 1910–1998. *International Journal of Climatology* **20**(13): 1533-1541. DOI:10.1002/1097-0088(20001115)20:13<1533::AID-JOC586>3.0.CO;2-J

He Y, Bárdossy A, Zehe E, 2011. A catchment classification scheme using local variance reduction method. *Journal of Hydrology* **411**(1–2): 140-154. DOI:doi:10.1016/j.jhydrol.2011.09.042

Heller KA, Ghahramani Z, 2005. Bayesian hierarchical clustering, Proceedings of the 22nd international conference on Machine learning. ACM, pp. 297-304.

Helsel D, Hirsch R, 2002. Statistical methods in water resources: US Geological Survey Techniques of Water Resources Investigations, book 4, chap. A3.

Hennessy KJ, Whetton PH, Walsh K, Smith IN, Bathols JM, Hutchinson M, Sharples J, 2008. Climate change effects on snow conditions in mainland Australia and adaptation at ski resorts through snowmaking. *Climate Research* **35**(3): 255-270.

Hughes J, James B, 1989. A hydrological regionalization of streams in Victoria, Australia, with implications for stream ecology. *Marine and Freshwater Research* **40**(3): 303-326. DOI:doi:10.1071/MF9890303

Hümann M, Schüler G, Müller C, Schneider R, Johst M, Caspari T, 2011. Identification of runoff processes – The impact of different forest types and soil properties on runoff formation and floods. *Journal of Hydrology* **409**(3–4): 637-649. DOI:10.1016/j.jhydrol.2011.08.067

Huntington TG, 2006. Evidence for intensification of the global water cycle: Review and synthesis. *Journal of Hydrology* **319**(1–4): 83-95. DOI:10.1016/j.jhydrol.2005.07.003

IBRA7, 2015. Interim Biogeographical Regionalisation for Australia - Regions and codes. Australian Government Department of Sustainability, Environment, Population and Communities, Canberra.

IBRA, 2013. Interim Biogeographic Regionalisation for Australia (IBRA). In: Department of Sustainability, E., Water, Population and Communities (Ed.), Australia.

Iversen CM, 2010. Digging deeper: fine-root responses to rising atmospheric CO_2 concentration in forested ecosystems. *New Phytologist* **186**(2): 346-357. DOI:10.1111/j.1469-8137.2009.03122.x

Jaramillo F, Destouni G, 2014. Developing water change spectra and distinguishing change drivers worldwide. *Geophysical Research Letters* **41**(23): 8377-8386. DOI:10.1002/2014GL061848

Jaramillo F, Destouni G, 2015. Local flow regulation and irrigation raise global human water consumption and footprint. *Science* **350**(6265): 1248-1251. DOI:10.1126/science.aad1010

Johnson N, Revenga C, Echeverria J, 2001. Managing Water for People and Nature. *Science* **292**(5519): 1071-1072. DOI:10.1126/science.1058821

Jones DA, Wang W, Fawcett R, 2009. High-quality spatial climate data-sets for Australia. *Australian Meteorological and Oceanographic Journal* **58**(4): 233-248.

Jothityangkoon C, Sivapalan M, 2009. Framework for exploration of climatic and landscape controls on catchment water balance, with emphasis on inter-annual variability. *Journal of Hydrology* **371**(1–4): 154-168. DOI:doi:10.1016/j.jhydrol.2009.03.030

Karoly DJ, 2014. Climate change: Human-induced rainfall changes. *Nature Geoscience* **7**(8): 551-552. DOI:10.1038/ngeo2207

Kennard MJ, Pusey BJ, Olden JD, Mackay SJ, Stein JL, Marsh N, 2010. Classification of natural flow regimes in Australia to support environmental flow management. *Freshwater Biology* **55**(1): 171-193. DOI:doi:10.1111/j.1365-2427.2009.02307.x

Klein C, Wilson K, Watts M, Stein J, Berry S, Carwardine J, Smith MS, Mackey B, Possingham H, 2009. Incorporating ecological and evolutionary processes into continental-scale conservation planning. *Ecological Applications* **19**(1): 206-217. DOI:10.1890/07-1684.1

Knauer J, Zaehle S, Reichstein M, Medlyn BE, Forkel M, Hagemann S, Werner C, 2017. The response of ecosystem water-use efficiency to rising atmospheric CO_2 concentrations: sensitivity and large-scale biogeochemical implications. *New Phytologist* **213**(4): 1654-1666. DOI:10.1111/nph.14288

Labat D, Godderis Y, Probst JL, Guyot JL, 2005. Reply to comment of Legates et al. *Advances in Water Resources* **28**(12): 1316-1319. DOI:10.1016/j.advwatres.2005.04.007

Labat D, Goddéris Y, Probst JL, Guyot JL, 2004. Evidence for global runoff increase related to climate warming. *Advances in Water Resources* **27**(6): 631-642. DOI:10.1016/j.advwatres.2004.02.020

Lacey GC, Grayson RB, 1998. Relating baseflow to catchment properties in south-eastern Australia. *Journal of Hydrology* **204**(1–4): 231-250. DOI:10.1016/S0022-1694(97)00124-8

Ladson A, Brown R, Neal B, Nathan R, 2013. A standard approach to baseflow separation using the Lyne and Hollick filter. *Australian Journal of Water Resources* **17**(1): 25-34.

Larsen JE, Sivapalan M, Coles NA, Linnet PE, 1994. Similarity analysis of runoff generation processes in real-world catchments. *Water Resources Research* **30**(6): 1641-1652. DOI:doi:10.1029/94WR00555

Legates DR, Lins HF, McCabe GJ, 2005. Comments on "Evidence for global runoff increase related to climate warming" by Labat et al. *Advances in Water Resources* **28**(12): 1310-1315. DOI:10.1016/j.advwatres.2005.04.006

Leigh C, Sheldon F, 2008. Hydrological changes and ecological impacts associated with water resource development in large floodplain rivers in the Australian tropics. *River Research and Applications* **24**(9): 1251-1270. DOI:doi:10.1002/rra.1125

Ley R, Casper MC, Hellebrand H, Merz R, 2011. Catchment classification by runoff behaviour with self-organizing maps (SOM). *Hydrol. Earth Syst. Sci.* **15**(9): 2947-2962. DOI:10.5194/hess-15-2947-2011

Li H, Sivapalan M, Tian F, Harman C, 2014. Functional approach to exploring climatic and landscape controls of runoff generation: 1. Behavioral constraints on runoff volume. *Water Resources Research* **50**(12): 9300-9322. DOI:doi:10.1002/2014WR016307

Li L, Maier HR, Lambert MF, Simmons CT, Partington D, 2013. Framework for assessing and improving the performance of recursive digital filters for baseflow estimation with application to the Lyne and Hollick filter. *Environmental Modelling & Software* **41**(0): 163-175. DOI:doi:10.1016/j.envsoft.2012.11.009

Li Q, Wei X, Zhang M, Liu W, Fan H, Zhou G, Giles-Hansen K, Liu S, Wang Y, 2017. Forest cover change and water yield in large forested watersheds: A global synthetic assessment. *Ecohydrology*: n/a-n/a. DOI:10.1002/eco.1838

Liang W, Bai D, Wang F, Fu B, Yan J, Wang S, Yang Y, Long D, Feng M, 2015. Quantifying the impacts of climate change and ecological restoration on streamflow changes based on a

Budyko hydrological model in China's Loess Plateau. *Water Resources Research* **51**(8): 6500-6519. DOI:10.1002/2014WR016589

Liu Q, McVicar TR, Yang Z, Donohue RJ, Liang L, Yang Y, 2016. The hydrological effects of varying vegetation characteristics in a temperate water-limited basin: Development of the dynamic Budyko-Choudhury-Porporato (dBCP) model. *Journal of Hydrology* **543**: 595-611. DOI:10.1016/j.jhydrol.2016.10.035

Liu YY, van Dijk AIJM, de Jeu RAM, Canadell JG, McCabe MF, Evans JP, Wang G, 2015. Recent reversal in loss of global terrestrial biomass. *Nature Climate Change* **5**(5): 470-474. DOI:10.1038/nclimate2581

Longobardi A, Villani P, 2008. Baseflow index regionalization analysis in a mediterranean area and data scarcity context: Role of the catchment permeability index. *Journal of Hydrology* **355**(1–4): 63-75. DOI:10.1016/j.jhydrol.2008.03.011

Lu X, Wang L, McCabe MF, 2016. Elevated CO_2 as a driver of global dryland greening. *Scientific Reports* **6**: 20716. DOI:10.1038/srep20716

Lymburner L, Tan P, Mueller N, Thackway R, Lewis A, Thankappan M, Randall L, Islam A, Senarath U, 2011. Dynamic Land Cover Dataset Version 1. In: Australia, G. (Ed.).

Lyne V, Hollick M, 1979. Stochastic time-variable rainfall runoff modelling, Hydrology and Water Resources Symposium. Institution of Engineers, Perth, Australia, pp. 89-92.

Lytle DA, Poff NL, 2004. Adaptation to natural flow regimes. *Trends in Ecology & Evolution* **19**(2): 94-100. DOI:10.1016/j.tree.2003.10.002

Mac Nally R, Bennett AF, Brown GW, Lumsden LF, Yen A, Hinkley S, Lillywhite P, Ward D, 2002. How well do ecosystem-based planning units represent different components of biodiversity? *Ecological Applications* **12**(3): 900-912. DOI:10.1890/1051-0761(2002)012[0900:HWDEBP]2.0.CO;2

Mackay SJ, Arthington AH, James CS, 2014. Classification and comparison of natural and altered flow regimes to support an Australian trial of the Ecological Limits of Hydrologic Alteration framework. *Ecohydrology* **7**(6): 1485-1507. DOI:10.1002/eco.1473

Mazvimavi D, Meijerink AMJ, Savenije HHG, Stein A, 2005. Prediction of flow characteristics using multiple regression and neural networks: A case study in Zimbabwe. *Physics and Chemistry of the Earth, Parts A/B/C* **30**(11–16): 639-647. DOI:10.1016/j.pce.2005.08.003

McAlpine CA, Syktus J, Deo RC, Lawrence PJ, McGowan HA, Watterson IG, Phinn SR, 2007. Modeling the impact of historical land cover change on Australia's regional climate. *Geophysical Research Letters* **34**(22): L22711. DOI:10.1029/2007GL031524

McAlpine CA, Syktus J, Ryan JG, Deo RC, McKeon GM, McGowan HA, Phinn SR, 2009. A continent under stress: interactions, feedbacks and risks associated with impact of modified land cover on Australia's climate. *Global Change Biology* **15**(9): 2206-2223. DOI:10.1111/j.1365-2486.2009.01939.x

McDonnell JJ, Sivapalan M, Vaché K, Dunn S, Grant G, Haggerty R, Hinz C, Hooper R, Kirchner J, Roderick ML, Selker J, Weiler M, 2007. Moving beyond heterogeneity and process complexity: A new vision for watershed hydrology. *Water Resources Research* **43**(7): W07301. DOI:doi:10.1029/2006WR005467

McDonnell JJ, Woods R, 2004. On the need for catchment classification. *Journal of Hydrology* **299**(1–2): 2-3. DOI:doi:10.1016/j.jhydrol.2004.09.003

McFarlane D, Stone R, Martens S, Thomas J, Silberstein R, Ali R, Hodgson G, 2012. Climate change impacts on water yields and demands in south-western Australia. *Journal of Hydrology* **475**(0): 488-498. DOI:10.1016/j.jhydrol.2012.05.038

McKenzie NJ, Jacquier D, Ashton L, Cresswell H, 2000. Estimation of soil properties using the Atlas of Australian Soils. CSIRO Land and Water Canberra.

McMahon TA, Vogel RM, Peel MC, Pegram GGS, 2007. Global streamflows – Part 1: Characteristics of annual streamflows. *Journal of Hydrology* **347**(3–4): 243-259. DOI:10.1016/j.jhydrol.2007.09.002

McVicar TR, Donohue RJ, O'Grady AP, Li L, 2010. The effects of climatic changes on plant physiological and catchment ecohydrological processes in the high-rainfall catchments of the Murray-Darling Basin: A scoping study. CSIRO Water for a Healthy Country National Research Flagship, Canberra.

McVicar TR, Roderick ML, Donohue RJ, Li LT, Van Niel TG, Thomas A, Grieser J, Jhajharia D, Himri Y, Mahowald NM, Mescherskaya AV, Kruger AC, Rehman S, Dinpashoh Y, 2012a. Global review and synthesis of trends in observed terrestrial near-surface wind speeds: Implications for evaporation. *Journal of Hydrology* **416–417**(0): 182-205. DOI:10.1016/j.jhydrol.2011.10.024

McVicar TR, Roderick ML, Donohue RJ, Van Niel TG, 2012b. Less bluster ahead? Ecohydrological implications of global trends of terrestrial near-surface wind speeds. *Ecohydrology* **5**(4): 381-388. DOI:10.1002/eco.1298

McVicar TR, Van Niel TG, Li L, Hutchinson MF, Mu X, Liu Z, 2007. Spatially distributing monthly reference evapotranspiration and pan evaporation considering topographic influences. *Journal of Hydrology* **338**(3–4): 196-220. DOI:doi:10.1016/j.jhydrol.2007.02.018

Miller VC, 1953. A Quantitative geomorphic study of drainage basin characteristics in the Clinch Mountain area Virginia and Tennessee.

Milly PCD, 1994. Climate, soil water storage, and the average annual water balance. *Water Resources Research* **30**(7): 2143-2156. DOI:doi:10.1029/94WR00586

Milly PCD, Betancourt J, Falkenmark M, Hirsch RM, Kundzewicz ZW, Lettenmaier DP, Stouffer RJ, 2008. Stationarity Is Dead: Whither Water Management? *Science* **319**(5863): 573-574. DOI:doi:10.1126/science.1151915

Milly PCD, Dunne KA, Vecchia AV, 2005. Global pattern of trends in streamflow and water availability in a changing climate. *Nature* **438**(7066): 347-350.

Minshall GW, Winger PV, 1968. The Effect of Reduction in Stream Flow on Invertebrate Drift. *Ecology* **49**(3): 580-582. DOI:10.2307/1934133

Moliere DR, Lowry JBC, Humphrey CL, 2009. Classifying the flow regime of data-limited streams in the wet-dry tropical region of Australia. *Journal of Hydrology* **367**(1–2): 1-13. DOI:10.1016/j.jhydrol.2008.12.015

Mosley MP, 1981. Delimitation of New Zealand hydrologic regions. *Journal of Hydrology* **49**(1–2): 173-192. DOI:10.1016/0022-1694(81)90211-0

Murphy BF, Timbal B, 2008. A review of recent climate variability and climate change in southeastern Australia. *International Journal of Climatology* **28**(7): 859-879. DOI:10.1002/joc.1627

Mwakalila S, Feyen J, Wyseure G, 2002. The influence of physical catchment properties on baseflow in semi-arid environments. *Journal of Arid Environments* **52**(2): 245-258. DOI:10.1006/jare.2001.0947

Nagelkerke NJD, 1991. A note on a general definition of the coefficient of determination. *Biometrika* **78**(3): 691-692. DOI:10.1093/biomet/78.3.691

Naiman RJ, Latterell JJ, Pettit NE, Olden JD, 2008. Flow variability and the biophysical vitality of river systems. *Comptes Rendus Geoscience* **340**(9–10): 629-643. DOI:10.1016/j.crte.2008.01.002

Nathan RJ, McMahon TA, 1990. Evaluation of automated techniques for base flow and recession analyses. *Water Resources Research* **26**(7): 1465-1473. DOI:doi:10.1029/WR026i007p01465

Nicholls N, 2010. Local and remote causes of the southern Australian autumn-winter rainfall decline, 1958–2007. *Clim Dyn* **34**(6): 835-845. DOI:10.1007/s00382-009-0527-6

Nicholls N, Collins D, 2006. Observed climate change in Australia over the past century. *Energy & Environment* **17**(1): 1-12. DOI:10.1260/095830506776318804

Ning T, Li Z, Liu W, 2016. Separating the impacts of climate change and land surface alteration on runoff reduction in the Jing River catchment of China. *CATENA* **147**: 80-86. DOI:10.1016/j.catena.2016.06.041

Nippgen F, McGlynn BL, Marshall LA, Emanuel RE, 2011. Landscape structure and climate influences on hydrologic response. *Water Resources Research* **47**(12): W12528. DOI:10.1029/2011WR011161

Norbiato D, Borga M, Merz R, Blöschl G, Carton A, 2009. Controls on event runoff coefficients in the eastern Italian Alps. *Journal of Hydrology* **375**(3–4): 312-325. DOI:10.1016/j.jhydrol.2009.06.044

Ogunkoya OO, 1988. Towards a delimitation of southwestern Nigeria into hydrological regions. *Journal of Hydrology* **99**(1–2): 165-177. DOI:10.1016/0022-1694(88)90085-6

Ogunkoya OO, Adejuwon JO, Jeje LK, 1984. Runoff response to basin parameters in southwestern Nigeria. *Journal of Hydrology* **72**(1–2): 67-84. DOI:10.1016/0022-1694(84)90185-9

Ohmura A, Wild M, 2002. Is the Hydrological Cycle Accelerating? *Science* **298**(5597): 1345-1346. DOI:10.1126/science.1078972

Oki T, 2006. The Hydrologic Cycles and Global Circulation, Encyclopedia of Hydrological Sciences. John Wiley & Sons, Ltd. DOI:10.1002/0470848944.hsa001

Olden JD, Kennard MJ, Pusey BJ, 2012. A framework for hydrologic classification with a review of methodologies and applications in ecohydrology. *Ecohydrology* **5**(4): 503-518. DOI:doi:10.1002/eco.251

Olden JD, Poff NL, 2003. Redundancy and the choice of hydrologic indices for characterizing streamflow regimes. *River Research and Applications* **19**(2): 101-121. DOI:doi:10.1002/rra.700

Ospina R, Ferrari SLP, 2012. A general class of zero-or-one inflated beta regression models. *Computational Statistics & Data Analysis* **56**(6): 1609-1623. DOI:10.1016/j.csda.2011.10.005

Ospina R, Ferrari SP, 2010. Inflated beta distributions. *Stat Papers* **51**(1): 111-126. DOI:10.1007/s00362-008-0125-4

Oudin L, Andréassian V, Perrin C, Michel C, Le Moine N, 2008. Spatial proximity, physical similarity, regression and ungaged catchments: A comparison of regionalization approaches based on 913 French catchments. *Water Resources Research* **44**(3): W03413. DOI:10.1029/2007WR006240

Oudin L, Kay A, Andréassian V, Perrin C, 2010. Are seemingly physically similar catchments truly hydrologically similar? *Water Resources Research* **46**(11): W11558. DOI:doi:10.1029/2009WR008887

Patil S, Stieglitz M, 2011. Hydrologic similarity among catchments under variable flow conditions. *Hydrol. Earth Syst. Sci.* **15**(3): 989-997. DOI:doi:10.5194/hess-15-989-2011

Pegg MA, Pierce CL, 2002. Classification of reaches in the Missouri and lower Yellowstone Rivers based on flow characteristics. *River Research and Applications* **18**(1): 31-42. DOI:10.1002/rra.635

Pelletier JD, Barron-Gafford GA, Breshears DD, Brooks PD, Chorover J, Durcik M, Harman CJ, Huxman TE, Lohse KA, Lybrand R, Meixner T, McIntosh JC, Papuga SA, Rasmussen C, Schaap M, Swetnam TL, Troch PA, 2013. Coevolution of nonlinear trends in vegetation, soils, and topography with elevation and slope aspect: A case study in the sky islands of southern Arizona. *Journal of Geophysical Research: Earth Surface* **118**(2): 741-758. DOI:10.1002/jgrf.20046

Peña-Arancibia JL, van Dijk AI, Guerschman JP, Mulligan M, Bruijnzeel LA, McVicar TR, 2012. Detecting changes in streamflow after partial woodland clearing in two large catchments in the seasonal tropics. *Journal of Hydrology* **416**: 60-71.

Peña-Arancibia JL, van Dijk AIJM, Mulligan M, Bruijnzeel LA, 2010. The role of climatic and terrain attributes in estimating baseflow recession in tropical catchments. *Hydrology and Earth System Sciences* **14**(11): 2193-2205. DOI:10.5194/hess-14-2193-2010

Piao S, Friedlingstein P, Ciais P, de Noblet-Ducoudré N, Labat D, Zaehle S, 2007. Changes in climate and land use have a larger direct impact than rising CO_2 on global river runoff trends. *Proceedings of the National Academy of Sciences* **104**(39): 15242-15247. DOI:10.1073/pnas.0707213104

Pitman AJ, Narisma GT, Pielke RA, Holbrook NJ, 2004. Impact of land cover change on the climate of southwest Western Australia. *Journal of Geophysical Research: Atmospheres* **109**(D18): D18109. DOI:10.1029/2003JD004347

Poff NL, Allan JD, Bain MB, Karr JR, Prestegaard KL, Richter BD, Sparks RE, Stromberg JC, 1997. The Natural Flow Regime. *BioScience* **47**(11): 769-784. DOI:10.2307/1313099

Poff NL, Olden JD, Pepin DM, Bledsoe BP, 2006. Placing global stream flow variability in geographic and geomorphic contexts. *River Research and Applications* **22**(2): 149-166. DOI:doi:10.1002/rra.902

Postel S, Richter B, 2012. Rivers for life: managing water for people and nature. Island Press.

Potter NJ, Zhang L, 2009. Interannual variability of catchment water balance in Australia. *Journal of Hydrology* **369**(1–2): 120-129. DOI:doi:10.1016/j.jhydrol.2009.02.005

Potter NJ, Zhang L, Milly PCD, McMahon TA, Jakeman AJ, 2005. Effects of rainfall seasonality and soil moisture capacity on mean annual water balance for Australian catchments. *Water Resources Research* **41**(6): W06007. DOI:10.1029/2004WR003697

Radford BJ, Thornton CM, Cowie BA, Stephens ML, 2007. The Brigalow Catchment Study: III.* Productivity changes on brigalow land cleared for long-term cropping and for grazing. *Soil Research* **45**(7): 512-523. DOI:10.1071/SR07062

Raupach MR, Briggs PR, Haverd V, King EA, Paget M, Trudinger CM, 2012. Australian Water Availability Project. CSIRO Marine and Atmospheric Research, Canberra, Australia. .

Reinfelds I, Swanson E, Cohen T, Larsen J, Nolan A, 2014. Hydrospatial assessment of streamflow yields and effects of climate change: Snowy Mountains, Australia. *Journal of Hydrology* **512**: 206-220. DOI:10.1016/j.jhydrol.2014.02.038

Risbey JS, Pook MJ, McIntosh PC, Wheeler MC, Hendon HH, 2009. On the Remote Drivers of Rainfall Variability in Australia. *Monthly Weather Review* **137**(10): 3233-3253. DOI:10.1175/2009MWR2861.1

Roderick ML, Farquhar GD, 2002. The Cause of Decreased Pan Evaporation over the Past 50 Years. *Science* **298**(5597): 1410-1411. DOI:10.1126/science.1075390-a

Roderick ML, Farquhar GD, 2011. A simple framework for relating variations in runoff to variations in climatic conditions and catchment properties. *Water Resources Research* **47**(12): W00G07. DOI:10.1029/2010WR009826

Roderick ML, Greve P, Farquhar GD, 2015. On the assessment of aridity with changes in atmospheric CO_2. *Water Resources Research* **51**(7): 5450-5463. DOI:10.1002/2015WR017031

Rodriguez DA, Tomasella J, Linhares C, 2010. Is the forest conversion to pasture affecting the hydrological response of Amazonian catchments? Signals in the Ji-Paraná Basin. *Hydrological Processes* **24**(10): 1254-1269. DOI:10.1002/hyp.7586

Sahin V, Hall MJ, 1996. The effects of afforestation and deforestation on water yields. *Journal of Hydrology* **178**(1–4): 293-309. DOI:10.1016/0022-1694(95)02825-0

Sanborn SC, Bledsoe BP, 2006. Predicting streamflow regime metrics for ungauged streamsin Colorado, Washington, and Oregon. *Journal of Hydrology* **325**(1–4): 241-261. DOI:doi:10.1016/j.jhydrol.2005.10.018

Sarojini BB, Stott PA, Black E, 2016. Detection and attribution of human influence on regional precipitation. *Nature Climate Change* **6**(7): 669-675. DOI:10.1038/nclimate2976

Sawicz KA, Kelleher C, Wagener T, Troch PA, Sivapalan M, Carrillo G, 2014. Characterizing hydrologic change through catchment classification. *Hydrology and Earth System Sciences* **18**(1): 273-285. DOI:doi:10.5194/hess-18-273-2014

Sawicz KA, Wagener T, Sivapalan M, Troch PA, Carrillo G, 2011. Catchment classification: empirical analysis of hydrologic similarity based on catchment function in the eastern USA. *Hydrology and Earth System Sciences* **15**(9): 2895-2911. DOI:doi:10.5194/hess-15-2895-2011

Scanlon BR, Jolly I, Sophocleous M, Zhang L, 2007. Global impacts of conversions from natural to agricultural ecosystems on water resources: Quantity versus quality. *Water Resources Research* **43**(3): W03437. DOI:10.1029/2006WR005486

Scanlon BR, Keese KE, Flint AL, Flint LE, Gaye CB, Edmunds WM, Simmers I, 2006. Global synthesis of groundwater recharge in semiarid and arid regions. *Hydrological Processes* **20**(15): 3335-3370. DOI:10.1002/hyp.6335

Schneider MK, Brunner F, Hollis JM, Stamm C, 2007. Towards a hydrological classification of European soils: preliminary test of its predictive power for the base flow index using river discharge data. *Hydrology and Earth System Sciences* **11**(4): 1501-1513. DOI:10.5194/hess-11-1501-2007

Schumm SA, 1956. Evolution of drainage systems and slopes in badlands at Perth Amboy, New Jersey. *Geological Society of America Bulletin* **67**(5): 597-646. DOI:doi:10.1130/0016-7606(1956)67[597:EODSAS]2.0.CO;2

Seddon AWR, Macias-Fauria M, Long PR, Benz D, Willis KJ, 2016. Sensitivity of global terrestrial ecosystems to climate variability. *Nature* **531**(7593): 229-232. DOI:10.1038/nature16986

Sefton CEM, Howarth SM, 1998. Relationships between dynamic response characteristics and physical descriptors of catchments in England and Wales. *Journal of Hydrology* **211**(1–4): 1-16. DOI:doi:10.1016/S0022-1694(98)00163-2

Sen PK, 1968. Estimates of the Regression Coefficient Based on Kendall's Tau. *Journal of the American Statistical Association* **63**(324): 1379-1389. DOI:10.1080/01621459.1968.10480934

Shamir E, Imam B, Gupta HV, Sorooshian S, 2005. Application of temporal streamflow descriptors in hydrologic model parameter estimation. *Water Resources Research* **41**(6): W06021. DOI:doi:10.1029/2004WR003409

Silberstein RP, Aryal SK, Durrant J, Pearcey M, Braccia M, Charles SP, Boniecka L, Hodgson GA, Bari MA, Viney NR, McFarlane DJ, 2012. Climate change and runoff in south-western Australia. *Journal of Hydrology* **475**(0): 441-455. DOI:10.1016/j.jhydrol.2012.02.009

Siriwardena L, Finlayson BL, McMahon TA, 2006. The impact of land use change on catchment hydrology in large catchments: The Comet River, Central Queensland, Australia. *Journal of Hydrology* **326**(1–4): 199-214. DOI:10.1016/j.jhydrol.2005.10.030

Sivakumar B, Singh V, Berndtsson R, Khan S, 2014. Catchment Classification Framework in Hydrology: Challenges and Directions. *Journal of Hydrologic Engineering* **20**(1): A4014002. DOI:doi:10.1061/(ASCE)HE.1943-5584.0000837

Sivapalan M, 2006. Pattern, Process and Function: Elements of a Unified Theory of Hydrology at the Catchment Scale, Encyclopedia of Hydrological Sciences. John Wiley & Sons, Ltd. DOI:doi:10.1002/0470848944.hsa012

Smakhtin VU, 2001. Low flow hydrology: a review. *Journal of Hydrology* **240**(3–4): 147-186. DOI:doi:10.1016/S0022-1694(00)00340-1

Snelder TH, Biggs BJF, Woods RA, 2005. Improved eco-hydrological classification of rivers. *River Research and Applications* **21**(6): 609-628. DOI:doi:10.1002/rra.826

Snyder FF, 1938. Synthetic unit-graphs. *Eos, Transactions American Geophysical Union* **19**(1): 447-454. DOI:10.1029/TR019i001p00447

Sopper WE, Lull HW, 1965. Streamflow characteristics of physiographic units in the northeast. *Water Resources Research* **1**(1): 115-124. DOI:10.1029/WR001i001p00115

Soulsby C, Tetzlaff D, Hrachowitz M, 2010. Are transit times useful process-based tools for flow prediction and classification in ungauged basins in montane regions? *Hydrological Processes* **24**(12): 1685-1696. DOI:10.1002/hyp.7578

Sriwongsitanon N, Taesombat W, 2011. Effects of land cover on runoff coefficient. *Journal of Hydrology* **410**(3–4): 226-238. DOI:10.1016/j.jhydrol.2011.09.021

Ssegane H, Tollner EW, Mohamoud YM, Rasmussen TC, Dowd JF, 2012. Advances in variable selection methods I: Causal selection methods versus stepwise regression and principal component analysis on data of known and unknown functional relationships. *Journal of Hydrology* **438–439**: 16-25. DOI:DOI:doi.org/10.1016/j.jhydrol.2012.01.008

Stasinopoulos DM, Rigby RA, 2007. Generalized Additive Models for Location Scale and Shape (GAMLSS) in R. *2007* **23**(7): 46. DOI:10.18637/jss.v023.i07

Stednick JD, 1996. Monitoring the effects of timber harvest on annual water yield. *Journal of Hydrology* **176**(1–4): 79-95. DOI:10.1016/0022-1694(95)02780-7

Sterling SM, Ducharne A, Polcher J, 2013. The impact of global land-cover change on the terrestrial water cycle. *Nature Climate Change* **3**(4): 385-390. DOI:10.1038/nclimate1690

Swann ALS, Hoffman FM, Koven CD, Randerson JT, 2016. Plant responses to increasing CO_2 reduce estimates of climate impacts on drought severity. *Proceedings of the National Academy of Sciences* **113**(36): 10019-10024. DOI:10.1073/pnas.1604581113

Syed TH, Famiglietti JS, Chambers DP, Willis JK, Hilburn K, 2010. Satellite-based global-ocean mass balance estimates of interannual variability and emerging trends in continental freshwater discharge. *Proceedings of the National Academy of Sciences* **107**(42): 17916-17921. DOI:10.1073/pnas.1003292107

Tan X, Gan TY, 2015. Contribution of human and climate change impacts to changes in streamflow of Canada. *Scientific Reports* **5**: 17767. DOI:10.1038/srep17767

Taylor RG, Scanlon B, Doll P, Rodell M, van Beek R, Wada Y, Longuevergne L, Leblanc M, Famiglietti JS, Edmunds M, Konikow L, Green TR, Chen J, Taniguchi M, Bierkens MFP, MacDonald A, Fan Y, Maxwell RM, Yechieli Y, Gurdak JJ, Allen DM, Shamsudduha M, Hiscock K, Yeh PJF, Holman I, Treidel H, 2013. Ground water and climate change. *Nature Climate Change* **3**(4): 322-329.

Thackway R, Cresswell I, 1995. An interim biogeographic regionalisation for Australia: a framework for establishing the national system of reserves. *Australian Nature Conservation Agency, Canberra*.

Thorburn P, 2013. Catchments to reef continuum: Minimising impacts of agriculture on the Great Barrier Reef. *Agriculture, Ecosystems & Environment* **180**: 1-3. DOI:10.1016/j.agee.2013.08.004

Thorburn PJ, Wilkinson SN, Silburn DM, 2013. Water quality in agricultural lands draining to the Great Barrier Reef: A review of causes, management and priorities. *Agriculture, Ecosystems & Environment* **180**: 4-20. DOI:10.1016/j.agee.2013.07.006

Thornton C, Cowie B, Freebairn D, Playford C, 2007. The Brigalow Catchment Study: II. Clearing brigalow (Acacia harpophylla) for cropping or pasture increases runoff. *Soil Research* **45**(7): 496-511.

Timbal B, Arblaster JM, 2006. Land cover change as an additional forcing to explain the rainfall decline in the south west of Australia. *Geophysical Research Letters* **33**(7): L07717. DOI:10.1029/2005GL025361

Timbal B, Fawcett R, 2012. A Historical Perspective on Southeastern Australian Rainfall since 1865 Using the Instrumental Record. *Journal of Climate* **26**(4): 1112-1129. DOI:10.1175/JCLI-D-12-00082.1

Tomer MD, Schilling KE, 2009. A simple approach to distinguish land-use and climate-change effects on watershed hydrology. *Journal of Hydrology* **376**(1–2): 24-33. DOI:10.1016/j.jhydrol.2009.07.029

Tooth S, 2000. Process, form and change in dryland rivers: a review of recent research. *Earth-Science Reviews* **51**(1–4): 67-107. DOI:10.1016/S0012-8252(00)00014-3

Toth E, 2013. Catchment classification based on characterisation of streamflow and precipitation time series. *Hydrol. Earth Syst. Sci.* **17**(3): 1149-1159. DOI:10.5194/hess-17-1149-2013

Traff DC, Niemann JD, Middlekauff SA, Lehman BM, 2015. Effects of woody vegetation on shallow soil moisture at a semiarid montane catchment. *Ecohydrology* **8**(5): 935-947. DOI:10.1002/eco.1542

Trancoso R, Larsen JR, McAlpine C, McVicar TR, Phinn S, 2016. Linking the Budyko framework and the Dunne diagram. *Journal of Hydrology* **535**: 581-597. DOI:10.1016/j.jhydrol.2016.02.017

Trancoso R, Larsen JR, McVicar TR, Phinn S, McAlpine CA, 2017a. CO_2 – vegetation feedbacks and other climate changes implicated in reducing baseflow. *Geophysical Research Letters* **44**(5): 2310-2318. DOI:10.1002/2017GL072759

Trancoso R, Phinn S, McVicar TR, Larsen JR, McAlpine CA, 2017b. Regional variation in streamflow drivers across a continental climatic gradient. *Ecohydrology*: e1816. DOI:10.1002/eco.1816

Troch PA, Carrillo G, Sivapalan M, Wagener T, Sawicz K, 2013. Climate-vegetation-soil interactions and long-term hydrologic partitioning: signatures of catchment co-evolution. *Hydrology and Earth System Sciences* **17**(6): 2209-2217. DOI:doi:10.5194/hess-17-2209-2013

Troch PA, Lahmers T, Meira A, Mukherjee R, Pedersen JW, Roy T, Valdés-Pineda R, 2015. Catchment coevolution: A useful framework for improving predictions of hydrological change? *Water Resources Research* **51**(7): 4903-4922. DOI:10.1002/2015WR017032

Ukkola AM, Prentice IC, 2013. A worldwide analysis of trends in water-balance evapotranspiration. *Hydrol. Earth Syst. Sci.* **17**(10): 4177-4187. DOI:10.5194/hess-17-4177-2013

Ukkola AM, Prentice IC, Keenan TF, van Dijk AIJM, Viney NR, Myneni RB, Bi J, 2016. Reduced streamflow in water-stressed climates consistent with CO_2 effects on vegetation. *Nature Climate Change* **6**(1): 75-78. DOI:10.1038/nclimate2831

van den Honert RC, McAneney J, 2011. The 2011 Brisbane Floods: Causes, Impacts and Implications. *Water* **3**(4): 1149-1173.

van der Velde Y, Vercauteren N, Jaramillo F, Dekker SC, Destouni G, Lyon SW, 2014. Exploring hydroclimatic change disparity via the Budyko framework. *Hydrological Processes* **28**(13): 4110-4118. DOI:doi:10.1002/hyp.9949

van Dijk AIJM, 2010. Climate and terrain factors explaining streamflow response and recession in Australian catchments. *Hydrology and Earth System Sciences* **14**(1): 159-169. DOI:10.5194/hess-14-159-2010

van Dijk AIJM, Beck HE, Crosbie RS, de Jeu RAM, Liu YY, Podger GM, Timbal B, Viney NR, 2013. The Millennium Drought in southeast Australia (2001–2009): Natural and human causes and implications for water resources, ecosystems, economy, and society. *Water Resources Research* **49**(2): 1040-1057. DOI:10.1002/wrcr.20123

van Dijk AIJM, Keenan RJ, 2007. Planted forests and water in perspective. *Forest Ecology and Management* **251**(1–2): 1-9. DOI:10.1016/j.foreco.2007.06.010

Vaze J, Davidson A, Teng J, Podger G, 2011. Impact of climate change on water availability in the Macquarie-Castlereagh River Basin in Australia. *Hydrological Processes* **25**(16): 2597-2612.

Vaze J, Post D, Chiew FHS, Perraud J-M, Viney N, Teng J, 2010. Climate non-stationarity–Validity of calibrated rainfall–runoff models for use in climate change studies. *Journal of Hydrology* **394**(3): 447-457.

Verdon-Kidd DC, Kiem AS, 2009. Nature and causes of protracted droughts in southeast Australia: Comparison between the Federation, WWII, and Big Dry droughts. *Geophysical Research Letters* **36**(22): L22707. DOI:10.1029/2009GL041067

Villarini G, Smith JA, 2010. Flood peak distributions for the eastern United States. *Water Resources Research* **46**(6): W06504. DOI:10.1029/2009WR008395

Wagener T, Sivapalan M, McGlynn B, 2006. Catchment Classification and Services—Toward a New Paradigm for Catchment Hydrology Driven by Societal Needs, Encyclopedia of Hydrological Sciences. John Wiley & Sons, Ltd. DOI:10.1002/0470848944.hsa320

Wagener T, Sivapalan M, Troch PA, Woods R, 2007. Catchment Classification and Hydrologic Similarity. *Geography Compass* **1**(4): 901-931. DOI:doi:10.1111/j.1749-8198.2007.00039.x

Walker J, Bullen F, Williams BG, 1993. Ecohydrological Changes in the Murray-Darling Basin. I. The Number of Trees Cleared Over Two Centuries. *Journal of Applied Ecology* **30**(2): 265-273. DOI:10.2307/2404628

Wang D, Hejazi M, 2011. Quantifying the relative contribution of the climate and direct human impacts on mean annual streamflow in the contiguous United States. *Water Resources Research* **47**(10): W00J12. DOI:10.1029/2010WR010283

Wang S, Zhang Z, McVicar TR, Zhang J, Zhu J, Guo J, 2012. An event-based approach to understanding the hydrological impacts of different land uses in semi-arid catchments. *Journal of Hydrology* **416–417**: 50-59. DOI:10.1016/j.jhydrol.2011.11.035

Wang S, Zhang Z, R. McVicar T, Guo J, Tang Y, Yao A, 2013. Isolating the impacts of climate change and land use change on decadal streamflow variation: Assessing three complementary approaches. *Journal of Hydrology* **507**(0): 63-74. DOI:10.1016/j.jhydrol.2013.10.018

Wardrop DH, Bishop JA, Easterling M, Hychka K, Myers W, Patil GP, Taillie C, 2005. Use of landscape and land use parameters for classification and characterization of watersheds in the mid-Atlantic across five physiographic provinces. *Environmental and Ecological Statistics* **12**(2): 209-223. DOI:10.1007/s10651-005-1042-5

Wilk J, Andersson L, Plermkamon V, 2001. Hydrological impacts of forest conversion to agriculture in a large river basin in northeast Thailand. *Hydrological Processes* **15**(14): 2729-2748.

Wilkinson SN, Hancock GJ, Bartley R, Hawdon AA, Keen RJ, 2013. Using sediment tracing to assess processes and spatial patterns of erosion in grazed rangelands, Burdekin River basin, Australia. *Agriculture, Ecosystems & Environment* **180**: 90-102. DOI:10.1016/j.agee.2012.02.002

Wilson N, Tickle PK, Gallant J, Dowling T, Read A, 2011. 1 second SRTM Derived Hydrological Digital Elevation Model (DEM-H) version 1.0. In: Australia), C.o.A.G. (Ed.). Geoscience Australia.

Winter TC, 2001. The concept of hydrologic landscapes. *Journal of the American Water Resources Association* **37**(2): 335-349. DOI:doi:10.1111/j.1752-1688.2001.tb00973.x

Wolock DM, McCabe GJ, 1999. Explaining spatial variability in mean annual runoff in the conterminous United States. *Climate Research* **11**(2): 149-159.

Wolock MD, Winter CT, McMahon G, 2004. Delineation and Evaluation of Hydrologic-Landscape Regions in the United States Using Geographic Information System Tools and Multivariate Statistical Analyses. *Environmental Management* **34**(1): S71-S88. DOI:10.1007/s00267-003-5077-9

Woods R, 2003. The relative roles of climate, soil, vegetation and topography in determining seasonal and long-term catchment dynamics. *Advances in Water Resources* **26**(3): 295-309. DOI:doi:10.1016/S0309-1708(02)00164-1

Woodward C, Shulmeister J, Larsen J, Jacobsen GE, Zawadzki A, 2014. The hydrological legacy of deforestation on global wetlands. *Science* **346**(6211): 844-847. DOI:10.1126/science.1260510

Wu P, Wood R, Ridley J, Lowe J, 2010. Temporary acceleration of the hydrological cycle in response to a CO2 rampdown. *Geophysical Research Letters* **37**(12): n/a-n/a. DOI:10.1029/2010GL043730

Xu X, Yang D, Yang H, Lei H, 2014. Attribution analysis based on the Budyko hypothesis for detecting the dominant cause of runoff decline in Haihe basin. *Journal of Hydrology* **510**: 530-540. DOI:10.1016/j.jhydrol.2013.12.052

Yadav M, Wagener T, Gupta H, 2007. Regionalization of constraints on expected watershed response behavior for improved predictions in ungauged basins. *Advances in Water Resources* **30**(8): 1756-1774. DOI:doi:10.1016/j.advwatres.2007.01.005

Yang Y, Donohue RJ, McVicar TR, 2016a. Global estimation of effective plant rooting depth: Implications for hydrological modeling. *Water Resources Research* **52**(10): 8260-8276. DOI:10.1002/2016wr019392

Yang Y, Donohue RJ, McVicar TR, Roderick ML, Beck HE, 2016b. Long-term CO_2 fertilization increases vegetation productivity and has little effect on hydrological partitioning in tropical rainforests. *Journal of Geophysical Research: Biogeosciences* **121**(8): 2125-2140. DOI:10.1002/2016JG003475

Yetemen O, Istanbulluoglu E, Duvall AR, 2015. Solar radiation as a global driver of hillslope asymmetry: Insights from an ecogeomorphic landscape evolution model. *Water Resources Research*: n/a-n/a. DOI:10.1002/2015WR017103

Yin J, Porporato A, Albertson J, 2014. Interplay of climate seasonality and soil moisture-rainfall feedback. *Water Resources Research* **50**(7): 6053-6066. DOI:10.1002/2013WR014772

Yokoo Y, Sivapalan M, Oki T, 2008. Investigating the roles of climate seasonality and landscape characteristics on mean annual and monthly water balances. *Journal of Hydrology* **357**(3–4): 255-269. DOI:10.1016/j.jhydrol.2008.05.010

Zhang L, Dawes W, Walker G, 2001. Response of mean annual evapotranspiration to vegetation changes at catchment scale. *Water resources research* **37**(3): 701-708. DOI:doi:10.1029/2000WR900325

Zhang L, Potter N, Hickel K, Zhang Y, Shao Q, 2008a. Water balance modeling over variable time scales based on the Budyko framework–Model development and testing. *Journal of Hydrology* **360**(1): 117-131. DOI:doi:10.1016/j.jhydrol.2008.07.021

Zhang M, Liu N, Harper R, Li Q, Liu K, Wei X, Ning D, Hou Y, Liu S, 2017. A global review on hydrological responses to forest change across multiple spatial scales: Importance of scale, climate, forest type and hydrological regime. *Journal of Hydrology* **546**: 44-59. DOI:10.1016/j.jhydrol.2016.12.040

Zhang X, Wan H, Zwiers FW, Hegerl GC, Min S-K, 2013. Attributing intensification of precipitation extremes to human influence. *Geophysical Research Letters* **40**(19): 5252-5257. DOI:10.1002/grl.51010

Zhang XS, Amirthanathan GE, Bari MA, Laugesen RM, Shin D, Kent DM, MacDonald AM, Turner ME, Tuteja NK, 2016a. How streamflow has changed across Australia since the

1950s: evidence from the network of hydrologic reference stations. *Hydrol. Earth Syst. Sci.* **20**(9): 3947-3965. DOI:10.5194/hess-20-3947-2016

Zhang Y, Chiew FHS, 2009. Relative merits of different methods for runoff predictions in ungauged catchments. *Water Resources Research* **45**(7): W07412. DOI:doi:10.1029/2008WR007504

Zhang Y, Peña-Arancibia JL, McVicar TR, Chiew FHS, Vaze J, Liu C, Lu X, Zheng H, Wang Y, Liu YY, Miralles DG, Pan M, 2016b. Multi-decadal trends in global terrestrial evapotranspiration and its components. *Scientific Reports* **6**: 19124. DOI:10.1038/srep19124

Zhang Y, Vaze J, Chiew FHS, Teng J, Li M, 2014. Predicting hydrological signatures in ungauged catchments using spatial interpolation, index model, and rainfall–runoff modelling. *Journal of Hydrology* **517**(0): 936-948. DOI:doi:10.1016/j.jhydrol.2014.06.032

Zhang Z, Wagener T, Reed P, Bhushan R, 2008b. Reducing uncertainty in predictions in ungauged basins by combining hydrologic indices regionalization and multiobjective optimization. *Water Resources Research* **44**(12): W00B04. DOI:10.1029/2008WR006833

Zhou G, Wei X, Chen X, Zhou P, Liu X, Xiao Y, Sun G, Scott DF, Zhou S, Han L, Su Y, 2015. Global pattern for the effect of climate and land cover on water yield. *Nat Commun* **6**. DOI:10.1038/ncomms6918

APPENDICES

Appendix 1 – Chapter 1

Table A1.1. List of the 355 streamflow stations selected for this PhD thesis

Id	Station code	Station name	State	Latitude	Longitude	Time-series length (years)	Area (km^2)	P (mm/year)	Q (mm/year)
1	102101A	PASCOE RIVER	QLD	-12.88	142.98	46.28	648.11	1541.38	9.10
2	104001A	STEWART RIVER	QLD	-14.17	143.39	43.98	473.43	1204.58	4.33
3	105001B	HANN RIVER	QLD	-15.22	143.85	45.07	980.02	1037.20	1.50
4	105102A	LAURA RIVER	QLD	-15.61	144.48	45.80	1321.55	1050.96	2.26
5	105105A	EAST NORMANBY RIVER	QLD	-15.77	145.01	44.88	296.51	1653.06	4.05
6	107001B	ENDEAVOUR RIVER	QLD	-15.42	145.07	46.28	340.12	1552.89	4.49
7	108002A	DAINTREE RIVER	QLD	-16.18	145.28	45.30	911.30	2032.10	9.67
8	108003A	BLOOMFIELD RIVER	QLD	-15.99	145.29	43.99	256.15	2228.09	23.91
9	110003A	BARRON RIVER	QLD	-17.26	145.54	88.31	221.05	1617.03	6.67
10	110011B	FLAGGY CREEK	QLD	-16.77	145.52	58.29	138.78	1613.52	8.19
11	111005A	MULGRAVE RIVER	QLD	-17.18	145.72	47.21	362.42	2709.00	17.43
12	111101D	RUSSELL RIVER	QLD	-17.39	145.97	33.96	316.65	3473.99	39.29
13	111105A	BABINDA CREEK	QLD	-17.35	145.87	47.22	39.20	3490.53	54.15
14	112002A	FISHER CREEK	QLD	-17.57	145.91	85.31	16.09	3196.09	26.03
15	112003A	NORTH JOHNSTONE RIVER	QLD	-17.38	145.65	55.29	171.64	1948.35	11.94
16	112101B	SOUTH JOHNSTONE RIVER	QLD	-17.61	145.98	39.28	397.50	2905.57	22.97
17	112102A	LIVERPOOL CREEK	QLD	-17.71	145.91	43.64	78.36	3111.33	22.06
18	113004A	COCHABLE CREEK	QLD	-17.74	145.63	47.06	93.64	2179.87	19.84
19	114001A	MURRAY RIVER	QLD	-18.11	145.81	43.63	155.84	1839.90	12.34
20	116008B	GOWRIE CREEK	QLD	-18.44	145.85	60.29	123.66	1726.56	14.25
21	116010A	BLENCOE CREEK	QLD	-18.20	145.54	53.29	227.31	1234.02	6.38
22	116012A	CAMERON CREEK	QLD	-18.07	145.34	52.29	351.15	1120.85	4.91

23	116015A	BLUNDER CREEK	QLD	-17.74	145.44	47.23	126.29	1711.98	7.72
24	116016A	RUDD CREEK	QLD	-17.92	145.15	43.28	1448.85	737.37	1.11
25	116017A	STONE RIVER	QLD	-18.77	145.95	43.54	165.82	1253.35	4.98
26	117002A	BLACK RIVER	QLD	-19.24	146.63	40.83	249.21	1117.34	4.31
27	117003A	BLUEWATER CREEK	QLD	-19.18	146.55	40.15	86.70	1359.95	7.61
28	119005A	HAUGHTON RIVER	QLD	-19.78	146.96	42.29	1121.20	787.86	1.95
29	119006A	MAJOR CREEK	QLD	-19.67	147.02	35.69	476.51	911.91	4.46
30	119101A	BARRATTA CREEK	QLD	-19.69	147.17	39.26	737.68	823.45	2.59
31	120102A	KEELBOTTOM CREEK	QLD	-19.37	146.36	46.39	193.10	1252.64	6.74
32	120106B	BASALT RIVER	QLD	-19.68	145.54	46.28	1308.86	666.50	0.69
33	120112A	STAR RIVER	QLD	-19.38	146.05	46.28	1204.65	1020.55	5.25
34	120216A	BROKEN RIVER	QLD	-21.19	148.45	44.62	96.06	1727.80	4.90
35	120304A	SUTTOR RIVER	QLD	-21.45	147.71	46.41	1957.54	631.77	0.71
36	120307A	CAPE RIVER	QLD	-20.48	145.48	44.95	772.57	677.93	0.82
37	121001A	DON RIVER	QLD	-20.29	148.12	56.88	593.39	727.60	0.50
38	121002A	ELLIOT RIVER	QLD	-19.93	147.84	40.84	270.10	822.46	2.44
39	122004A	GREGORY RIVER	QLD	-20.30	148.55	41.22	46.61	1548.98	8.17
40	124002A	ST.HELENS CREEK	QLD	-20.91	148.76	40.93	121.10	1753.71	11.94
41	124003A	ANDROMACHE RIVER	QLD	-20.58	148.47	37.96	231.38	1291.75	4.27
42	125006A	FINCH HATTON CREEK	QLD	-21.11	148.64	37.95	35.83	1713.15	16.89
43	126003A	CARMILA CREEK	QLD	-21.92	149.40	40.18	84.09	1153.65	5.45
44	129001A	WATERPARK CREEK	QLD	-22.84	150.67	61.91	248.25	1314.03	4.53
45	130004A	RAGLAN CREEK	QLD	-23.82	150.82	50.29	391.83	803.50	0.36
46	130316A	MIMOSA CREEK	QLD	-24.34	149.58	57.00	2480.45	638.28	0.35
47	130319A	BELL CREEK	QLD	-24.15	150.52	53.29	299.43	736.28	0.31
48	130334A	SOUTH KARIBOE CREEK	QLD	-24.56	150.75	41.24	285.56	689.92	0.12
49	130335A	DEE RIVER	QLD	-23.77	150.36	42.44	475.30	767.20	0.97

50	130336A	GREVILLEA CREEK	QLD	-24.58	150.62	41.24	243.80	641.45	0.18
51	130348A	PROSPECT CREEK	QLD	-24.45	150.42	38.90	384.49	618.40	0.25
52	130349A	DON RIVER	QLD	-23.97	150.39	37.09	593.39	727.60	0.50
53	130403A	CONNORS RIVER	QLD	-22.04	149.13	48.09	1284.60	930.31	4.51
54	130406A	FUNNEL CREEK	QLD	-21.78	148.93	48.10	1046.22	1191.67	5.06
55	130413A	DENISON CREEK	QLD	-21.77	148.79	42.10	764.94	931.45	2.54
56	132001A	CALLIOPE RIVER	QLD	-23.98	151.10	75.30	1287.17	799.59	1.05
57	134001B	BAFFLE CREEK	QLD	-24.51	151.74	41.11	1401.02	1004.83	2.08
58	135002A	KOLAN RIVER	QLD	-24.75	151.59	48.21	550.54	870.64	1.16
59	135004A	GIN GIN CREEK	QLD	-24.97	151.89	48.21	537.19	806.66	0.93
60	136108A	MONAL CREEK	QLD	-24.61	151.11	51.50	91.63	803.76	0.62
61	136111A	SPLINTER CREEK	QLD	-24.75	151.26	49.28	141.42	775.12	0.65
62	136112A	BURNETT RIVER	QLD	-24.99	151.35	48.28	369.46	769.92	0.70
63	136202D	BARAMBAH CREEK	QLD	-26.30	152.04	49.28	650.17	833.94	0.79
64	137003A	ELLIOTT RIVER	QLD	-24.99	152.38	55.29	232.26	918.84	0.88
65	138003D	GLASTONBURY CREEK	QLD	-26.22	152.52	34.45	110.13	993.01	1.77
66	138004B	MUNNA CREEK	QLD	-25.90	152.35	39.28	1189.98	824.94	1.18
67	138009A	TINANA CREEK	QLD	-26.08	152.78	39.50	101.67	1266.59	2.94
68	138110A	MARY RIVER	QLD	-26.63	152.70	54.29	487.44	1292.79	3.57
69	138113A	KANDANGA CREEK	QLD	-26.39	152.64	42.17	170.62	1024.10	2.39
70	140002A	TEEWAH CREEK	QLD	-26.06	153.04	42.01	58.74	1387.66	6.28
71	141003C	PETRIE CREEK	QLD	-26.62	152.96	35.28	39.28	1740.08	8.14
72	141006A	MOOLOOLAH RIVER	QLD	-26.76	152.98	42.08	39.64	1650.07	6.85
73	141008A	EUDLO CREEK	QLD	-26.66	153.02	32.01	57.30	1661.79	6.25
74	141009A	NORTH MAROOCHY RIVER	QLD	-26.49	152.96	31.90	42.00	1614.78	6.01
75	142001A	CABOOLTURE RIVER	QLD	-27.10	152.89	48.28	97.66	1289.14	4.35
76	142202A	SOUTH PINE RIVER	QLD	-27.35	152.92	48.28	161.95	1156.35	3.63

77	143010B	EMU CREEK	QLD	-26.98	152.29	37.13	916.19	772.14	0.52
78	143028A	ITHACA CREEK	QLD	-27.45	152.99	41.28	7.06	1063.62	5.01
79	143032A	MOGGILL CREEK	QLD	-27.49	152.89	37.50	22.75	1031.43	3.00
80	143033A	OXLEY CREEK	QLD	-27.73	152.95	37.08	50.54	855.91	1.35
81	143110A	BREMER RIVER	QLD	-27.83	152.51	45.28	126.49	950.50	1.52
82	143113A	PURGA CREEK	QLD	-27.68	152.73	40.13	212.85	814.85	0.69
83	143219A	MURPHYS CREEK	QLD	-27.47	151.99	34.28	15.93	819.95	1.18
84	143303A	STANLEY RIVER	QLD	-26.84	152.84	86.56	104.53	1480.47	6.97
85	143307A	BYRON CREEK	QLD	-27.14	152.64	35.57	55.59	1144.93	3.23
86	145003B	LOGAN RIVER	QLD	-28.20	152.77	60.29	174.80	1069.99	2.68
87	145010A	RUNNING CREEK	QLD	-28.25	152.89	48.13	132.40	1356.90	3.20
88	145011A	TEVIOT BROOK	QLD	-28.15	152.57	47.93	82.88	1054.63	1.60
89	145018A	BURNETT CREEK	QLD	-28.22	152.61	43.69	81.78	970.65	1.69
90	145101D	ALBERT RIVER	QLD	-28.05	153.04	60.29	166.97	1113.12	2.83
91	145103A	CAINBABLE CREEK	QLD	-28.09	153.08	51.62	42.18	1195.36	1.44
92	145107A	CANUNGRA CREEK	QLD	-28.00	153.16	40.96	100.23	1476.85	3.96
93	146010A	COOMERA RIVER	QLD	-28.03	153.19	51.29	97.49	1414.54	3.81
94	146012A	CURRUMBIN CREEK	QLD	-28.18	153.42	43.89	30.65	1853.59	8.31
95	146014A	BACK CREEK	QLD	-28.12	153.19	42.61	6.86	1565.44	6.67
96	422306A	SWAN CREEK	QLD	-28.16	152.28	94.65	82.32	988.73	1.06
97	422313B	EMU CREEK	QLD	-28.23	152.23	41.28	916.19	772.14	0.52
98	422319B	DALRYMPLE CREEK	QLD	-28.04	152.01	45.28	246.06	765.23	0.84
99	422321B	SPRING CREEK	QLD	-28.35	152.33	41.28	33.89	1123.89	3.03
100	422326A	GOWRIE CREEK	QLD	-27.52	151.94	44.28	123.66	1726.56	14.25
101	422334A	KINGS CREEK	QLD	-27.93	151.86	44.74	515.08	691.71	0.51
102	422338A	CANAL CREEK	QLD	-28.03	151.59	41.79	395.63	653.83	0.38
103	422341A	CONDAMINE RIVER	QLD	-28.33	152.31	37.63	95.54	1003.69	2.16

104	917107A	ELIZABETH CREEK	QLD	-18.13	144.31	45.47	461.93	740.10	0.93
105	919005A	RIFLE CREEK	QLD	-16.68	145.23	45.36	366.81	1327.80	5.86
106	919013A	MCLEOD RIVER	QLD	-16.50	145.00	40.98	533.92	1506.00	3.33
107	919201A	PALMER RIVER	QLD	-16.11	144.78	46.09	535.68	1344.45	2.56
108	922001A	ARCHER RIVER	QLD	-13.42	142.92	45.08	2914.54	1306.04	5.89
109	922101B	COEN RIVER	QLD	-13.96	143.17	46.18	171.18	1328.02	6.83
110	923001A	WATSON RIVER	QLD	-13.13	142.05	40.97	994.46	1450.89	5.28
111	926002A	DULHUNTY RIVER	QLD	-11.83	142.42	43.15	330.26	1572.81	6.97
112	927001B	JARDINE RIVER	QLD	-11.15	142.35	35.32	2419.12	1795.35	9.27
113	201001	OXLEY RIVER AT EUNGELLA	NSW	-28.35	153.29	66.66	216.38	1592.27	525.61
114	201012	COBAKI CREEK AT COBAKI	NSW	-28.20	153.46	31.59	10.15	1696.18	592.40
115	202001	BRUNSWICK RIVER AT DURRUMBUL (SHERRYS CROSSING)	NSW	-28.53	153.46	59.24	36.48	1798.23	555.45
116	203002	COOPERS CREEK AT REPENTANCE	NSW	-28.64	153.41	93.95	63.59	1943.67	945.13
117	203005	RICHMOND RIVER AT WIANGAREE	NSW	-28.50	152.97	70.64	702.64	1163.11	280.38
118	203010	LEYCESTER RIVER AT ROCK VALLEY	NSW	-28.74	153.16	62.40	177.26	1373.48	412.27
119	203012	BYRON CREEK AT BINNA BURRA	NSW	-28.71	153.50	62.39	38.71	1889.54	897.44
120	203030	MYRTLE CREEK AT RAPPVILLE	NSW	-29.11	153.00	44.62	388.24	1089.22	130.12
121	204008	GUY FAWKES RIVER AT EBOR	NSW	-30.40	152.35	90.16	32.89	1387.15	920.30
122	204017	BIELSDOWN CREEK AT DORRIGO NO.2 & NO.3	NSW	-30.31	152.71	66.93	82.32	1600.58	1085.57
123	204030	ABERFOYLE RIVER AT ABERFOYLE	NSW	-30.26	152.01	62.32	209.26	860.06	75.70
124	204031	MANN RIVER AT SHANNON VALE	NSW	-29.72	151.85	62.27	358.24	923.20	88.30
125	204033	TIMBARRA RIVER AT BILLYRIMBA	NSW	-29.19	152.25	62.15	1268.63	995.24	115.47
126	204034	HENRY RIVER AT NEWTON BOYD	NSW	-29.76	152.21	62.23	400.94	884.31	101.41
127	204036	CATARACT CREEK AT SANDY HILL(BELOW SNAKE CREEK)	NSW	-28.93	152.22	61.84	245.32	949.15	177.56
128	204037	CLOUDS CREEK AT CLOUDS CREEK	NSW	-30.09	152.63	61.56	63.14	1361.80	202.38

129	204039	MARYLAND RIVER D/S WYLIE CREEK	NSW	-28.47	152.20	60.30	386.11	834.95	77.40
130	204043	PEACOCK CREEK AT BONALBO	NSW	-28.73	152.67	53.81	47.75	1162.24	115.26
131	204055	SPORTSMANS CREEK AT GURRANANG SIDING	NSW	-29.47	152.98	41.87	201.49	1116.58	200.01
132	204056	DANDAHRA CREEK AT GIBRALTAR RANGE	NSW	-29.48	152.45	41.67	113.45	1154.22	607.81
133	204067	GORDON BROOK AT FINEFLOWER	NSW	-29.40	152.65	30.72	313.29	1096.81	216.74
134	205002	BELLINGER RIVER AT THORA	NSW	-30.43	152.78	58.57	445.92	1429.67	526.17
135	205006	NAMBUCCA RIVER AT BOWRAVILLE	NSW	-30.64	152.86	51.97	256.75	1495.66	467.62
136	206001	STYX RIVER AT JEOGLA	NSW	-30.59	152.16	95.74	160.42	1210.47	552.05
137	206009	TIA RIVER AT TIA	NSW	-31.19	151.83	86.23	266.12	986.18	149.53
138	206014	WOLLOMOMBI RIVER AT CONINSIDE	NSW	-30.48	152.03	65.76	377.45	771.20	63.05
139	206018	APSLEY RIVER AT APSLEY FALLS	NSW	-31.05	151.77	61.10	863.99	803.18	48.63
140	206025	SALISBURY WATERS NEAR DANGAR FALLS	NSW	-30.68	151.71	41.04	650.34	767.99	39.03
141	206026	SANDY CREEK AT NEWHOLME	NSW	-30.42	151.66	39.32	8.96	749.65	31.21
142	206027	PIPECLAY CREEK AT KIRBY FARM	NSW	-30.47	151.63	39.12	6.22	725.46	34.46
143	207006	FORBES RIVER AT BIRDWOOD(FILLY FLAT)	NSW	-31.38	152.33	58.53	334.03	1400.43	493.43
144	207013	ELLENBOROUGH RIVER D/S BUNNOO RIVER JUNCTION	NSW	-31.48	152.45	38.80	498.75	1385.93	307.09
145	208001	BARRINGTON RIVER AT BOBS CROSSING	NSW	-32.03	151.47	69.97	19.96	1243.29	1192.07
146	208007	NOWENDOC RIVER AT NOWENDOC	NSW	-31.52	151.72	67.51	222.61	965.67	214.55
147	208009	BARNARD RIVER AT BARRY	NSW	-31.58	151.32	64.92	157.55	935.24	224.79
148	208015	LANSDOWNE RIVER AT LANSDOWNE	NSW	-31.79	152.51	44.56	95.57	1270.68	472.57
149	208019	DINGO CREEK AT MUNYAREE FLAT	NSW	-31.84	152.29	42.47	523.35	1206.18	262.63
150	209002	MAMMY JOHNSONS RIVER AT PIKES CROSSING	NSW	-32.24	151.98	46.07	157.62	1123.35	263.53
151	209006	WANG WAUK RIVER AT WILLINA	NSW	-32.16	152.26	44.73	148.32	1109.14	211.24
152	209018	KARUAH RIVER AT DAM SITE	NSW	-32.27	151.90	34.06	293.09	1170.09	309.40
153	210006	GOULBURN RIVER AT COGGAN	NSW	-32.34	150.10	101.27	820.58	675.84	73.23
154	210011	WILLIAMS RIVER AT TILLEGRA	NSW	-32.32	151.69	82.92	196.20	1153.39	385.16
155	210014	ROUCHEL BROOK AT ROUCHEL BROOK (THE VALE)	NSW	-32.15	151.05	79.46	401.43	850.63	105.69

156	210017	MOONAN BROOK AT MOONAN BROOK	NSW	-31.94	151.28	73.61	102.64	963.24	232.82
157	210022	ALLYN RIVER AT HALTON	NSW	-32.31	151.51	73.10	189.56	1114.37	380.85
158	210040	WYBONG CREEK AT WYBONG	NSW	-32.27	150.64	58.67	664.48	681.07	27.26
159	210061	PAGES RIVER AT BLANDFORD (BICKHAM)	NSW	-31.81	150.93	53.66	298.29	783.45	89.46
160	210068	POKOLBIN CREEK AT POKOLBIN SITE 3	NSW	-32.80	151.33	50.17	25.64	811.12	41.54
161	210076	ANTIENE CREEK AT LIDDELL	NSW	-32.34	150.98	45.41	13.13	647.38	81.33
162	210080	WEST BROOK AT U/S GLENDON BROOK	NSW	-32.47	151.28	44.71	73.18	825.77	108.35
163	210093	KINGDON PONDS CREEK AT NEAR PARKVILLE	NSW	-31.96	150.86	41.75	178.57	723.80	28.20
164	211008	JIGADEE CREEK AT AVONDALE	NSW	-33.07	151.47	44.10	67.10	1055.21	179.94
165	211010	JILLIBY CREEK AT U/S WYONG RIVER (DURREN LANE)	NSW	-33.24	151.39	41.06	92.83	1161.28	185.77
166	211013	OURIMBAH CREEK AT U/S WEIR	NSW	-33.35	151.34	37.14	83.72	1245.16	227.46
167	211014	WYONG RIVER AT YARRAMALONG	NSW	-33.22	151.28	37.13	180.87	1089.15	184.00
168	212018	CAPERTEE RIVER AT GLEN DAVIS	NSW	-33.12	150.28	43.41	1026.13	701.70	19.11
169	212320	SOUTH CREEK AT MULGOA ROAD	NSW	-33.88	150.77	58.25	90.20	740.37	83.59
170	213005	TOONGABBIE CREEK AT BRIENS ROAD	NSW	-33.80	150.98	34.85	71.07	854.78	306.17
171	213006	FISHERS GHOST CREEK AT BRADBURY PARK	NSW	-34.07	150.81	33.09	2.44	813.84	235.89
172	213200	O HARES CREEK AT WEDDERBURN	NSW	-34.16	150.84	35.94	74.08	1123.75	273.53
173	214003	MACQUARIE RIVULET AT ALBION PARK	NSW	-34.58	150.71	64.38	35.51	1459.46	382.84
174	215004	CORANG RIVER AT HOCKEYS	NSW	-35.15	150.03	89.38	163.76	850.82	240.49
175	215008	SHOALHAVEN RIVER AT KADOONA	NSW	-35.79	149.64	63.33	283.48	850.99	169.97
176	215014	BUNGONIA CREEK AT BUNGONIA	NSW	-34.82	149.99	32.74	164.47	656.70	40.97
177	216004	CURRAMBENE CREEK AT FALLS CREEK	NSW	-34.97	150.60	44.22	93.48	1079.76	145.16
178	216008	BUTLERS CREEK AT KIOLOA	NSW	-35.54	150.36	33.12	0.62	1125.78	63.51
179	217002	DEUA RIVER AT WAMBAN	NSW	-35.92	150.03	54.31	1216.10	836.86	146.28
180	218001	TUROSS RIVER AT TUROSS VALE	NSW	-36.26	149.51	65.57	90.15	817.91	223.50
181	218007	WADBILLIGA RIVER AT WADBILLIGA	NSW	-36.26	149.69	39.58	124.57	818.88	220.94
182	219001	RUTHERFORD CREEK AT BROWN MOUNTAIN	NSW	-36.59	149.44	89.81	15.75	854.18	284.21

183	219006	TANTAWANGALO CREEK AT TANTAWANGALO MOUNTAIN (DAM)	NSW	-36.78	149.54	89.37	81.84	843.16	183.13
184	219017	DOUBLE CREEK NEAR BROGO	NSW	-36.60	149.81	47.52	157.30	829.93	165.96
185	220003	PAMBULA RIVER AT LOCHIEL	NSW	-36.94	149.82	47.37	106.31	846.03	162.78
186	221010	IMLAY CREEK AT IMLAY ROAD BRIDGE	NSW	-37.23	149.70	32.50	74.70	887.67	162.84
187	222004	LITTLE PLAINS RIVER AT WELLESLEY (ROWES)	NSW	-37.00	149.09	72.86	614.56	859.07	95.99
188	222016	PINCH RIVER AT THE BARRY WAY	NSW	-36.79	148.40	38.82	158.16	849.27	289.75
189	222017	MACLAUGHLIN RIVER AT THE HUT	NSW	-36.65	149.11	35.36	313.77	589.82	57.16
190	401009	MARAGLE CREEK AT MARAGLE	NSW	-35.93	148.10	66.13	216.54	997.01	122.25
191	401012	MURRAY RIVER AT BIGGARA	NSW	-36.32	148.05	65.49	1258.20	1109.23	324.62
192	401016	WELUMBA CREEK AT THE SQUARE	NSW	-36.03	148.12	30.72	50.64	909.39	114.94
193	410024	GOODRADIGBEE RIVER AT WEE JASPER (KASHMIR)	NSW	-35.17	148.69	99.35	989.63	1153.37	246.48
194	410025	JUGIONG CREEK AT JUGIONG (INVERLOCKIE)	NSW	-34.79	148.38	99.98	1361.65	682.47	62.99
195	410026	YASS RIVER AT YASS	NSW	-34.84	148.91	98.42	1236.33	653.42	48.57
196	410038	ADJUNGBILLY CREEK AT DARBALARA	NSW	-35.02	148.25	81.75	389.38	1065.21	177.69
197	410057	GOOBARRAGANDRA RIVER AT LACMALAC	NSW	-35.33	148.35	69.08	667.09	1165.07	356.60
198	410061	ADELONG CREEK AT BATLOW ROAD	NSW	-35.33	148.07	66.36	146.90	1071.69	210.10
199	410076	STRIKE-A-LIGHT CREEK AT JERANGLE ROAD	NSW	-35.92	149.24	59.42	212.91	696.65	45.61
200	410081	COOMA CREEK AT COOMA NO.2 (THE GRANGE)	NSW	-36.26	149.14	57.08	97.19	537.80	70.66
201	410107	MOUNTAIN CREEK AT MOUNTAIN CREEK	NSW	-35.03	148.83	41.65	185.69	956.70	150.40
202	410114	KILLIMCAT CREEK AT WYANGLE	NSW	-35.23	148.31	38.62	21.68	893.43	176.02
203	410141	MICALIGO CREEK AT MICHELAGO	NSW	-35.70	149.15	59.65	190.98	649.12	33.46
204	411003	BUTMAROO CREEK AT BUTMAROO	NSW	-35.26	149.54	42.29	63.92	752.76	66.44
205	412029	BOOROWA RIVER AT PROSSERS CROSSING	NSW	-34.14	148.81	75.84	1557.44	650.59	45.12
206	412066	ABERCROMBIE RIVER AT HADLEY NO.2	NSW	-34.11	149.60	53.57	1635.75	752.36	76.46
207	412080	FLYERS CREEK AT BENEREE	NSW	-33.51	149.04	45.76	86.26	805.23	93.01
208	416003	TENTERFIELD CREEK AT CLIFTON	NSW	-29.03	151.72	92.54	555.37	823.69	64.07

209	416008	BEARDY RIVER AT HAYSTACK	NSW	-29.22	151.38	79.45	898.57	757.27	57.21
210	416023	DEEPWATER RIVER AT BOLIVIA	NSW	-29.29	151.92	46.85	539.51	866.95	67.32
211	418005	COPES CREEK AT KIMBERLEY	NSW	-29.92	151.11	84.76	238.58	841.30	74.08
212	418014	GWYDIR RIVER AT YARROWYCK	NSW	-30.47	151.36	59.08	826.95	764.48	52.09
213	418021	LAURA CREEK AT LAURA	NSW	-30.23	151.19	48.61	357.48	836.63	66.72
214	419010	MACDONALD RIVER AT WOOLBROOK	NSW	-30.97	151.35	86.24	843.94	892.30	119.32
215	419035	GOONOO GOONOO CREEK AT TIMBUMBURI	NSW	-31.27	150.92	48.58	459.64	764.10	39.47
216	419054	SWAMP OAK CREEK AT LIMBRI	NSW	-31.04	151.17	39.65	393.70	815.45	60.13
217	419076	WARRAH CREEK AT OLD WARRAH	NSW	-31.66	150.64	31.57	142.17	805.48	55.18
218	421026	TURON RIVER AT SOFALA	NSW	-33.08	149.69	64.38	884.89	744.33	71.41
219	221201	CANN RIVER (WEST BRANCH) @ WEERAGUA	VIC	-37.37	149.20	56.90	329.50	903.02	120.15
220	221207	ERRINUNDRA RIVER @ ERRINUNDRA	VIC	-37.45	148.92	42.46	159.97	1005.86	324.42
221	221208	WINGAN RIVER @ WINGAN INLET NATIONAL PARK	VIC	-37.69	149.49	31.07	420.84	919.24	159.22
222	221209	CANN RIVER (EAST BRANCH) @ WEERAGUA	VIC	-37.36	149.21	41.22	149.70	850.05	108.75
223	221210	GENOA RIVER @ THE GORGE	VIC	-37.42	149.52	41.39	840.10	864.85	114.38
224	221211	COMBIENBAR RIVER @ COMBIENBAR	VIC	-37.44	148.98	39.42	179.95	951.60	153.22
225	222206	BUCHAN RIVER @ BUCHAN	VIC	-37.50	148.17	87.83	847.99	955.09	125.35
226	222210	DEDDICK RIVER @ DEDDICK (CASEYS)	VIC	-37.09	148.42	40.77	846.74	759.29	61.94
227	222213	SUGGAN BUGGAN RIVER @ SUGGAN BUGGAN	VIC	-36.96	148.33	39.55	364.40	1013.63	121.56
228	222217	RODGER RIVER @ JACKSONS CROSSING	VIC	-37.41	148.36	37.61	432.64	884.46	115.19
229	223202	TAMBO RIVER @ SWIFTS CREEK	VIC	-37.27	147.73	36.84	895.98	857.72	61.52
230	223204	NICHOLSON RIVER @ DEPTFORD	VIC	-37.59	147.70	52.68	321.58	747.43	81.12
231	223212	TIMBARRA RIVER @ D/S OF WILKINSON CREEK	VIC	-37.45	148.06	31.68	431.74	872.61	130.22
232	224201	WONNANGATTA RIVER @ WATERFORD	VIC	-37.49	147.17	37.49	1976.18	1092.29	243.76
233	224213	DARGO RIVER @ LOWER DARGO ROAD	VIC	-37.50	147.27	40.64	667.50	1116.75	226.72
234	224214	WENTWORTH RIVER @ TABBERABBERA	VIC	-37.50	147.39	39.52	441.46	836.76	81.88
235	225209	MACALISTER RIVER @ LICOLA	VIC	-37.63	146.62	61.46	1238.37	1028.50	280.64

236	225213	ABERFELDY RIVER @ BEARDMORE	VIC	-37.85	146.43	50.55	312.13	1068.04	180.23
237	225218	FREESTONE CREEK @ BRIAGALONG	VIC	-37.81	147.10	38.50	305.09	751.34	98.11
238	225224	AVON RIVER @ THE CHANNEL	VIC	-37.80	146.88	41.50	557.83	781.75	126.25
239	225230	GLENMAGGIE CREEK @ THE GORGE	VIC	-37.91	146.66	38.70	138.99	1024.53	109.98
240	226209	MOE RIVER @ DARNUM	VIC	-38.21	146.00	53.24	229.60	962.56	202.76
241	226218	NARRACAN CREEK @ THORPDALE	VIC	-38.27	146.19	58.57	66.37	1008.26	305.67
242	226220	LOCH RIVER @ NOOJEE	VIC	-37.87	146.01	35.71	106.57	1278.40	235.48
243	226222	LATROBE RIVER @ NEAR NOOJEE (US ADA R JUNCT.)	VIC	-37.88	145.89	42.68	64.93	1297.63	343.01
244	226226	TANJIL RIVER @ TANJIL JUNCTION	VIC	-37.98	146.19	53.64	314.52	1226.31	399.14
245	226407	MORWELL RIVER @ BOOLARRA	VIC	-38.41	146.31	41.68	116.37	1065.84	249.23
246	226410	TRARALGON CREEK @ KOORNALLA	VIC	-38.32	146.53	60.52	85.83	1114.00	224.98
247	227205	MERRIMAN CREEK @ CALIGNEE SOUTH	VIC	-38.35	146.65	48.08	39.38	1067.73	274.57
248	227210	BRUTHEN CREEK @ CARRAJUNG LOWER	VIC	-38.40	146.74	61.44	18.76	915.39	148.97
249	227211	AGNES RIVER @ TOORA	VIC	-38.64	146.37	57.01	66.43	1058.30	347.77
250	227213	JACK RIVER @ JACK RIVER	VIC	-38.53	146.54	51.12	35.22	1016.74	291.23
251	227225	TARRA RIVER @ FISCHERS	VIC	-38.47	146.56	45.72	20.49	998.00	374.72
252	227226	TARWIN RIVER EAST BRANCH @ DUMBALK NORTH	VIC	-38.50	146.16	45.01	128.43	1096.37	250.06
253	227227	WILKUR CREEK @ LEONGATHA	VIC	-38.39	145.96	43.45	105.66	937.16	314.94
254	227236	POWLETT RIVER @ D/S FOSTER CREEK JUNCTION	VIC	-38.56	145.71	34.65	140.65	1016.23	329.50
255	227237	FRANKLIN RIVER @ TOORA	VIC	-38.63	146.31	30.76	74.93	910.77	299.23
256	230209	BARRINGO CREEK @ BARRINGO (U/S OF DIVERSION)	VIC	-37.41	144.63	47.58	5.21	777.30	189.65
257	230210	SALTWATER CREEK @ BULLENGAROOK	VIC	-37.47	144.52	45.68	46.38	847.58	70.88
258	231211	LERDERDERG RIVER @ U/S GOODMAN CREEK JUNCTION	VIC	-37.63	144.43	57.63	236.78	837.76	80.01
259	231225	WERRIBEE RIVER @ BALLAN (U/S OLD WESTERN HWY)	VIC	-37.60	144.25	114.08	108.68	515.82	129.94
260	231231	TOOLERN CREEK @ MELTON SOUTH	VIC	-37.73	144.58	34.69	89.96	583.89	30.45
261	233223	WARRAMBINE CREEK @ WARRAMBINE	VIC	-37.93	143.87	43.61	53.87	844.93	21.22
262	234203	PIRRON YALLOCK CREEK @ PIRRON YALLOCK	VIC	-38.35	143.42	49.71	165.11	860.31	80.71

		(ABOVE H'WY BR.)							
263	234209	DEAN CREEK @ LAKE COLAC	VIC	-38.34	143.56	38.16	54.67	1175.57	68.04
264	235203	CURDIES RIVER @ CURDIE	VIC	-38.44	142.96	48.58	780.47	824.99	102.14
265	235204	LITTLE AIRE CREEK @ BEECH FOREST	VIC	-38.65	143.53	58.76	11.33	1621.65	940.49
266	235205	ARKINS CREEK WEST BRANCH @ WYELANGTA	VIC	-38.64	143.44	35.65	4.48	1616.62	887.92
267	235210	LARDNER CREEK @ GELLIBRAND	VIC	-38.53	143.54	49.57	51.92	1453.83	401.81
268	235211	KENNEDYS CREEK @ KENNEDYS CREEK	VIC	-38.59	143.26	49.58	268.81	933.37	122.47
269	235216	CUMBERLAND RIVER @ LORNE	VIC	-38.57	143.95	38.66	39.51	1275.07	462.87
270	235232	PAINKALAC CREEK @ PAINKALAC CREEK DAM	VIC	-38.44	144.07	34.75	36.26	965.10	75.18
271	235233	BARHAM RIVER EAST BRANCH @ APOLLO BAY PARADISE	VIC	-38.76	143.62	36.25	44.47	1262.03	491.41
272	235234	LOVE CREEK @ GELLIBRAND	VIC	-38.48	143.57	34.69	81.52	988.19	104.73
273	236202	HOPKINS RIVER @ WICKLIFFE	VIC	-37.70	142.72	31.93	1399.84	562.02	17.20
274	236205	MERRI RIVER @ WOODFORD	VIC	-38.32	142.48	45.70	904.18	723.86	54.68
275	236212	BRUCKNELL CREEK @ CUDGEE	VIC	-38.35	142.65	48.61	219.37	811.36	114.32
276	237200	MOYNE RIVER @ TOOLONG	VIC	-38.32	142.23	32.61	559.71	716.26	64.70
277	237202	FITZROY RIVER @ HEYWOOD	VIC	-38.19	141.96	50.81	424.94	689.09	52.31
278	237205	DARLOT CREEK @ HOMERTON BRIDGE	VIC	-38.15	141.77	51.01	733.74	665.83	70.70
279	237207	SURRY RIVER @ HEATHMERE	VIC	-38.24	141.66	43.73	306.50	774.53	83.34
280	238207	WANNON RIVER @ JIMMY CREEK	VIC	-37.37	142.50	63.98	48.14	753.77	162.79
281	238208	JIMMY CREEK @ JIMMY CREEK	VIC	-37.37	142.51	63.98	22.76	697.54	117.27
282	238223	WANDO RIVER @ WANDO VALE	VIC	-37.50	141.43	49.75	176.13	670.98	70.18
283	238229	CHETWYND RIVER @ CHETWYND	VIC	-37.32	141.48	46.79	70.82	662.17	85.94
284	238230	STOKES RIVER @ TEAKETTLE	VIC	-37.87	141.41	47.55	200.29	714.29	68.07
285	238231	GLENELG RIVER @ BIG CORD	VIC	-37.31	142.37	45.72	58.35	689.44	147.89
286	238235	CRAWFORD RIVER @ LOWER CRAWFORD	VIC	-37.98	141.45	43.64	631.46	699.26	59.16
287	401208	CUDGEWA CREEK @ BERRINGAMA	VIC	-36.21	147.68	46.29	357.83	1107.96	212.00

288	401210	SNOWY CREEK @ BELOW GRANITE FLAT	VIC	-36.57	147.41	81.28	413.56	1437.89	444.71
289	401212	NARIEL CREEK @ UPPER NARIEL	VIC	-36.45	147.83	59.76	264.16	1274.12	473.16
290	401215	MORASS CREEK @ UPLANDS	VIC	-36.87	147.70	46.87	538.79	920.54	51.11
291	401216	BIG RIVER @ JOKERS CREEK	VIC	-36.93	147.47	79.19	359.80	1637.50	575.96
292	401217	GIBBO RIVER @ GIBBO PARK	VIC	-36.76	147.71	42.47	389.66	1124.58	272.27
293	401220	TALLANGATTA CREEK @ MCCALLUMS	VIC	-36.21	147.34	37.80	456.01	1082.93	158.12
294	402204	YACKANDANDAH CREEK @ OSBORNES FLAT	VIC	-36.30	146.91	46.95	280.83	1084.54	171.32
295	402206	RUNNING CREEK @ RUNNING CREEK	VIC	-36.54	147.04	42.77	127.83	1307.11	232.45
296	403213	FIFTEEN MILE CREEK @ GRETA SOUTH	VIC	-36.62	146.24	55.08	227.32	1044.65	243.07
297	403214	HAPPY VALLEY CREEK @ ROSEWHITE	VIC	-36.58	146.82	52.55	141.42	1131.78	158.04
298	403218	DANDONGADALE RIVER @ MATONG NORTH	VIC	-36.81	146.63	51.43	381.88	1221.65	73.16
299	403222	BUFFALO RIVER @ ABBEYARD	VIC	-36.91	146.70	48.54	416.18	1255.68	354.24
300	403232	MORSES CREEK @ WANDILIGONG	VIC	-36.75	146.98	31.87	126.98	1428.93	319.39
301	405205	MURRINDINDI RIVER @ MURRINDINDI ABOVE COLWELLS	VIC	-37.41	145.56	74.61	108.37	1307.65	457.90
302	405209	ACHERON RIVER @ TAGGERTY	VIC	-37.32	145.71	52.98	626.17	1298.48	443.82
303	405214	DELATITE RIVER @ TONGA BRIDGE	VIC	-37.16	146.11	45.85	360.04	1016.28	268.93
304	405217	YEA RIVER @ DEVLINS BRIDGE	VIC	-37.38	145.47	38.74	360.50	1068.68	245.31
305	405218	JAMIESON RIVER @ GERRANG BRIDGE	VIC	-37.29	146.19	30.28	367.12	1153.53	528.52
306	405226	PRANJIP CREEK @ MOORILIM	VIC	-36.62	145.31	48.62	788.68	631.13	62.03
307	405227	BIG RIVER @ JAMIESON	VIC	-37.37	146.06	55.94	628.75	1356.94	445.57
308	405229	WANALTA CREEK @ WANALTA	VIC	-36.63	144.87	44.74	102.82	539.76	30.17
309	405230	CORNELLA CREEK @ COLBINABBIN	VIC	-36.60	144.80	43.85	236.50	563.36	31.67
310	405238	MOLLISON CREEK @ PYALONG	VIC	-37.12	144.86	47.68	164.61	735.17	105.83
311	405241	RUBICON RIVER @ RUBICON	VIC	-37.29	145.83	64.52	127.78	1486.20	823.74
312	405245	FORD CREEK @ MANSFIELD	VIC	-37.04	146.05	43.67	117.47	867.00	87.00
313	405246	CASTLE CREEK @ ARCADIA	VIC	-36.59	145.35	43.69	102.70	611.58	119.12

314	405248	MAJOR CREEK @ GRAYTOWN	VIC	-36.85	144.91	39.73	292.31	602.38	38.65
315	405251	BRANKEET CREEK @ ANCONA	VIC	-36.97	145.79	42.64	118.98	793.19	121.56
316	405263	GOULBURN RIVER @ U/S OF SNAKE CREEK JUNCTION	VIC	-37.46	146.25	38.68	327.97	1244.59	394.62
317	405274	HOME CREEK @ YARCK	VIC	-37.11	145.61	36.59	186.54	754.99	125.30
318	406208	CAMPASPE RIVER @ ASHBOURNE	VIC	-37.39	144.45	54.58	38.13	922.66	143.19
319	406216	AXE CREEK @ SEDGEWICK	VIC	-36.90	144.36	44.68	35.04	810.44	60.91
320	406224	MOUNT PLEASANT CREEK @ RUNNYMEDE	VIC	-36.55	144.64	39.56	242.33	526.65	25.91
321	406235	WILD DUCK CREEK @ U/S OF HEATHCOTE-MIA MIA ROAD	VIC	-36.95	144.66	33.13	212.72	698.03	82.94
322	407221	JIM CROW CREEK @ YANDOIT	VIC	-37.21	144.10	36.92	8.58	625.04	248.00
323	407230	JOYCES CREEK @ STRATHLEA	VIC	-37.16	143.96	35.88	150.79	694.55	54.28
324	407246	BULLOCK CREEK @ MARONG	VIC	-36.73	144.14	41.59	186.52	569.32	38.03
325	408202	AVOCA RIVER @ AMPHITHEATRE	VIC	-37.18	143.41	47.20	76.81	654.60	52.53
326	415207	WIMMERA RIVER @ EVERSLEY	VIC	-37.19	143.18	40.64	305.98	648.69	52.32
327	415226	RICHARDSON RIVER @ CARRS PLAINS	VIC	-36.74	142.79	42.71	129.68	482.90	23.12
328	415237	CONCONGELLA CREEK @ STAWELL	VIC	-37.03	142.82	37.90	241.06	552.99	38.13
329	415238	WATTLE CREEK @ NAVARRE	VIC	-36.90	143.11	37.86	139.49	572.50	34.13
330	415244	SHEPHERDS CREEK @ WARRAK	VIC	-37.25	143.19	30.34	13.40	719.37	76.86
331	30	RINGAROOMA RIVER	TAS	-41.13	147.87	36.34	553.73	1248.96	5.35
332	76	NORTH ESK RIVER	TAS	-41.50	147.39	90.60	374.04	1133.16	4.36
333	181	SOUTH ESK RIVER	TAS	-41.60	147.20	56.82	3299.27	822.05	2.23
334	499	TYENNA RIVER	TAS	-42.71	146.71	49.41	206.16	1318.29	8.95
335	2200	SWAN RIVER	TAS	-42.05	148.08	49.38	421.97	671.21	2.81
336	2204	APSLEY RIVER	TAS	-41.94	148.24	45.37	158.90	747.44	2.42
337	2206	SCAMANDER RIVER	TAS	-41.45	148.18	45.51	268.73	908.20	2.26
338	2208	MEREDITH RIVER	TAS	-42.12	148.04	43.57	86.13	644.67	2.23
339	2209	CARLTON RIVER	TAS	-42.87	147.70	44.59	141.93	738.34	1.26

340	2214	ANSONS RIVER	TAS	-41.05	148.22	34.39	229.36	982.85	2.34
341	2216	ALLAN CREEK	TAS	-43.07	147.89	30.56	8.07	1011.95	3.51
342	3203	COAL RIVER	TAS	-42.43	147.45	42.25	54.35	628.23	1.15
343	5202	SNUG RIVULET	TAS	-43.07	147.24	48.14	17.53	1004.56	3.05
344	14200	MONTAGU RIVER	TAS	-40.79	144.93	48.38	297.45	1182.42	2.81
345	14207	LEVEN RIVER	TAS	-41.25	146.09	50.33	500.42	1829.49	10.28
346	14212	CAN RIVER	TAS	-41.06	145.84	45.57	234.87	1476.05	6.53
347	14213	BLACK RIVER	TAS	-40.87	145.30	45.38	319.22	1272.73	6.21
348	14214	DUCK RIVER	TAS	-40.87	145.12	47.48	361.94	1238.34	5.00
349	14215	FLOWERDALE RIVER	TAS	-40.97	145.61	47.57	152.47	1415.96	7.47
350	14223	WELCOME RIVER	TAS	-40.78	144.75	32.51	280.58	1105.44	1.72
351	17200	RUBICON RIVER	TAS	-41.25	146.56	46.31	263.97	964.71	2.55
352	18217	MACQUARIE RIVER	TAS	-42.18	147.60	34.25	317.67	636.36	2.03
353	18221	JACKEYS CREEK	TAS	-41.68	146.66	31.53	30.20	1103.84	6.18
354	19200	BRID RIVER	TAS	-41.02	147.37	48.30	140.11	993.86	3.03
355	19201	GREAT FORESTER RIVER	TAS	-41.11	147.61	43.65	194.11	1173.97	4.14

Appendix 2 – Chapter 2

Supplementary material

Linking the Budyko framework and the Dunne diagram

Contents of this file

A2.1 Introduction

This supporting information provides a full description of the eight streamflow signatures used in this research. The supporting figures show the results of assessment for hierarchical classification model choice (**Figure A2.1**), classification tree based on five of the eight streamflow signatures to allocate further gauged catchments into the five clusters with similar streamflow behaviour (**Figure A2.2**), and evaluation of assumptions for mixed effect modelling (**Figure A2.3**). The supporting table displays the pairwise comparisons among flow signatures, Dryness Index and Evaporative Index by catchment clusters (**Table A2.1**).

A2.2 Description of the eight streamflow signatures

Long-term runoff ratio – RQP

The long-term runoff ratio (RQP) is the ratio between the long-term cumulative streamflow (Q) and long-term cumulative precipitation (P), where:

$$RQP = \frac{Q}{P}. \quad \text{(S1)}$$

RQP is important in the context of the long-term catchment water balance because it determines the faction of water intake (precipitation) that is released as runoff (streamflow). Assuming that the long-term catchment water storage is stationarity (and there are no interactions with regional groundwater systems), RQP represents the partition of water yielded from a catchment as runoff, with the complement being the actual evapotranspiration from the catchment (Milly, 1994; Milly et al., 2008).

Streamflow elasticity – EQP

It is widely recognised that streamflow is sensitive to the local effects of climate seasonality and climate variability and change (Chiew, 2006; Donohue et al., 2011; Sankarasubramanian et al., 2001). Streamflow elasticity provides a measure of the sensitivity of long-term streamflow to changes in long-term precipitation. It is an annual hydrological signature obtained by the proportional change in mean annual streamflow divided by the proportional change in mean annual precipitation (Chiew, 2006; Dooge, 1992; Sankarasubramanian et al., 2001; Schaake, 1990). We used the non-parametric estimator proposed by Sankarasubramanian et al. (2001), although other variations of the streamflow elasticity are available (Fu et al., 2007). This non-parametric estimator is more appropriate to the aims of this research because it is only dependent on streamflow and precipitation and uses the median, thereby providing a more stable value. In addition, it can be easily applied in comparative studies of many catchments and over a large spatial extent (Chiew, 2006). The EQP non-parametric estimator is expressed as:

$$EQP = median\left(\frac{(Q_t - \bar{Q})}{(P_t - \bar{P})}\frac{\bar{P}}{\bar{Q}}\right); \quad \text{(S2)}$$

where Q_t and P_t are the total annual streamflow and precipitation for each year respectively while $\bar{Q}$ and $\bar{P}$ are the long-term mean annual streamflow and precipitation. EQP gives the

percentage of change on streamflow expected for a 1% of change in mean annual precipitation.

Rising Limb Density – RLD

Rising Limb Density (RLD) is the ratio between the number of rising limbs within the streamflow time series (N_{RL}) and the total amount of time (days in this instance, defined by the temporal resolution of the streamflow data) where the streamflow is rising (TR). It is defined as:

$$RLD = \frac{N_{RL}}{T_R}. \quad \text{(S3)}$$

This signature captures the shape and smoothness of a hydrograph and is insensitive to flood magnitude and timing (Shamir et al., 2005). The larger the RLD value, the "flashier" the catchment's hydrological response.

Baseflow Index – BFI

The separation of streamflow into slower water release components (termed baseflow) and quicker runoff components (stormflow) is widely used when considering water supply, water allocation, contamination impacts and flood hydrology (Arnold and Allen, 1999; Lacey and Grayson, 1998; Peña-Arancibia et al., 2010; Wittenberg, 1999). To perform this separation five main methods have been proposed, including use of: (i) simple graphical visualisation; (ii) chemical tracers; (iii) filtering methods; (iv) recursive digital filtering; and (v) unit hydrograph (see Gonzales et al. (2009) for a brief explanation and comparison of methods). Here, we used the recursive digital filtering method as it can be automated for multiple streamflow time series and provides reproducible and comparable results (Eckhardt, 2005; Li et al., 2013). Although several recursive digital filtering are available, the algorithm choice is still subjective because the true values of baseflow index are often unknown (Eckhardt, 2008). We use the digital filter proposed by Lyne and Hollick (1979) because it has been extensively tested for Australian conditions, and is objective, repeatable, and therefore useful for comparative hydrology (Nathan and McMahon, 1990). The Lyne and Hollick digital filter was applied to the daily streamflow time series according to:

$$q_f(i) = \alpha q_f(i-1) + \frac{(1+\alpha)}{2}[q(i) - q(i-1)] \quad for\ q_f(i) > 0\ ; \quad \text{(S4)}$$

where $q_f(i)$ is the filtered quickflow response at the i^{th} sampling instant; $q(i)$ is the original streamflow at the i^{th} sampling instant; and α is the filter parameter which was fitted as 0.925 for daily data of Australian streams following Lyne and Hollick (1979).

Three passes are recommended to fit the daily streamflow data. Passes, in order, should be: forward, backward, forward.

The value of the baseflow $q_b(i)$ is then given by;

$$q_b(i) = q(i) - q_f(i). \quad \text{(S5)}$$

The baseflow index (*BFI)* is given by the summation of all time steps of the studied time series, as:

$$BFI = \sum_{i=1}^{n} \frac{q_b(i)}{q(i)}. \quad \text{(S6)}$$

Slope of the Flow Duration Curve – SFDC

The Slope of the Flow Duration Curve (SFDC) quantifies the flow variability between the 33rd and 66th percentiles of the flow duration curve (Yadav et al., 2007) and hence provides a metric of the shape of the flow duration curve. The algorithm uses the semi-log scale to estimate the slope because the region of FDC encompassed between these percentiles is often relatively linear (Zhang et al., 2008). The higher the slope, the more variable is the flow regime. A low slope denotes streams with low baseflow recession and a relatively larger baseflow contribution. The signature is defined as:

$$SFDC = \frac{\ln(Q_{33\%}) - \ln(Q_{66\%})}{(0.66 - 0.33)}. \quad \text{(S7)}$$

where *SFDC* is the slope of the flow duration curve, $Q_{33\%}$ is the streamflow value at 33rd percentile, and $Q_{66\%}$ is the streamflow value at 66th percentile.

Normalized 10th percentile streamflow - Q10N

The Normalized 10th percentile streamflow (Q10N) is an indicator of high flow intensity and variability. It is the daily streamflow value that exceeds 10% of the time normalized by the mean streamflow. The Q10N is related to the catchment "flashiness" and magnitude of high flow (Ogunkoya, 1988). The greater the number the more erratic the flow regime is. This

signature denotes how many times the top 10% highest flows are greater than the average flow within a time series. Q10N is calculated as:

$$Q10N = \frac{Q_{10}}{\bar{Q}}; \quad \text{(S8)}$$

where Q_{10} is the streamflow at 10th percentile and $\bar{Q}$ is the long-term average daily streamflow.

Normalized 90th percentile streamflow - Q90N

The Normalized 90th percentile streamflow (Q90N) addresses the intensity and variability of low streamflow. It is the ratio of the value of the daily streamflow being exceeded 90% of the time and the mean streamflow. The Q90N value indicates proportionally how small the low flows are in relation to average flows. Values can range from 0 to 1, being 0 for intermittent streams at 10th percentile flow and 1 for regular streams where the streamflow at 10th percentile has the same value of the average flow. Therefore, streams with a small Q90N value indicate lower and more variable low flows and are normally located in regions with a marked dry season. Conversely, high Q90N values indicate reduced low flow magnitude and variability. Q90N is calculated as:

$$Q90N = \frac{Q_{90}}{\bar{Q}}. \quad \text{(S8)}$$

where Q_{90} is the streamflow at 90th percentile and $\bar{Q}$ is the long-term average daily streamflow.

Frequency of no flow - FNF

The frequency of no flow (FNF) indicates the relative amount of time a stream is ephemeral. It is a daily hydrological metric that reports the proportional duration of no flow within a streamflow time series (Zhang et al., 2014). Australia is primarily a water-limited environment and intermittent streams are common in semi-arid and arid regions and in the upper catchments of the coastal ranges. Therefore, a signature that shows the ephemeral condition of lower order parts of the drainage network is crucial to evaluating the hydrological behaviour of Australian catchments. The signature is defined as:

$$FNF = \frac{N_{NF}}{N_S}. \quad \text{(S10)}$$

where *FNF* is the frequency of no flow days. N_{NF} is the number of zero flow days, and N_S is the total number of days within the streamflow time series.

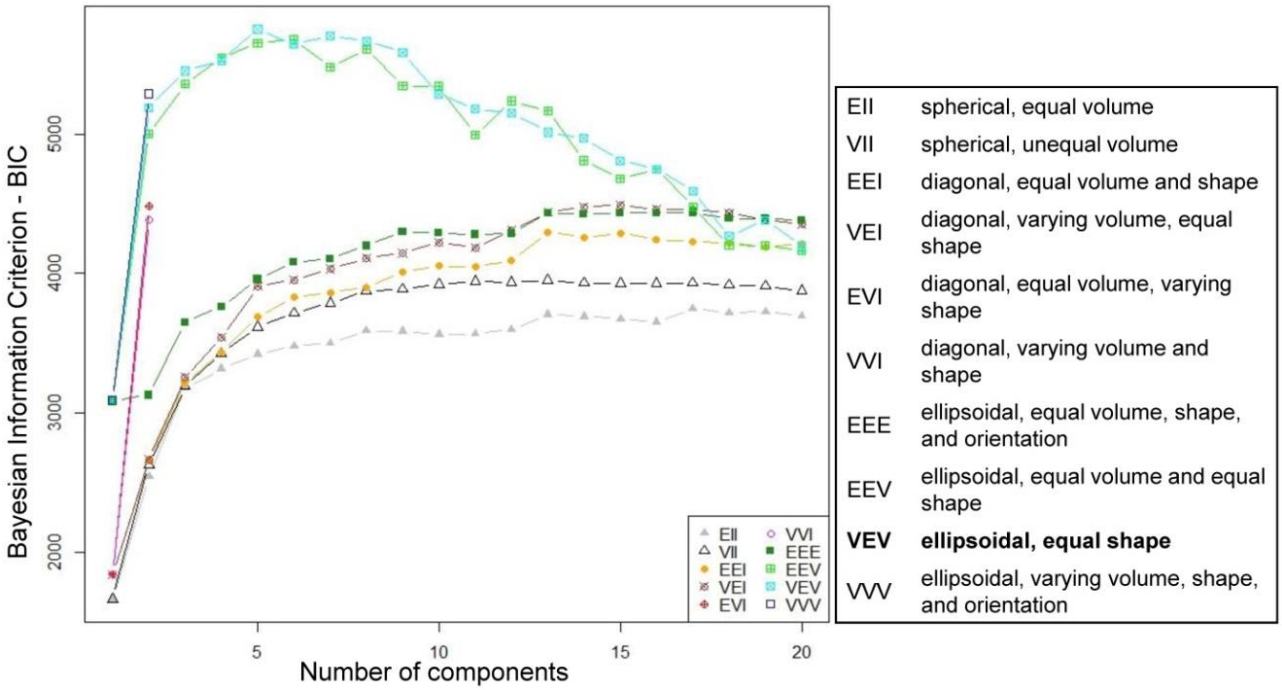

Figure A2.1 Results of the assessment for hierarchical classification model choice. The Bayesian Information Criterion (BIC) was used to assess models with differing parameterizations and/or numbers of clusters (10 models with 20 components). The ellipsoidal Gaussian finite mixture model with equal shape and five components was selected because of maximum BIC (5752.7).

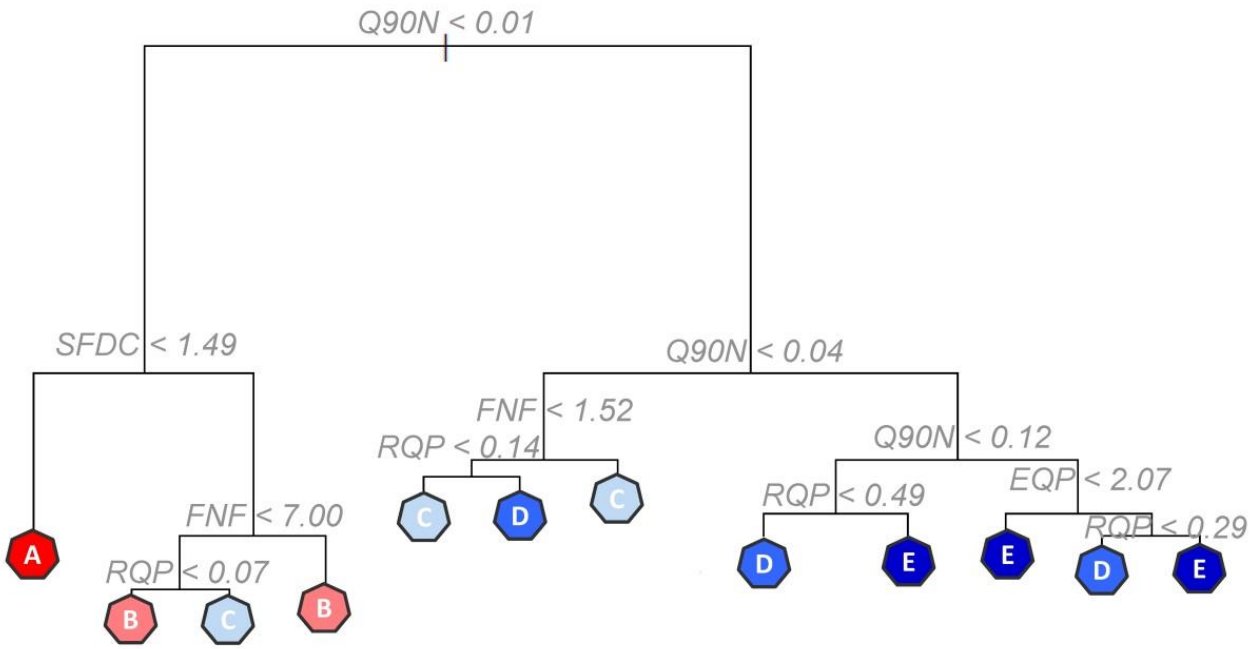

Figure A2.2 Classification tree based on five of the eight streamflow signatures to allocate further gauged catchments into the five clusters with similar streamflow behaviour identified along the Australian east seaboard with 91.81% of accuracy. The five clusters are denoted A to E and with more cluster-specific information provided in Figures 4 and 5 of the paper.

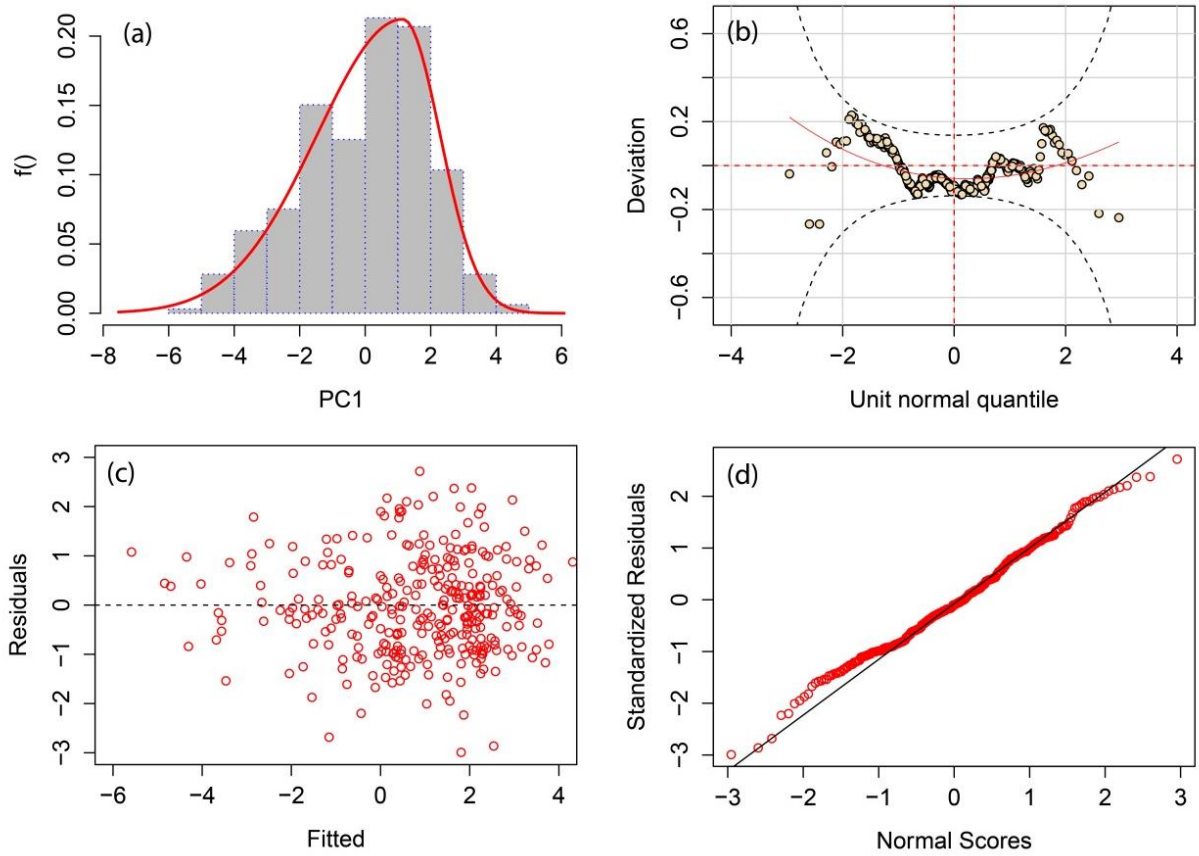

Figure A2.3 (a) The skew normal type 2 distribution curve fitted for to the response variable (PC1) with minimum generalized Akaike Information Criterion (GAIC) of 146.2; (b) worm plot for checking the residuals within different ranges; (c) distribution of residuals in relation to fitted values; and (d) Q-Q plot.

Table A2.1 Statistical significance of an unpaired Wilcoxon rank sum test on the differences of the distributions of eight streamflow signatures (see Table 2 and section 1 of the Supporting Information for a description of streamflow signatures), Dryness Index (PET/P) and Evaporative Index (AET/P) among catchment clusters (see Figures 4 and 5 for a graphical display of flow signatures and indexes variability respectively). Significant differences (p-value < 0.5) are highlighted with an asterisk.

Combinations	RQP	EQP	RLD	BFI	SFDC	Q10N	Q90N	FNF	PET/P	AET/P
A-B	0.000*	0.128	0.000*	0.000*	0.000*	0.003*	0.003*	0.000*	0.000*	0.416
A-C	0.000*	0.062	0.000*	0.000*	0.000*	0.000*	0.000*	0.000*	0.000*	0.005*
A-D	0.000*	0.000*	0.012*	0.000*	0.000*	0.000*	0.000*	0.000*	0.000*	0.000*
A-E	0.000*	0.000*	0.003*	0.000*	0.000*	0.000*	0.000*	0.000*	0.000*	0.000*
B-C	0.008*	0.385	0.984	0.004*	0.000*	0.000*	0.000*	0.000*	0.001*	0.134
B-D	0.000*	0.000*	0.107	0.000*	0.000*	0.000*	0.000*	0.000*	0.000*	0.000*
B-E	0.000*	0.000*	0.000*	0.000*	0.000*	0.000*	0.000*	0.000*	0.000*	0.000*
C-D	0.088	0.000*	0.134	0.000*	0.000*	0.000*	0.000*	0.000*	0.000*	0.005*
C-E	0.000*	0.000*	0.000*	0.000*	0.000*	0.000*	0.000*	0.000*	0.000*	0.000*
D-E	0.000*	0.000*	0.000*	0.000*	0.000*	0.000*	0.000*	0.000*	0.000*	0.000*

A2.3 References

Arnold, J.G., Allen, P.M., 1999. Automated methods for estimating baseflow and ground water recharge from streamflow records. JAWRA Journal of the American Water Resources Association, 35(2): 411-424. DOI:doi:10.1111/j.1752-1688.1999.tb03599.x

Chiew, F.H.S., 2006. Estimation of rainfall elasticity of streamflow in Australia. Hydrological Sciences Journal, 51(4): 613-625. DOI:doi:10.1623/hysj.51.4.613

Donohue, R.J., Roderick, M.L., McVicar, T.R., 2011. Assessing the differences in sensitivities of runoff to changes in climatic conditions across a large basin. Journal of Hydrology, 406(3–4): 234-244. DOI:10.1016/j.jhydrol.2011.07.003

Dooge, J.C.I., 1992. Sensitivity of Runoff to Climate Change: A Hortonian Approach. Bulletin of the American Meteorological Society, 73(12): 2013-2024. DOI:doi:10.1175/1520-0477(1992)073<2013:SORTCC>2.0.CO;2

Eckhardt, K., 2005. How to construct recursive digital filters for baseflow separation. Hydrological Processes, 19(2): 507-515. DOI:doi:10.1002/hyp.5675

Eckhardt, K., 2008. A comparison of baseflow indices, which were calculated with seven different baseflow separation methods. Journal of Hydrology, 352(1–2): 168-173. DOI:doi:10.1016/j.jhydrol.2008.01.005

Fu, G., Charles, S.P., Chiew, F.H.S., 2007. A two-parameter climate elasticity of streamflow index to assess climate change effects on annual streamflow. Water Resources Research, 43(11): W11419. DOI:doi:10.1029/2007WR005890

Gonzales, A.L., Nonner, J., Heijkers, J., Uhlenbrook, S., 2009. Comparison of different base flow separation methods in a lowland catchment. Hydrology and Earth System Sciences, 13(11): 2055-2068. DOI:doi:10.5194/hess-13-2055-2009

Lacey, G.C., Grayson, R.B., 1998. Relating baseflow to catchment properties in south-eastern Australia. Journal of Hydrology, 204(1–4): 231-250. DOI:10.1016/S0022-1694(97)00124-8

Li, L., Maier, H.R., Lambert, M.F., Simmons, C.T., Partington, D., 2013. Framework for assessing and improving the performance of recursive digital filters for baseflow estimation with application to the Lyne and Hollick filter. Environmental Modelling & Software, 41(0): 163-175. DOI:doi:10.1016/j.envsoft.2012.11.009

Lyne, V., Hollick, M., 1979. Stochastic time-variable rainfall runoff modelling, Hydrology and Water Resources Symposium. Institution of Engineers, Perth, Australia, pp. 89-92.

Milly, P.C.D., 1994. Climate, soil water storage, and the average annual water balance. Water Resources Research, 30(7): 2143-2156. DOI:doi:10.1029/94WR00586

Milly, P.C.D. et al., 2008. Stationarity Is Dead: Whither Water Management? Science, 319(5863): 573-574. DOI:doi:10.1126/science.1151915

Nathan, R.J., McMahon, T.A., 1990. Evaluation of automated techniques for base flow and recession analyses. Water Resources Research, 26(7): 1465-1473. DOI:doi:10.1029/WR026i007p01465

Ogunkoya, O.O., 1988. Towards a delimitation of southwestern Nigeria into hydrological regions. Journal of Hydrology, 99(1–2): 165-177. DOI:10.1016/0022-1694(88)90085-6

Peña-Arancibia, J.L., van Dijk, A.I.J.M., Mulligan, M., Bruijnzeel, L.A., 2010. The role of climatic and terrain attributes in estimating baseflow recession in tropical catchments. Hydrol. Earth Syst. Sci., 14(11): 2193-2205. DOI:10.5194/hess-14-2193-2010

Sankarasubramanian, A., Vogel, R.M., Limbrunner, J.F., 2001. Climate elasticity of streamflow in the United States. Water Resources Research, 37(6): 1771-1781. DOI:doi:10.1029/2000WR900330

Schaake, J.C., 1990. From climate to flow. In: Waggoner, P.E. (Ed.), Climate change and US water resources. John Wiley and Sons, New York, pp. 177-206.

Shamir, E., Imam, B., Morin, E., Gupta, H.V., Sorooshian, S., 2005. The role of hydrograph indices in parameter estimation of rainfall–runoff models. Hydrological Processes, 19(11): 2187-2207. DOI:doi:10.1002/hyp.5676

Wittenberg, H., 1999. Baseflow recession and recharge as nonlinear storage processes. Hydrological Processes, 13(5): 715-726. DOI:doi:10.1002/(SICI)1099-1085(19990415)13:5<715::AID-HYP775>3.0.CO;2-N

Yadav, M., Wagener, T., Gupta, H., 2007. Regionalization of constraints on expected watershed response behavior for improved predictions in ungauged basins. Advances in Water Resources, 30(8): 1756-1774. DOI:doi:10.1016/j.advwatres.2007.01.005

Zhang, Y., Vaze, J., Chiew, F.H.S., Teng, J., Li, M., 2014. Predicting hydrological signatures in ungauged catchments using spatial interpolation, index model, and rainfall–runoff modelling. Journal of Hydrology, 517(0): 936-948. DOI:doi:10.1016/j.jhydrol.2014.06.032

Zhang, Z., Wagener, T., Reed, P., Bhushan, R., 2008. Reducing uncertainty in predictions in ungauged basins by combining hydrologic indices regionalization and multiobjective optimization. Water Resources Research, 44(12): W00B04. DOI:10.1029/2008WR006833

Appendix 3 – Chapter 3

Supplementary material

Regional variation in streamflow drivers across a continental climatic gradient

Contents of this file

A3.1 Introduction

This supplementary information provides supporting table and figures showing the variability of explanatory variables across the regions (**Table A3.1**) and correlograms from streamflow characteristics (**Figure A3.1)** and residuals of cross-validation of models across different regions and scales (**Figure A3.2**).

Table A3.1. Listing of the 24 explanatory variables assessed to model streamflow characteristics with sources and average ± standard deviation by region, where: EC = East Coast of Australia; R1 = Region 1 - tropical; R2 = Region 2 - sub-tropical; R3 = Region 3, temperate. Metrics with empty brackets are non-dimensional.

Explanatory variables (Units)	Average ± Standard deviation			
	EC	**R1**	**R2**	**R3**
Climatic				
1. Dryness index ( )	1.45 ± 0.49	1.28 ± 0.64	1.32 ± 0.39	1.13 ± 0.35
2. Long-term average maximum air temperature (° C)	20.34 ± 3.7	27.85 ± 1.95	24.62 ± 1.46	17.53 ± 1.27
3. Long-term average minimum air temperature (° C)	9.05 ± 3.39	18.19 ± 1.88	13.21 ± 1.53	6.55 ± 1.38
4. Seasonality index ( )	0.004 ± 0.004	0.011 ± 0.003	0.005 ± 0.**0**01	0.002 ± 0.002
5. Long-term annual average of precipitation (mm)	929.77 ± 272.07	1671.65 ± 744.4	1188.87 ± 341.8	1030.93 ± 245.56
Topography				
6. Fraction of erosional landscapes ( )	0.73 ± 0.2	0.69 ± 0.2	0.82 ± 0.13	0.9 ± 0.1
7. Average slope (%)	12.36 ± 7.37	12.57 ± 7.09	15.67 ± 6.02	17.28 ± 7.02
8. Maximum slope (%)	62.79 ± 29.32	68.65 ± 27.34	80.1 ± 37.83	62.67 ± 19.45
Vegetation				
9. Long-term monthly average of fPAR ( )	0.69 ± 0.11	0.66 ± 0.16	0.75 ± 0.09	0.75 ± 0.08
10. Long-term monthly range of fPAR ( )	0.07 ± 0.04	0.06 ± 0.02	0.05 ± 0.02	0.05 ± 0.02
11. Fraction of woody vegetation cover ( )	0.78 ± 0.26	0.93 ± 0.11	0.89 ± 0.09	0.83 ± 0.2
12. Long-term annual average of actual evapotranspiration (mm)	726.72 ± 150.09	1046.76 ± 238.08	955.9 ± 142.81	747.15 ± 79.35
Soils				
13. Long-term monthly average of soil moisture ( )	0.38 ± 0.1	0.38 ± 0.14	0.35 ± 0.08	0.47 ± 0.1
14. Average soil depth ($AB_{horizon}$) (m)	0.99 ± 0.26	1.24 ± 0.33	0.91 ± 0.24	1.05 ± 0.24
15. Saturated Hydraulic Conductivity (mm/h)	699.47 ± 650.39	167.13 ± 90.42	107.87 ± 75.24	165 ± 91.66
16. Average clay content (%)	27.7 ± 10.51	26.35 ± 12.78	34.67 ± 11.52	30.21 ± 10.91
17. Average pH ( )	5.17 ± 0.65	5.2 ± 0.45	5.24 ± 0.77	4.67 ± 0.33
18. Average plant available water capacity (mm)	102.05 ± 32.1	72.1 ± 27.96	94.01 ± 30.88	130.24 ± 33.02
19. Average bulk density in top 30 cm (g/cm^3)	1.30 ± 0.18	1.51 ± 0.15	1.36 ± 0.19	1.15 ± 0.18
Physiography				
20. Area (km^2)	361.37 ± 429.35	572.01 ± 656.37	264.2 ± 341.49	287.93 ± 320.2
21. Perimeter (km)	173.75 ± 107.31	181.22 ± 108.3	130.28 ± 86.43	154.95 ± 94.09
22. Circularity Ratio( )	0.13 ± 0.04	0.18 ± 0.04	0.15 ± 0.03	0.13 ± 0.03
23. Shape factor( )	0.36 ± 0.06	0.42 ± 0.05	0.38 ± 0.04	0.35 ± 0.04
24. Compactness coefficient ( )	2.87 ± 0.49	2.41 ± 0.33	2.63 ± 0.33	2.86 ± 0.3

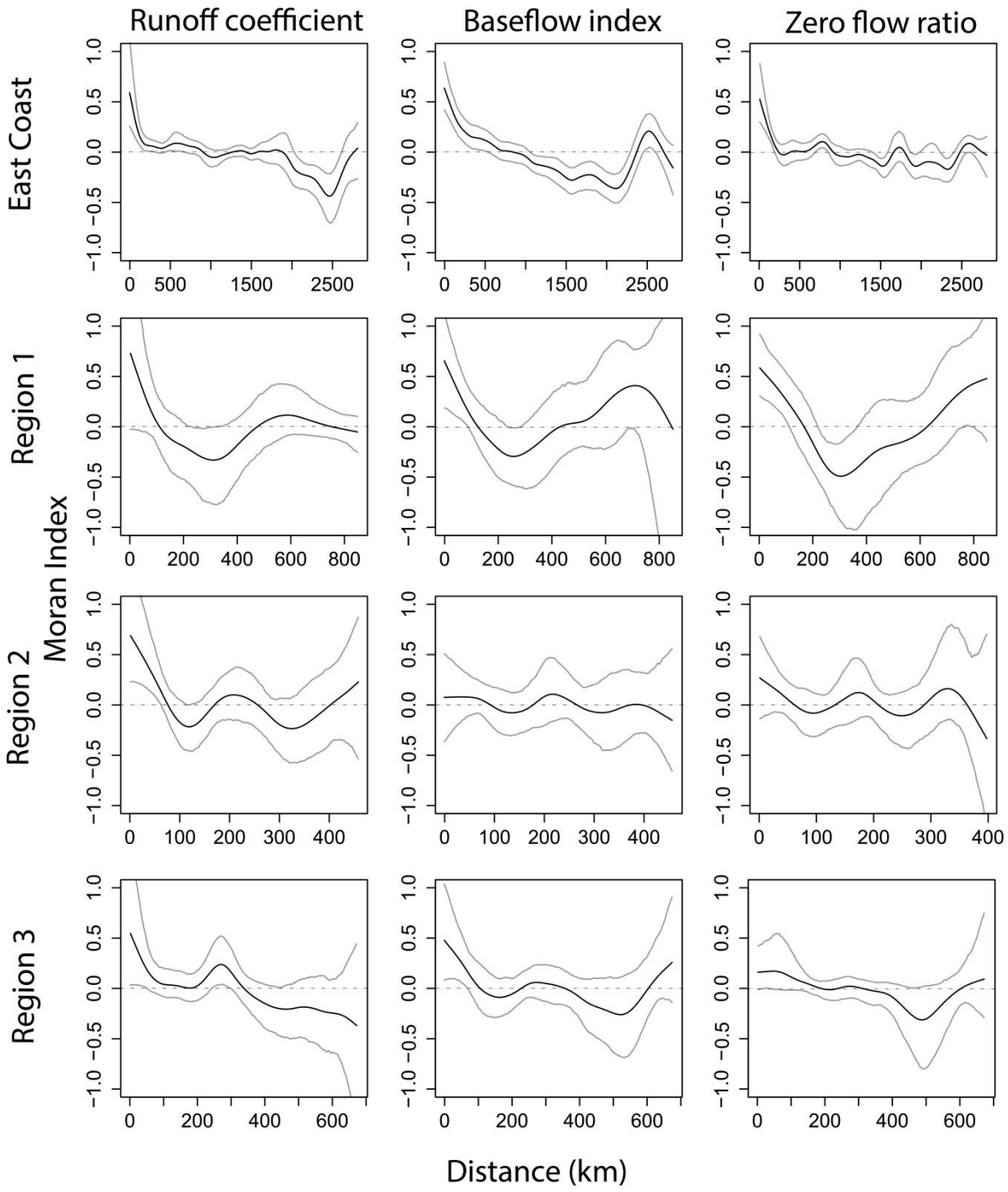

Figure A3.1. Spline correlograms from residuals of three streamflow characteristics (runoff ratio, baseflow index and zero flow ratio) across the entire east coast and three distinct regions. The black lines are the average spatial autocorrelation from 1000 resamples and the grey lines are the confidence envelope corresponding to the null distribution.

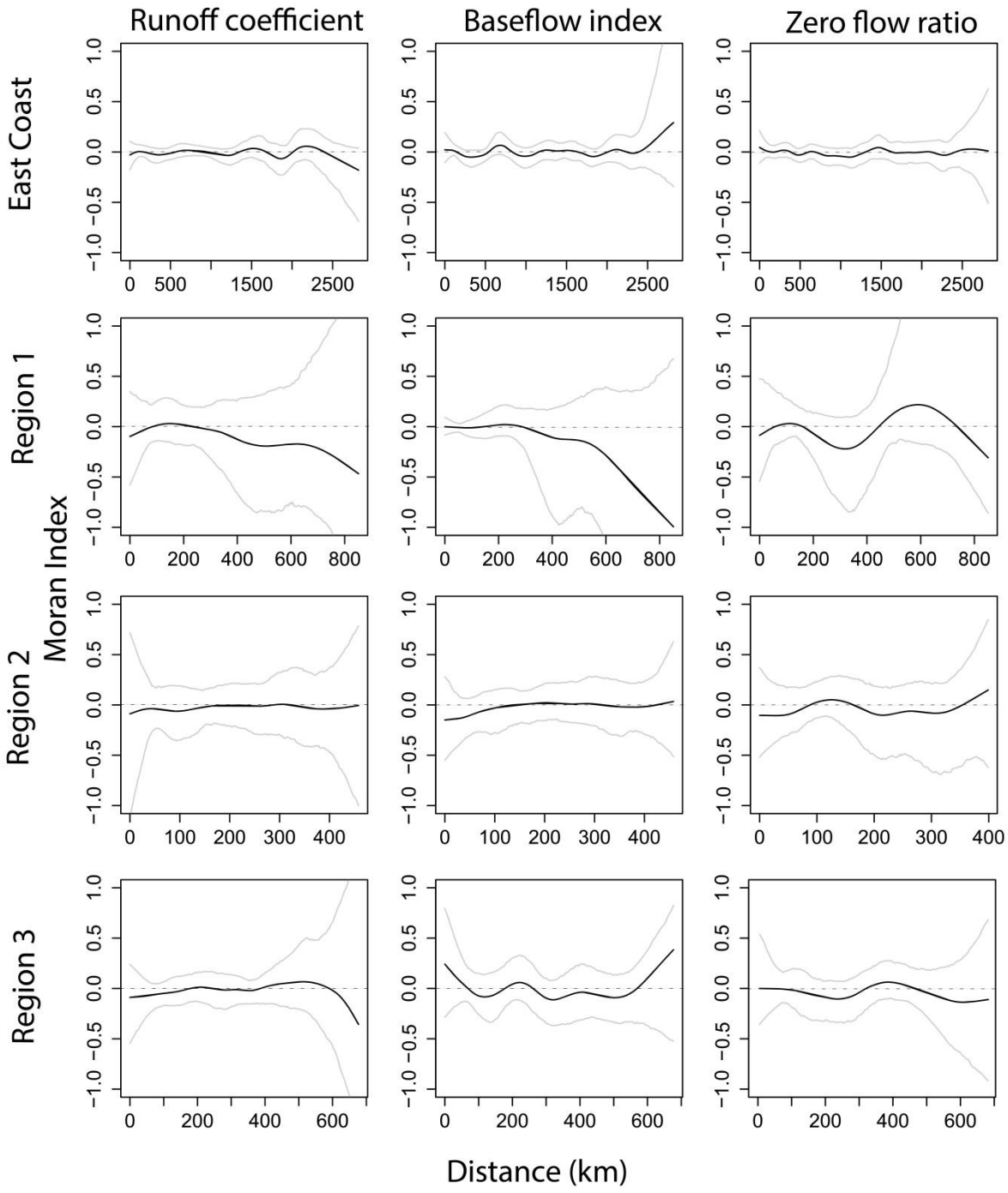

Figure A3.2. Spline correlograms from residuals of cross-validation of generalized additive models for location, scale and shape with penalised B-splines for three streamflow characteristics (runoff ratio, baseflow index and zero flow ratio) across the entire east coast and three distinct regions.

Appendix 4 – Chapter 4

Supplementary material

Disentangling vegetation gain and climate contributions to long-term streamflow changes

Contents of this file

A4.1 Introduction

This supplementary material provides a supporting figure showing the Conceptual diagram of (a) possible changes in the water and energy balances due to climate- (ΔQ^C) and land cover-induced (ΔQ^L) changes in the Budyko framework (**Figure A4.1)**.

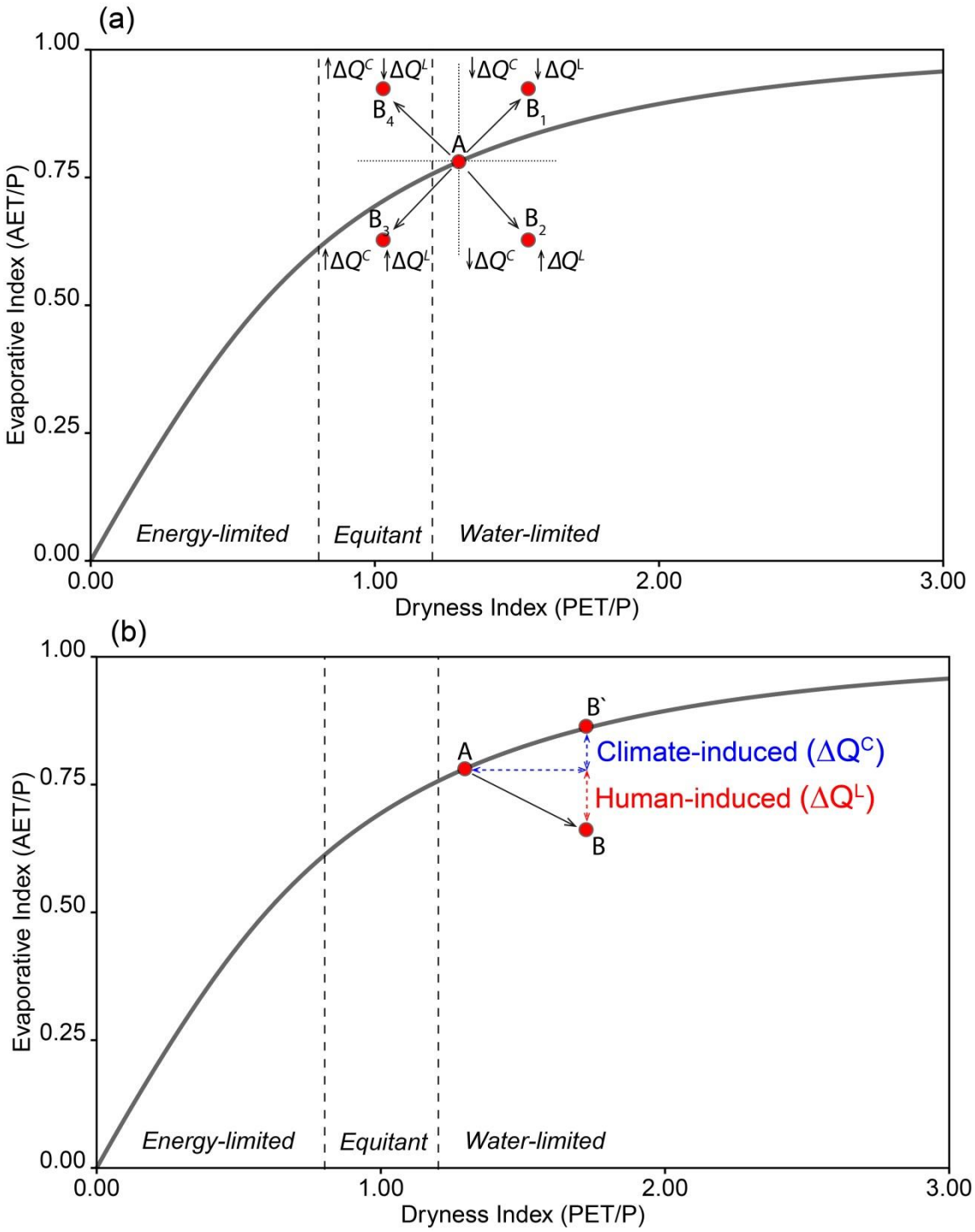

Figure A4.1. Conceptual diagram of (a) possible changes in the water and energy balances due to climate- (ΔQ^C) and human-induced (ΔQ^L) changes in the Budyko framework according to the trajectory described. Catchments moving towards B_1 have decreasing ΔQ^C and ΔQ^L; catchments moving towards B_2 have decreasing ΔQ^C and increasing ΔQ^L; catchments moving towards B_3 have increasing ΔQ^C and ΔQ^L; and catchments moving towards B_4 have increasing ΔQ^C and decreasing ΔQ^L. (b) Decomposition of climate- and human-direct impacts where the changes in AET (vertical displacement) is partitioned into ΔQ^C and ΔQ^L (adapted from Wang and Hejazi (2011)).

Appendix 5 – Chapter 5

Supplementary material

CO_2 – vegetation feedbacks and other climate changes implicated in reducing baseflow

Contents of this file

Figure A5.1 to A5.11

A4.1 Introduction

This Supporting Information provides additional figures showing trends in baseflow, precipitation and potential evapotranspiration for 1950 - 2013 (**Figure A5.1**); the influence of time-series length and wet and dry periods in trends (**Figure A5.2**); sensitivity of trends to the length of time-series (**Figure A5.3**); trends in baseflow in the context of the Budyko framework (**Figure A5.4**); scatterplots of trends in Qb and P and PET (**Figure A5.5**); ternary plot of relative contributions of P, PET and other factors for 1950 - 2013 (**Figure A5.6**); relationship of Qb and Qbr trends and fPAR and fPARr trends (**Figure A5.7**); ternary plots of relative contributions of P, PET and other factors in Qb trends in light of P max – PET max phase offset and spectrum of streamflow regimes (**Figure A5.8**); trends for Qbr and fPARr (**Figure A5.9**); relationship between atmospheric CO_2 concentrations and fPARr (**Figure A5.10**); and relative impact of eCO_2 –Veg and climate (P + PET) on baseflow changes in relation to long-term annual baseflow for 1950 - 2013 (**Figure A5.11**).

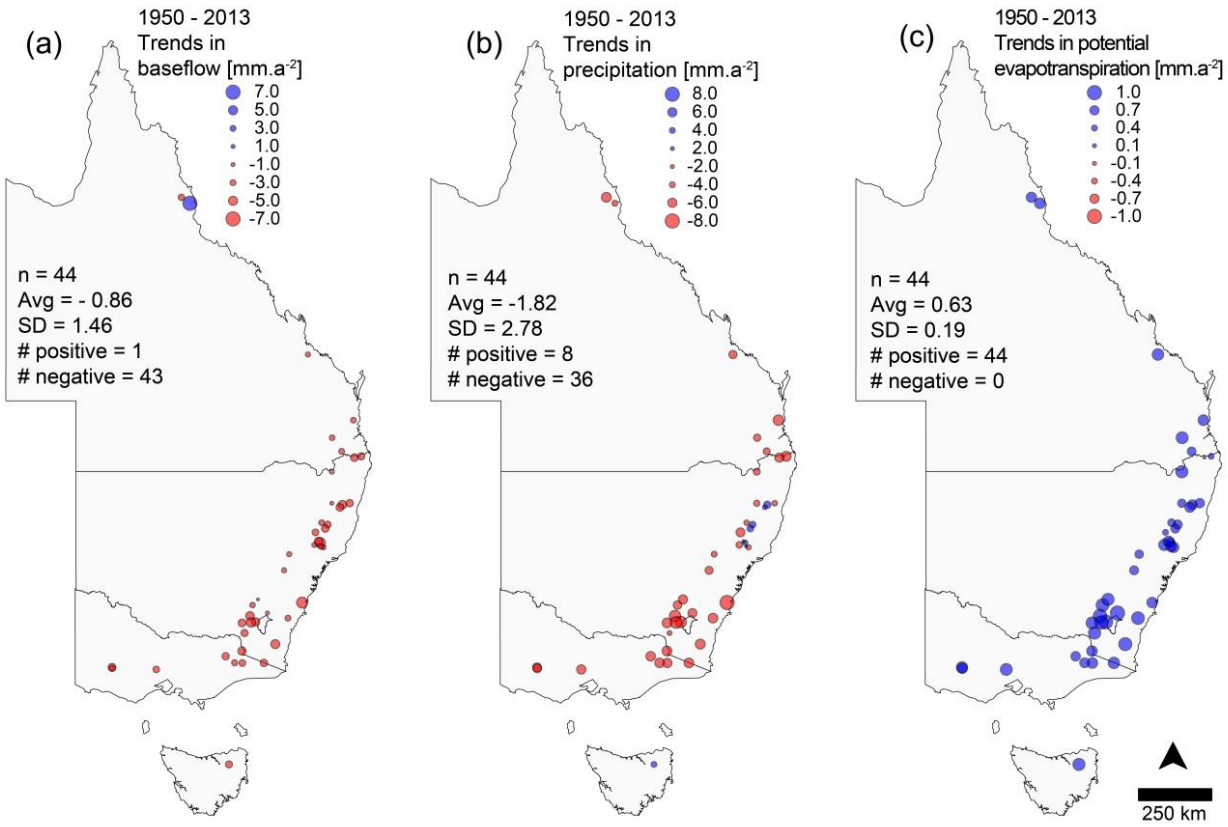

Figure A5.1. Trends in (a) baseflow, (b) precipitation and (c) potential evapotranspiration for 1950–2013.

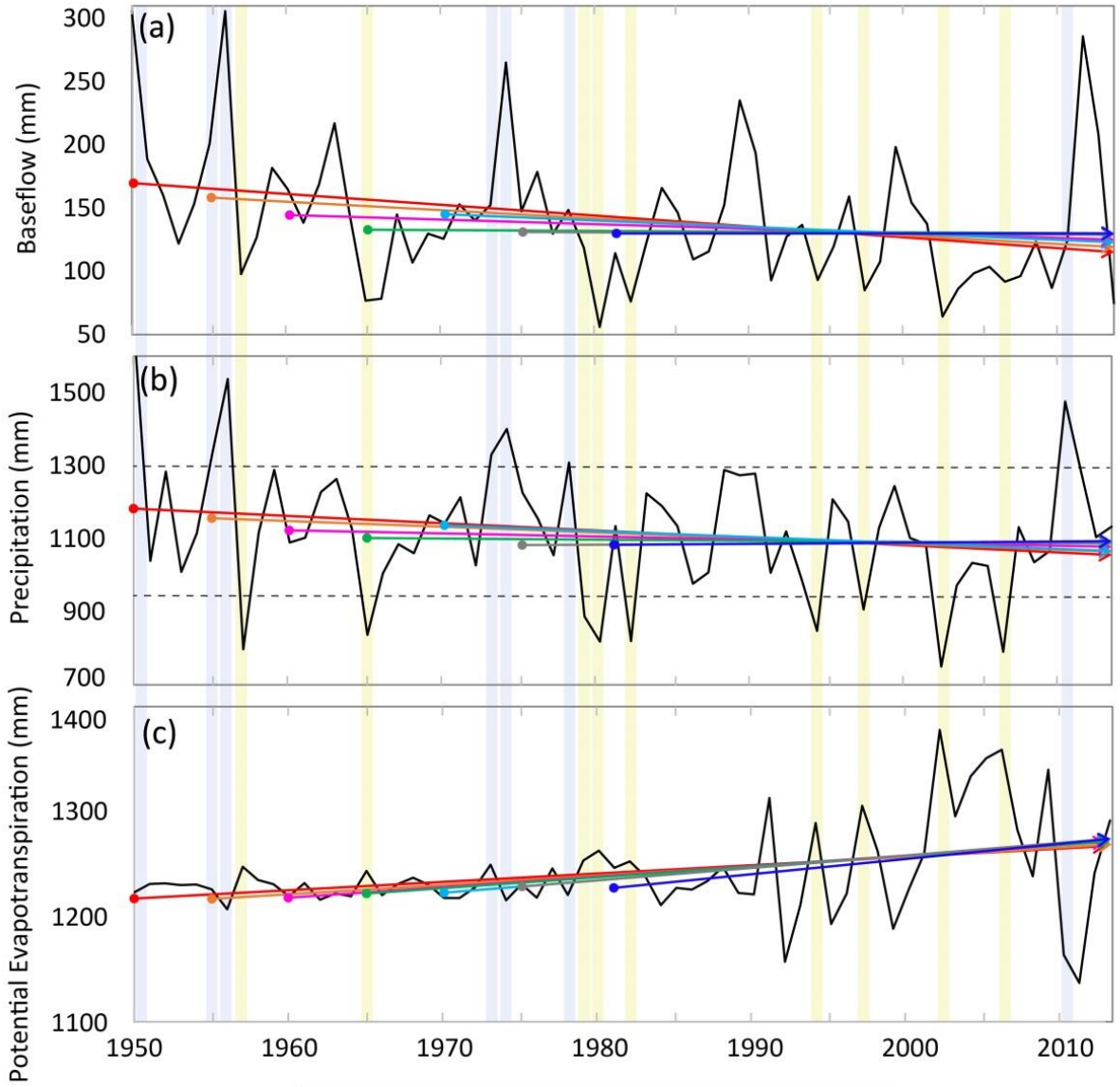

(d)

Period	Trends ($mm.a^{-2}$) Qb	P	PET
1950 - 2013	-0.86	-2.02	0.79
1955 - 2013	-0.67	-1.58	0.89
1960 - 2013	-0.38	-0.85	1.00
1965 - 2013	-0.06	-0.31	1.03
1970 - 2013	-0.51	-1.64	1.18
1975 - 2013	-0.06	0.20	1.20
1981 - 2013	-0.05	0.31	1.45

Figure A5.2. Influence of time-series length, from 1950 onwards incrementing by roughly 5-year steps, and wet and dry periods in trend detection and trend magnitudes of hydroclimatic variables averaged for the 44 catchments for: (a) baseflow; (b) precipitation, (c) potential evapotranspiration, and (d) linear trends. In part (b) years with precipitation under the lower horizontal dashed line (i.e. P ≤ average (P) - standard deviation (P)) are considered dry (yellow shaded strips) while years with precipitation above the upper horizontal dashed line (i.e. P ≥ average (P) + standard deviation (P)) are considered wet (blue shaded strips). On (a) to (c) the coloured arrows display the changes in trend slopes according to the length of time-series considered, with the trends be reported in (d).

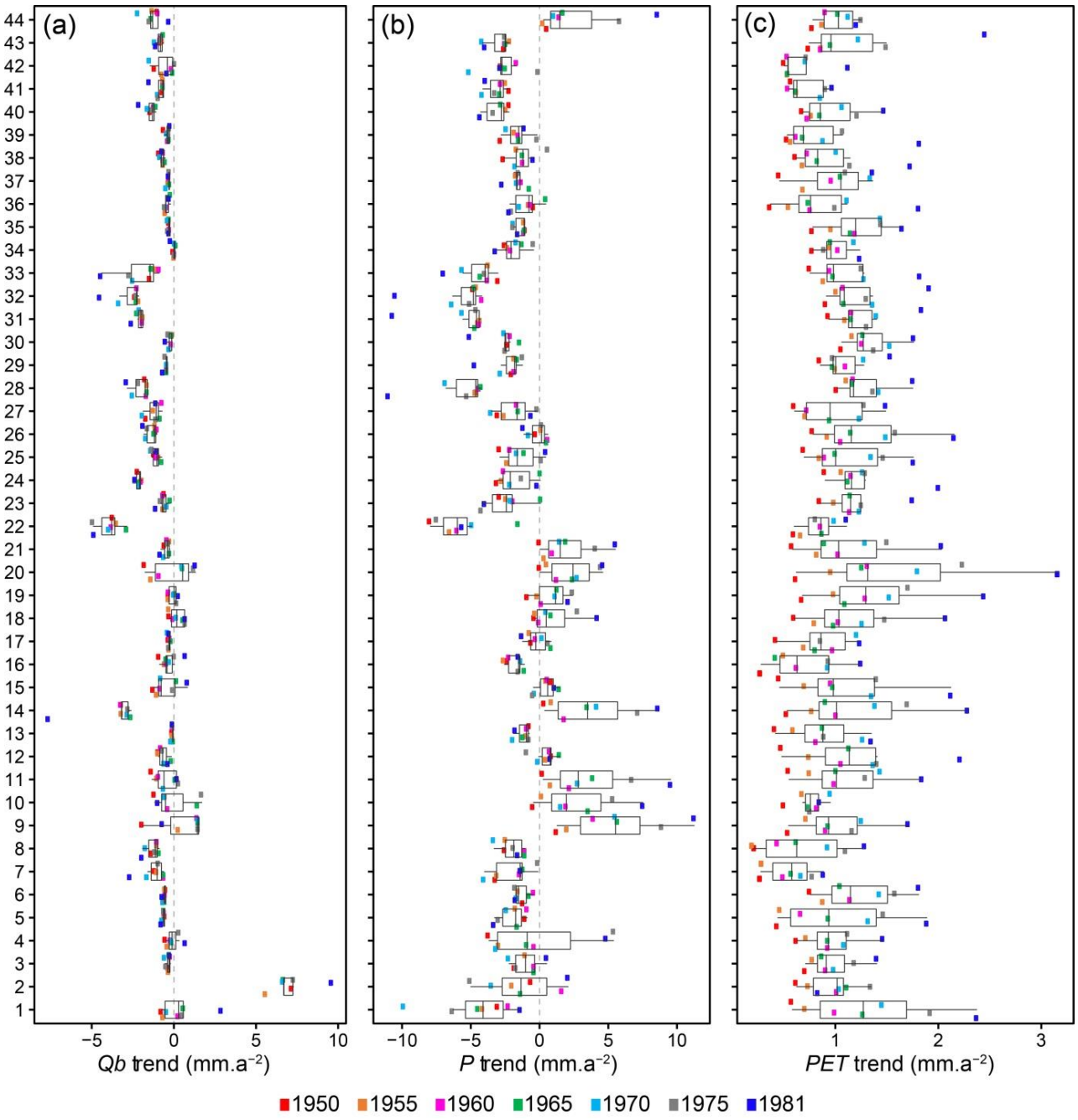

Figure A5.3. Sensitivity of trends to the length of time-series for the 44 catchments with streamflow data from 1950 to 2013: (a) baseflow; (b) precipitation; and (c) potential evapotranspiration. Coloured squares refer to the starting year used to calculate the trends. Box plot statistics include the median (internal vertical line), interquartile range (*IQR* - denoted by the box), and horizontal lines (or whiskers) are calculated as $\pm 1.58 \times IQR\sqrt{n}$.

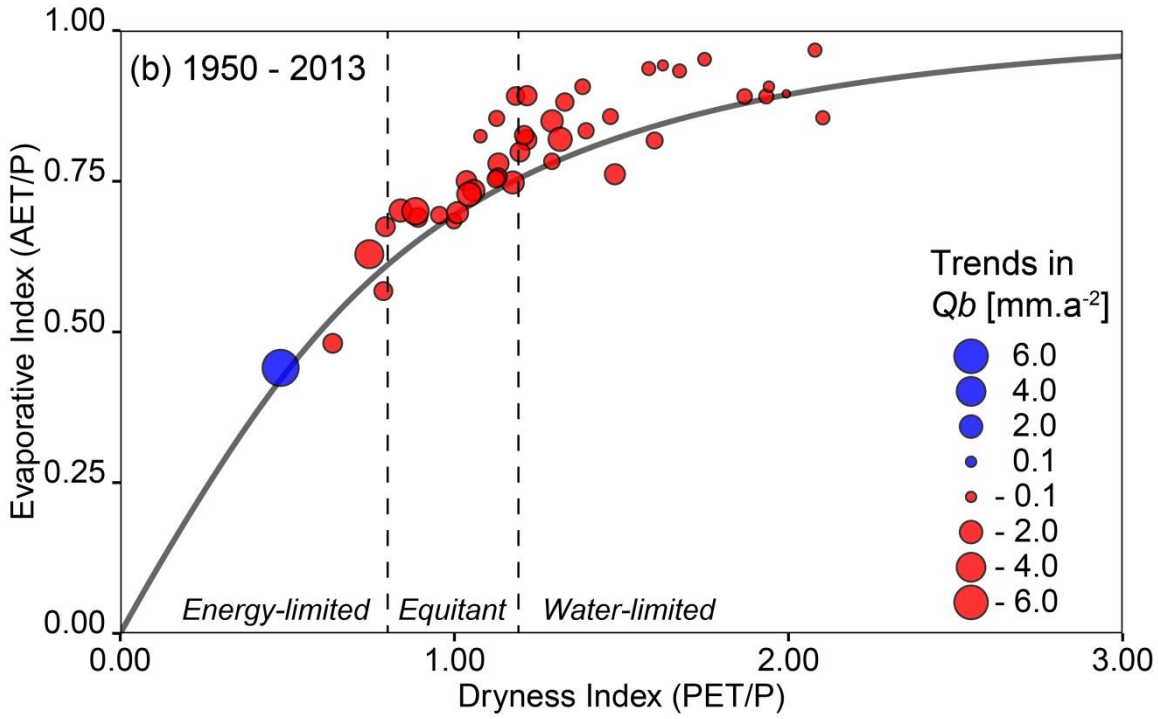

Figure A5.4. Trends in baseflow (Qb) in the context of the Budyko framework for 1950 – 2013 period. Solid grey line is the Budyko curve and vertical dashed lines are the thresholds defining the water-limited, equitant and energy-limited regions.

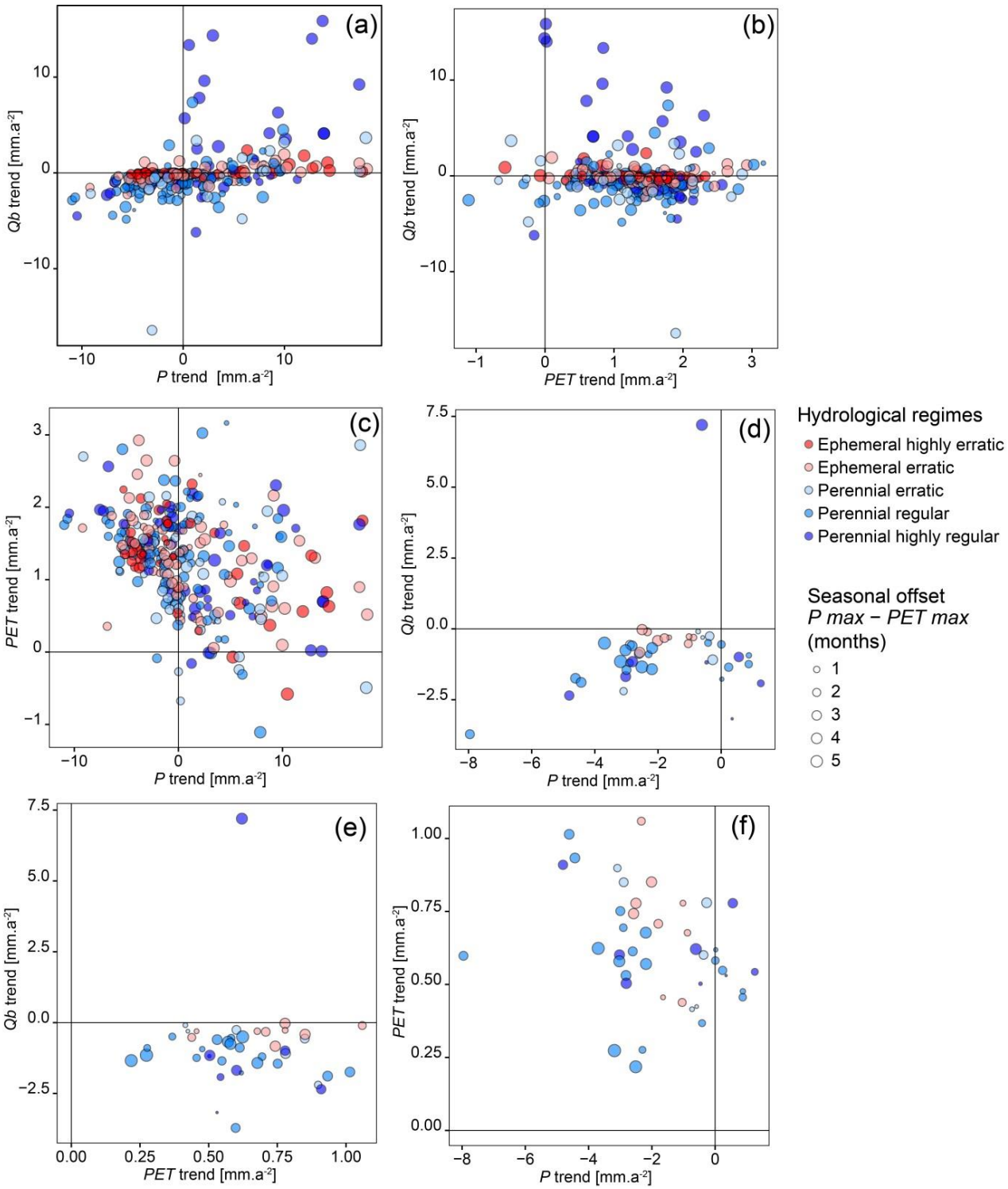

Figure A5.5. Scatterplots of trends in Qb and P, Qb and PET, and PET and P for 1981 - 2013 (a, b and c respectively) and 1950 - 2013 (d, e and f respectively). Symbol colours refer to the hydrological regimes (see Trancoso et al, 2016 for a full description). Symbol size refers to the temporal phase offset between month of P maxima and month of PET maxima averaged across the per catchment entire time-series.

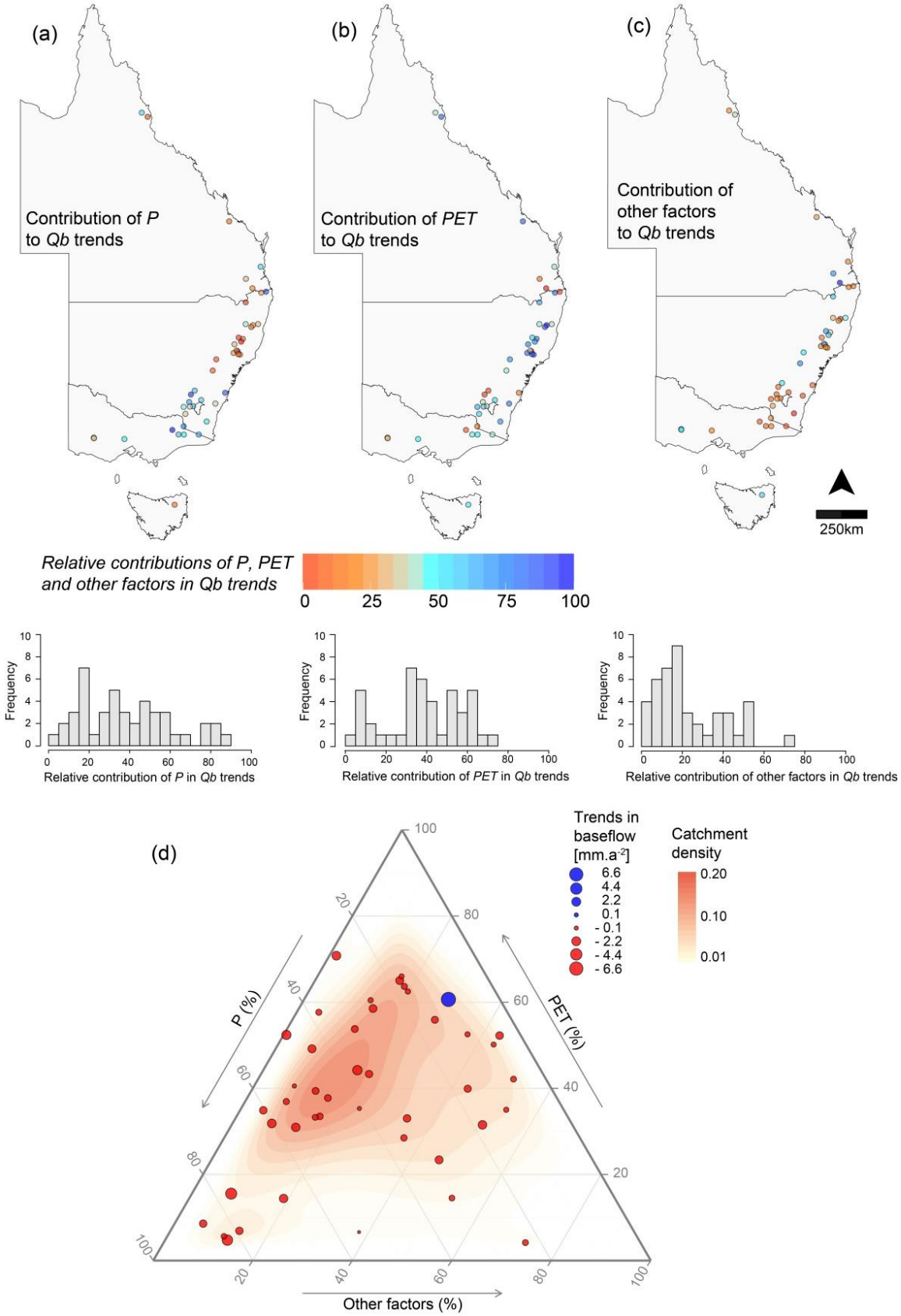

Figure A5.6. Histograms and spatial distribution of the relative contributions of (a) P, (b) PET and (c) other factors on Qb trends for 1950-2013. (d) Ternary diagram integrating the relative contributions of P, PET and other factors on Qb trends. Catchment density refers to the relative frequency of catchments within the ternary space.

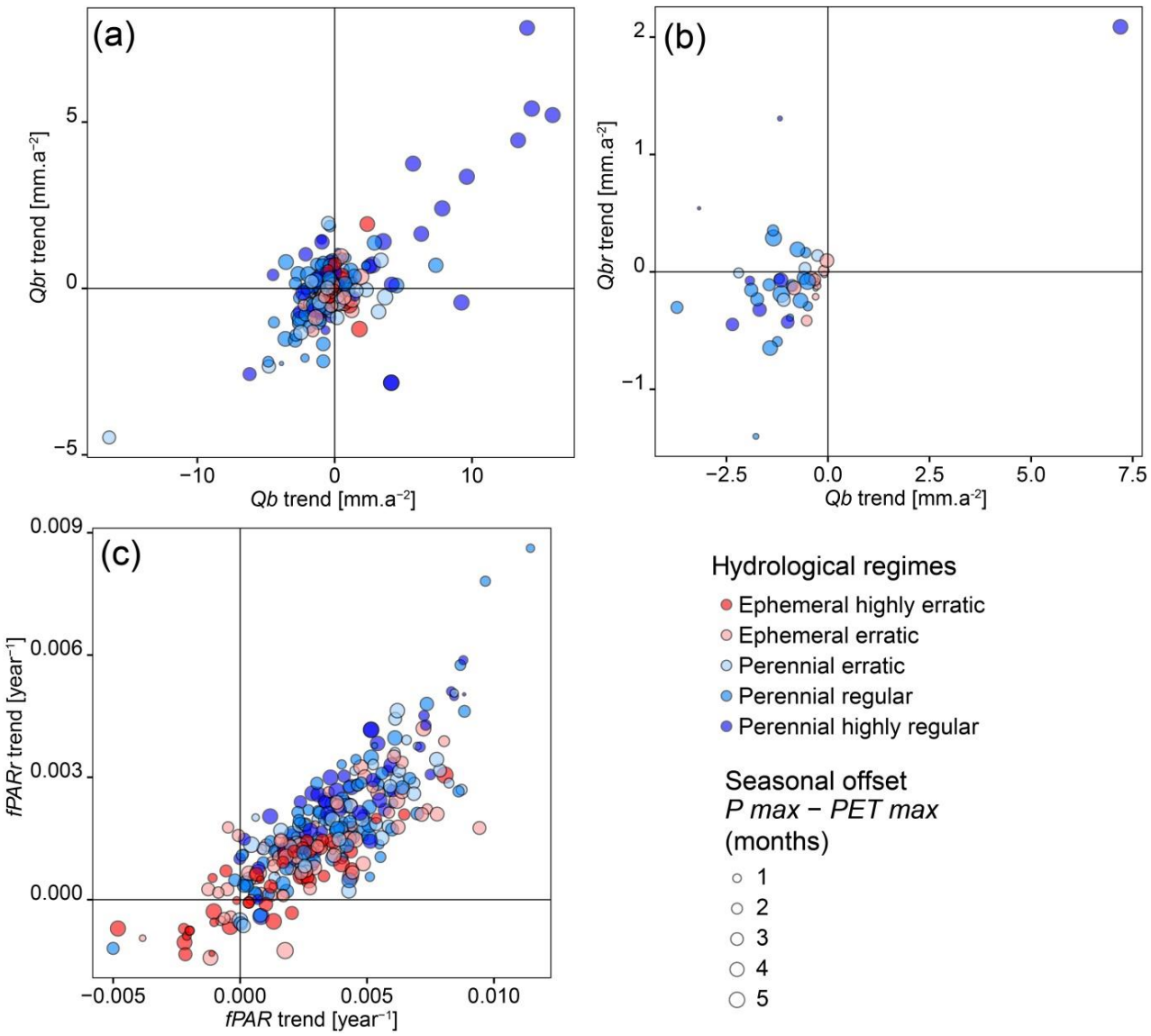

Figure A5.7. Scatterplots of Qb and Qbr trends for: (a) 1981-2013 and (b) 1950-2013. Part (c) is a scatterplot for fPAR and fPARr trends for 1981-2013. Symbol colours refer to the hydrological regimes (see Trancoso et al, 2016 for a full description). Symbol size refers to the temporal phase offset between month of P maxima and month of PET maxima averaged across the per catchment entire time-series.

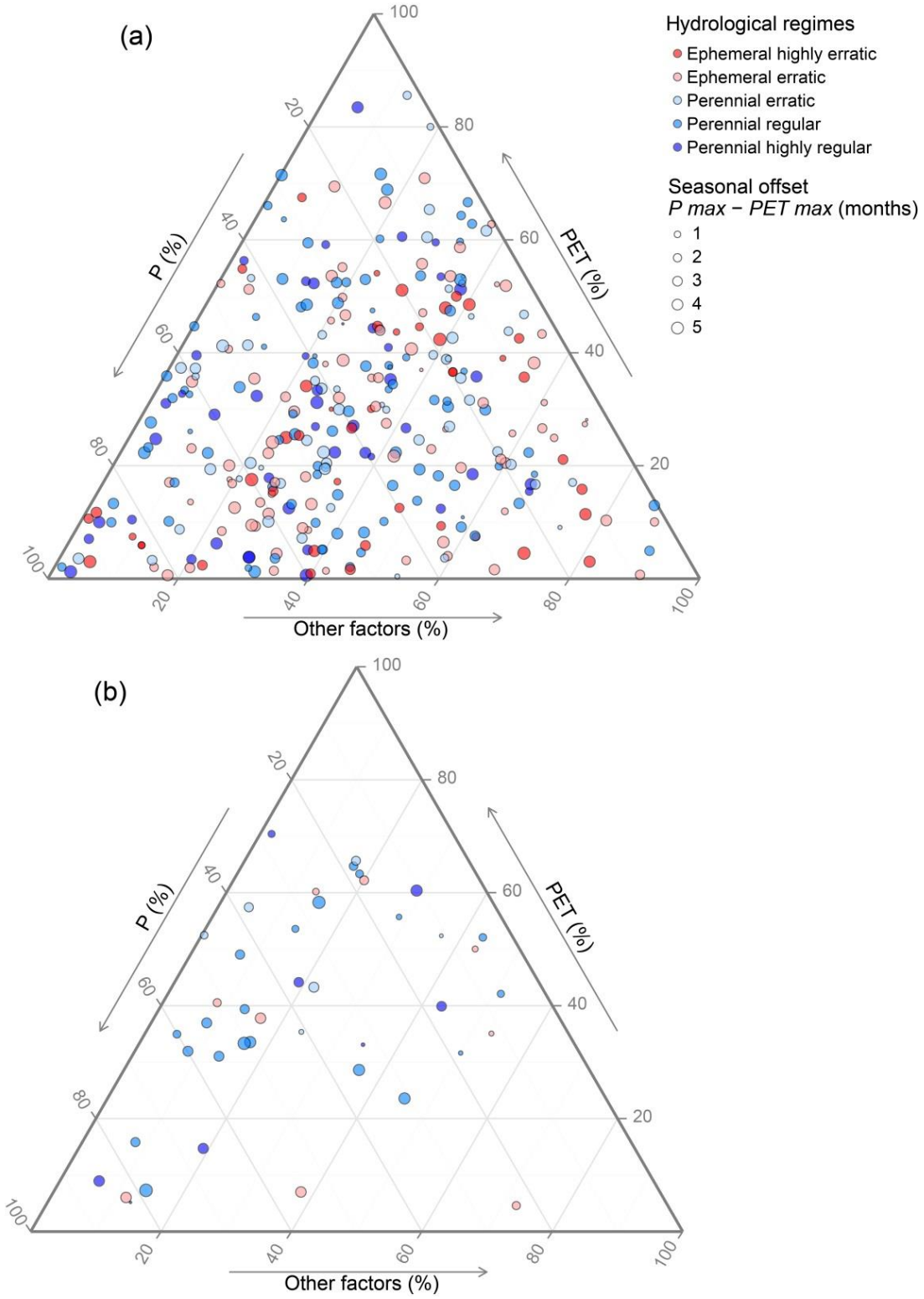

Figure A5.8. Relative contributions of P, PET and other factors on Qb trends for (a) 1981-2013 and (b) 1950-2013. Symbol colours refer to the hydrological regimes (see Trancoso et al, 2016 for a full description). Symbol size refers to the temporal phase offset between month of P maxima and month of PET maxima averaged across the per catchment entire time-series.

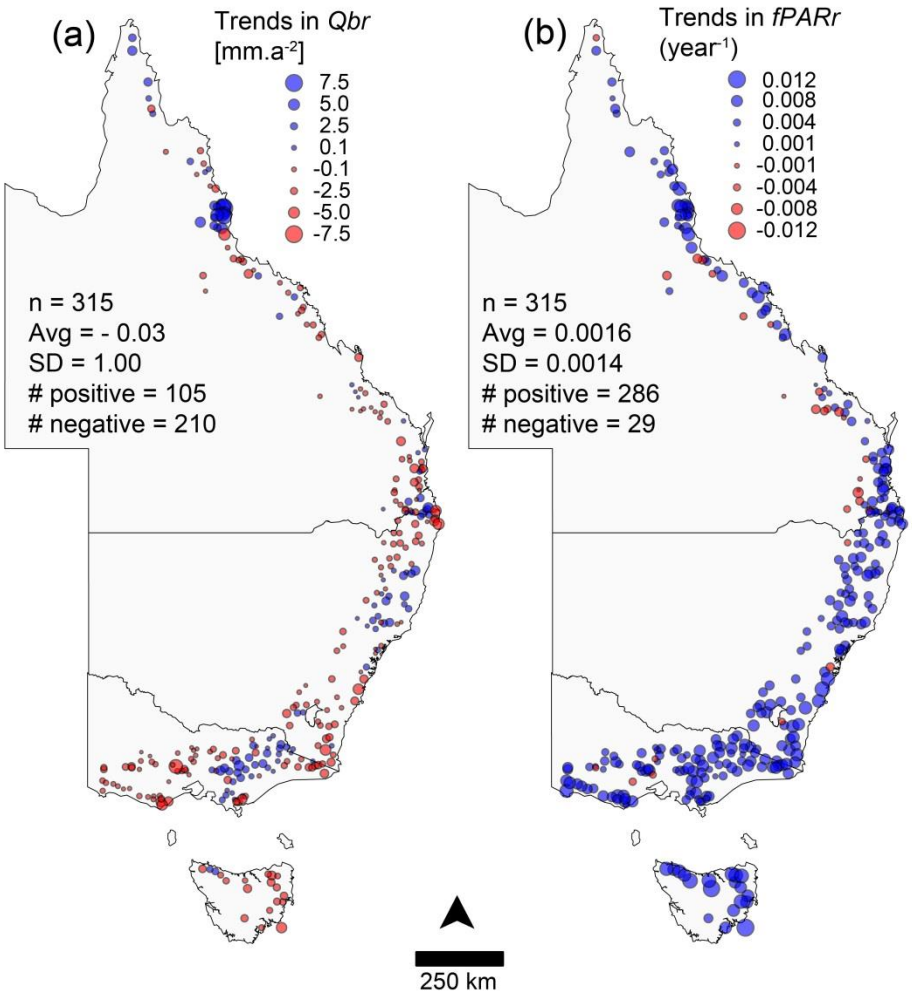

Figure A5.9 Trends of (a) detrended baseflow (Qbr) and (b) detrended fPAR (fPARr) for 1981 – 2013.

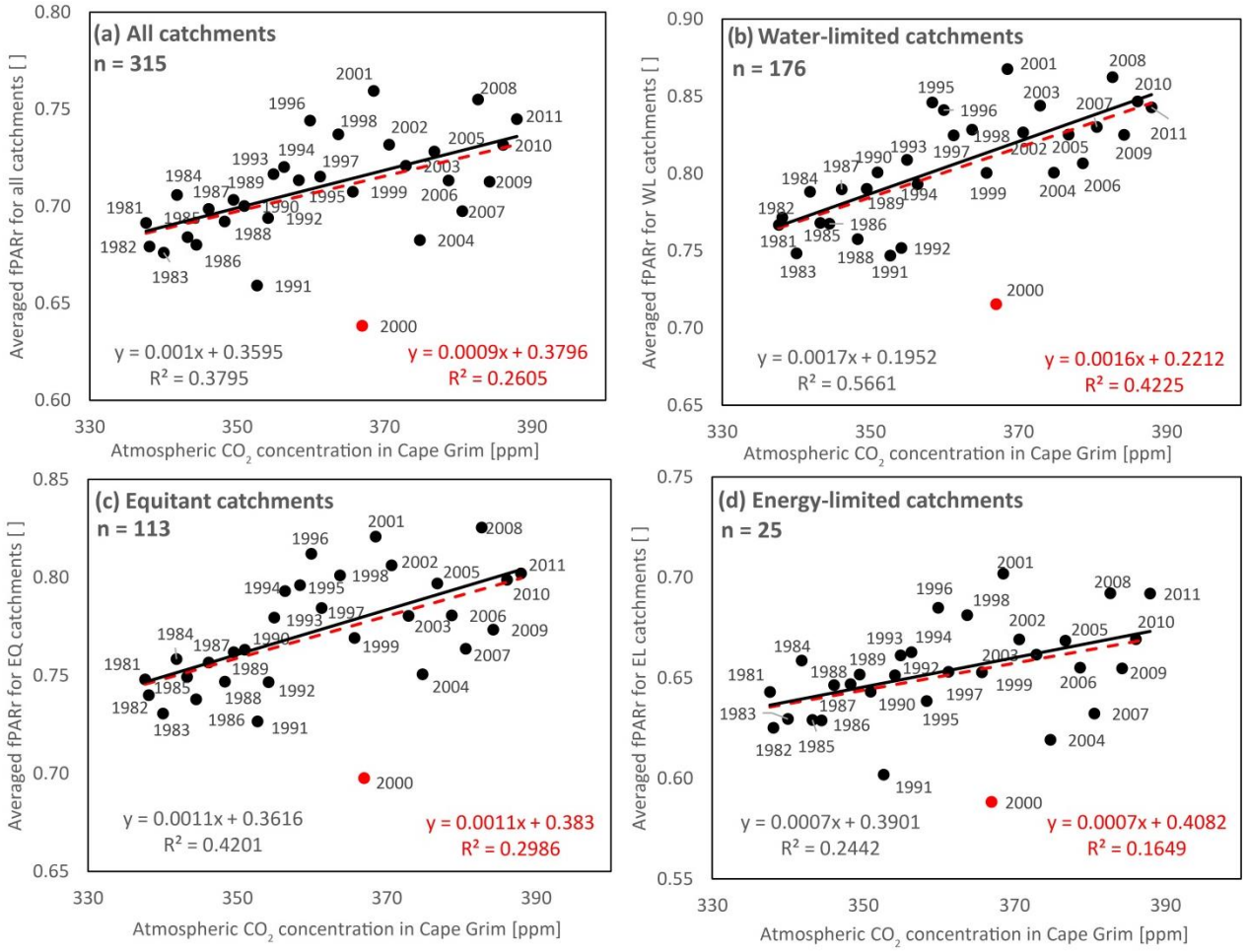

Figure A5.10 Relationship between atmospheric CO2 concentration in Cape Grim (Tasmania) and averaged fPARr for (a) all catchments, (b) water-limited catchments, (c) equitant catchments and (d) energy-limited catchments. Trend lines, linear equations and R2 values are displayed excluding (in black) and including 2000 (in red), which was a wet year identified as an outlier. Note that all the dry years (limited resources) are above the line of best fit (when resource use efficiency is high to maintain the high levels of fPAR – what vegetation have evolved to do – keep living when dry with a slow response in canopy-level fPAR). Note that the gain of line-of-best fit is highest for WL > Equitant > EL, which means that the less of a resource (in this case water) a catchment has, the more efficient it is used and there is less Q as a proportion of P. Note also that R2 follows similar pattern going from EL < Equitant < WL. These patterns suggest that these plots are tracking a biophysically important process related to water use efficiency.

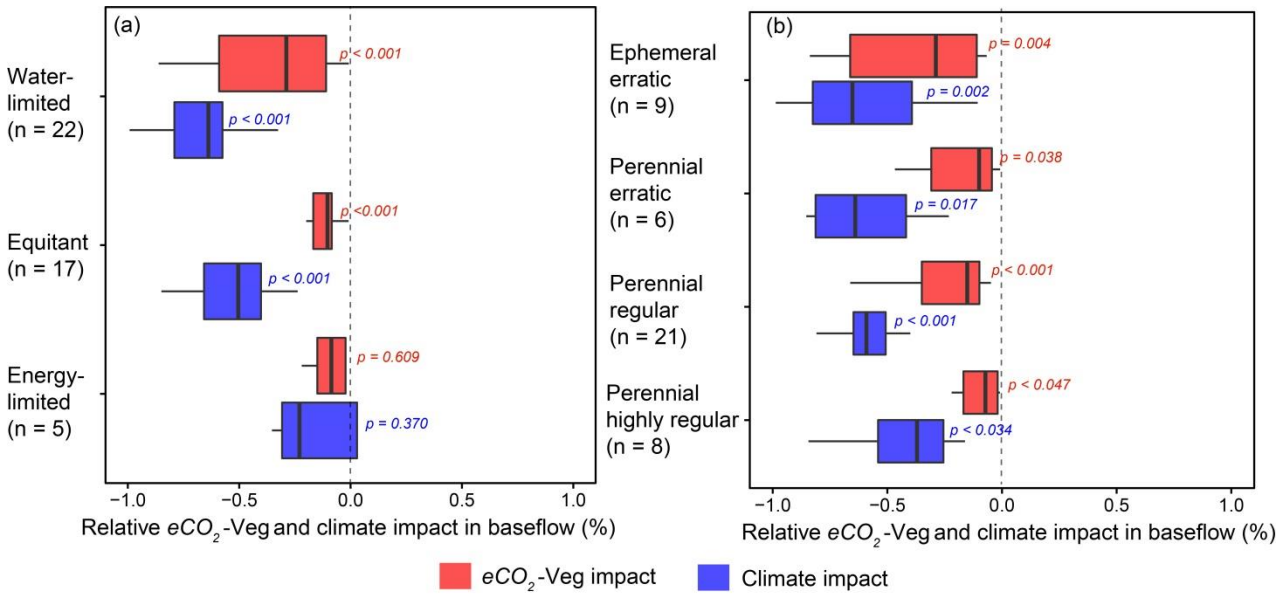

Figure A5.11 Relationship between atmospheric CO_2 concentration in Cape Grim (Tasmania) and averaged fPARr for (a) all catchments, (b) water-limited (PET/P ≥ 1.2) catchments, (c) equitant (0.8 > PET/P < 1.2) catchments and (d) energy-limited (PET/P ≤ 0.8) catchments. Trend lines, linear equations and R^2 values are displayed excluding (in black) and including 2000 (in red), which was a wet year identified as an outlier. Note that all the dry years (when resources are limited) are located above the line of best fit (when resource use efficiency is high to maintain the high levels of fPAR). The gain of line-of-best fit is highest for WL > Equitant > EL, which means that the less of a resource (in this case water) a catchment has, the more efficiently it is used and there is less Q as a proportion of P. Note also that R^2 follows similar pattern going from EL < Equitant < WL. These patterns suggest that these plots are tracking a biophysically important process related to water use efficiency.